A Multiple Defect Approach to Bridge Life Cycle Modelling

Gareth Samuel Calvert

Thesis submitted to the University of Nottingham
for the degree of Doctor of Philosophy

2021

Abstract

Bridges are critical assets for the safe, reliable and functional operation of transportation networks. Infrastructure asset managers are responsible for ensuring that these bridges adhere to rigorous safety standards using the finite resources available to transportation agencies. Predicting future condition, forecasting required interventions and developing equitable resource allocations from limited budgets is a challenging task for bridge asset managers. To facilitate the decision making process at network level and to present decisions to stakeholders, it is common that a life cycle analysis is performed to evaluate the outcomes of different potential management strategies. An accurate bridge life cycle analysis is contingent on an appropriate bridge deterioration model being employed.

In many jurisdictions, stochastic deterioration models are calibrated using condition records from visual bridge examinations, however, condition records typically report bridge condition on a single condition scale. In this thesis, defect specific condition scales are defined to incorporate multiple defect specific indicators in the modelling of deterioration. These additional indicators enable the modelling of the interactions between defects during bridge deterioration, with examples shown for bridge components constructed out of masonry and metal. The multiple defect deterioration models are presented as Dynamic Bayesian Networks, which are calibrated using condition records from railway bridges in the United Kingdom.

Decision modelling in a life cycle analysis enables the evaluation of different asset management strategies. Typical specifications of intervention types in life cycle analysis models are often arbitrarily defined as qualitative actions, e.g. minor and major repair. However, the additional condition indicators developed in this thesis enable the modelling of targeted defect specific maintenance intervention types. Modelling defect specific interventions provides scope to quantitatively assess the effects of strategies that favour increased volumes of preventative maintenance. A Petri net model is used to perform a life cycle analysis, which incorporates a novel dynamic conditional approach to utilise the multiple condition indicators. The model is enhanced by incorporating intrinsic structural and material properties of bridge components alongside local factors such as coastal proximity.

Acknowledgements

My doctoral studies have been transformational for me in many ways, and I will be forever grateful for the opportunity to be supervised by Dr Luis Neves and Professor John Andrews. The success of this PhD project has been achieved due to their continuous support, encouragement, and guidance. In particular, the mentorship of Luis has allowed me to achieve things I could merely dream of a few years ago.

A massive thank you is also owed to Kate Sanderson for her never-ending support with research matters, providing counsel and assisting me with the many opportunities I enjoyed during my time at the research group. Thanks also to Dr Rasa Remenyte-Prescott for her helpful suggestions and critique during my annual progression reviews and viva voce examination. I also appreciate the efforts and expertise of Professor Dan Frangopol during his examination of this thesis. Additionally, a shout out to all my colleagues, past and present, from the Resilience Engineering Research Group who made my time an enjoyable and productive endeavour. It would also be remiss of me to not state my immense gratitude to Network Rail and the Engineering and Physical Sciences Research Council for their financial support that made this all possible.

A huge source of enjoyment of this project has been the tangible impact it could have on industry and this has been achieved with the collaboration with Dr Matthew Hamer at Network Rail, whom a debt of gratitude is owed.

I have been blessed to have the most supportive friends that one could wish for. All of you have made the years I have spent at Nottingham an enjoyable and fulfilling period of my life.

Finally, a massive thank you is owed to my mother for her love, support, and patience.

Author's Declaration

Some chapters of this thesis have been partly based on the following publications of the author.

Journal Papers

- Calvert G., Neves L., Andrews J., and Hamer M. (2020) Multi-defect modelling of bridge deterioration using truncated inspection records, *Reliability Engineering and System Safety*, 200 (106962), DOI: `https://doi.org/10.1016/j.ress.2020.106962`

- Calvert G., Neves L., Andrews J., and Hamer M. (2020) Modelling interactions between multiple bridge deterioration mechanisms, *Engineering Structures*, 221 (111059), DOI: `https://doi.org/10.1016/j.engstruct.2020.111059`

- Litherland J., Calvert G., Andrews J., Modhara S., and Kirwan A. (2021) An alternative approach to railway asset management value analysis: framework development, *Infrastructure Asset Management* DOI: `https://doi.org/10.1680/jinam.20.00002`

- Litherland J., Calvert G., Andrews J., Modhara S., and Kirwan A. (2021) An alternative approach to railway asset management value analysis: application to a UK railway corridor, *Infrastructure Asset Management* DOI: `https://doi.org/10.1680/jinam.21.00003`

- Calvert G., Neves L., Andrews J., and Hamer M. (Submitted) Incorporating defect specific condition indicators in a bridge life cycle analysis, *Engineering Structures*

Conference Contributions

- Calvert G., Neves L., Andrews J. and Hamer M. (2019) Multi-Defect Modelling of Bridge Deterioration, *SIAM UKIE National Student Conference*, 10-11 June 2019, Manchester, UK, DOI: `https://doi.org/10.13140/RG.2.2.14850.22725`

- Litherland J., Calvert G., Andrews J., Kirwan A. (2019) Development of an Extended RAMS Framework for Railway Networks, *29th European Safety and Reliability Conference (ESREL 2019)*, 22-26 September 2019, Hanover, Germany, DOI: `doi.org/10.3850/978-981-11-2724-3`

- Calvert G., Neves L., Andrews J. and Hamer M. (2019) Modelling dependencies between multiple bridge deterioration mechanisms, *IALCCE LCM Workshop 2019*, 27-29 October 2019, Rotterdam, Netherlands

- Calvert G., Neves L., Andrews J. and Hamer M. (2019) Multi-Defect, Bridge Asset Management, *UKRRIN Annual Conference*, 21 November 2019, Birmingham, UK

- Calvert G., Neves L., Andrews J. and Hamer M. (2020) A Multi Defect Approach to Bridge Asset Management, *22nd IStructE Young Researchers Conference*, 4 September 2020, London, UK, DOI: `https://doi.org/10.13140/RG.2.2.31394.17602`

- Calvert G., Neves L., Andrews J., and Hamer M. (2021) Modelling the interactions between defect mechanisms on metal bridges, *10th International Conference on Bridge Maintenance, Safety and Management (IABMAS 2020)*, 11-18 April 2021, Sapporo, Japan, DOI: `https://doi.org/10.1201/9780429279119-374`

Contents

List of Figures

List of Tables

List of Acronyms

AI	Artificial Intelligence
AIC	Akaike Information Criterion
ANN	Artificial Neural Networks
ASCE	American Society of Civil Engineers
ATPC	Average Time in Poor Condition
BBN	Bayesian Belief Network
BIC	Bayesian Information Criterion
BMS	Bridge Management System
BO	Overbridge
BPM	Backward Prediction Model
BU	Underbridge
CAPM	Causal Arc Place Marking
CBR	Case Based Reasoning
CDF	Cumulative Distribution Function
CM	Cracked Masonry/Coating-Metal
CNN	Convolutional Neural Networks
CPN	Coloured Petri Net
CPT	Conditional Probability Table
CTMC	Continuous Time Markov Chain
DAG	Directed Acyclic Graph
DBN	Dynamic Bayesian Network
DCT	Dynamic Conditional Transition
DTMC	Discrete Time Markov Chain
EMGTPA	Equivalent Million Gross Tonnes Per Annum

FEA	Finite Element Analysis
FMEA	Failure Modes and Effects Analysis
GA	Genetic Algorithm
GPU	Graphical Processing Units
HSE	Health and Safety Executive
KFF	Known Failed Function
KPI	Key Performance Indicator
LDF	Lifetime Distribution Function
MGE	Exposed Main Girder
MGI	Inner Main Girder
MLE	Maximum Likelihood Estimator
MSE	Mean Squared Error
MTTP	Mean Time To Poor
MU	Monetary Units
NBI	National Bridge Inventory
NDE	Non-Destructive Evaluation
NDT	Non-Destructive Testing
PCT	Place Conditional Transition
PDF	Probability Density Function
PLBE	Principal Load Bearing Element
PN	Petri Net
PPDAC	Problem, Plan, Data, Analysis, Conclusion
PRNG	Pseudo-Random Number Generator
PSO	Particle Swarm Optimisation
SCF	Structural Component Failure
SevEx	Severity Extent
SHM	Structural Health Monitoring
SPN	Stochastic Petri Net
TPM	Transition Probability Matrix
TRM	Transition Rate Matrix
WLCC	Whole Life Cycle Cost

Chapter 1

Introduction

Transportation networks are widely regarded as critical national infrastructure (Cabinet Office, 2019; Department of Homeland Security, 2013); these networks comprise a wide range of civil infrastructure including bridges. In most developed countries the civil infrastructure portfolio composing the transportation networks is mature and increasingly requiring investment in maintenance, repair and replacement to ensure the continued provision of the safety, reliability and functionality of the networks (Dobbs et al., 2013).

Infrastructure asset managers have the responsibility of ensuring that the bridges are maintained to a suitable safety threshold as the consequence of structural failures poses huge safety, economic and social risks (Smale, 2018; Xie and Levinson, 2011). As part of the efforts to avert such failures infrastructure owners devise asset management strategies. In general, asset management can be defined as the "*coordinated activity of an organisation to realise values from assets*" (British Standards Institution, 2014). For bridges this requires an array of measures to be implemented including inspection, maintenance, renewal and enhancement strategies alongside life cycle modelling to inform the strategy development.

The asset management of structural assets can require major resource allocations and investments, with the forecasted requirements of infrastructure portfolios increasing (Institute of Civil Engineers, 2018). However, many infrastructure asset managers only have finite resources available to them. Moreover, many infrastructure asset managers are publicly funded by the taxpayer, and thus have regulatory

oversight into how funding is used to manage assets. In response to this challenge many infrastructure owners have invested in developing decision support tools and their life cycle modelling capabilities.

Life cycle modelling is used to predict future asset condition, forecast required interventions, evaluate the effects of different management strategies and determine optimal resource allocation. Furthermore, life cycle cost models are used to present strategies to infrastructure stakeholders, aid in the determination of optimal strategies and provide an accountable way to justify decisions.

The American Society of Civil Engineers (ASCE) Grand Challenge tasks civil engineers to "*significantly enhance the performance and value of infrastructure projects over their life cycles by 2025*" and to "*foster the optimization of infrastructure investments*" (ASCE, 2017). Such objectives require multi-faceted solutions with life cycle modelling being a constituent part of any solution.

1.1 Research Motivation

The railway in Great Britain includes a sizeable portfolio of over 26,000 bridges (Network Rail, 2019b), see Figure 1.1. Network Rail is the infrastructure asset manager for the railway network in England, Scotland, and Wales. Consequently, Network Rail is responsible for the inspection, assessment, maintenance, and repair of this portfolio of bridges. The risk of structural failure is reduced by performing inspections and maintenance as per the industry guidelines (Network Rail, 2014a) and by following a prescribed asset management strategy (Network Rail, 2018).

An asset life cycle consists of "*all stages from construction, operation and maintenance to end-of-life, including decommissioning*" (British Standards Institution, 2017). The Whole Life Cycle Cost (WLCC) captures all initial and future costs of an asset through the course of its life cycle and is calculated to establish the total cost of asset ownership and assess different asset management strategies. Many infrastructure managers want to identify and avoid scenarios which have lower initial costs but have considerably higher ongoing costs. Life cycle cost modelling can be used to determine the WLCC. Whilst WLCC is a key modelling output, it is criti-

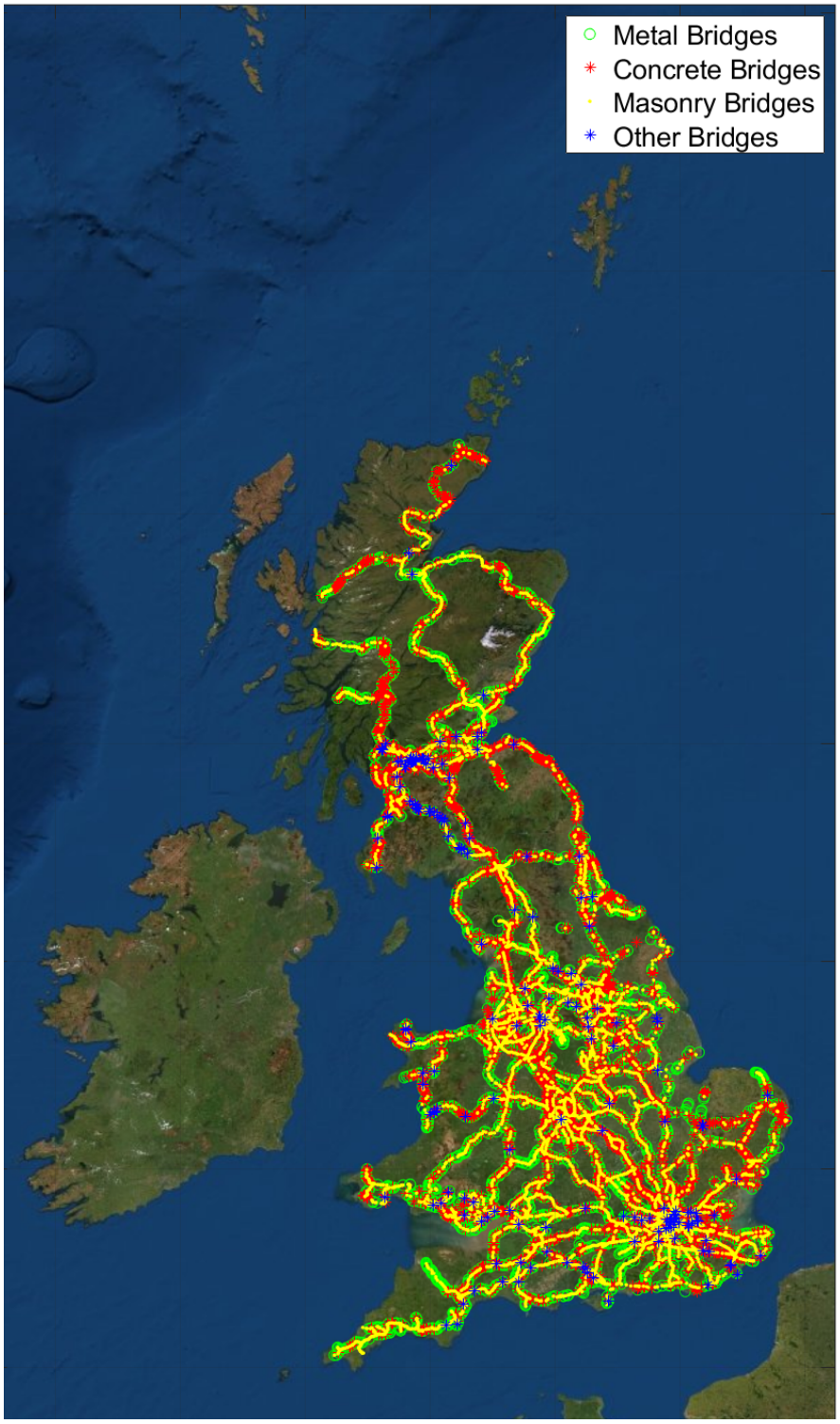

Figure 1.1: The Network Rail bridge portfolio (Network Rail, 2019b).

cal that any analysis approach is capable of ascertaining the impact the evaluated strategy has on additional factors such as safety, capability and service disruption.

There are two fundamental components to any life cycle analysis: a deterioration model and a decision model (Frangopol et al., 2004). The future condition of a bridge component under a do-nothing maintenance strategy is predicted using a deterioration model. The decision model is used to evaluate the impact of different maintenance strategies to the deterioration model output, and thus it enables comparisons of different maintenance strategies and the consequence on bridge condition and WLCC. When using both components, it is possible to determine the optimal WLCC for the considered strategies, given the priorities and constraints of the asset stakeholders.

It is critical to asset managers that both the deterioration model and the decision model have sufficient prediction accuracy in their own right. However, it is also paramount that the deterioration model is well understood and is reflective of the physical deterioration process, otherwise the output of the decision model will have added uncertainty.

Across academic literature and industry there have been an extensive range of decision support tools researched and developed to support asset managers in their decision making for network level bridge management, see Chapter 3. Many transportation agencies have implemented modelling frameworks which assume that the condition at the lowest hierarchical asset level can be denoted by a single score. However, this is an oversimplification of the diverse physical process of deterioration; it results in a limited ability to model different strategies that have targeted defect specific maintenance strategies.

1.2 Aims and Objectives

1.2.1 Aims

The aim of this research project is to develop enhanced methodologies to model the deterioration of bridges, in order to facilitate enhanced life cycle modelling that maximises the impact of investments and minimises the safety risk to infrastructure

users.

More specifically, can bridge condition be predicted using multiple defect specific indicators, and if so, what relationships exist between different defect mechanisms? Upon answering this research question, the capabilities of existing life cycle models would need to be adapted accordingly to incorporate the additional indicators and provide enhanced decision making capabilities.

1.2.2 Objectives

- Develop a stochastic multiple defect bridge deterioration model calibrated using data that is available for an entire portfolio of bridges and determine the most appropriate calibration methods given the constraints of the available data.
- Identify and quantify interactions between defect modes and propose a method to model any identified relationships.
- Develop a life cycle model which incorporates multiple degradation condition indicators and facilitates the evaluation of defect specific maintenance intervention strategies.
- Identify additional factors and properties that can cause a variation in the life cycle profile of a bridge component.

1.3 Thesis Outline

The thesis is structured as follows:

- **Chapter 2:** *Stochastic modelling methods* - This chapter presents the mathematical principles that underpin the stochastic modelling methodologies commonly employed in literature and in this thesis to model bridge deterioration.
- **Chapter 3:** *Bridge asset management* - A comprehensive review of bridge performance evaluation, asset management, deterioration modelling and the the availability of data for model calibration.

- **Chapter 4:** *Modelling multiple deterioration mechanisms* - In existing literature and industrial practice, bridge component deterioration is modelled using a single condition indicator. However, bridge deterioration is not one single process but rather an amalgamation of several simultaneous processes, which all result in the degradation of structural performance. This chapter introduces a Markov chain model to predict the independent progression of multiple bridge deterioration mechanisms.

- **Chapter 5:** *Modelling interactions between multiple deterioration mechanisms* The development and progression of one deterioration mechanism may be influenced by the occurrence or extensiveness of another. In this chapter the interactions between defects are modelled using Dynamic Bayesian Networks.

- **Chapter 6:** *Incorporating defect specific condition indicators in a bridge life cycle analysis* - A deterioration model that simultaneously considers multiple deterioration mechanisms and the interactions between mechanisms is capable of outputting multiple condition indicators. These additional indicators can be used in decision modelling and incorporated in maintenance strategies which specify targeted defect specific interventions. In this chapter, a life cycle model is presented as a Petri net model which enables the specification of targeted maintenance strategies and facilitates the evaluation of the quantitative benefits of strategies that favour earlier interventions.

- **Chapter 7:** *Incorporating the effects of local, material and structural properties on metallic bridge deterioration* - The deterioration profile of a bridge component can be influenced by many different factors. In this chapter, a bridge's coastal proximity, material type and structural properties are assessed to determine whether these factors influence the rate of progression for particular mechanisms. Additionally, the consequences of differing deterioration profiles on the life cycle are evaluated.

- **Chapter 8:** *Conclusions* - This chapter summarises the research contributions of the material presented in the thesis, commenting on the fulfilment of the research aims and objectives, and identifies areas for future work.

Chapter 2

Stochastic Modelling Methods

Bridge deterioration is an aggregation of several dynamic processes which all result in the reduction of the structural integrity of a bridge. A stochastic process is used for the modelling of random time-dependent phenomena, with the term stochastic being a derivation of the Greek word *stokhastikos*, meaning "*capable of guessing*" or "*conjecture*" (Privault, 2013). Moreover, for bridge deterioration modelling, stochastic techniques are favoured over deterministic methodologies for their intrinsic ability to incorporate the uncertainty of the deterioration process (Frangopol et al., 2004).

Stochastic models (and mathematical models in general) are used to describe a system and study the effects and interactions of system components, inter-system relationships and the system environment, as well as to make predictions on future system behaviour. The purpose of a stochastic structural deterioration model for an asset portfolio is:

- to elicit an estimation of the probability of structural failure within a defined time frame;
- to complement decision modelling in a life cycle analysis to present optimal maintenance strategies to infrastructure stakeholders.

Nonetheless, one must always recall the adage popularised by George Box, "*All models are wrong*" (Box, 1976). Box later appended "*but some are useful*" (Box, 1979). The task for engineers, scientists and statisticians, is to ensure the applicability of the models they develop.

To achieve the desired useful outputs from a developed model it is critical that one takes a holistic problem-based approach, with specific statistical tools deemed to be only one component of a complete cycle of investigation (Spiegelhalter, 2019). Frameworks such as the PPDAC Cycle encapsulate this problem-driven approach into an investigation/research workflow (MacKay and Oldford, 2000; Wild and Pfannkuch, 1999). PPDAC stands for:

- Problem - Understanding and defining the problem, as well as evaluating different approaches to answering the research question.
- Plan - Identify what is required to be measured and recorded.
- Data - Collect, manage and cleanse the required data for the study.
- Analysis - Sort data, look for patterns and test hypothesis.
- Conclusion

Each stage feeds directly into the next, with the study conclusions feeding back into future problem developments. This thesis considers each of these stages in the development and implementation of bridge deterioration modelling.

The purpose of this chapter is to review the methodologies commonly used in bridge deterioration modelling during the analysis stage of an investigation. Markov based approaches are recognised to be the most prevalent for bridge deterioration modelling (Agrawal et al., 2009; Frangopol et al., 2004), and are the first method considered. However, there are a plethora of different methodologies that have been employed in addition to Markov based models. The remainder of the chapter considers two alternative methods: Petri nets and Bayesian Belief Networks.

2.1 Markov Models

The Markovian approach can be applied to systems that have discrete or continuous variations, temporally and spatially (Andrews and Moss, 2002). However, for civil engineering applications, finite-state Markov processes are more prevalent.

Markov models assume the Markov property, or memoryless property, which can be described by "*a sequence of random variables; which correspond to the states of a certain system in such a way that the state at one time depends only on the state in the previous time step*" (Ching et al., 2013). Moreover, the Markov property is the notion that a future state is only determined by the present state and it does not consider the history in determining the future, i.e. its past and future are independent.

2.1.1 Finite-State Markov Processes

Consider a stochastic process X, such that

$$X = \{X^{(t)}, t \in \mathcal{T}\}, \tag{2.1.1}$$

where $X^{(t)}$ represents the state of X at time t and $\mathcal{T}$ is the set that describes time. Moreover, $\mathcal{S}$ is the finite state space that describes the possible states that X can assume. An element of the state space $\mathcal{S}$ is known as a state of the process. When a process is in state i, there is a probability $p_{i,j}$ that its subsequent state will be in state j,

$$p_{ij} = \mathbb{P}(X^{(n+1)} = x_{n+1} | X^{(n)} = x_n, X^{(n-1)} = x_{n-1}, \dots, X^{(0)} = x_0) = \mathbb{P}(X^{(n+1)} = x_{n+1} | X^n = x_n) \tag{2.1.2}$$

where $n \geq 0$ and $x_0, x_1, \dots, x_{n+1} \in \mathcal{S}$. Such a stochastic process is called a Markov process (Rubino and Sericola, 2014).

2.1.2 Discrete Time Markov Chain

Consider the Markov chain, $X_t, t \in \mathcal{T}$, where $T = \{t_0, t_1, t_2, \dots\}$. Moreover, the Markov chain is time-homogeneous, i.e. $t_j - t_i = \delta t$, $\forall i, j \in \mathbb{Z}^*, i \neq j$, where δt is a unit time step. The probability of X transitioning from state i to state j per δt is defined by,

$$p_{i,j} = \mathbb{P}\{X^{(t_{n+1})} = j | X^{(t_n)} = i\} = \mathbb{P}\{X^{(t_1)} = j | X^{(t_0)} = i\}. \tag{2.1.3}$$

All the possible (i, j) permutations for transition probabilities p_{ij}, can be used as elements to construct a matrix P of order $(n \times n)$,

$$\mathbf{P} = \begin{bmatrix} p_{1,1} & p_{1,2} & \cdots & p_{1,n} \\ p_{2,1} & p_{2,2} & \cdots & p_{2,n} \\ \vdots & \vdots & \ddots & \vdots \\ p_{n,1} & p_{n,2} & \cdots & p_{n,n} \end{bmatrix}, \tag{2.1.4}$$

where n is the total number of condition states and the matrix $\mathbf{P}$ is known as the Transition Probability Matrix (TPM). $\mathbf{P}$ is a stochastic matrix, which means the following constraints apply:

$$0 \leq p_{i,j} \leq 1, \quad \forall i, j = 1, \ldots, n, \tag{2.1.5}$$

$$\sum_{j=1}^{n} p_{i,j} = 1, \quad \forall i. \tag{2.1.6}$$

Markov Chain Directed Graphs

Discrete Time Markov Chains (DTMC) can be stated in purely abstract terms to define the stochastic process over time but it is common for a Markov model to be graphically represented using a Markov directed graph. For a DTMC with the following TPM,

$$\mathbf{P} = \begin{bmatrix} p_{1,1} & p_{1,2} & p_{1,3} \\ p_{2,1} & p_{2,2} & p_{2,3} \\ p_{3,1} & p_{3,2} & p_{3,3} \end{bmatrix}, \tag{2.1.7}$$

an example of its associated directed graph is shown in Figure 2.1.

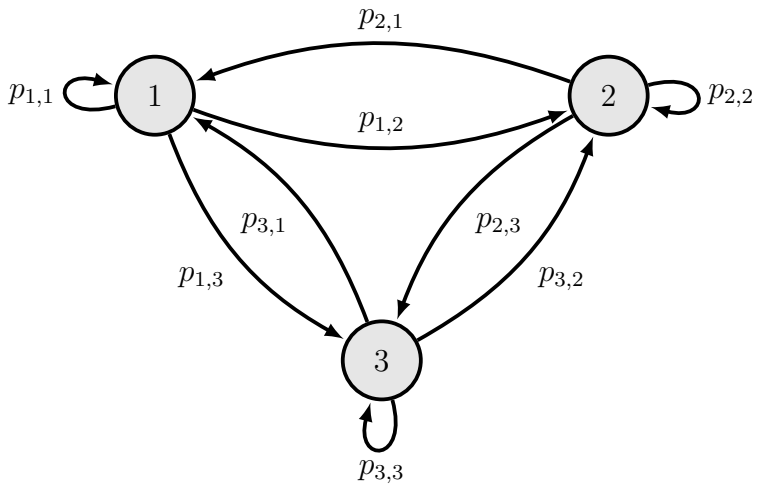

Figure 2.1: Three state, discrete time Markov chain model.

Common DTMC Structures for Bridge Deterioration Models

Commonly when DTMCs are used to model the deterioration of a structure, the model assumes a do-nothing maintenance strategy which results in the continual degradation of a structure, i.e. there is no improvement in condition. Thus, the structure of the DTMC TPM will require that any entries below the main diagonal assume a value of zero. Two common TPM structures that adhere to this constraint are the progressive Markov chain,

$$\mathbf{P} = \begin{bmatrix} p_{1,1} & p_{1,2} & p_{1,3} & p_{1,4} & p_{1,5} \\ 0 & p_{2,2} & p_{2,3} & p_{2,4} & p_{2,5} \\ 0 & 0 & p_{3,3} & p_{3,4} & p_{3,5} \\ 0 & 0 & 0 & p_{4,4} & p_{4,5} \\ 0 & 0 & 0 & 0 & 1 \end{bmatrix}, \tag{2.1.8}$$

and the sequential Markov chain,

$$\mathbf{P} = \begin{bmatrix} 1-p_{1,2} & p_{1,2} & 0 & 0 & 0 \\ 0 & 1-p_{2,3} & p_{2,3} & 0 & 0 \\ 0 & 0 & 1-p_{3,4} & p_{3,4} & 0 \\ 0 & 0 & 0 & 1-p_{4,5} & p_{4,5} \\ 0 & 0 & 0 & 0 & 1 \end{bmatrix}, \tag{2.1.9}$$

where both examples have five discrete condition states. Modelling bridge deterioration using DTMCs requires that the following characteristics are satisfied:

- The discrete states denote specific condition states. Moreover, the states are strictly ordered by severity of degradation.
- The process encapsulates the monotonic progression through the distinct condition states.

Both the progressive and sequential structures as shown in (2.1.8) and (2.1.9) possess these characteristics (Kallen, 2007). The progressive structure permits the 'jumping' of condition states which could be indicative of instances of sudden or rapid deterioration, for example a bridge in state 1 could transition directly to state 3 without having to transition via state 2. Deterioration due to the ageing of an asset is typically deemed to be a gradual process and the sequential structure enforces the gradual deterioration through successive states and prohibits states being skipped.

Chapman-Kolmogorov Equation

The *n-step transition probability* is the probability that a process in state i at time t will be in state j after a further n time steps,

$$p_{i,j}^{(n)} = \mathbb{P}\{X^{(t+n)} = j | X^{(t)} = i\}, \quad n, i, j \geq 0. \tag{2.1.10}$$

The Chapman-Kolmogorov equation enables a method to compute these probabilities,

$$p_{i,j}^{(n+m)} = \sum_{k=0}^{\infty} p_{i,k}^{(n)} p_{k,j}^{(m)} \tag{2.1.11}$$

The $p_{i,k}^{(n)} p_{k,j}^{(m)}$ term represents the probability of a process starting in state i and transitioning to state j in $n+m$ steps, where the transition path uses state k as an intermediate at the n^{th} transition. Thus, the probability of being in state j after $n+m$ transitions is determined by summing over all possible intermediate states k (Ross, 2006). Moreover, if $\mathbf{P}$ is the one-step matrix, it can be stated that,

$$\mathbf{P}^{(m)} \cdot \mathbf{P}^{(n)} = \mathbf{P}^{(m+n)}. \tag{2.1.12}$$

Consequently, the probability of $p_{i,j}^{(m+n)}$ will be the $(i,j)^{th}$ element of $\mathbf{P}^{(m+n)}$. Using this result, the changes in the distribution of a portfolio's condition, $\mathbf{C}$, with N condition states, from time 0, to t, can be determine using,

$$\begin{bmatrix} c_1^t & c_2^t & \dots & c_N^t \end{bmatrix} = \begin{bmatrix} c_1^0 & c_2^0 & \dots & c_N^0 \end{bmatrix} \begin{bmatrix} p_{1,1} & p_{1,2} & \dots & p_{1,N} \\ 0 & \ddots & \ddots & p_{2,n} \\ \vdots & \ddots & \ddots & \vdots \\ 0 & 0 & 0 & 1 \end{bmatrix}^t , \tag{2.1.13}$$

where c_i^t is the proportion of the portfolio predicted to be in state i at year t.

Absorption States

A state s_i of a Markov chain is called an absorbing state if it is impossible to leave that state, i.e. $p_{i,i} = 1$. A state that is not an absorbing state is known as a transient state. A Markov chain is described as being an absorbing Markov chain if every non-absorbing state in the chain can transition into an absorbing state (Grinstead and Snell, 1997). If there are t transient states and r absorbing states, then the canonical form of the transitions matrix $\mathbf{P}$ is denoted as,

$$\mathbf{P} = \left(\begin{array}{c|c} \mathbf{Q} & \mathbf{R} \\ \hline 0 & \mathbf{I}_r \end{array}\right), \tag{2.1.14}$$

where $\mathbf{Q}$ is a t-by-t matrix, $\mathbf{R}$ is a t-by-r matrix, 0 is a r-by-t zero matrix and $\mathbf{I}_r$ is the r-by-r identity. The probability of transitioning from one transient state to another is described by $\mathbf{Q}$, and the probability of transitioning from a transient state to an absorbing state is described by $\mathbf{R}$ (Grinstead and Snell, 1997).

Theorem 2.1.1 In an absorbing Markov chain, the probability that the process will be absorbed after n steps is 1. ($Q^n \to 0$ as $n \to \infty$).

Theorem 2.1.2 For an absorbing Markov chain P, the fundamental matrix is described by

$$\mathbf{N} = \mathbf{I} + \mathbf{Q} + \mathbf{Q}^2 + \cdots = \sum_{k=0}^{\infty} Q^k = (\mathbf{I}_t - \mathbf{Q})^{-1},$$

where I_t is the t-by-t identity matrix. The $i - j^{th}$ entry of N, $n_{i,j}$, indicates the expected number of times the chain is in state s_j given that the chain started in s_i.

Theorem 2.1.3 Let t_i be the expected number of steps before the chain is absorbed, given that the chain starts in state s_i and let t be the column vector whose i^{th} entry is t_i. Then

$$\mathbf{t} = \mathbf{N} \cdot \mathbf{c},$$

where $\mathbf{c}$ is a column vector all of whose entries are one.

The deterioration models shown in (2.1.8) and (2.1.9) are both absorbing Markov chains, where the fifth state is the absorbing state. Now consider the fifth state to be defined as the 'poor' bridge condition. A practical application of Theorem 2.1.3 is that it enables the calculation of the expected time to poor condition of a bridge from each starting condition and provides insight into the remaining useful life of a bridge.

2.1.3 Semi-Markov Processes

Semi-Markov processes are Markov processes that have a random sojourn time allocated between state transitions (Howard, 1971). Consider the stochastic process X^T, which has n states, which assumes $S_0 = i$, $\forall i \in \mathcal{S}$ at the initial time step and the state after k transitions is denoted as S_k, where $k = 1, 2, \ldots, m$. The state transitions occur at stepwise iterations at $t = \tau_k$.

The probability of the process transitioning into state j with a sojourn time ($T = \tau_k - \tau_{k-1}$) less than or equal to t, given that it has just transitioned into state i is,

$$\mathbb{P}\{\tau_k - \tau_{k-1} \leq t, S_k = j | S_{k-1} = i\} = p_{ij} \cdot F_{ij}(t), \tag{2.1.15}$$

where,

$$F_{i,j}(t) = \mathbb{P}\{T \leq t | S_k = j, S_{k-1} = i\}. \tag{2.1.16}$$

$F(t)$ does not necessarily need to be described by a memoryless distribution, hence the designation of 'semi-Markov', however, at the instance of state transition the Markov property holds. If $F(t)$ is described by an exponential distribution, the stochastic process is Markovian for all $t \geq 0$ and is known as a continuous time Markov chain (Limnios and Oprisan, 2001).

2.1.4 Continuous Time Markov Chain

For Continuous Time Markov Chains (CTMC), the transition probability function can be expressed as,

$$\mathbf{P}(t) = \exp(\mathbf{Q} \cdot t) = \sum_{k=0}^{\infty} \mathbf{Q}^k \frac{t^k}{k!}, \tag{2.1.17}$$

where $\mathbf{Q}$ is known as the Transition Rate Matrix (TRM) or an intensity matrix. The structure of the matrix follows the q_{ij} nomenclature, which is used to express the rate at which an element will leave state i and transition to state j (Norris, 1997). The elements of $\mathbf{Q}$ are required to satisfy the following conditions,

$$q_{ij} \geq 0, \quad \text{for } i \neq j, \tag{2.1.18}$$

$$q_{ii} = -\sum_{j \neq i} q_{ij}. \tag{2.1.19}$$

Note that $\mathbf{Q}$ is a square matrix and the function $\exp(\mathbf{A})$, where $\mathbf{A}$ is a square matrix, is known as the matrix exponential. The matrix exponential is defined by the same power series as the scalar exponential i.e.

$$\exp(X) = 1 + X + \frac{X^2}{2!} + \frac{X^3}{3!} + \cdots = \sum_{k=0}^{\infty} \frac{1}{k!} X^k, \tag{2.1.20}$$

however, the X^k term for the matrix exponential[1] is defined by matrix products and not element-wise scalar multiplication (Jackson, 2011). For simple models, it is possible to determine analytical expressions, however to generalise for more complex models numerical analysis techniques are used. Moler and Van Loan (2003) describe methods to compute the matrix exponential and the challenges in computing an approximant. The inbuilt `expm` in MATLAB uses the scaling and squaring method algorithm described by Higham (2005) and Al-Mohy and Higham (2009), which relies on determining Padé approximants to the matrix exponential.

[1] X^0 is the identity matrix.

2.2 Petri Nets

Petri Nets (PN) were invented by Carl Adam Petri and were initially used for the description of chemical processes (Petri and Reisig, 2008). Petri formalised his ideas in his PhD thesis (Petri, 1962).

PNs are a graphical and mathematical methodology which are used to describe and study systems that are characterised as being "*concurrent, asynchronous, distributed, parallel, nondeterministic, and/or stochastic*" (Murata, 1989). In many research disciplines, a physical phenomenon is studied through the medium of a model rather than direct study. A model is a representation developed to contain the most important attributes of the system. By manipulating the developed model, it is hoped that research can acquire a greater understanding of the system without the physical costs of interacting with it (Peterson, 1981).

The application of PNs in reliability engineering models have become well established in the research community (Jensen, 1997; Schneeweiss, 1999; Trivedi and Bobbio, 2017). Furthermore, there has been some work on the use of PNs within the contexts of railway networks, with numerous studies showing that they can be effective in the modelling of deterioration and maintenance processes in this industry (Andrews, 2013; Kilsby et al., 2017, 2018; Le et al., 2017; Yianni et al., 2017).

2.2.1 Petri Net Terminology

A PN is a mathematical modelling language which is used to create a directed, weighted, bipartite graph and is composed of five sets (Murata, 1989). A PN has a finite set, called the *initial marking*, which specifies the initial state. The graph being described as bipartite is due to the nodes of the graph being divided into two different types: *places* and *transitions*, which form a finite set of places P and a finite set of transitions T. Furthermore, the set of places, P and set of transitions, T, are disjoint.

The two node types, places and transitions, can be connected by directed arcs, from places to transitions, called *input arcs*, and from transitions to places, called *output arcs*. Mathematically, this can be described as an *input* function, I, and an

output function, O. Both the input and output functions are used to relate places and transitions. An input function, I, is a mapping from transition t_j to a collection of places $I(t_j)$, known as the *input places* of t_j. Similarly, an output function, O, is a mapping from a transition t_j to a collection of places $O(t_j)$, called the *output places* of t_j.

The final element of a PN are *tokens*, which are used to denote the elements in the studied system, or particular states of the system (Murata, 1989; Peterson, 1977). Thus, a PN structure can be mathematically described by a quintuple containing its places, transitions, input function and output function (Hopcroft and Ullman, 1969; Peterson, 1981). A formal definition of a Petri Net can be found in Definition 2.2.1, (Murata, 1989).

Definition 2.2.1 A Petri Net is a quintuple, $PN = (P, T, F, W, M_0)$ where:

$P = \{p_1, p_2, \ldots, p_m\}$ is a finite set of places,

$T = \{t_1, t_2, \ldots t_n\}$ is a finite set of transitions,

$F \subseteq (P \times T) \cup (T \times P)$ is a set of arcs (flow relation),

$W : F \to \{1, 2, 3, \ldots\}$ is a weight function,

$M_0 : P \to \{0, 1, 2, 3, \ldots\}$ is the initial marking,

$P \cap T = \emptyset$ and $P \cup T \neq \emptyset$.

A Petri net $N = (P, T, F, W)$ without any specific initial marking is denoted by N. A Petri net with the given initial marking is denoted by (N, M_0).

2.2.2 Petri Net Graphical Representation

A graphical interpretation of a PN has two node types which are the *places* and *transitions*. Circles are typically used to denote places and a rectangle or square is used to denote a transition. The transitions and places are interconnected mathematically by input and output functions but visually by arrows, known as an *arc* or *edge*, which show the direction of flow. The connection of one node type to the same node type is not permissible as the sets of places and transitions are disjoint, and thus no two places or transitions can be directly connected with an arc (Reisig, 2013). Figure 2.2 shows the different PN graphical components.

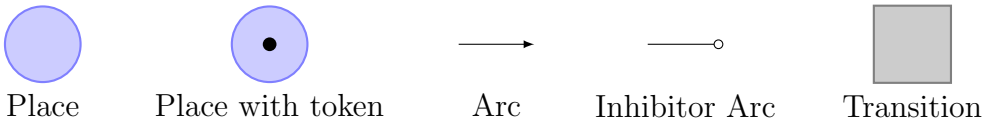

Figure 2.2: Petri net graphical components.

2.2.3 Petri Net Examples

The function of a transition in a PN is to absorb tokens from the input places and generate tokens in the output places. If a transition has multiple input places, the transition requires all of the input places to contain a token before it can fire.

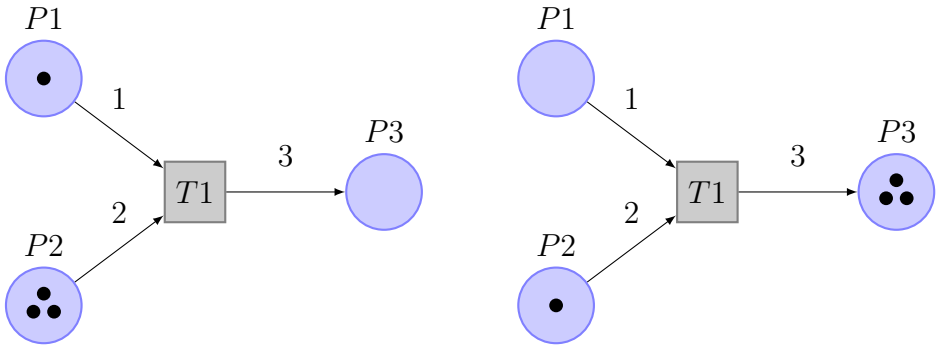

(a) Example Petri net before firing

(b) Example Petri net after firing

Figure 2.3: An example Petri net with (a) showing the net before it fires and (b) showing the net after firing T1.

A transition will become enabled if all its input places are marked with the number of tokens specified by their connected arc weight. An example of a PN before and after firing is shown in Figure 2.3. In the example, observe that for $T1$ to fire, 1 token from $P1$ and 2 tokens from $P2$ are required. When firing, these tokens are removed from the input places and 3 tokens are added to $P3$.

An inhibitor arc can only go from a place to a transition, i.e. it is a type of inbound arc. A transition with a connected inhibitor arc can only become enabled if there are no tokens present in the connected place. Thus, in the example shown in Figure 2.4, the transition can not become enabled and fire a token into $P2$.

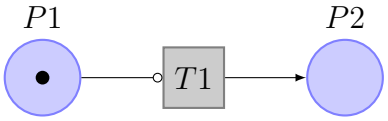

Figure 2.4: Example Petri net with an inhibitor arc.

2.2.4 Stochastic Petri Nets

In the PNs introduced thus far, there was no inclusion for a temporal parameter. Many systems are time dependent and if an accurate model is to be developed, the chosen modelling methodology must have the capacity for temporal properties.

An initial introduction of time to the PN modelling framework can be found in Ramamoorthy and Ho (1980), and Zuberek (1980). Although, it should be noted that whilst temporal attributes were added to PNs, the time intervals were fixed in nature, i.e. the time introduction was used to create a fixed time delay between the transition being enabled and the instant at which the transition fires.

The concept of a Stochastic Petri Net (SPN) was introduced by Molloy (1982); this work assigned an exponentially distributed firing delay time to each transition for continuous time systems. After the initial proposal of SPNs by Molloy, several different defined classes were proposed in literature; the generalised SPN (Marsan et al., 1984), the extended SPN (Dugan et al., 1985) and PNs with deterministic and exponentially distributed firing times (Ajmone Marsan and Chiola, 1987).

A random time interval value can be assigned using different probability distributions. The different types of SPNs outline how the different transition extensions or server semantics work; the server semantics outline how to process tokens and how the transition becomes enabled and fires for each time step. There are further examples of transition extensions to add additional functionality to Petri nets including, reset transitions, conditional transitions and probabilistic transitions (Andrews, 2013).

2.2.5 Continuous Probability Distributions

Deterioration models describe a random time-dependent phenomenon, with each transition between condition states having a time delay. The value of the time delay is sampled from a probabilistic time distribution. There are a plethora of potential distributions one can use although, in this review, two are considered: the Weibull and the Exponential distributions. Before considering the distributions themselves, a few concepts should be defined.

Time is a continuous variable and this is reflected in the distributions of time represented by a continuous probability distribution. A Cumulative Distribution Function (CDF), $F(t)$, is defined as the probability that a random variable T, assumes a value, less than or equal to the specific value of t,

$$F(t) = P(T \leq t), \tag{2.2.21}$$

where $F(t)$ is a probability such that

$$0 \leq F(t) \leq 1. \tag{2.2.22}$$

Weibull Distribution

The Weibull Distribution, named after Waloddi Weibull, is a continuous probability distribution and it is a widely used lifetime distribution in reliability engineering (ReliaSoft, 2020). The Weibull Probability Distribution Function (PDF) can have up to three input parameters: η, the scale parameter, β, the shape parameter and γ, the location parameter (Andrews and Moss, 2002). Thus, the 3-parameter Weibull PDF is given by:

$$f(t) = \frac{\beta}{\eta}\left(\frac{t-\gamma}{\eta}\right)^{\beta-1} e^{-\left(\frac{t-\gamma}{\eta}\right)^{\beta}} \tag{2.2.23}$$

where

$$\begin{aligned} f(t) &\geq 0, \\ t &\geq \gamma, \\ \beta &> 0, \\ -\infty < \gamma &< +\infty. \end{aligned} \tag{2.2.24}$$

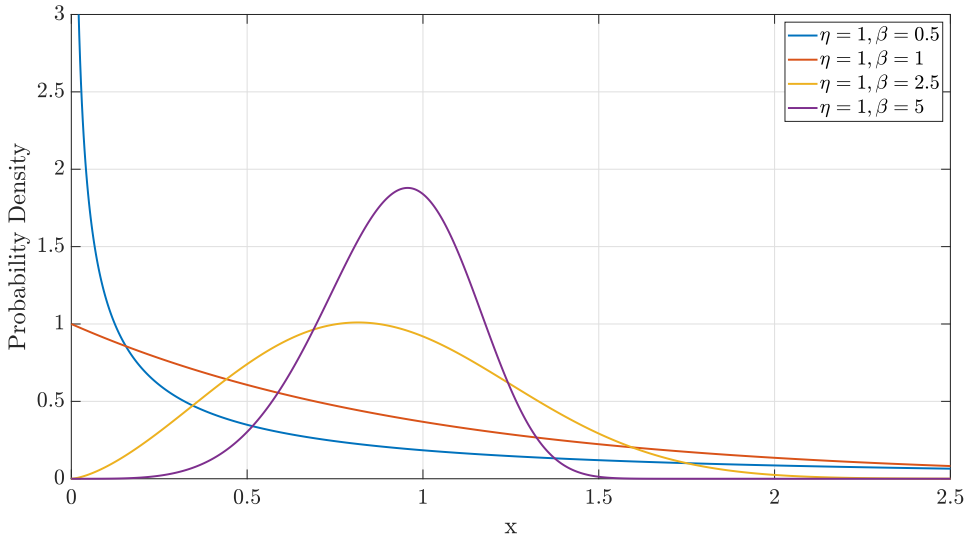

Figure 2.5: Weibull probability density function, with varying shape parameter values.

If the location parameter, γ, is set to zero, then the 2-parameter Weibull PDF is given by,

$$f(t) = \frac{\beta}{\eta}\left(\frac{t}{\eta}\right)^{\beta-1} e^{-\left(\frac{t}{\eta}\right)^{\beta}}. \tag{2.2.25}$$

See Figure 2.5 for an example plot of the Weibull PDF.

Finally, the shape parameter provides an indication of the rate of the hazard. Thus, if $\beta < 1$, the hazard rate is decreasing, $\beta = 1$, the rate is constant and $\beta > 1$ the hazard rate is increasing (Le and Andrews, 2015).

The CDF of the Weibull distribution can be obtained by integrating the PDF,

$$F(t) = 1 - e^{-\left(\frac{t}{\eta}\right)^{\beta}}, \tag{2.2.26}$$

where $F(t)$ is the CDF of the Weibull distribution. Random times, t, can be sampled from a rearrangement of the CDF and sampling a random number,

$$\begin{aligned} X &= 1 - e^{-\left(\frac{t}{\eta}\right)^{\beta}}, \\ e^{-\left(\frac{t}{\eta}\right)^{\beta}} &= 1 - X, \\ \left(\frac{t}{\eta}\right)^{\beta} &= -\ln(1-X), \\ t &= \eta[-\ln(1-X)]^{\frac{1}{\beta}}. \end{aligned} \tag{2.2.27}$$

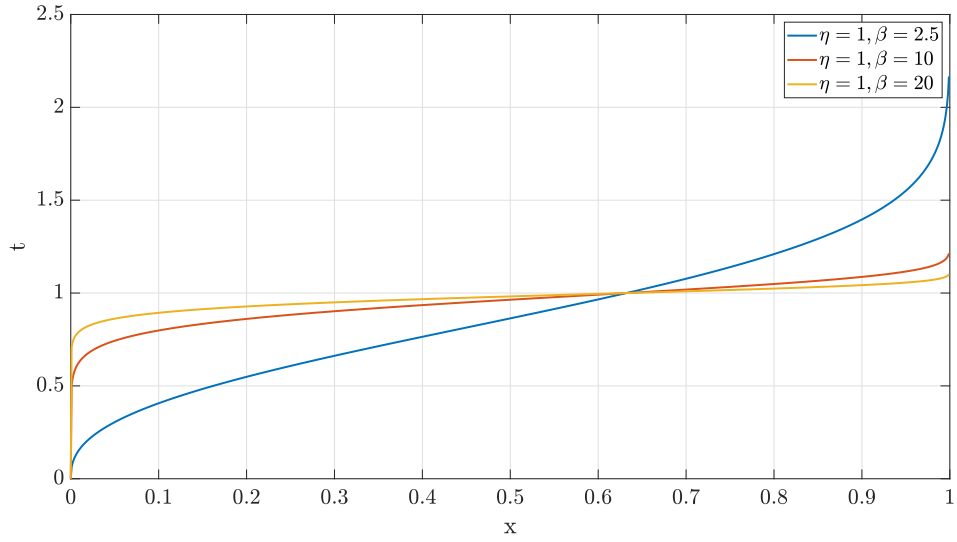

Figure 2.6: Random time values sampled from Weibull distributions.

X is a sampled random number from the uniform distribution over $[0, 1]$, and thus $(1 - X)$ must be also, hence a random time t can be defined by the following,

$$t = \eta[-\ln(X)]^{\frac{1}{\beta}}. \tag{2.2.28}$$

Random time samples from example Weibull distributions are shown in Figure 2.6.

Exponential Distribution

The exponential distribution is another continuous probability distribution that outlines the progression of continuous and independent events at a constant average rate. Furthermore, the exponential distribution is again a commonly used distribution in reliability engineering models (Andrews and Moss, 2002).

The exponential distribution can be shown to be a special case of the Weibull distribution, where the shape parameter, $\beta = 1$. Thus, considering (2.2.23) and defining $\beta = 1$, one obtains the 2-parameter exponential PDF,

$$f(t) = \lambda e^{-\lambda(t-\gamma)} \quad f(t) \geq 0, \lambda \geq 0, t \geq \gamma. \tag{2.2.29}$$

As the exponential PDF has only one shape, there is no shape parameter. The 1-parameter exponential PDF is obtained by setting $\gamma = 0$ which results in,

$$f(t) = \lambda e^{-\lambda t}. \tag{2.2.30}$$

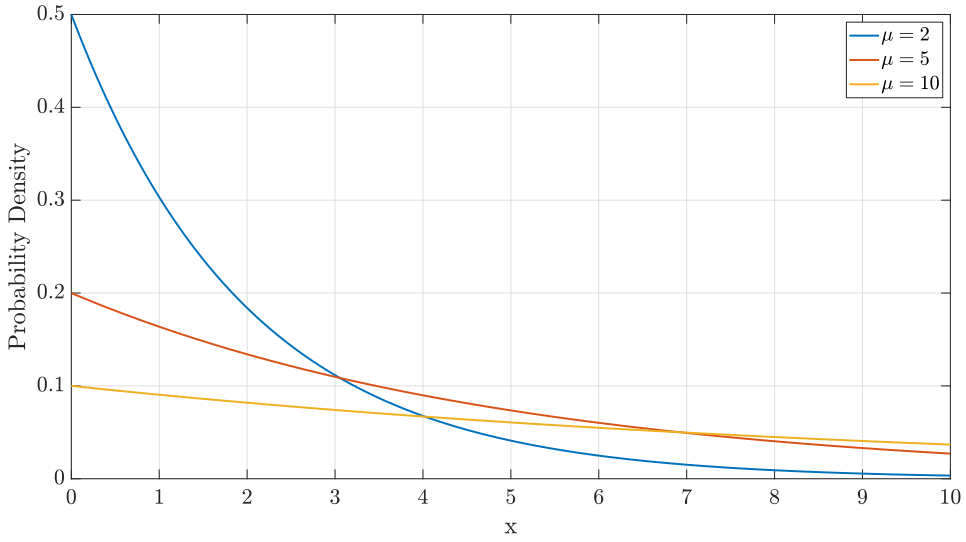

Figure 2.7: Exponential probability density function, with varying μ values.

Example exponential PDF plots are shown in Figure 2.7. The CDF of the exponential distribution is given by

$$F(t) = 1 - e^{-\lambda t}, \tag{2.2.31}$$

where $F(t)$ is the CDF of the exponential distribution. For the 1-parameter exponential distribution it can be shown that

$$\lambda = \frac{1}{\mu}, \tag{2.2.32}$$

where μ is the mean time between failures, and thus the CDF of the exponential distribution can be expressed as,

$$F(t) = 1 - e^{-\frac{t}{\mu}}. \tag{2.2.33}$$

Again, consider a random number X, uniformly distributed over the interval [0, 1] and equate it to $F(t)$,

$$X = 1 - e^{-\frac{t}{\mu}} \tag{2.2.34}$$

with rearrangement, the sample time to failure can be expressed as,

$$t = -\mu[\ln(X)]. \tag{2.2.35}$$

Random time samples from example exponential distributions are shown in Figure 2.8.

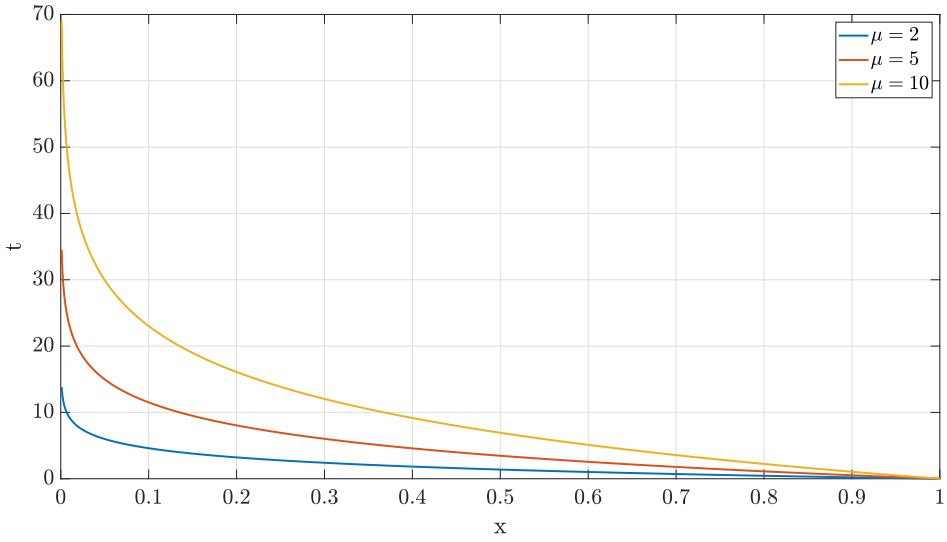

Figure 2.8: Random time values sampled from exponential distributions.

Bathtub curve

In reliability engineering, the bathtub curve alludes to the concept that the hazard rate can be observed to comprise three distinct phases in an asset life cycle (Andrews and Moss, 2002). The three phases are:

- **Phase I - Burn-in** - The hazard rate reduces in value over time. The reduction in rate is attributed to weak components failing early in the life cycle of a system.
- **Phase II - Useful-life** - The hazard rate remains relatively constant during this phase of a life cycle.
- **Phase III - Wear-out** - The hazard rate increases in value over time. The increase in hazard rate is attributed to components starting to wear out or age.

The dynamics of each phase are shown in Figure 2.9. If the hazard rate is constant, it is also referred to as failure rate and is commonly characterised by the exponential distribution. However, for Phase I and III where the hazard rate changes over time, a different characterisation is required. A commonly used probability distribution to capture the non-constant hazard rate is the Weibull distribution.

It is critical that any non-constant hazard rate is incorporated into a deterioration model to provide accurate reliability predictions. When performing a life cycle analysis it is critical a non-constant hazard rate is incorporated as it can have huge consequences on the development of asset management strategies. Depending on what phase an asset is in during its life cycle, the asset may require different inspection regimes, maintenance intervention strategies and/or asset monitoring.

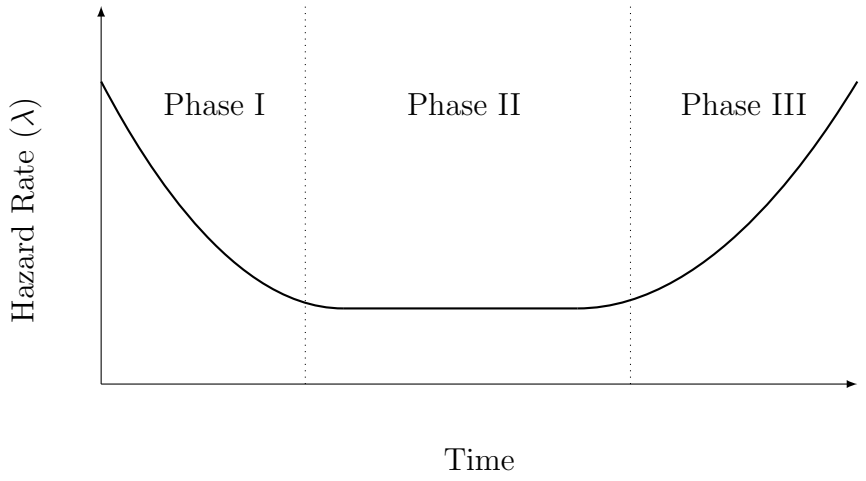

Figure 2.9: Bathtub curve depicting the three phases of the hazard function during an asset life cycle.

2.2.6 Coloured Petri Nets

Traditionally PNs can be classified as high level PNs or low level PNs, with high level PNs being a combination of PNs and programming languages (Jensen, 1997; Jensen and Krietensen, 2009). Coloured Petri Nets (CPNs) are a graphical language for the construction of concurrent system models and analysing the associated properties and belong to the high level PN class. CPNs are a discrete-event modelling language combining the capabilities of PNs with the capabilities of a high level programming language.

CPNs have the same defined rules associated to the enabling and firing of transitions as PNs but now allow for more than one token type to be defined. Whilst the word colour is used, it is merely meant that each token represents a different data value, and is thus typically represented by a different colour on a graph.

An example CPN is shown in Figure 2.10, denoting the markings before and after the firing of $T1$. For $T1$ to be enabled it requires that $P1$ contains at least 1 black token and 1 red token with other token colours being irrelevant to enabling $T1$. Upon $T1$ being enabled and firing, it produces 2 black tokens in $P2$ and one blue token and one red token in $P3$.

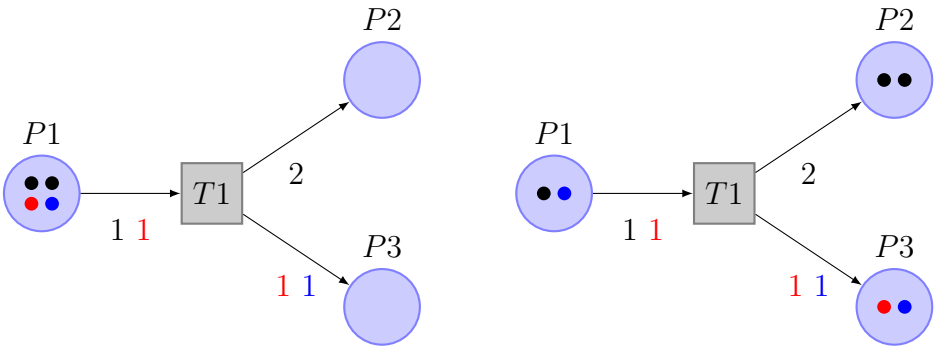

(a) Example Coloured Petri net before firing

(b) Example Coloured Petri net after firing

Figure 2.10: An example Coloured Petri net with (a) showing the net before it fires and (b) showing the net after firing T1.

An advantage of CPNs over traditional PNs is that it can be used to reduce the size of a net or the required instances of the net to model a whole system, as more information can be stored in the token as well as being able to be manipulated by transitions.

2.2.7 Petri Net Analysis

To analyse PNs that include transitions other than instantaneous or fixed time transitions, it is common to use Monte Carlo methods. Monte Carlo methods are a computational technique for performing random sampling to determine numerical results for problems. Monte Carlo methods have been applied to a wide range of problems including deterministic problems that require numerical integration, as well as for executing simulations that require random samples from a probability distribution (Kroese et al., 2014).

When analysing a PN, the marking of the net at particular time points during

a simulation period will be of interest. Monte Carlo analysis uses sample means to estimate the population or true mean (Dunn and Shultis, 2011). Thus, the sample mean for each place marking is computed to determine the true marking of each place in the PN. The sample mean of a function z of a random variable x is an estimate of the true mean $\langle z \rangle$,

$$\hat{z} = \frac{1}{N} \sum_{i=1}^{N} z(x_i), \tag{2.2.36}$$

$$\hat{z} = \langle z \rangle, \quad \text{for } N \to \infty. \tag{2.2.37}$$

The sample mean is determined by the execution of random sampling, which results in obtaining a large number of random samples of output results from a PN model (Thomopoulos, 2013). The random sample requires a large stream of random numbers which are generated using a Pseudo-Random Number Generator (PRNG) algorithm (Kroese et al., 2011). PRNG algorithms are included in many programming languages, although caution is required when implementing a simulation using a parallel solution, to ensure the independence of the sequence of random numbers for each computational thread (Tan, 2002).

One of the limitations of PNs is the required computational expense to execute Monte Carlo simulations. There are several studies that have introduced techniques to reduce the computational expense of analysing PNs (Naybour et al., 2019; Neumann et al., 2019), however they do not typically generalise well for all net designs.

There are several publicly available PN software packages, (Bonet and Lladó, 2007; Dingle and Knottenbelt, 2009; Freytag and Sänger, 2014; Zimmermann, 2017) with one of the most popular implementations being CPN Tools (Jensen et al., 2007). Despite international standards existing for PN software design and file exchange (ISO/IEC, 2010, 2011), there are still notable discrepancies in simulation implementations and modelling functionality.

2.3 Bayesian Networks

Conditional probability is the notion that a probability of an event occurring is determined by the contextual information of another event i.e. it describes the probability of an event occurring based on *a priori* knowledge of conditions that may be related to the event. Bayes' theorem (Bayes, 1763) presents the formulation that describes how to update the probability of one event given information regarding another, and can be expressed as,

$$P(A|B) = \frac{P(B|A)P(A)}{P(B)} \tag{2.3.38}$$

where A and B are events and $P(B) \neq 0$.

Bayesian Belief Networks (BBN) are a probabilistic graphical model based on Bayes' theorem, with Pearl (1988), and Jensen (2001) often cited as authoritative literature. BBNs have been shown to be a useful method in reliability analysis, risk assessment and maintenance studies (Hossain et al., 2019; Langseth and Portinale, 2007; Reeves et al., 2018; Weber et al., 2012), particularly for their ability to incorporate expert knowledge.

2.3.1 Definition

BBNs are composed of a set of nodes and a set of arcs: the set of nodes, $\mathbf{X} = \{X_1, \ldots, X_n\}$, denotes n variables and the set of arcs are directed causal relationships between the variables. A Directed Acyclic Graph (DAG) is used to visualise the causal relationships between variables and the condition probabilities for variables given their causal relationships are tabulated in a Conditional Probability Table (CPT) (Jensen, 2001; Pearl, 1988).

The node that is at the start of an arc is known as a parent node and a node at the end of an arc is known as a child node. A node that has no parent nodes is known as a root node, a node that has no child nodes is known as a leaf node and a node with both parent nodes and child nodes is known as an intermediate node.

In general, the chain rule, or general product rule, can be used to determine the

joint probability distribution for a set of n variables,

$$P(X_1 \cap \cdots \cap X_n) = \prod_{k=1}^{n} P(X_k | \bigcap_{j=1}^{k-1} X_j). \tag{2.3.39}$$

However, BBNs encapsulate parent-child relationships, so the joint probability distribution can be calculated using recursive factorisation,

$$P(X_1 \cap \cdots \cap X_n) = \prod_{j=1}^{n} P(X_j | pa(X_j)), \tag{2.3.40}$$

where: $pa(X_j)$ denotes the set of all variables X_i, such that there is an arc from node i to node j in the graph (Pearl, 1988).

2.3.2 BBN Example

The BBN shown in Figure 2.11 has five nodes to denote the five discrete random variables $\mathbf{X} = \{X_1, X_2, X_3, X_4, X_5\}$. The joint probability distribution for the example is,

$$P(X_1, X_2, X_3, X_4, X_5) = P(X_5|X_4) \cdot P(X_4|X_2, X_3) \cdot P(X_2|X_1) \cdot P(X_3) \cdot P(X_1) \tag{2.3.41}$$

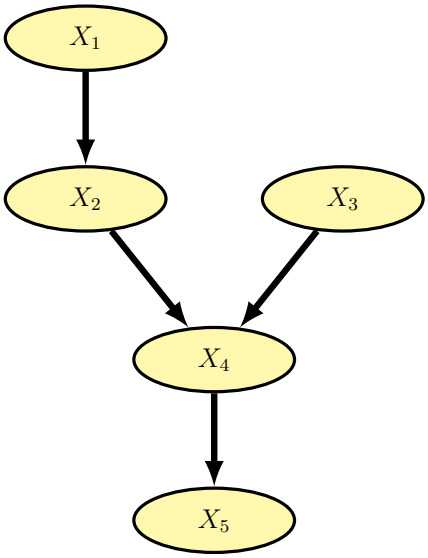

Figure 2.11: An example five node BBN.

Marginalisation by Variable Elimination

The marginal probability of a variable assuming a particular value, is the probability of a particular variable assuming a particular value independent of the values other variables have assumed. To calculate the marginal probability for a variable, the joint probability distribution can be restated for marginalisation by variable elimination. Marginalisation is a distributive operation over combinations of local joint probabilities: a variable's marginal probability can be obtained from marginalising the global joint probability distribution by marginalising the local variable CPTs (Fenton and Neil, 2013).

For example, if one wanted to determine the marginal probability for $P(X_2)$, marginalisation gives,

$$P(X_2) = \sum_{X_1,X_3,X_4,X_5} P(X_1)P(X_3)P(X_2|X_1)P(X_4|X_2,X_3)P(X_5|X_4). \tag{2.3.42}$$

However, as marginalisation is a distributive operation over combinations it can be restated as,

$$P(X_2) = \left(\sum_{X_1} P(X_1)P(X_2|X_1)\left(\sum_{X_4}\left(\sum_{X_3} P(X_3)P(X_4|X_2,X_3)\left(\sum_{X_5} P(X_5|X_4)\right)\right)\right)\right). \tag{2.3.43}$$

Belief Propagation

The observation of any of the variables can provide evidence and BBNs have the capability to update the marginal probabilities accordingly, i.e. belief propagation. Consider $\mathcal{H}$ as the set of variables that are of interest, $\mathcal{E}$ as the set of observed variables given evidence and $\mathcal{S}$ as the set of variables which are not in $\mathcal{H}$ or $\mathcal{E}$, then

$$P(\mathcal{H}|\mathcal{E}) = \frac{P(\mathcal{E}|\mathcal{H})P(\mathcal{H})}{P(\mathcal{E})} = \frac{\sum_{\mathcal{S}} P(\mathcal{H},\mathcal{E},\mathcal{S})}{\sum_{\mathcal{H}}\sum_{\mathcal{S}} P(\mathcal{H},\mathcal{E},\mathcal{S})}. \tag{2.3.44}$$

Consider the BBN as shown in Figure 2.11, with each variable being a boolean. Using (2.3.44), the probability of $X_4 = true$ given that $X_2 = true$ is

$$P(X_4 = t|X_2 = t) = \frac{\sum_{X_1,X_3} P(X_1, X_2 = t, X_3, X_4 = t)}{\sum_{X_4}\sum_{X_1,X_3} P(X_1, X_2 = t, X_3, X_4)}. \tag{2.3.45}$$

An example of propagating evidence backwards is, if $X_4 = true$ the probability of $X_3 = true$ is

$$P(X_3 = t|X_4 = t) = \frac{\sum_{X_1,X_2} P(X_1, X_2, X_3 = t, X_4 = t)}{\sum_{X_3}\sum_{X_1,X_2} P(X_1, X_2, X_3, X_4 = t)}. \tag{2.3.46}$$

2.3.3 Dynamic Bayesian Networks

A BBN is useful for modelling a system of variables and their conditional dependencies, where the system is in a static state. Dynamic Bayesian Networks (DBN) are an extension of the BBN formalism which introduces additional mechanisms for modelling the conditional dependencies between variables temporally (Dagum and Galper, 1995; Dagum et al., 1992; Dean and Kanazawa, 1989; Murphy, 2002).

Consider a pair $(B_1, B_{\rightarrow})$, where B_1 is a BBN which defines the prior $P(\mathbf{X}^1)$ and $B_{\rightarrow}$ is a two slice temporal Bayes net (2TBN) which defines $P(\mathbf{X}^t|\mathbf{X}^{t-1})$ as a DAG and is expressed as,

$$P(\mathbf{X}^t|\mathbf{X}^{t-1}) = \prod_{i=1}^{N} P(X_i^t|Pa(X_i^t)), \tag{2.3.47}$$

where X_i^t is the i'th node at time t, N is the number of nodes on a time slice and $Pa(X_i^t)$ are the parents of X_i^t (Murphy, 2002).

Each discretisation of time is known as a time slice. In a 2TBN, the nodes featuring in the first time slice do not have any parameters associated with them, but the nodes in the second time slice of a 2TBN have a CPT associated with them, which defines $P(X_i^t|Pa(X_i^t))\ \forall i, t > 1$.

Typically, the parents of a node, i.e. $Pa(X_i^t)$, will be either on the same time slice or the previous time slice, although this is primarily for notational simplicity and is not strictly required. Consequently, 2TBN typically assume the Markov property, i.e. the probability distribution for a future time step is dependent on the current time step and is independent of past events. Moreover, any defined CPTs are time invariant: CPTs are not functions of time and the topology of the net remains consistent across different time steps (Murphy, 2002).

A DBN can be obtained by "unrolling" a 2TBN until we have T time slices. The

joint probability distribution can be calculated using recursive factorisation,

$$P(X_1^1, X_2^1, \ldots, X_{n-1}^T, X_n^T) = \prod_{t=1}^{T} \prod_{j=1}^{n} P(X_j^t | pa(X_j^t)), \tag{2.3.48}$$

DBN models are an effective means for evaluating the reliability and resiliency of engineering systems (Kammouh et al., 2020), and can be useful for three distinct tasks: predicting the value of variables at future time steps, predicting the value of unobserved variables for the current time step and predicting the value of unobserved variables in previous time steps. Moreover, DBNs can be used as a generalisation of other temporal state-space models including: hidden Markov models (Rabiner, 1989) and Kalman filter models (Kalman, 1960).

2.3.4 DBN Example

Consider three variables α, β and γ, where γ has a conditional dependency to both α and β. The relationship between these three variables could be expressed as a BBN as shown in Figure 2.12.

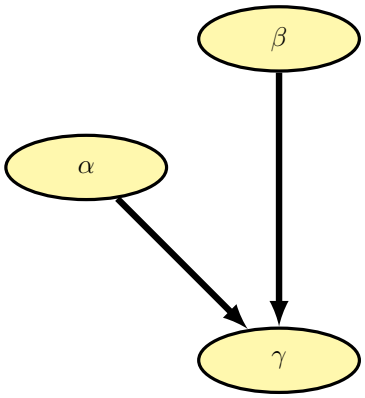

Figure 2.12: Example BBN model for α, β and γ variables.

Now consider that α, β and γ evolve temporally and γ retains its dependence to α and β. If the state of each of the processes is known for a given time, the state of each process for a future increment of time τ can be determined using a 2TBN, see Figure 2.13.

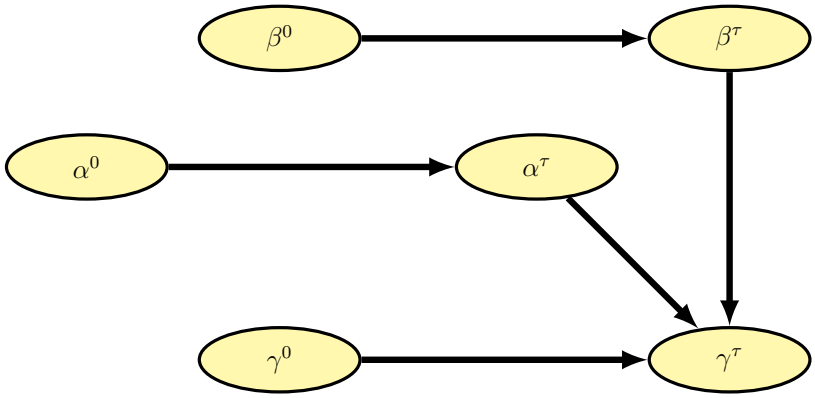

Figure 2.13: Example 2TBN model for α, β and γ processes.

The probability of the state of each of the three variables at time T can be determined by DBN which requires the "unrolling" of the discrete instances of the 2TBN until T is reached. The DBN structure is shown in Figure 2.14. The solid black lines in Figure 2.14 show the causal relationship required to evaluate α, β and γ at time t. The dashed grey lines show the causal relationships between the variables on an inter- and intra- time slice basis.

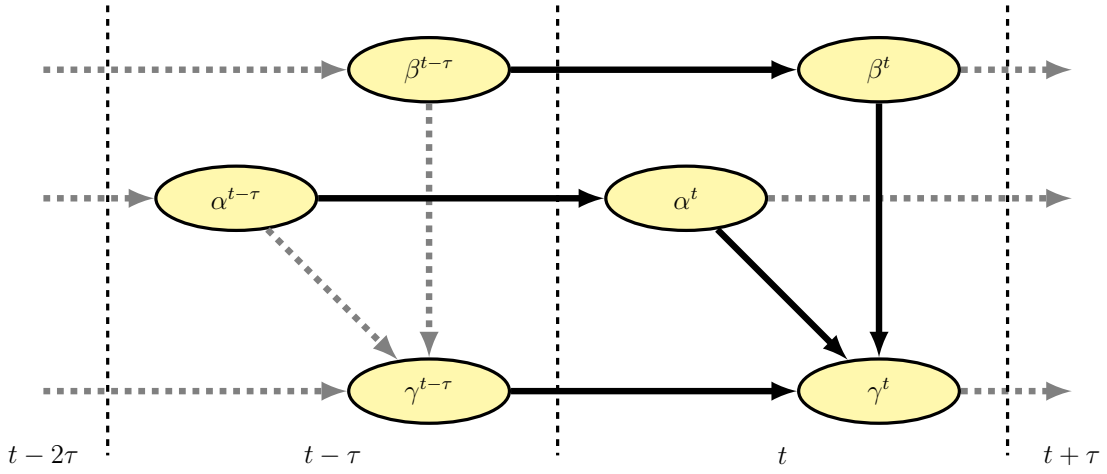

Figure 2.14: Example DBN model for α, β and γ processes.

Alternatively, a DBN model can be expressed as a BBN model by treating each time step's instance of a variable as its own distinct node. Figure 2.15 shows the example DBN model from $t = t_0$ to $t = t_3$.

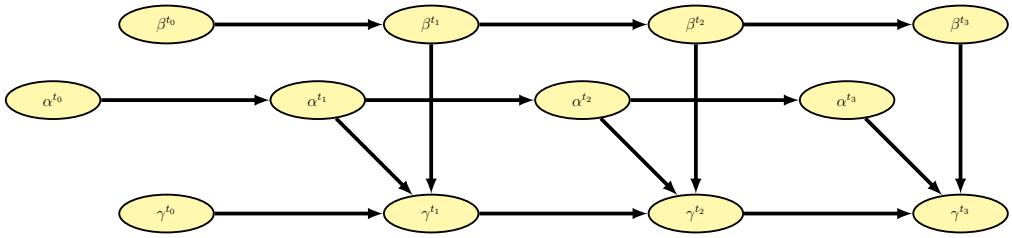

Figure 2.15: Example DBN model unrolled as a BBN model until $t = t_3$.

2.4 Summary of Methodologies

This chapter presented an overview of several commonly employed methodologies for bridge deterioration modelling that will be used in this thesis: Markov models, PNs, BBNs and DBNs. Each of the presented methods can be used for state based models, however there are several differences between them. Markov models are relatively simple to implement computationally, and discrete or continuous time can be used to model a process, however they assume the memoryless property and can suffer from state explosion. PNs offer more flexibility when developing a model of a system and additional functionality can be incorporated by using different transition types. However, PNs are commonly resolved using Monte Carlo simulation which is computationally expensive. BBN/DBN models can be resolved analytically and offer the ability to include conditional relationships between different variables, however the methods require discretisation of time alongside being time invariant.

All of the methods presented can be characterised graphically which facilitates the understanding of any developed model. However, a PN graphical implementation is particularly useful as the model can be visualised at various stages of a process by tracking the position of the tokens in the net.

Determining the most appropriate method requires a well defined problem and an understanding of the limitations that the calibration data may have. Consequently, further analysis of the advantages and limitations of each method is deferred to Chapter 3 where a review of bridge asset management is conducted.

Chapter 3

Bridge Asset Management

3.1 Introduction

Infrastructure investment requires efficient resource allocation to maximise the impact from the finite investment that infrastructure asset managers can make. Bridge management can be defined as the procedural responsibility of a portfolio of bridges from conception to the end of their safe and useful life (Ryall, 2010). Many tasks associated with the maintenance of bridges can be more efficiently coordinated and implemented by following good bridge management techniques. Examples of these tasks are:

- Maintenance of an inventory of the bridge stock.
- Regular inspections for the assessment of bridge condition and strength.
- Prioritisation and scheduling of bridge interventions.
- Optimised resource allocation with consideration of organisational priorities.
- Safety and capability assessments.

A life cycle analysis of bridge condition and intervention strategy is commonly employed as an effective means to determine the optimal allocation of resources for interventions across an asset portfolio. A critical component required to perform a life cycle analysis of bridges is performance evaluation and prediction. In particular,

the degradation of bridge condition and performance should be well understood. The structural performance of bridges can be defined at many different hierarchical asset levels including, cross-section, component, whole structure and network (Frangopol et al., 2017).

The American Society of Civil Engineers (ASCE) recently identified that technical capabilities in managing risk and uncertainty were increasingly vital to the practising civil engineer, with the ASCE Technical Council drafting a collection of state-of-the-art papers on "*lifecycle performance assessment and risk-informed decision making in structural engineering* " (Biondini and Frangopol, 2016; Ellingwood and Frangopol, 2016; Ghosn et al., 2016; Lounis and McAllister, 2016; Sánchez-Silva et al., 2016).

The purpose of this chapter is to outline the existing literature for different indicators used for bridge performance evaluation and the stochastic methods that can be employed to facilitate network level decision making. The chapter is organised as follows: Section 3.2 provides a review of the different indicators to evaluate bridge performance, with a particular focus on network level decision making. Section 3.3 considers bridge asset management and the systems used by network asset managers. To assist in strategic decision making, deterioration models are developed to provide performance predictions and to identify potential intervention requirements. The data available for model calibration is discussed in Section 3.4. Different deterioration models that exist in literature are evaluated in Section 3.5.

3.2 Performance Evaluation

Bridge managers aim at finding the best balance between structural reliability, risk, utility, sustainability and life-cycle cost (Frangopol et al., 2017). These performance indicators can be defined at different scales and different levels of detail. The primary focus of a bridge asset manager is to ensure that the bridge provides a safe load capability during its service life. The assessment of structural reliability and risk facilitate the evaluation of safety. Reliability analysis assesses the probability of failure of structures, or structural components but unlike risk analysis, reliability

analysis does not account for the consequences of failure.

Aside from safety, an asset manager will have several other constraints and demands from network stakeholders, and thus the remainder of this section will consider additional performance indicators to assess life cycle cost, utility and sustainability.

3.2.1 Structural Reliability

One key objective of bridge managers is to ensure the safety of the infrastructure and its users. Structural safety has been an area of intense research for decades and has been widely applied to the safety assessment of existing bridges (Ang and Tang., 2007; Ghosn et al., 2016; Ghosn and Moses, 1986; Jacinto et al., 2016; Melchers and Beck, 2018; Thoft-Christensen and Baker, 1982). Although the generalised use of structural reliability for bridge assessment is too complex and expensive to be applied at network level, some of the key properties are relevant to develop simpler safety indicators.

The fundamental reliability problem can be expressed in terms of the loading, material properties and degradation mechanisms as,

$$M(t) = R(t) - S(t), \tag{3.2.1}$$

where $M(t)$ is a random variable describing the time-dependent margin of safety (also known as the limit state function), $R(t)$ denotes the strength of the structure (also known as its resistance) and $S(t)$ is the effect of applied loads on the structure. Thus, a structure has not failed as long as $M(t) \geq 0$. At the instance where $R(t) = S(t)$ i.e. $M(t) = 0$, the structure has reached the limit state and failure is imminent.

Consider a structural component has a resistance R and load effect S, and their respective PDFs f_R and f_S. The probability that S does not exceed R, $P(R \geq S)$ denotes the reliability of the structural component. The time-variant probability of failure $p_F(t)$ is,

$$p_F(t) = P(M(t) \leq 0) = \int_0^\infty \int_0^s f_{R,S}(t)\mathrm{d}r\mathrm{d}s, \tag{3.2.2}$$

where $f_{R,S}(t)$ is the joint PDF of $R(t)$ and $S(t)$. Moreover, the reliability index can be expressed as,

$$\beta(t) = \Phi^{-1}(1 - p_F(t)) = -\Phi^{-1}(p_F(t)), \tag{3.2.3}$$

where $\Phi^{-1}(t)$ is the inverse of the standard normal CDF. The relationship in values between the failure probability and reliability index are shown in Table 3.1.

Table 3.1: Value relationship between p_F and β.

p_F	10^{-1}	10^{-2}	10^{-3}	10^{-4}	10^{-5}	10^{-6}	10^{-7}
β	1.3	2.3	3.1	3.7	4.2	4.7	5.2

EN 1990 (CEN, 2010) charts outs target reliability index values for the ultimate limit state of new structures, for three different consequence classes, which incorporate the consequence to human life and/or economic, social and environmental consequences. The reliability index values for each class are shown in Table 3.2. The target levels stated in EN 1990 are primarily for newly constructed structures, whereas ISO 2394 (International Organization for Standardization, 2015) provides target levels for a structure during its service life. Additionally the Joint Committee of Structural Safety created the probabilistic model code as "*a first attempt to put together in a consistent way some of the rules, regulations, and explanations that are necessary for the design of new structures, or the assessment of existing ones from a probabilistic point of view*" (JCSS, 2001).

Table 3.2: Recommended minimum values for reliability index.

Consequence Class	Consequence of Failure		Reliability Index (β_n)	
	Human Life Consequence	Economic Consequence	$t_{ref} = 1$ year	$t_{ref} = 50$ years
1	Low	Small	4.2	3.3
2	Medium	Considerable	4.7	3.8
3	High	Very Great	5.2	4.3

The evaluation of (3.2.2) is a robust application of probability theory. Theoretically, there is the scope to apply it across a vast asset portfolio. However, when

practically evaluating the expression for assets across an entire network, there are limited capabilities of acquiring realistic values for R and S from sample data.

Bridges are heterogeneous assets each with its own distinct configuration of structural components. To model the reliability of a bridge, the bridge is assumed to be a configuration of bridge components, where the components are assumed to be a system of series, parallel or a combination of series and parallel components (Hendawi & Frangopol 1994).

Finite Element Analysis (FEA) can also be used to evaluate the structural reliability of a bridge system. FEA can be used to analyse different responses such as stress, displacement and bending moment, which can be compared with the strength of materials or members. However, to perform sufficient samples of the structure's random variables to obtain an appropriate solution makes the computational cost prohibitively high to be practical. Whilst alternative methods do exist, ultimately the computational overhead is still not practical for life cycle decision making at the network level and proxies for structural reliability are commonly used.

Semi-Probabilistic Analysis

A simpler approach to the design and assessment of structures is based on the concept of partial safety factors. In this approach, the probability of failure is not explicitly computed. The probability of failure is limited to acceptable values by comparing a design strength with a design effect of actions. Each of these are computed using the mean values of variables, if their variability is small, or pessimistic estimates, if variability is significant. These pessimistic (e.g. design) values are computed based on pessimistic percentile of properties, affected by partial safety factors.

To avoid structural failure, the designed load bearing capacity R_d must be greater than the design value for bridge strength S_d, i.e. $R_d \geq S_d$. The probability of $R_d \geq S_d$ being adhered to can be calculated using the real mean properties and/or use a set of conservative properties as if they were real.

Partial safety factors are used in limit state design which ensures the survivability of a bridge by underestimating bridge strength and overestimating the applied

load. The semi-probabilistic approach requires that there is a low probability of exceedance of $S \geq S_d$ and a high probability of exceedance for $R \geq R_d$ such that there is a low probability of failure i.e. $P(R < S) \rightarrow 0$. If there is an overlap between the distributions for S and R, the probability of failure is larger than zero. The area of possible failure is shown as the shaded blue area in Figure 3.1.

When calibrating partial safety factors, the objective is to determine factors that ensure that a certain threshold of reliability is achieved with a high degree of confidence. Although, this design philosophy will result in conservative assessments, it requires much less data and computational cost, making them feasible for critical structures. Semi-probabilistic analysis is outlined in several international standards including EN 1990 and ISO 2394.

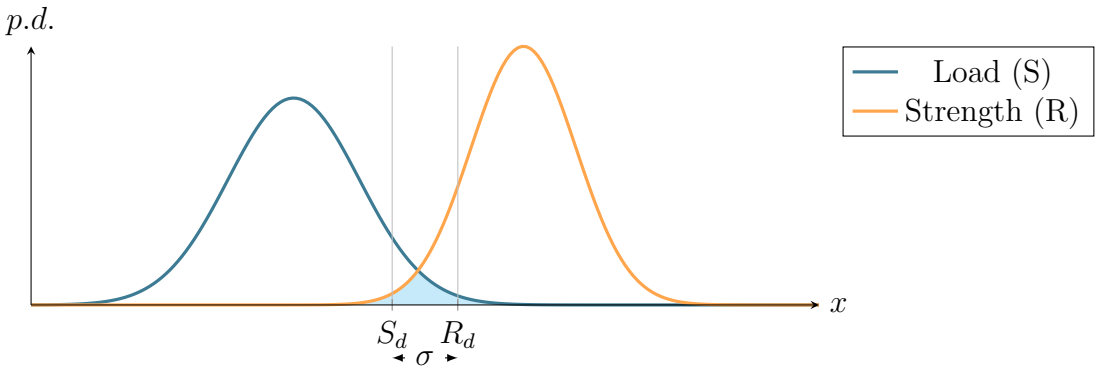

Figure 3.1: Semi -probabilistic analysis of failure probability.

Qualitative Analysis

Determining structural reliability for a portfolio of bridges in operation is a challenging task. Thus, to evaluate the performance of a structure or its constituent components, visual examination records are commonly used. Particular condition states used to record asset condition are designated as a threshold to trigger further investigation or intervention, namely structural assessment using partial safety factors. Quantifying consequences is an extremely difficult endeavour, nonetheless for decision making it is common to define an acceptable probability of failure based on consequence class. Moreover, by qualitative assessments such as visual inspection, it is possible to assign thresholds to instigate particular actions when there is

a perceived level of risk deemed by engineering judgement. Additionally, if the consequence of failure remains fixed, the urgency of intervention or investigation being executed can be defined for different probabilities of failure. Measures have been developed to ascertain whether investment is required to intervene on an asset to save human life (Nathwani et al., 1997; Pandey and Nathwani, 2004; Pandey et al., 2006).

An example of a consequence indicator is the Health and Safety Executive's (HSE) *Tolerability of Risk Framework*, which considers risk on a scale which can be *"measured by individual risk and the societal concerns it engenders"* (Health and Safety Executive, 2001). The framework has three regions of risk; "*acceptable*", "*tolerable*" and "*unacceptable*". The threshold between tolerable and unacceptable is known as the Basic Safety Limit. The HSE defines the Basic Safety Limit in terms of societal outcomes.

An additional example is given by Network Rail which defined the Basic Safety Limit in terms of particular condition states for each asset sub-group using engineering expertise and a Failure Modes and Effects Analysis (FMEA), see Figure 3.2. For different asset sub-group a intervention/investigation trigger has been defined to ensure that the asset sub-group condition is equal or greater than the defined Basic Safety Limit. For underline and overline bridges, the Basic Safety Limit at Network Rail is expressed in terms of a Bridge Condition Marking Index (BCMI) score. BCMI is a numeric score between 0 and 100, where 100 indicates perfect condition. A BCMI score for a whole structure is an aggregated score of its constituent components' scores. A BCMI that is lower than its specified Basic Safety Limit thresholds will be identified as a potential safety risk and reviewed by a suitably qualified structural engineer, to determine if a priority intervention is required. Condition based intervention trigger levels are also defined with consideration of the criticality of the route a bridge is situated on, to maintain service performance and to reduce safety risk by intervening earlier (Network Rail, 2014b).

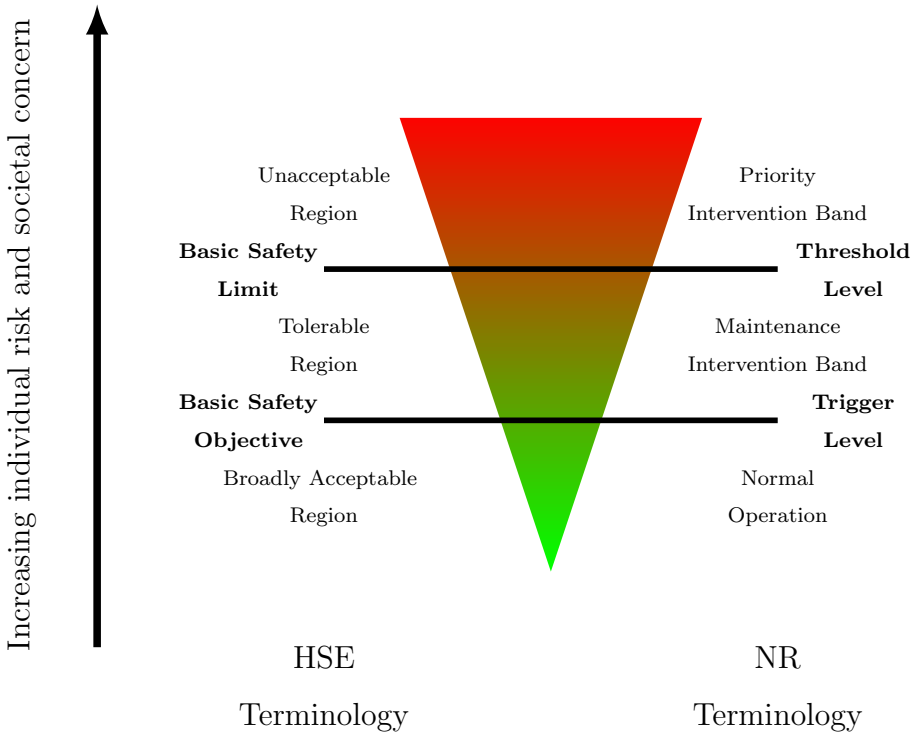

Figure 3.2: Risk Framework - Health and Safety Executive and Network Rail.

3.2.2 Risk Analysis

For asset management purposes, risk analysis is used to compare the risk of a structure failing with the cost of improving its safety. Risk can be evaluated as the product of the probability of failure by its consequences.

Consider a bridge that is exposed to n mutually exclusive hazard events H_i. The probability of structural failure can be expressed as,

$$P_F(t) = \sum_{i=1}^{n} P(F|H_i^t) \cdot P(H_i^t), \tag{3.2.4}$$

where $P(F|H_i^t)$ is the conditional probability of failure occurring given a particular hazard occurring and $P(H_i^t)$ is the probability of hazard H_i occurring at time t (Ellingwood, 2001). The conditional probability of failure for each hazard event can be computed using (3.2.2) for the postulated structural consequence of the hazard event.

Risk is the quantification of the consequence of events generated by the occurrence of hazardous events. The total risk of structural failure was expressed by

Ellingwood (2005) as,

$$\mathcal{R}(t) = \sum_{i=1}^{n} C_m(t) \cdot P(F|H_i^t) \cdot P(H_i^t), \tag{3.2.5}$$

where $\mathcal{R}(t)$ is the risk at time t, $C_m(t)$ is the consequence of structural failure at time t. From these equations, there are three potential actions for an asset owner to reduce the risk:

- Design and maintain the structural asset to reduce the $P(F|H_i)$ term.
- Minimise the likelihood of a hazard occurring such that $P(H_i) \to 0$.
- Minimise the consequences of failure by mitigation measures.

In this thesis the hazard being considered is the deterioration of the structural integrity of a bridge through the gradual development of multiple defects. A robust inspection regime alongside prompt intervention scheduling could be used to minimise the probability of a bridge being in poor condition. Additionally, preventative maintenance could also be used to minimise the hazard of structural deterioration.

If significant deterioration has occurred, the probability of structural failure can be minimised by a robust and resilient structural design that has redundancy in the design for instances of damage. Moreover, the probability of failure given deterioration can be reduced by implementing operational restrictions, such as reducing the permitted loading of the bridge, the line speed for rail traffic or bridge closure to avoid catastrophic failure. The consequence of structural failure can be minimised by ensuring that there are fast repairs upon failure and that there are alternative routes or temporary structures in place to facilitate diversion or continued service.

Several studies in literature have adopted risk-based approaches to aid bridge management. Decò and Frangopol (2011) proposed a methodology to evaluate the time-dependent total risk of a bridge under multiple hazards (e.g. live loads, corrosion, scour, and earthquakes), with several studies devoted to developing computational frameworks for risk of bridge networks under seismic activity (Decò et al., 2013; Dong et al., 2014; Shekhar and Ghosh, 2020; Shekhar et al., 2018).

An impediment to assessing risk at network level is the fragmented ownership of civil infrastructure which causes systematic discrepancies in available data for

different structures, especially when trying to incorporate local and environmental factors. In the UK, the ownership and management of bridge portfolios is distributed between many different agencies at both local and national level. Whilst Network Rail own most of the bridges that feature on the national rail network, bridges on metro rail networks are sometimes owned by the local transportation authorities, for example, Transport for London. Moreover, the road bridges associated with motorways and trunk roads are typically under the jurisdiction of Highways England, Traffic Wales and Transport Scotland, whereas other road types can be under different council jurisdictions and/or metropolitan authorities. Consequently, there is no national structures database and Middleton (2004) states that it is "*notoriously difficult to obtain reliable figures on the number of bridges in the UK*", making detailed analysis beyond asset count even more challenging.

To facilitate a more holistic risk assessment which can analyse the exposure of the bridge portfolio, assess hazards and study asset vulnerability, Pregnolato (2019) proposed a 20 point bridge taxonomy, considering road and rail bridges at risk of flooding or scour. The study exhibited the potential capabilities of having a consolidated national database for providing predictive insights into failures and disruptions. Fiorillo and Nassif (2020a) provide an example approach of incorporating a probabilistic risk analysis into network level decision modelling.

3.2.3 Life Cycle Cost

The evaluation of life cycle cost is critical to support decision during bridge management planning. An asset manager has finite resources and they are tasked with minimising the total cost to maintain the bridge system to adhere to mandated safety levels. A common expression of expected total cost during the life time of a bridge was proposed by Frangopol et al. (1997),

$$C_{ET} = C_T + C_{PM} + C_{INS} + C_{REP} + C_F, \tag{3.2.6}$$

where C_T is the initial cost of construction, C_{PM} is the expected cost of routine maintenance cost, C_{INS} is the cost of the inspection regime, C_{REP} is the expected cost of repair and C_F is the expected cost of failure. If monitoring equipment is in-

stalled on the bridge, Frangopol and Messervey (2007) proposed a revised expression for the expected total cost,

$$C_{ET}^{0} = C_{T}^{0} + C_{PM}^{0} + C_{INS}^{0} + C_{REP}^{0} + C_{F}^{0} + C_{MON}, \tag{3.2.7}$$

where the zero superscript denotes costs from (3.2.6) that are affected by monitoring and C_{MON} denotes the expected cost of the monitoring, which is given by,

$$C_{MON} = M_{T} + M_{OP} + M_{INS} + M_{REP}, \tag{3.2.8}$$

where M_T is the expected design and construction cost of the monitoring system, M_{OP} is the expected operational costs of the monitoring system, M_{INS} is the expected cost for inspecting the monitoring system and M_{REP} is the expected costs for repairing the monitoring system (Frangopol, 2011). The expected benefit, B_{MON}, of installing monitoring equipment can be calculated as,

$$B_{MON} = C_{ET} - C_{ET}^{0}. \tag{3.2.9}$$

Thus, the installation of monitoring equipment is only cost effective when

$$B_{MON} > 0. \tag{3.2.10}$$

Unless mandated by safety standards, infrastructure managers are not incentivised to install monitoring equipment across their asset portfolios, as the M_T is prohibitively high for typical structures, such that $B_{MON} < 0$. Ultimately the installation of monitoring equipment will be incremental across a network and will likely be targeted to new infrastructure or high risk infrastructure in the first instance.

3.2.4 Sustainability

The social and economics benefits of transportation networks are critical to the geographic regions they serve. However, the infrastructure must be provided in a sustainable way. Brundtland (1987) defines sustainability as *"development that meets the needs of the present without compromising the ability of future generations to meet their own needs"*. Infrastructure asset managers are not only tasked with ensuring the safe, reliable and functional operation of transportation networks

but also to do so in a sustainable way. Sustainability frameworks have been proposed that include metrics that encapsulate the social, economic and environmental concerns of the asset portfolio (Dong and Frangopol, 2016; Lundie et al., 2004).

Stein et al. (1999) proposed an array of metrics to quantify the economic and social factors to monitor sustainability. For example, the study proposed that the social cost for sustainability can be calculated based on the downtime of travel due to the closure of a bridge, which can be reported as a value of time or as a financial amount. However, such metrics typically analyse the downtime by calculating the delay caused from a detour from not using the bridge, this is applicable for highway bridges but is not necessarily applicable for all railway bridges. Another metric to monitor the social sustainability is to measure the life lost cost which incorporates fatalities and an implied cost of averting a fatality (Rackwitz, 2002).

Additional studies have built on Stein et al. (1999) and adapted economic cost metrics to consider environmental impact (Dong et al., 2014; Kendall et al., 2008; Padgett et al., 2009). Environmental cost can be assessed in terms of the traffic detour and cost associated with a repair action. A generalised environmental metric for a repair action is:

$$E_{REP} = (Eu_{Steel} \cdot V_{Steel} + Eu_{Concrete} \cdot V_{Concrete}) \cdot RCR, \tag{3.2.11}$$

where Eu_{Steel} and $Eu_{Concrete}$ are the environmental metrics per unit volume of their respective materials, V_{Steel} and $V_{Concrete}$ are the volumes of each material on a bridge and RCR is the repair cost ratio for a bridge in a particular damage state (Frangopol et al., 2017). Dong et al. (2014) expresses the environmental metric to consider multiple bridges on a network, the conditional probability of bridges being in particular damage states after a hazardous event and iterates across the multiple bridges and damage states with specific RCR values. An economic cost can also be associated to a repair action.

The sustainability metrics, if measured in economic terms, can be used to calculate the total economic consequence of a hazardous event,

$$C_S = C_{REP} + C_{RUN} + C_{TL} + C_{SL} + C_{EN}, \tag{3.2.12}$$

where C_{REP} is the repair cost, C_{RUN} is the running costs for following a detour to

incorporate fuel costs etc, C_{TL} is the monetary value assigned to the loss of users' time due to a detour, C_{SL} is the life loss cost attributed for any resultant fatalities, C_{EN} is the cost of the additional carbon emissions (Dong et al., 2014). It should be noted that

$$C_F \approx C_S - C_{REP}, \tag{3.2.13}$$

where C_F is the expected cost of failure shown in (3.2.6).

Global infrastructure expenditure is forecasted to grow from an annual spending of $4 trillion in 2012 to $9 trillion per annum in 2025 (PwC, 2014). In this context, Goodfellow-Smith et al. (2020a,b) considers how the financing of infrastructure can be a vehicle to drive the uptake in sustainable design and construction techniques. In particular, by changing the criteria and objectives in investment decision making to mandate consideration of sustainable and resilient engineering solutions when presenting the economic, social and environmental value delivered by investment propositions.

3.2.5 Utility

Asset investment planning decisions are typically supported by consolidating several metrics into a value framework to ascertain the relative value an asset or portfolio of assets provide to stakeholders. However, transportation infrastructure has many different stakeholders including transportation agencies, governmental regulators and infrastructure users, amongst others (Chen et al., 2015). Each stakeholder will have a range of objectives and some of these objectives may be in conflict with the priorities of other stakeholders, and thus asset managers must be able to appropriately distinguish and analyse the objectives to be able to facilitate effective collaboration between parties (Harmon, 2003). An example of a value framework that encapsulated a multiple stakeholder approach was presented by Litherland et al. (2019), which proposed an Extended RAMS (Reliability, Availability, Maintainability, and Safety) framework that included metrics for social and environmental properties of an operational railway.

Brownlow and Watson (1987) proposes that using a hierarchical approach when performing multi-attribute value analysis is desirable as it ensures a comprehensive

coverage of metrics and objectives in the decision making process and facilitates identification of any redundancy or double-counting in the analysis. A multi-attribute value function can be used to assess the value or utility of an asset portfolio and a common functional decomposition of system is by additive formulation. The additive form of the multi-attribute value function is,

$$V(s) = \sum_{i=1}^{n} w_i \cdot v_i(s), \tag{3.2.14}$$

where V is the multi-attribute value of the system for strategy S, w_i is the weighting of the attribute i v_i is the observed value of attribute i for strategy S, and there are n attributes. The selection of appropriate weighting factors for attributes is a challenging task. Jiménez et al. (2003) considered the imprecise nature of these weights by implementing lower and upper bounds for the value of each weight. These bounds enabled a sensitivity analysis to be performed and to enable a more informed decision to be made when selecting an optimal strategy. The study by Jiménez et al. (2003) presented a case study related to the restoration of a contaminated lake.

A multi-attribute value framework for assessing the utility of a bridge/bridge network was proposed by Dong et al. (2015). The function summed the appropriate terms for the social, economic and environmental utility of bridges to determine the multi-attribute value function,

$$V(s) = w_{Soc}v_{Soc} + w_{Eco}v_{Eco} + w_{Env}v_{Env}. \tag{3.2.15}$$

Determining value in non-economic terms is a challenging task, in particular as economic, environmental and social value are all interrelated. Economic value should include group value, e.g. governmental spending, and individual value, e.g. the direct cost that an infrastructure user pays. Environmental value, for example, can be reported in terms of the reduced environmental costs between alternative scenarios. However, social value should consider the fulfilment of the individual needs of each potential user, as each individual will economically value the same social value differently. Social value can be assessed using factors such as safety, security, comfort/ambience and convenience, where the ill defined quantitative nature of some of these social value indicators would make qualitative assessments more

appropriate than quantitative (Kalyviotis et al., 2020). Nonetheless, a common approach to determining social value is to perform a social cost benefit analysis which seeks to determine monetised values for attributes that deliver social value (Hauck et al., 2017; Vickerman, 2007).

Srinivasan and Parlikad (2017) also identified that many existing asset management decisions are driven on life cycle costing, negating the value the infrastructure may bring to various stakeholders. The returned value from infrastructure depends on the achieved benefits of the asset delivering effective service and performance, the risk manifested by the operation of the asset, and the required resource investment during the asset life cycle. Srinivasan and Parlikad (2017) suggests a three stage process to evaluate the value proposition from an asset. The three stages are

- Stage A: Establishment of the context - e.g. objectives, scope, problem statement and evaluation period
- Stage B: Value mapping - e.g. identification of stakeholders, stakeholder priorities, value metrics, direct and indirect influences between assets and metrics
- Stage C: Value assessment - e.g. modelling requirements, model development, solution selection and sensitivity analysis.

The proposed value mapping facilitates the inclusion of the requirements of multiple stakeholders and multiple metrics to support asset management decision making.

3.3 Bridge Asset Management

The performance of civil infrastructure including bridges can be evaluated using a range of indicators as aforementioned. Bridge asset managers are responsible for developing strategy and allocating resources to ensure the continued performance of their portfolio of bridges. However, delivering continued performance is not a trivial task as asset managers are under several constraints such as budget, workforce availability and service commitments, when making decisions.

3.3.1 Bridge Management Systems

During the 1960s and start of the 1970s maintenance, rehabilitation, and repair activities were typically performed on a "*as-needed*" basis (Thompson et al., 1998). Towards the end of the 1960s, in the United States, there were a number of bridge failures with fatalities, such as the Silver Bridge failure, which prompted the US federal government to authorise more rigorous legislation in respect to the inspection, maintenance and management of bridges. The increased legislative burden placed on Departments of Transportation lead to the recognition of the need for a defined methodology.

A Bridge Management System (BMS) is defined by the US Department of Transportation, Federal Highway Administration as, "*a systematic process that provides, analyzes, and summarizes bridge information for use in selecting and implementing cost-effective bridge construction, rehabilitation, and maintenance programs*" (US Department of Transportation, Federal Highway Administration, 2018). Furthermore, the United States Code, 23 U.S.C §500.107, states that; "*an effective BMS should include, as a minimum, formal procedures for:*

(a) *Collecting, processing, and updating data;*

(b) *Predicting deterioration;*

(c) *Identifying alternative actions;*

(d) *Predicting costs;*

(e) *Determining optimal policies;*

(f) *Performing short- and long-term budget forecasting; and*

(g) *Recommending programs and schedules for implementation within policy and budget constraints."*

An early example of a BMS is Bridgit, which was developed in 1985 under the National Cooperative Highway Research Program (NCHRP) to provide "*guidance*

on optimal resource allocation to the bridge network, given constrained and/or unconstrained budgets" (Hawk and Small, 1998) and "*guidance on network-level management decisions and project level actions*" (Hawk, 1999).

In 1991, the United States Congress passed the Intermodal Surface Transportation Efficiency Act (ISTEA) which mandated that that all state Departments of Transportation make use of Bridge Management Systems (BMSs) (Agrawal et al., 2010). This Act of Congress resulted in an American Association of State Highway and Transportation Officials (AASHTO) task force being created to provide guidance in the development of a BMS named Pontis in 1992. Golabi and Shepard (1997) provide a comprehensive account of the objectives and design philosophy of the system. Thompson et al. (1998) summarise the computational capabilities of Pontis and discuss the deterioration, preservation and improvement models.

Pontis has been the most widely used BMS in the United States since its entry to the market, with over 50 agencies in the USA and internationally using it in 2015 (Bentley-Systems, 2015). Pontis was renamed to be AASHTOWare Bridge Management (BrM) with the release of 5.1.3 in May 2013 (AASHTOWare, 2013).

DANBRO is a BMS in current use in Denmark by the Road Directorate and the counties of Denmark. The DANBRO BMS was designed with a modular design philosophy with the first modules implemented in 1988. The modular structure was a result of the development mindset that a BMS is only a tool to aid decision making by bridge owners and that different bridge owners have different requirements. Lauridsen and Lassen (1999) provide a detailed overview of the system and design philosophy. DANBRO has been implemented in various other national administrations including in Mexico, Saudi Arabia and Ireland (Duffy, 2004).

The American and Danish efforts in developing a BMS are recognised to be world leading, with Flaig and Lark (2000) providing a history of the development of BMSs in the USA, Denmark and the UK. More recently, the IABMAS Bridge Management Committee completed reports which outline 25 existing BMSs that are in use in 18 countries (Mirzaei et al., 2012, 2014).

3.3.2 Life Cycle Management

Life cycle management is recognised across industry and literature to be an effective tool for maximising the cost-effectiveness of asset interventions and delivered value from an asset. Developing life cycle management strategy for bridge portfolios requires the capability of predicting future asset condition alongside with being able to ascertain the impact of different intervention types during a bridge life cycle. After construction the evaluation of these concerns is performed using a life cycle model, which is composed of two critical modelling components: a deterioration model and a decision model. A deterioration model is used to model the process of deterioration and predict future bridge condition. A decision model uses the prediction of bridge condition and is used to apply particular intervention strategies and determine any uplift in condition or extension of predicted service life.

A life cycle model is used to support decision making and present particular strategies to stakeholders. A generalised model framework for life cycle modelling is shown in Figure 3.3, which is able to output the Key Performance Indicators (KPIs) for a particular strategy.

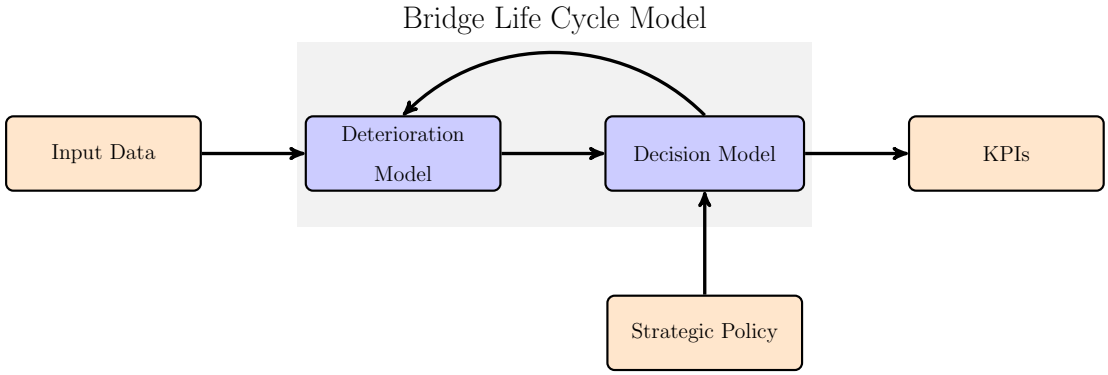

Figure 3.3: Bridge life cycle model - policy evaluation.

If the interventions types are well defined and the model has an appropriate parametrisation of the physical processes, it is possible to use a life cycle model to not only output KPIs but determine the 'optimal' policy. Moreover, it is possible to incorporate multiple constraints into the optimisation e.g. budget, workforce availability etc. A generalised model framework for the optimisation approach is shown in Figure 3.4.

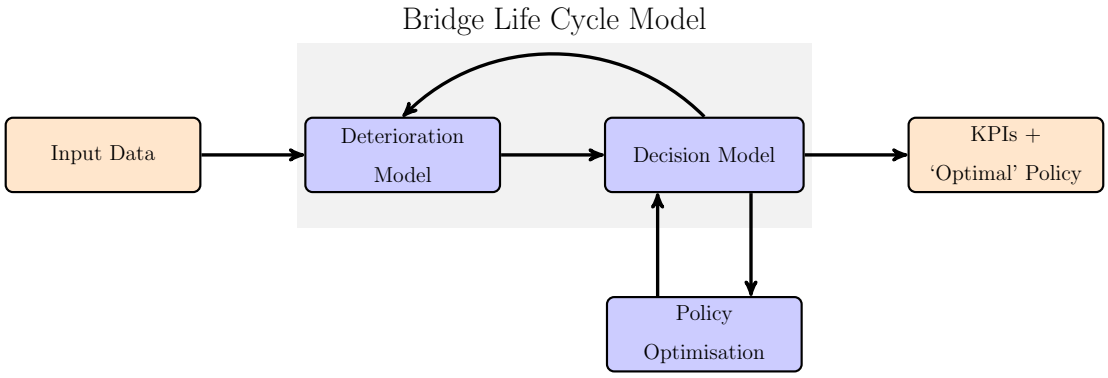

Figure 3.4: Bridge life cycle model - policy optimisation.

The purpose of a model can be broadly categorised into three classes: Generator, Mediator and Predictor (Heath et al., 2009). A generator model is used to generate hypotheses, mediator models are employed to make comparisons between competing strategies, and predictor models are used when a system is well understood and can provide accurate insights into future bridge condition states (Bush et al., 2017). In bridge management, a mediator model can be used to investigate the benefits of different maintenance strategies. A predictor model can compare different maintenance strategies but could also affix accurate costings to any output, which is an objective of infrastructure asset managers.

Bridge stakeholders commonly stipulate that any selected management strategy requires a degree of accountability to support the rationale behind any decision being made. The task in developing decision support models and tools is to provide a solution which provides accurate insights, appropriate indicators and effective representations of physical processes, akin to a generator model. However, the modelling of life cycle is contingent on having a deterioration model that simulates the structural reliability of a bridge and how the reliability changes over time. Section 3.4 evaluates potential data sources for calibrating deterioration models to predict future asset condition.

3.3.3 Optimisation in Life Cycle Management

Infrastructure can be managed using different asset policies which outline the implementation of processes, such as an inspection regime, structural monitoring and

maintenance interventions. Structural performance is a function of structural deterioration alongside the different processes outlined in asset policies and can be measured using an array of different indicators, such as condition, safety and reliability. A task for infrastructure asset managers is to select an asset policy that maximises the structural performance of their bridges over a time period; however, this is not an unconstrained problem. Asset managers typically have cost constraints alongside constraints on asset access time, equipment and workforce availability, which limit the deliverable volumes of inspection, monitoring and maintenance interventions. To support decision making, optimisation is used to determine optimal asset policies given the constraints of the infrastructure asset managers.

Whilst maintenance costs are only one type of cost in a WLCC analysis, funds allocated for life cycle management activities are commonly directed towards the maintenance of assets (Frangopol, 2011). A core objective function for the optimisation of the life cycle of structures is the minimisation of the total expected maintenance cost. Consequently, there is a range of examples in literature where an expression for life cycle cost has been the only objective in an optimisation (Ang and De Leon, 1997; Estes and Frangopol, 1999; Yang et al., 2006). In a single objective optimisation where cost is required to be minimised, thresholds for structural performance should be set to ensure that the optimisation maintains a serviceable bridge and does not minimise the cost in absolute terms.

When determining an optimal asset policy which maximises structural performance the problem can be stated with multiple objectives, some of which may compete against each other. A multi-criteria optimisation can be used to maintain the optimum compromise solution between the competing objectives. In particular, cost and performance have a conflicting relationship and there are many optimisation studies that considered the maximisation of structural performance alongside the minimisation of cost (Neves et al., 2006a,b).

Evolutionary optimisation algorithms, such as a Genetic Algorithm (GA) (see Appendix A), are commonly used for optimisation problems with multiple performance indicators (Okasha and Frangopol, 2009). However, the required use of evolutionary algorithms for maintenance optimisation is dependent on whether pre-

ventative maintenance and/or essential maintenance actions are being evaluated (Frangopol, 2011). In particular, if only one type of essential maintenance action is being modelled, performance thresholds can be set to trigger the maintenance action (Neves et al., 2006a). However, if multiple essential maintenance actions are being evaluated, an optimisation can be performed to select an appropriate maintenance action that returns an optimal cost whilst providing a service life extension or determining a maintenance strategy that maintains a specified service length. Additionally, aspects of the inspection regime may also be included in the optimisation process.

For models that evaluate preventative maintenance, the optimisation algorithm can be used to determine the number of applications of a preventative maintenance action as well as the timing between multiple applications (Frangopol, 2011; Frangopol and Bocchini, 2012; Neves et al., 2006b). Whilst uniform application of preventative maintenance simplifies the complexity of the optimisation problem, Frangopol et al. (1997) shown that non-uniform intervals between actions are typically more economically advantageous.

More recently, there has been an increased interest from infrastructure asset managers in maximising sustainability and utility metrics, rather than focusing only on performance and cost (see Sections 3.2.4 and 3.2.5). An example of a maintenance optimisation framework that encapsulates indicators for economic, societal and environmental outcomes was developed by Sabatino et al. (2015). The sustainability-based maintenance optimisation decision-support framework used the multi-attribute utility theory to quantify the multiple competing objectives. Optimisation was used to evaluate different maintenance action types on bridge components and the respective application timings, whilst assuming equal weightings in economic, societal and environmental factors.

3.4 Data Availability

When developing a model to predict future bridge performance, indicators for structural reliability and risk are most commonly modelled, with the remaining perfor-

mance indicators calculated as a consequence. It may be possible to model these indicators on a theoretical basis, given the design specification of the structure (Stewart, 2001). Nevertheless, it is desirable for performance models to be calibrated using data collected during the service life of a structure to capture any uncertainty in the deterioration of performance. In general the following data sources are available:

- Experimental/empirical measurements including: Non-Destructive Testing (NDT) / Non-Destructive Evaluation (NDE) and Structural Health Monitoring (SHM).
- Condition records from visual examinations.
- Maintenance records outlining intervention activities and date of occurrence.

3.4.1 Experimental Measurements

Engineering measures can be collected from a structure using a range of techniques. Typically, these data gathering activities are divided into continuous (if data is collected at very high frequency) or discrete (when data is collected once or with low frequency) measures.

Continuous data gathering, usually denoted as SHM, is necessarily non-destructive and measures structural response of the structure, including displacements and accelerations. Discrete data gathering includes both destructive and non-destructive tests, and the outputs can be used to determine the structural performance, in addition to its geometrical, mechanical and material properties

NDT is used to provide additional insight into the structural performance of a bridge/bridge component. Examples of NDT include: crack measurements, strain gauges, infrared thermography, radiography and ultrasonic measurements. However, these monitoring mechanisms are typically only employed for bridges/bridge components which have been identified as a concern, NDT does not necessarily adhere to a regular inspection regime and is an expensive monitoring mechanism for asset managers to utilise. Consequently, data from NDT is commonly used to evaluate performance for specific structures rather than supporting network level decision making. However, NDT has the advantage of inducing no damage on the structure, and thus can be repeated as often as required.

SHM involves the installation of monitoring equipment on civil infrastructure to detect damage and monitor structural loading. The use of SHM data can be utilised in a reliability assessment (Frangopol et al., 2008; Liu et al., 2009a,b; Strauss et al., 2008). Vagnoli et al. (2018) provides a recent literature review of SHM methods applied to bridges.

For network level decision making there is a distinct difference in priorities between SHM and life cycle management (Frangopol, 2011). SHM is primarily interested in damage detection, load capacity and component structural failure, whereas life cycle management is used by infrastructure managers to provide insight into strategic concerns such as: cost predictions, condition, serviceability and safety (Glaser et al., 2007). There are ongoing efforts to incorporate SHM into reliability assessments and strategic decision making (Okasha et al., 2012; Orcesi and Frangopol, 2011). However, in the short and medium terms there is limited scope to have widespread installation of monitoring equipment across entire asset portfolios, in particular for portfolio owners with a mature asset base. Moreover, in the advent of possessing SHM data for structures in an entire portfolio, further research is required into efficient methods to manage and utilise such vast quantities of data.

3.4.2 Maintenance Data

If the construction date of a bridge is known and a full intervention history exists for each of its elements, it is possible to perform a lifetime analysis for each bridge element. A lifetime analysis considers the degradation of a bridge element by analysing the instances of interventions and the time between each intervention being required (Le and Andrews, 2013, 2015).

For example, consider that a bridge element was installed during the construction of a bridge at time t_0 and is in a 'perfect' condition state s_i. The condition states after partial or complete degradation can be defined as the states at which particular interventions are scheduled. Thus, if considering three scheduled interventions types, minor repair, major repair and replace, three further condition states could be defined, s_j as 'good', s_k as 'poor' and 's_l' as 'very poor'. Assuming that each intervention type restores the bridge element to s_i, it is possible to analyse the

times taken to reach a particular condition state of triggering an intervention. An example deterioration pattern is shown in Figure 3.5.

One should identify the complete records which indicate the full time required to reach a particular condition state and censored records where it has not been possible to observe the complete lifetime or time required to reach a state. For example, if minor repair or major repair interventions have been triggered, the full time required to reach the replace threshold has not been observed, however it is known to be at least that observed time interval. Moreover, the intervention based condition rating scale is defined for scheduled interventions, however unscheduled intervention may be necessary. For example, if a bridge element is damaged during a bridge strike, an emergency repair may be scheduled, in which case the record would be right-censored even for the first non-perfect state of s_j.

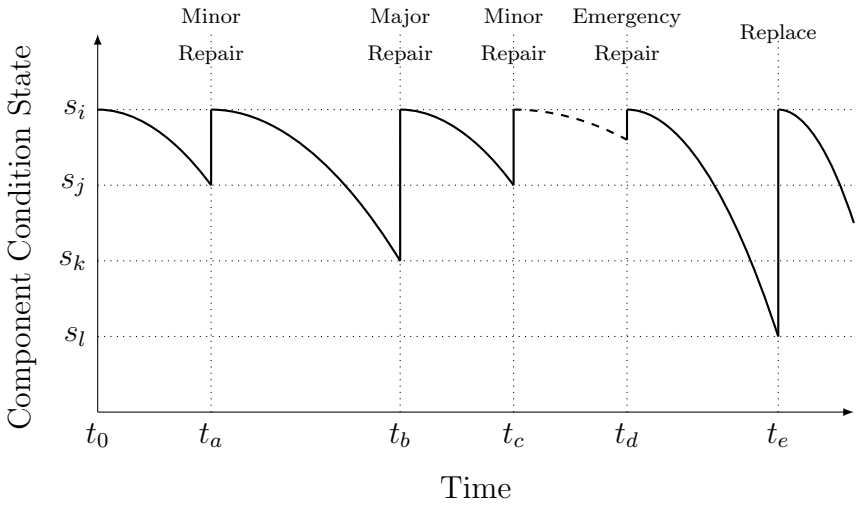

Figure 3.5: Example deterioration pattern and historical maintenance interventions on a bridge component (Le and Andrews, 2015).

Different components will degrade at different rates, however cohorts of components can be formed for components that perform a similar structural function and experience similar degradation rates and mechanisms. By performing a lifetime analysis for all components, it is then possible to calibrate distributions for condition transition times using these cohorts.

Calibrating a deterioration model using maintenance records and lifetime analysis addresses some of the concerns of the subjectivity of condition records from

visual inspection. However, a deterioration model with an intervention based condition scale has the following limitations:

- Whilst for principal load bearing elements the decision to schedule an intervention can be triggered based on the condition of one element, in general the decision to intervene on a bridge is seldom based on the condition of one bridge element. Thus, the records that show an intervention being scheduled could in reality be indicating a shorter time (or longer) to reach a particular state than the actual lifetime of the component condition. Moreover, the scheduling of maintenance interventions can vary due to strategic and fiscal priorities in addition to the condition of the asset. For example, the constraints on a budget vary over time and this will impact the scheduling of interventions which would alter the time interval between interventions.

- The differentiation between maintenance interventions into a consolidated discrete condition scale is in itself a subjective endeavour.

- Many transportation agencies have limited availability of complete and detailed intervention histories, particularly for asset portfolios with a mature asset composition. The limited data availability curtails the effectiveness of any model calibration.

3.4.3 Condition Data

A regular inspection of bridges is typically mandated by a transportation agency or their regulator. The primary purpose of inspection is to confirm that each bridge is structurally sound and that there are minimal safety risks for continued operation. Moreover, condition assessment aids the forecasting and prioritisation of future maintenance interventions.

A bridge is composed of substructure, superstructure and deck components, with the overall bridge having a particular designed service life. However, each of the substructure, superstructure and deck components, and their constituent elements will also have a unique service life. Over the lifespan of the bridge, particular components or elements may require maintenance or replacement at a shorter interval than

the service life of the entire bridge. However, it may be cost effective to intervene to enable larger and more expensive components to remain in continued operation over a longer time period (Li, 2019).

To facilitate component level decision making, condition ratings are commonly assigned to components during a bridge inspection. For example, in the USA, all federally funded bridges are required to be inspected every two years adhering to two standards:

- Federal National Bridge Inspection Standards (NBIS) (FHWA, 1987; FHWA, 1995).
- AASHTO Guide for Commonly-Recognised (CoRe) Structural Elements (AASHTO, 1997; AASHTO, 2010).

The National Bridge Inventory (NBI) records the results of these inspections and the condition states used are shown in Table 3.3.

Table 3.3: NBI Condition Ratings for substructure, superstructure and deck components (FHWA, 1995).

Rating	Bridge Element Condition	Description
9	Excellent	As new.
8	Very Good	No problems reported.
7	Good	Some minor problems.
6	Satisfactory	Structural elements show minor deterioration.
5	Fair	All primary structural elements are sound, but may have minor section loss, cracking, spalling or scour.
4	Poor	Advanced section loss, deterioration, spalling or scour.
3	Serious	Loss of section, deterioration, spalling or scour has seriously affected primary structural components; local failures are possible; and fatigue cracks in steel, or shear cracks in concrete may be present.
2	Critical	Advanced deterioration of primary structural elements; fatigue cracks in steel or shear cracks in concrete may be present or scour may have removed substructure support; unless closely monitored it may be necessary to close the bridge until corrective action is taken.
1	"Imminent" Failure	Major deterioration, or section loss present in critical structural components or obvious vertical or horizontal movements affecting structure stability; bridge is closed to traffic, but corrective action may resume the bridge in light service.
0	Failed	Out of service and beyond corrective action.

In the United Kingdom, a condition rating scale using severity and extent codes is used by organisations such as Network Rail and Highways England. A condition is recorded for each bridge element, where the Extent code denotes "*the area, length or number (as appropriate) of the bridge element affected by the defect/damage*" and Severity code denotes "*the degree to which the defect/damage affects the function of the element or other elements of the bridge*" (Highways Agency, 2007a,b). The severity and extent codes are used to inform maintenance planning and strategic decisions. The purpose of two separate codes is to enable the distinction between a single but severe defect and a defect that is extensive but primarily superficial. The generic Severity and Extent codes are shown in Tables 3.4 and 3.5. Note that the definitions shown are generic and that Highways Agency (2007a) provides a detailed breakdown of Severity codes by material type.

Table 3.4: Extent Codes - UK Highway (Highways Agency, 2007a).

Code	Description
A	No significant defect.
B	Slight, not more than 5% of surface area/length/number.
C	Moderate, 5%-20% of surface area/length/number.
D	Wide, 20%-50% of surface area/length/number.
E	Extensive, more than 50% of surface area/length/number.

Table 3.5: Generic Severity Codes - UK Highway (Highways Agency, 2007a).

Code	Description
1	As new condition or defect has no significant effect on the element.
2	Early signs of deterioration, minor defect/damage, no reduction in functionality of element.
3	Moderate defect/damage, some loss of functionality could be expected.
4	Severe defect/damage, significant loss of functionality and/or element is close to failure/collapse.
5	The element is non-functional/failed.

Condition rating scales are not always a discretised rating of defect, damage or deterioration. For example, in Sweden condition is reported in terms of physical, functional and economic cost, with the physical and functional condition articulated as time to intervention/service disruption. The physical and functional condition ratings are shown in Table 3.6. The economic condition is used an indication of the extent of the damage present and the required quantity of repairs, computed as the product of the quantity of the defect and the unit cost for repair (Hearn et al., 2005). An additional example is the *Image de la Qualité des Ouvrages d'Art (IQOA)* condition scale used in France, which is defined by the presence of defects and the perceived urgency of repair (Everett et al., 2008; SETRA, 1996), see Table 3.7.

Table 3.6: Swedish bridge condition ratings (Hearn et al., 2005).

Rating	Physical Condition	Functional Condition
3	Repair needed now	Service impaired now, at time of inspection
2	Repair within 3 years	Service impaired within 3 years
1	Repair within 10 years	Service impaired within 10 years
0	Repair beyond 10 years	Service impairment greater than 10 years

Table 3.7: French (IQOA) condition ratings (Everett et al., 2008).

Class	Physical Condition	Functional Condition
1	Bridges in apparently good condition.	Common maintenance.
2	Bridges with defects on equipment or protection elements or minor structural damages.	Needs specialised maintenance without urgency to repair.
2E	Bridges with defects on equipment or protection elements or minor structural damages.	Need specialised maintenance with urgency to repair in order to prevent increase of defects in the structure.
3	Damaged structure.	Needs repair without urgency to repair.
3U	Damaged structure.	Needs repair with urgency to repair.

From reviewing the different condition scales it is apparent that how condition is defined varies a great deal between different countries and infrastructure asset managers. In some scales the condition is used to indicate the structural performance and damage mechanisms. For example, the NBI condition ratings considered elements from new condition to a failed condition which denoted a bridge element being out of service or beyond corrective action. Additionally, the Severity Extent scales used in the UK denotes the development of distinct defect mechanisms and monitors their extensiveness. However, not all condition ratings are a direct discretised rating of structural deterioration, but rather an indication of required maintenance actions and/or urgency to repair, as exemplified in the Swedish and French condition scales. Such differences in the implied meaning of the condition rating must be considered when developing and implementing condition deterioration models to support life cycle analysis.

Reliability of Condition Data

Deterioration models calibrated from asset condition data have two fundamental sources of variability (Ben-Akiva et al., 1993; Madanat, 1993): the current condition of the asset and the projected condition of the asset. The variability in the current condition of an asset can be caused by measurement errors, defect misdiagnosis and/or data input errors. Any variability of the current condition of an asset will increase the uncertainty of the method used to predict future conditions. Moreover, the variability in a projected asset condition may lead to suboptimal scheduled maintenance which will increase the life cycle cost of the asset.

An investigation into the variability of the inspection results of Federal Highway bridges in the USA was performed by Phares et al. (2004) and Moore et al. (2001). The results of the study found that 78% of condition scores recorded were correct with 95% confidence. However, 95% of reported condition scores were within two condition scores of the true value. There is a number of factors affecting the quality of the inspection data: the experience of the inspector, availability of access to the element being inspected, the configuration of the bridge and the type of defect (Neves and Frangopol, 2010). Kuhn and Madanat (2005) investigated the impact of the increased uncertainty on deterioration modelling of civil infrastructure, given the variability of inspections, and concluded the increased uncertainty can result in significant financial and operational consequences. However, quantifying the uncertainty brought by condition record variability is a challenging task which is often remedied by expert judgement, which unfortunately has its own uncertainty.

Yianni et al. (2018) evaluated the sources of variability in the modelling of bridge asset management and quantified the impact on the WLCC. The study by Yianni et al. (2018) built on the findings of Phares et al. (2004) which determined that recorded conditions from visual inspections are typically correct to within two condition states on a one-dimensional scale. Yianni et al. (2018) studied condition using a two-dimensional SevEx condition scale and assumed a variability of one neighbouring condition state in the SevEx scale. For some states in the SevEx scale, an assumed variability of one neighbouring condition state could mean that there are up to 8 possible states to consider. From the assumed variability of the SevEx con-

dition scale, probabilities for the scheduling of the correct maintenance intervention were calculated and it was found that on average, maintenance actions are scheduled correctly 72% of the time. Imperfect interventions were also evaluated in the WLCC model, whereby each maintenance action was not assumed to always return the bridge component to perfect, A1 condition. Yianni et al. (2018) concluded that models that incorporate variability will ultimately yield less returned value from a constrained budget, but the model will be more reflective of the real-world system and its complexities.

3.4.4 Data Summary

Whilst experimental data from NDT and SHM exists and has been shown in literature to facilitate reliability analysis, the data from such monitoring activities is expensive to obtain and not readily available for entire asset portfolios but rather a small subset of assets limiting the applicability for network level modelling. Similarly, the use of maintenance records in bridge lifetime analysis suffers from the affliction of low data availability. Additionally, bridge lifetime analysis using maintenance records is also limited by the subjective definition of interventions and the uncertainty in scheduling rationale.

The use of condition records from visual inspections to calibrate deterioration models for portfolio level decision support is the most common practice (Frangopol et al., 2017). Although it should be noted that data using a condition rating scale is not necessarily indicative of the loading capability of a structural element (Liu and Frangopol, 2006; Neves and Frangopol, 2005; Saydam et al., 2013). Nonetheless, bridges or bridge components with poor or unacceptable condition scores are typically prioritised when scheduling interventions (Frangopol and Liu, 2007).

A plethora of methodologies can be employed to model bridge deterioration and be calibrated using condition records. These methods include,

- Deterministic models,
- Markov chain models,
- Bayesian Belief Networks (BBNs),

- Petri net models,
- Artificial Intelligence (AI) models.

Section 3.5 will provide further insight into each technique. Fault tree methods can be used to model future bridge condition, however these methods are only useful for predicting catastrophic failure events rather than intermediate condition events, and thus are not appropriate for modelling bridge condition over an extended period of time (LeBeau and Wadia-Fascetti, 2000; Sianipar and Adams, 1997).

3.5 Characterisation of Deterioration: Models and Approaches

3.5.1 Deterministic Methods

Deterministic modelling of bridge deterioration requires the assumption that the process can be defined with certainty using a given mathematical expression. Common techniques include: linear extrapolation, regression models and curve-fitted models (Morcous et al., 2002b).

Deterministic models are simple to implement and calibrate, however they negate the inherent stochastic properties of structural deterioration. Moreover, deterministic model typically disregard the interactions between deterioration of different constituent components of a bridge.

Polynomial regression

A common example of a deterministic model is polynomial regression. For example, consider a third-order polynomial, which is a defined function for condition rating given a bridge age,

$$C_i(t) = \beta_0 + \beta_1 t_i + \beta_2 t_i^2 + \beta_3 t_i^3 + \epsilon_i, \tag{3.5.16}$$

where $C_i(t)$ is the condition rating of a bridge at age t_i, t_i is the bridge age, and ϵ_i is the error term. β_0 was set to equal nine as that is the score for excellent condition using the NBI condition scale, which is the assumed condition at time $t = 0$. The

remaining β_i terms can be calibrated from historical condition records using the method of least squares, although the bridge age must be known for all bridges featuring in the condition records not just the date of inspection. Moreover, it is possible to estimate the expected service life of a bridge by analysing how long it takes to reach a particular condition rating, e.g. $C_i(t) = 3$, see Figure 3.6.

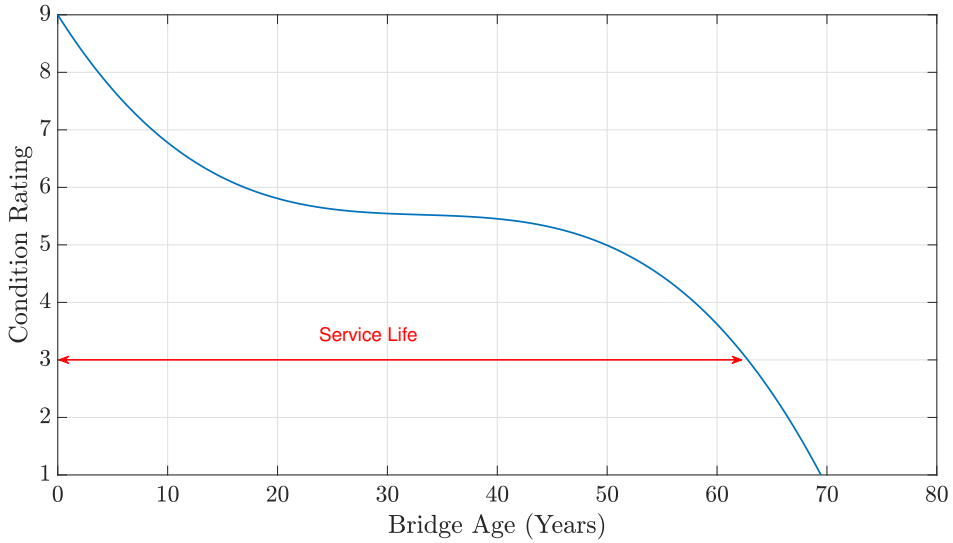

Figure 3.6: Performance curve for the condition of concrete bridges (Jiang et al., 1988).

Time-Dependent, Structural Deterioration Equations

Historically, structural deterioration was modelled as a time-dependent process using simple rate equations such as,

$$X(t) = \alpha(t - T_i)^{\beta}\epsilon_1(t), \quad t > T_i, \tag{3.5.17}$$

$$X(t) = \alpha(t - T_i)^{\beta} + \epsilon_2(t), \quad t > T_i, \tag{3.5.18}$$

where $X(t)$ is the deterioration parameter (indicative of a physical property e.g. loss of section, depth of penetration etc.), T_i is the induction period, α and β are parameters calibrated from experimental data and $\epsilon_1(t)$ and $\epsilon_2(t)$ are random error terms (Ellingwood, 2005).

Applying time-dependent equations to model structural deterioration across an entire portfolio is challenging as the equations are dependent on the calibration of

the α and β parameters from experimental data. Experimental data is expensive to obtain, it is quite sensitive to the environmental properties of the data sample and does not generalise well to environments that do not feature in the data sample.

Bilinear and Non-linear Deterioration Models

A limitation of most methodologies that require the assumption of the Markov property and are time-invariant is that the history of the bridge and any applied maintenance actions are disregarded. Moreover, such models are unable to incorporate a delay or reduced rate of defect occurrence immediately after an intervention has taken place. Thus, the modelling capability of assessing the true efficacy of interventions is constrained. One approach to address this limitation is to define piecewise functions for your deterioration metric. An expression for zero deterioration or reduced deterioration is defined for the time period immediately after an intervention. After a period of time has elapsed, deterioration then starts to occur or occur at a greater rate.

An example of a bi-linear deterioration model was presented by Neves and Frangopol (2005), which models condition and safety profiles under a do-nothing maintenance scenario. For a defined time period after t_0, there is no deterioration of condition or safety, which is justified with the physical reality. For example, the time required for chloride to reach the reinforcement bars of a concrete component, or the time required for a protective coating to deteriorate and metal corrosion to start on metallic components. Subsequent to this initial defined time period of no deterioration, deterioration is modelled as a linear function of time,

$$C(t) = \begin{cases} C_0, & \text{if } t \leq t_{ic}, \\ C_0 - \alpha_C(t - t_{ic}), & \text{if } t > t_{ic}, \end{cases} \tag{3.5.19}$$

$$S(t) = \begin{cases} S_0, & \text{if } t \leq t_{is}, \\ S_0 - \alpha_S(t - t_{is}), & \text{if } t > t_{is}, \end{cases} \tag{3.5.20}$$

where $C(t)$ and $S(t)$ are the condition and safety profiles respectively, C_0 and S_0 are the initial condition and safety indices at time $t = 0$, α_C and α_S are the deterioration rates for condition and safety respectively, and finally t_{ic} and t_{is} are the initial time periods of deterioration initiation for the condition and safety profiles respectively.

Defining deterioration profiles as a linear function of time is an idealised assumption. Petcherdchoo et al. (2004) presents non-linear deterioration profiles which adhere to engineering experience. Such models require the assumption that deterioration occurs in a certain way, however an advantage of the bilinear model is that it includes a reduced rate of deterioration earlier in the life cycle, which is more reflective of the reality.

3.5.2 Stochastic Methods

The indicators for evaluating performance shown in Section 3.2 are used in network level decision making. For forecasting purposes, future asset condition is of interest, which requires a methodology for modelling bridge deterioration and evaluating structural reliability. Estes and Frangopol (1999) proposed a system reliability framework to determine the optimal maintenance strategies for bridges. For network level decision making, condition records from visual examinations are the most abundant and their use for model calibration is often mandated by the regulators of transportation agencies.

Deterministic expressions can be used to predict future condition, however this approach would negate the inherent randomness of the deterioration process. Stochastic methods are favoured for making predictions on future asset condition due to the capability of incorporating the uncertainty of the deterioration process. The remainder of this section will review a variety of stochastic techniques and models that have been applied to model bridge deterioration.

Time-based Models

Time-based bridge deterioration models consider bridge deterioration as a function of bridge condition over time, i.e. time-based models simulate deterioration by predicting future condition or bridge failure by considering the time between changes in condition. Bridge condition is commonly denoted by a set of discrete condition states, however a continuous metric of condition is possible. The sojourn time for transitions between condition states can be expressed using deterministic methods,

however the sojourn time can also be modelled using stochastic methods, e.g. sampling the sojourn time from a probability distribution.

Pandey and van Noortwijk (2004) and Pandey et al. (2005) shown that the deterioration process is better reflected using a stochastic approach which encapsulates the variability of the deterioration process with time. Deterioration occurs at an increasing rate as time progresses, and thus if deterioration is modelled with time-invariance, the model will overestimate the probability of survival in the later stages of an asset's lifespan. This deterioration property was also empirically shown by Nicolai et al. (2007) in their assessment of coating degradation on steel bridges. These studies employed stochastic gamma processes to model deterioration stochastically, a method first proposed by Moran (1954) to model water flow into dams. Abdel-Hameed (1975) is often cited as the first example of gamma processes being applied to model deterioration.

There now exists an extensive array of applications of the process to model deterioration in optimisation models. The time-dependent structural reliability of a bridge was modelled using gamma processes by van Noortwijk et al. (2007), which considered both the deteriorating resistance and variable loading of the structure. However, van Noortwijk (2009) provided a survey of the applications of gamma processes in maintenance modelling, and acknowledged that gamma processes had more commonly been applied to decision modelling for single components opposed to whole systems of multiple components.

Yang et al. (2004) employed lifetime functions to compute the probability of system survival. The study shows that a bridge can be modelled as a combination of series and parallel components. The failure of one component typically does not result in the failure of the overall structure as bridges are typically redundant structural systems. Components from the same bridge are inherently subjected to similar environmental conditions, thus correlation between the failure of components must be considered in any reliability calculation.

Bridges are extremely complex systems that in most cases cannot be modelled solely as series or parallel systems. However, it is possible to identify components (e.g. individual spans in multi-span bridges) where the failure of any component

leads to bridge closure. In some cases, loads are distributed across multiple elements (e.g. multi-girder bridges) where failure of an element does not cause structural failure. Although, this structural design can only be defined as a parallel system as a first approach, as loading in surviving girders will increase and cause an increase in their probability of failure.

Lifetime Distribution Functions (LDF) can be defined for different types of components and environmental conditions and can be used to approximate a value for the probability of survival, P_s for a component deteriorating under a do-nothing maintenance scenario (Leemis, 1995). LDFs must satisfy the following conditions,

$$P_s = 1 \quad \text{at } t = 0, \tag{3.5.21}$$

$$P_s = 0 \quad \text{at } t \to \infty, \tag{3.5.22}$$

$$\frac{\delta P_s}{\delta t} \leq 0. \tag{3.5.23}$$

Exponential and Weibull survivor functions are common LDFs used to calculated P_s, which are defined as,

$$S(t) = e^{-\lambda \cdot t}, \tag{3.5.24}$$

where $S(t)$ is the exponential survival function, λ is the failure rate and t is time. The Weibull survival function is defined as,

$$S(t) = e^{-(\lambda_s t)^{\kappa}}, \tag{3.5.25}$$

where λ_s is the scale factor and κ is the shape factor. As aforementioned, the failure of one component does not typically lead to the failure of the whole structure due to designed system redundancy. Bridges are prone to several failure modes, each associated with the failure of one or more components. The structure failure of the whole bridge can be determined by calculating the probability of survival of the bridge, as a system of n components, which can be configured in series or parallel configuration (Yang et al., 2004). The probability of system survival for a series configuration is calculated as,

$$P_s = \prod_{i=1}^{n} P_{si}, \tag{3.5.26}$$

where P_{si} is the probability of survival for component i. For a system with a parallel configuration the probability of survival is calculated as,

$$P_s = 1 - \prod_{i=1}^{n}(1 - P_{si}). \tag{3.5.27}$$

Engineering expertise suggests that correlation between the probability of survival of components exists. However, accurately quantifying the correlation between components is a difficult task. Consequently, an intermediate endeavour is to ascertain bounds for the probability of failure for the correlation values of zero and one, i.e. no correlation and fully correlated.

If components are fully correlated, a series system will assume a probability of failure equal in value to the component with the largest probability of failure, and for components with no correlation, the probability of system failure can be calculated from the probabilities for independent components (Yang et al., 2004). Consequently, the probability of system failure P_f satisfies the following,

$$\max(P_{fi}) \leq P_f \leq 1 - \prod_{i}^{n}(1 - P_{fi}), \tag{3.5.28}$$

where $P_f = 1 - P_s$ and $P_{fi} = 1 - P_{si}$.

For a system with components in a parallel configuration, the probability of system failure when the components are fully correlated is equal in value to the component with the lowest probability of failure. If the components are not correlated at all, the probability of system failure can be calculated from the probabilities for independent components (Ang and Tang, 1984). The bounds for a parallel system are,

$$\prod_{i}^{n} P_{fi} \leq P_f \leq \min(P_{fi}). \tag{3.5.29}$$

Modelling a system's reliability as probability of failure of the systems component is a rigorous approach. However, instances of component failure and system failure are rare, which makes the calibration of any model of failure challenging.

Markov Models

As aforementioned, condition records from visual bridge inspections are commonly used to calibrate deterioration models. Such records report the condition of a bridge

or bridge component using a discrete condition scale. These visual inspections are part of examination regimes that typically only mandate an inspection every couple of years. Moreover, for mature asset portfolios these records may only exist for the late stages of a bridge's lifespan. Consequently, these records form a longitudinal study that are reported with discrete condition states and discrete time increments.

The properties of such condition records make the use of DTMCs an appropriate method to employ to predict future condition. An early example of modelling deterioration in this fashion is Golabi et al. (1982), which used DTMCs to predict future road condition to determine an optimal maintenance strategy.

A analysis of 5700 bridges in Indiana, USA by Jiang et al. (1988) and Jiang and Sinha (1989) is an early example of DTMCs being employed to model bridge deterioration. Cesare et al. (1992) also applied the technique to model bridge condition for a portfolio of 850 bridges in New York state. Numerous other studies have since employed DTMCs to predict future bridge condition (DeStefano and Grivas, 1998; Golabi and Shepard, 1997; Morcous, 2006; Scherer and Glagola, 1994) and the use of DTMCs were recognised by Frangopol et al. (2004) and Agrawal et al. (2009) as the most popular stochastic technique used for modelling bridge deterioration.

Note that a DTMC can be either time invariant or time variant dependent on the transition probability matrices that are defined. For example, Jiang et al. (1988), defined transition probabilities for different groups of bridge age, and thus it was a time variant model, which was calibrated using the percentage prediction method. The percentage prediction method requires that the inspection interval occurs regularly and is of a fixed interval size with minimal variance.

The transition probabilities for a DTMC can be determined by analysing historical condition records or set by expert judgement (Thompson and Shephard, 1994). It is preferable to calibrate the transition probabilities using historical data in the first instance, with the expert judgement used to generate probabilities for scenarios that have sparse or incomplete datasets. To compute transition probabilities from historical condition data there are two frequent methodologies used, (Morcous and Lounis, 2006);

- regression-based optimisation (expected value method),

- percentage prediction (frequency method).

The estimation of transition probabilities using a regression-based optimisation method requires the solution of a non-linear optimisation problem which minimises the sum of absolute differences between the regression curve that best fits the condition data and the conditions predicted using the Markov chain model.

The probability of a bridge element transitioning from condition i to j is denoted as $p_{i,j}$ and using the percentage prediction method, is calculated as,

$$p_{i,j} = \frac{n_{i,j}}{n_i} \tag{3.5.30}$$

where n_{ij} is the number of transitions from state i to state j within the stated time period and n_i is the total number of bridges in i before the transition (Jiang and Sinha, 1989). Using the percentage prediction method requires data from at least two consecutive inspections which occurred without any major maintenance interventions. Alternatively, the data from two consecutive inspections can be filtered to remove results showing an increase in condition score, excluding the improved results accounts for the effects of maintenance interventions.

For condition records which have varying inspection records, i.e. are non-periodical, Mašović and Hajdin (2014) shown that using the Expectation Maximisation algorithm is an effective way of calibrating DTMC transition probabilities. An alternative method is the statistical estimation of transition rates for a CTMC using a maximum likelihood estimation technique (Kallen and Noortwijk, 2006). Moreover, Kallen and Noortwijk (2006) performed a comparative analysis of different CTMCs that were state dependent and state independent, as well as CTMCs that were time variant and time invariant, concluding that the state dependent, time variant model provided the best fit for the training data and was more reflective of the physical reality of deterioration.

CTMCs are a special example of Semi-Markov models. In general, semi-Markov models assume the memoryless property at the instant of state transition, however the time between transitions, the sojourn time, is sampled from a probability distribution that does not necessarily need to be memoryless, hence use of the 'semi' prefix. Nonetheless, CTMCs assume the memoryless property $\forall t \geq 0$, as the sojourn

time is sampled from the exponential distribution. There are several examples of semi-Markov models being used to model bridge deterioration (Kleiner, 2001; Mishalani and Madanat, 2002; Ng and Moses, 1998; Thomas and Sobanjo, 2016), with the Weibull distribution commonly used in lieu of the exponential distribution.

Markov models can be used to predict future condition for specific bridge components and these condition predictions can be amalgamated to predict lifetime indicators for specific structures. These calculations can then be executed across an asset portfolio to inform network decisions. This approach to network level modelling enables the evaluation of the diverse structural configurations that would feature across a bridge portfolio. Additionally, it would be possible to incorporate further factors such as local climate and traffic loading. An alternative approach is to calibrate Markov models that directly predict the number of bridges that are in each condition state across the asset portfolio (Orcesi and Cremona, 2010).

Modelling deterioration to predict future condition is conducted to facilitate life cycle analysis and support an infrastructure manager's asset investment planning. BMS decision support tools have been developed by/for many transportation agencies to aid their asset management practices, as discussed in Section 3.3.1. Many of these BMS utilise Markov chain methodology to model deterioration and predict future condition, including: AASHTOWare Bridge Management (formerly *Pontis*) developed in the United States; KUBA, used in Switzerland; Ontario Bridge Management System (OBMS) used in Ontario, Canada and Quebec Bridge Management System (QBMS) used in Quebec, Canada (Mirzaei et al., 2014; Thompson et al., 1998).

Visual inspections and condition data have their limitations (see Section 3.4.3), however for many infrastructure managers this is the most abundant data source to calibrate models used for network level decision support. Consequently, for many infrastructure asset managers, Markov models have been widely adopted as they are well suited to modelling stochastic processes using a discrete condition scale. Moreover, the nature of many condition longitudinal studies requires the assumption of the memoryless property which is fulfilled in Markovian methods.

Whilst in literature the calculation for TPMs, is routinely shown using frequency

and regression methods, BMSs like Pontis previously used only the frequency approach, with expert judgement used to fill any gaps in the data (Ng and Moses, 1996). In more recent years BMSs such as Pontis and KUBA compute TPMs using regression (Fu and Devaraj, 2008; Roelfstra et al., 2004).

The use of Markov models are quite widespread in literature and industry, however there several limitations of the method to note:

- Markov models inherently assume the memoryless property, which several studies have shown may not be reflective of the physical process (Mishalani and Madanat, 2002; Sobanjo and Thompson, 2011). Consequently, deterioration is modelled as occurring at a constant rate (not necessarily the case for semi-Markov models).

- Probabilities for transitions that have sparse or incomplete data often require value assignment based on the subjective decisions of expert judgement (Frangopol et al., 2004). Moreover, the discrete condition states used at inspection are also vulnerable to the subjectivity of the bridge inspector.

- Careful consideration is required when developing Markov models for network level decision making due to Markov models being vulnerable to combinatorial state space explosion (Norris, 1997). Scherer and Glagola (1994) presented a classification system based on road system, climate and traffic loading to group similar bridges and improve the computational tractability of the problem. However, this resulted in the number of bridges being in particular states and the loss of individual identity for each bridge in the sample portfolio.

- The effects of maintenance interventions are difficult to ascertain and commonly neglected in Markov models. A particular challenge is determining appropriate inclusion/exclusion rules for records which exhibit an improvement in condition (Robelin and Madanat, 2007).

Despite of these limitations, Markov models are the most commonly employed stochastic technique used for bridge deterioration modelling due to their ability to incorporate the inherent randomness of bridge deterioration and their computational efficiency (Morcous, 2006).

Bayesian Belief Networks

BBNs are a type of probabilistic graphical model that enable the incorporation of conditional relationships between variables. The class of methods have been found to be applicable to a range of problems in reliability engineering, risk analysis and maintenance studies in particular for their ability to incorporate expert judgement (Langseth and Portinale, 2007; Weber et al., 2012).

An early example of BBN model being employed to predict bridge condition was introduced by Attoh-Okine and Bowers (2006). The proposed model evaluated the causal influences between different bridge elements and was used to compute the probabilities of being in particular conditions states across a range of different structural hierarchical levels i.e. deck, sub-structure, super-structure and overall. The general structure is shown in Figure 3.7. The root variables in the BBN for bridge elements had a distribution defined for multiple distinct defect states, however the BBN did not model how these defects interacted with each other, nor how they progressed.

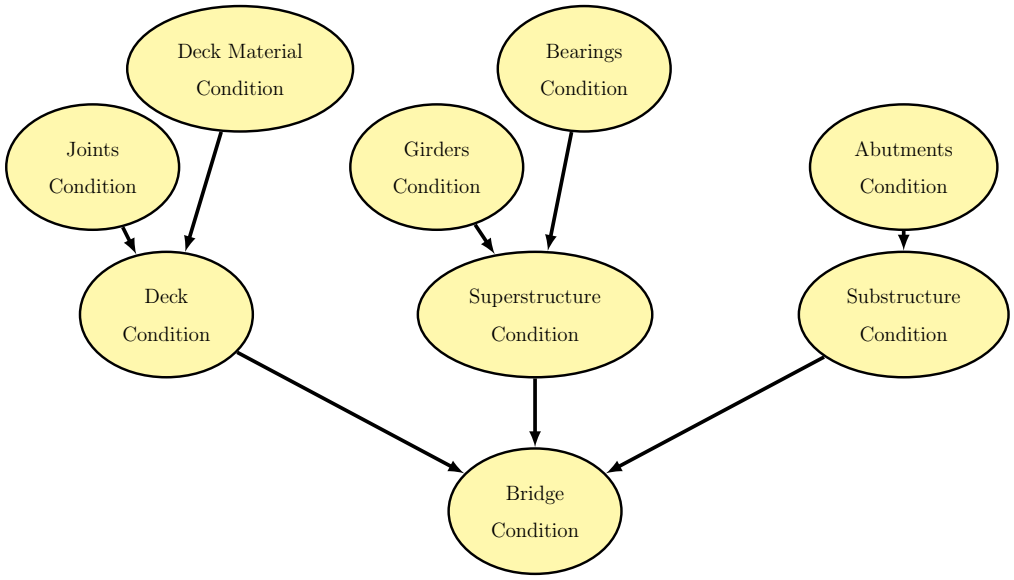

Figure 3.7: Bridge condition BBN (Attoh-Okine and Bowers, 2006).

DBNs extend the capabilities of BBNs over the temporal domain, see Section 2.3.3. DBNs have been successfully applied to reliability and deterioration problems (Foulliaron et al., 2015; Luque and Straub, 2016; Straub, 2009; Weber and Jouffe,

2003) as well as been used in strategy development (Luque and Straub, 2019; Yang and Frangopol, 2018).

Rafiq et al. (2015) developed a DBN model to predict future bridge condition, exploiting a similar hierarchical structure to predict condition for bridge elements and then amalgamate them to the overall structure proposed by Attoh-Okine and Bowers (2006). The inclusion of the temporal relationship between variables enabled the analysis of 'what-if' scenarios in terms of choosing particular maintenance or inspection strategies.

The DBN (Rafiq et al., 2015) was used to model a UK railway masonry arch bridge, which has a well defined structural hierarchy and weighted summation for determining overall condition given the condition of constituent elements. Using the BBN for a particular instance of time, it was possible to perform a sensitivity analysis to determine the influencing effect of different constituent elements' condition on the major element or overall levels. The evaluation of condition was limited to a single condition scale of *Poor, Fair* and *Good*.

An additional bridge deterioration model was developed by Zhang et al. (2017) and Zhang and Marsh (2018) that modelled the sojourn time between condition state transitions with a Weibull distribution. For the prior probabilities, the Weibull distribution was determined by expert judgement. The Weibull distribution was parametrised by hyper-parameters, whereby the shape and scale parameters were characterised by triangular distributions. The triangular distributions for hyper-parameters are used as experts typically prefer giving intervals for values as opposed to point estimates (Scholten et al., 2013). The posterior distribution can be updated upon the availability of failure data. The incorporation of this expert judgement into a BBN model by Zhang and Marsh followed the framework outlined by Marquez et al. (2010). The model also incorporated aggressive environmental factors as outlined by Yianni et al. (2016), alongside having a similar representation of the structural hierarchy as Attoh-Okine and Bowers (2006) and Rafiq et al. (2015).

One presented application of the Zhang and Marsh (2018) model was maintenance planning, however condition was on a single condition scale and the model had not been calibrated using industrial data. Zhang and Marsh (2021) provide ad-

ditional insight into how the BBN approach can be used to improve the inspection and maintenance decision making process, based on evaluating assets composed of multiple components. The BBN models are effective at determining when inspection or maintenance interventions should occur and for applying outcomes, however it is challenging to model the constraints of these processes, i.e. lead times, workforce availability, periodic volume/cost constraints.

To address modelling challenges of limited data for calibrating deterioration models, which have considerable uncertainty, Zhang and Marsh (2020) extended their established BBN framework to calibrate deterioration between groups of similar assets. Moreover, the BBN models in this study were tested using example NBI records from Wyoming, USA and were found to provide better prediction accuracy when compared to Markov models in a constrained data scenario.

An altered DBN framework termed covariate-DBN was applied to a case study of a network of steel bridges in the Netherlands (Kosgodagan-Dalla Torre et al., 2017). The model used Cooke's method (Cooke, 1991) to elicit a structure from experts, such that traffic and load could be incorporated into a bridge element deterioration model. Whilst such factors can influence the rate of bridge deterioration, the bridge condition was monitored using a single, four-point, condition scale. There are several other studies in the literature that calibrate BBN models using expert judgement (LeBeau and Wadia-Fascetti, 2010; Wang et al., 2012).

The modelling of condition for civil infrastructure is commonly performed on a single condition scale moving from a qualitative 'good' state to some 'poor' state. However, civil infrastructure can degrade under many different distinct mechanisms. Elmasry et al. (2017) provides an example of defect based deterioration model, which used a BBN to determine the static probabilities of particular defects occurring on sewer pipelines. Moreover, the study extended the BBN model to a DBN to analyse deterioration temporally.

The application of Bayesian statistical methods for structural reliability predictions is a mature discipline (Enright and Frangopol, 1999; Jacinto et al., 2016; Matos et al., 2016; Ni et al., 2020; Strauss et al., 2008), utilising both past condition data and also measurements from Structural Health Monitoring (SHM) equipment. More-

over, there are examples of BBNs being implemented to make reliability predictions using SHM data (Vagnoli, 2019; Vagnoli et al., 2018). However, the applications of such techniques for network level decision making is challenging as monitoring data is specific to particular bridges and monitoring activities require too many resources to scale to network level currently. Straub and Der Kiureghian (2010a,b) developed a computational framework that combined BBNs and structural reliability methods, which could be used to determine occurrences of rare events for infrastructure systems.

BBNs and associated techniques have an extensive range of applications in reliability analysis, bridge condition prediction and strategy development scenarios. BBNs are often used for their ability to incorporate conditional dependencies between variables and expert judgement in a model. They are a powerful tool for performing '*what-if*' analysis through propagation analysis and for conducting sensitivity analysis between variables. Moreover, BBNs can avoid the state explosion problem that Markov models suffer from (Kabir and Papadopoulos, 2019). Nonetheless, the determination of network structure can be challenging and requires careful consideration, alongside the challenge of calibrating the prior probabilities.

Petri Nets

Petri net (PN) models have been proposed for a diverse range of applications in science, engineering and business studies (Jensen, 1997), and have been shown to be an appropriate technique for deterioration and failure modelling (Andrews, 2013; Andrews et al., 2014; Chew et al., 2008; Kilsby et al., 2017).

Le (2014) and Le et al. (2017) developed a bridge asset management PN model that considered deterioration, inspection and maintenance interventions. The condition of a bridge component was denoted using a maintenance based condition scale, where there were four condition states, '*new*', '*good*', '*poor*' and '*very poor*' that were aligned with the triggering of the maintenance interventions of '*minor repair*', '*major repair*' and '*replace*', see Figure 3.8. The transition times between condition states were calibrated from maintenance records and as a lifetime analysis was performed deterioration could be modelled as a non-constant process using a

Weibull distribution. However, the available maintenance records for model calibration existed for only a small fraction of the entire asset portfolio. Moreover, the use of maintenance records for modelling civil infrastructure are vulnerable to the limitations mentioned in Section 3.4.2.

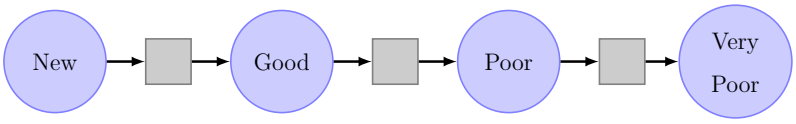

Figure 3.8: Four state bridge deterioration PN model (Le et al., 2017).

In another study, Le and Andrews (2016) proposed modelling bridge condition as a series of different degradation mechanisms, with a different model defined for each material type. Moreover, the condition scale used in this study was defined to both align with maintenance intervention and the conditions revealed from visual inspections. This is possible due to the nature of condition scale used at bridge inspection in the UK, see Tables 3.4 and 3.5 in Section 3.4.3. Le and Andrews (2016) calibrated the model using maintenance data and fitting a Weibull distribution to define condition sojourn times. However, it would be possible to determine transition times from condition records and use those instead.

An alternative Petri net model was proposed by Yianni et al. (2017), that models bridge condition on a two-dimensional scale, where each place denotes a Severity-Extent condition state, i.e. the type of defect present and its extensiveness, see Figure 3.9. Yianni et al. (2017) calibrated their deterioration model using condition records from visual inspection, however the nature of the available data constrained the model calibration to an exponential distribution. Moreover, the model only monitors the score for the worst defect present, disregarding others. An additional study (Yianni et al., 2016), considered the effects that local environmental factors had on deterioration rates and their consequence on the WLCC.

Petri nets are commonly solved using Monte Carlo simulations, however this can be computational expensive. Yianni et al. (2018) shown the applicability of utilising Graphical Processing Units (GPU) to complete Monte Carlo simulations of PN models, exploiting a GPUs parallelisation capabilities and the fact Monte Carlo simulations of PN models are *embarrassingly parallel*. The term embarrassingly

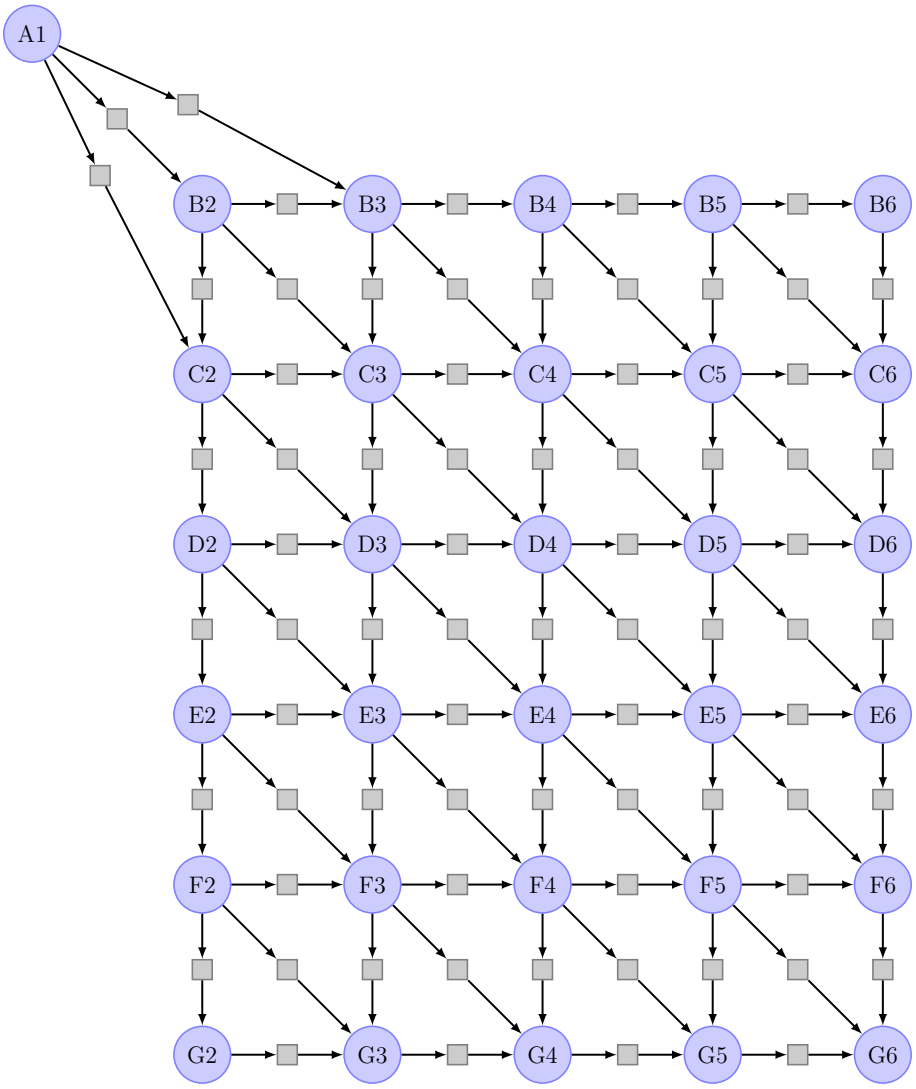

Figure 3.9: Bridge deterioration PN model based on the Network Rail Severity Extent Scale (Yianni et al., 2017).

parallel is used to *"emphasize the fact that, while there is a high degree of parallelism [in the problem] and it is possible to make efficient use of many processors, the granularity is large enough that no cooperation between the processors is required"* (Moler, 1986). Using GPUs to resolve a solution for Petri net, does not necessarily reduce the computational expense, however it does greatly reduce the time required to execute simulations.

Despite the computational expense, PN models have several advantages that include, being able to use an extensive range of stochastic processes to model physical phenomena, simulation of specific instances of states such that specific actions can

be scheduled and modelled and a flexible modelling framework and extensions to model complex processes.

Artificial Intelligence Models

The field of Artificial Intelligence (AI) seeks to "[automate] *activities that we associate with human-thinking, activities such as decision-making, problem solving and learning...*" (Bellman, 1978), moreover, it is "*the study of the design of intelligent agents*" (Poole et al., 1998).

AI covers a diverse range of applications and methodologies with techniques such as Case Based Reasoning (CBR), Artificial Neural Networks (ANN) and backward propagation methods being applied in bridge condition prediction models (Srikanth and Arockiasamy, 2020).

Morcous et al. (2002a,b) modelled bridge deterioration using CBR. CBR is a technique which considers the attributes of previous cases or examples that have similar characteristics to a current problem and applies an appropriate solution accordingly. Consider that a prediction of future condition for a bridge is the query case, with the data for all remaining bridges stored in a case library. The prediction of future condition is obtained by following the four steps of CBR,

1. Retrieve - A search of the case library is performed and case indices are employed to reduce the search space. A similarity measure/function will be assigned to evaluate the similarity between the query case and each case in the case library.

2. Reuse - Upon selecting a case from the case library based on similarity, the properties of the retrieved case are compared to determine how well the retrieved case and the query case map to each other and if any revisions are required.

3. Revise - If the retrieved case does not match the query case perfectly, the retrieved case can undergo 'case adaption', which applies domain expertise to alter the retrieved case to provide a more appropriate solution for the query case.

4. Retain - Any revised cases can be stored in the case library. Moreover, any new data that becomes available from inspection may also be input into the case library. This process is known as 'case accumulation'.

Whilst, CBR is a powerful tool to model bridge deterioration, it can be limited by the size of the case library, an insufficiently detailed case description and the difficulty of determining the most appropriate weights and degrees of similarity. Additionally, the application of domain expert knowledge to the model is a challenging task.

A more common AI technique used to model bridge deterioration are ANNs. ANNs are inspired by biological neural networks and are composed of a set of nodes known as artificial neurons. The set of nodes are arranged in groups forming layers with the nodes in each layer interconnected to nodes in other layers. Several variables can be input into the model in the first layer and with subsequent layers having nodes and arcs, with a defined series of weighted sums, values for particular variables can be returned in an output layer.

Early examples of ANNs being implemented to model bridge deterioration were presented by Sobanjo (1997), Cattan and Mohammadi (1997) and Tokdemir et al. (2000). In the study by Cattan and Mohammadi (1997), ANNs were initially designed to predict values for condition ratings using the physical design properties of the sample bridges as input data e.g. bridge dimensions, number of spans, span dimensions, structure type etc., which returned reasonable prediction accuracy. Later in the paper, ANNs were developed to use analytical ratings for bridges, that were based on empirical measurements, to predict the subjective condition rating. Moreover, it should be noted that the study by Cattan and Mohammadi (1997) had fixed time condition predictions and did not consider temporal evolution. These later models were not as effective in predicting bridge condition, however the paper exhibited the applicability of ANNs for this application if given appropriate data and input parameters.

Effective bridge asset management models require time-series condition predictions, however the selection of a modelling framework is typically limited by the availability of data over a sufficiently long period. It is common that for asset man-

agers with mature bridge stocks, inspection records only exist for the latter stages of a bridge life cycle. In recognition of this problem, Lee et al. (2008) introduced an ANN that could be used to generate records for previous time periods when inspections were not performed. The generation of missing data was achieved using a Backward Prediction Model (BPM) and training the ANN using the limited inspection records that do exist alongside 'non-bridge' factors such as local climate, number of vehicles and population growth in the local vicinity of a bridge. The study yielded reasonable prediction accuracy again, however caution is required when implementing such a method as further insight and research is required when selecting appropriate non-bridge factors. An example of the ANN model is shown in Figure 3.10.

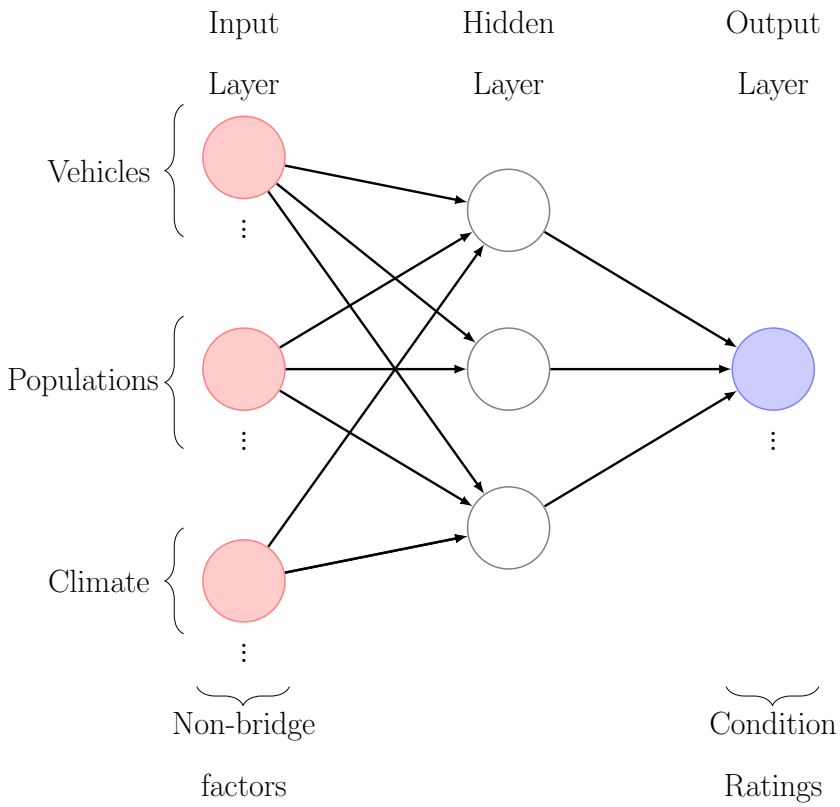

Figure 3.10: Structure of the Lee et al. (2008) AAN.

Bu et al. (2013) utilised the BPM method to generate unavailable historic data and analysed the effect that different numbers of non-bridge factors had on the prediction accuracy of deterioration models. The study calibrated linear and non-linear

regression deterioration models, alongside a Markov-based model and determined that using BPM-generated records in model calibration improved prediction accuracy and that the inclusion of additional non-bridge factors as inputs in the BPM model generate more favourable data for model calibration. An additional study by Bu et al. (2014), also utilised BPM methods to generate historic data and enabled the calibration of appropriate condition transition probabilities for a bespoke probabilistic bridge deterioration model.

An ANN condition model calibrated using maintenance and inspection data from Wisconsin, USA was present by Huang (2010). The model incorporated 11 significant factors that could influence deterioration including: deck age, maintenance history, previous condition, geographical location, average daily traffic, environment, deck length, deck area, design load, degree of skew, and number of spans. An interesting result from the study was that deck age and maintenance history were both statistically significant factors that influenced the deterioration process, which indicates that the assumptions required for Markov models, i.e. condition is independent of age and history, may be invalid.

Callow et al. (2013) proposed a novel hybrid optimisation method for AI based deterioration models that also consolidated many of the aforementioned AI models into a single process. The presented process had three stages:

- Stage 1: Generation of missing condition ratings - Any missing historic condition records were generated using the BPM technique.

- Stage 2: Optimisation of the condition ratings - CBR and Genetic Algorithms were used to optimise the query case and determine optimal input parameters for the next stage.

- Stage 3: Long term prediction of condition ratings using optimal condition rating scenarios. - A Time-Delay Neural Network (TDNN) was employed to predict long term condition predictions.

Chojaczyk et al. (2015) provide a review of ANN models used in structural reliability analysis, however the models considered are primarily focused on empirical

structural properties opposed to calibrating models for network decisions using condition records.

Deep learning models employ multiple processing layers to aid in the representation of data with multiple levels of abstraction (LeCun et al., 2015) and are commonly used for pattern classification and feature learning. Convolutional Neural Networks (CNN) or (ConvNet) are a type of ANN that comprise at least one convolution operation as a layer. CNNs have been widely applied to computer vision problems but increasingly find applications in structural health monitoring, for example in crack damage detection (Cha et al., 2017; Zhang et al., 2019). Liu and Zhang (2020) developed a CNN model for predicting bridge conditions for a time-dependent reliability analysis. The CNN model was calibrated using historical NBI data from the Maryland and Delaware highway bridges and incorporated 24 features including condition ratings, geographic properties, structural configuration and other attributes such as traffic and bridge age. The study found that with sufficient data, the trained CNN model is an effective technique for incorporating a plethora of factors in condition prediction, with the case study returning prediction accuracies of over 85% when tested on independent datasets.

Fiorillo and Nassif (2019) investigated the efficacy of five machine learning techniques for mapping indexes for bridge elements to NBI condition ratings for decks, superstructures and substructures. All techniques were found to yield relatively high predictive accuracy for predicting NBI ratings within ± 1 state, with the accuracy ranging between 79.8% and 100%. A method known as as the k-nearest neighbour classifier was found to be the most accurate technique of the methods considered. However, the authors concede that the study did employ an exhaustive list of techniques that can be found in literature. Fiorillo and Nassif (2020b) then employed a CNN model to map indexes for bridge elements to the NBI ratings and yielded an improved prediction accuracy. The mapping between elements and NBI ratings enables deterioration profiles to be set for elements that only have records for a short period of time. A further analysis by Martinez et al. (2020) of classification models for predicting future bridge condition found that all of the models considered in the study could predict the bridge index with a relative error of less than 1%.

AI methods are a versatile class of techniques that can be used to populate records for sparse data sets and develop deterioration models that encapsulate a plethora of different factors of inputs to tailor the predicted outputs for specific scenarios. Moreover, AI enables extensive analysis capabilities for different inspection and maintenance strategies given the inclusion of structural and non-structural factors. Nonetheless, whilst AI models can be computationally cheap when they have been trained, the training process can be computational expensive. Moreover, appropriate application of AI domain expertise is required to ensure that improved model outcomes are due to the model being more reflective of the physical phenomena rather than solely due to the increased parametrisation. Additionally, the calibration of an AI model is contingent on sizeable dataset for particular variables to generate missing condition records or to predict future condition records.

3.5.3 Modelling Summary

Deterministic models are relatively straightforward to calibrate and implement for informing condition predictions and decision making. However, such models evaluate deterioration neglecting the uncertainty of the process and provide the same outcome for any given initial condition state. Moreover, deterministic models are more effective in determining event outcomes for 'worst case' scenarios (Stewart, 2001). Deterministic models are well suited for modelling measurable physical indicators, however as aforementioned such metrics are difficult to deploy for network level decision making.

The use of stochastic models for evaluating life cycle performance of deteriorating bridges were identified by Frangopol et al. (2004) as being an effective means of modelling the uncertainty of deterioration and such techniques have been widely recorded in literature and applied in industry. A range of methods were reviewed:

- Time-based models represented a versatile approach for modelling bridge deterioration, in particular for their ability to assume a range of different probability distributions. Moreover, expressions exist such that distinct structural components can be modelled distinctly but then appropriately amalgamated into an overall value for the entire structure. Time-based models are the

basis of many deterioration modelling frameworks, however are commonly parametrised in a different methodological framework to facilitate inspection and intervention modelling, e.g. as the distribution defining the firing delay for a transition in a Petri net model.

- Markov chains are widely favoured as they are relatively computationally cheap to implement and are well suited to model discrete state condition scales. However they require the assumption of the memoryless property which has been shown in multiple studies to be non-reflective of the physical reality of bridge deterioration and they suffer from combinatorial state explosion.

- BBN/DBN models are favoured for their ability to easily incorporate expert knowledge and causal influences, however they also suffer from assuming the memoryless property.

- Petri nets are a very flexible modelling methodology, which enables the bespoke development of sophisticated process modelling for deterioration as well as inspection and intervention planning. Petri nets are commonly resolved using Monte Carlo simulations, which is expensive to deploy for network level decision making, however research has been conducted to determine manageable ways of computing solutions.

- The greatest strength of AI techniques is that they can utilise a diverse range of data sources to predict indicators and the techniques can be used to determine predictions for contextualised problems. However, the calibration or training of AI models can require a considerable amount of data in general, but also for time series data to have been captured over a long period of time which is not ordinarily available for many infrastructure managers.

3.6 Chapter Summary

The use of modelling in life cycle performance evaluation has been identified as being critical to supporting asset managers' decision making. An extensive body of research has been reviewed for the performance evaluation of bridges and bridge

portfolios, which included metrics for structural reliability, risk, utility, sustainability and life cycle cost. However, it can be concluded that the structural reliability of a bridge is not only important in its own right but also drives the performance of the other metrics. Moreover, for prediction purposes it is critical that structural reliability is understood on the temporal domain.

Structural reliability has analytical expressions that are derived from the physical phenomena of structural loading capability. However, for network level modelling and decision making, these expressions are too computationally expensive alongside there being insufficient data to calibrate models. Thus, the temporal evolution of structural reliability is commonly modelled using a proxy indicator, that is selected based on available data and an appropriate modelling framework. Section 3.4 evaluated data sources that are commonly available to bridge asset managers and determined despite its limitations, condition data from visual inspections remains the most readily available and appropriate data type for model calibration. Section 3.5 proceeded to evaluate the different modelling techniques that can be used to model the deterioration of bridge or structural component. The techniques considered included deterministic methods and a range of stochastic methods including: time-based models, Markov models, Bayesian networks, Petri nets and Artificial Intelligence techniques. An evaluation of the advantages and disadvantages of each stochastic modelling method was outlined in Section 3.5.3. However, there should be no recommendation of the most appropriate technique as to do so would require an understanding of the decision/problem being addressed and the data that is available.

For life cycle modelling of bridges or their structural components, there is a plethora of techniques that have been proposed. However, further work is required in developing 'blended approaches', whereby multiple methods can be used simultaneously, with each process having the most appropriate method implemented. For example, using an AI technique, such as a Mixture Density Network, to incorporate multiple data sources to predict future asset condition, with Petri nets used to model inspection and intervention due to their techniques flexibility in developing bespoke modelling solutions. Additionally, efforts should be made to predict mul-

tiple indicators beyond an arbitrary single condition scores, for example indicators for the distinct deterioration mechanisms, or indicators aligned with outputs from monitoring equipment.

Finally, there should be more continual evaluation of the life cycle problem, adhering to frameworks such as the PPDAC cycle. In particular, there has been considerable research conducted to develop and evaluate modelling techniques for bridge deterioration, however there has been limited revaluation of the decision making problem and collection of different data sources across entire asset portfolios in recent years. Future development of bridge deterioration modelling for network level decision making will not succeed by methodology development alone but rather a holistic problem-based approach.

Chapter 4

Modelling Multiple Deterioration Mechanisms

In Chapter 3 it was outlined that whilst there are a variety of deterministic and stochastic modelling approaches for bridge asset management at network level, stochastic modelling is more advantageous for modelling structural deterioration (Frangopol et al., 2004). These stochastic models can be calibrated using a variety of data sources including condition data from visual inspections, maintenance records and empirical data. Whilst condition data does not necessarily reflect the integrity of a load bearing structural element (Liu and Frangopol, 2006; Neves and Frangopol, 2005; Saydam et al., 2013), maintenance interventions should typically be prioritised to bridges with unacceptable and poor condition rating levels. Moreover, condition records are typically the most abundant source of data across an entire portfolio of assets and their use is the most common for calibrating deterioration models (Frangopol et al., 2017).

Bridges can degrade under a variety of different deterioration mechanisms, consequently any scale that seeks to consolidate the different deterioration modes into one condition index will have a level of subjectivity and arbitrariness. Ceravolo et al. (2009) proposed 'symptom-based' reliability models to overcome the limitations of ad hoc reliability indexes and to incorporate engineering knowledge gained from structural monitoring activities. However, the empirical measurements required for such models are often not available across large, diverse asset portfolios.

The research presented in this chapter introduces an approach for modelling the multiple different deterioration modes, such that more comprehensive predictions of bridge condition can be made. The simultaneous modelling of multiple defect mechanisms in a deterioration model will facilitate the development of more detailed decision models that can evaluate maintenance strategies based on particular defect types rather than the traditional ambiguous repair actions (e.g. minor repair, major repair and replacement).

It should be noted that the service life of civil infrastructure is characterised in part by the effects of progressive deterioration and sudden deterioration (Guo et al., 2020; Yang and Frangopol, 2019). Progressive deterioration describes the development of various defect mechanisms and sudden deterioration is the result of hazards such as earthquakes, fires and floods, amongst others. The models described in this chapter are used to predict progressive deterioration behaviour and they do not model sudden deterioration outright. Nonetheless, the modelling of distinct defect mechanisms permits the evaluation of how vulnerable a structure may be to sudden deterioration.

4.1 Masonry Multiple Defect Deterioration Model

4.1.1 Condition Records

Bridges are heterogeneous assets and the composition of each asset can vary greatly. However, to ensure there is a standardised approach for data collection across a portfolio of bridges, the structural configuration of a bridge can be expressed using a defined hierarchical decomposition. For example, a bridge inspected by Network Rail will be described by its composition of minor elements and major elements. Major elements include: inner supports, end supports and decks, and each major element is composed of a set of minor elements. Moreover, each minor element type may be assigned the status of being a '*principal load bearing element*'. At each detailed examination of a bridge, a condition will be recorded for each minor element on the bridge asset. Network Rail use an alpha-numeric condition scale known as Severity Extent (SevEx) to record the observed condition of the elements

of bridges at a detailed inspection. The SevEx scale is similar to the scale outlined in Highways Agency (2007a), as shown in Tables 3.4 and 3.5. However, at Network Rail the letter grade indicates the severity score and the number grade indicates the extent score.

Network Rail manage a diverse range of bridge assets in their portfolio that are constructed out of many different material types. The condition records indicate the primary material of a minor element and example denoted materials include: concrete, metal, masonry, timber and composites. The primary material of a minor element is recorded as the SevEx scale is defined differently for particular materials.

The definition for each severity score for a masonry bridge element aligns with a different defect mode. The possible defects that can be observed are: shallow spalling, deterioration of pointing, deep spalling, hollowness/drumming, loose or missing block work from the surface of bridge element and displaced or missing blockwork to the full depth of the element. The extent score details the coverage of the observed defect on the bridge element. Full definitions for the severity and extent scores can be found in Tables 4.1 and 4.2 respectively.

At inspection, each element is assessed and any defects can be assigned an alpha-numeric score on the SevEx scale. All the possible masonry SevEx scores range from A1 (no visible defect) to F6 (over 50% of the element surface having displaced or missing blocks), forming

$$\begin{aligned}\mathcal{C} =\{&A1, B2, \dots B6, C2, \dots, C6, \dots D2, \dots, D6,\\ &E2, \dots, E6, EX2, \dots, EX6, F2, \dots, F6\}.\end{aligned} \tag{4.1.1}$$

At each inspection, for each bridge element, the two 'worst' scores are recorded alongside the date of the inspection. When several inspections have taken place on the same bridge, the repeated observations form a longitudinal study. The longitudinal study can be split into 'exam pairs' and stated in the following format for n exam pairs,

Record	**Inspection 1**		**Inspection 2**		**Time Interval**
	SevEx 1	SevEx 2	SevEx 1	SevEx 2	(Years)
r_i	$\alpha_{i,1}$	$\beta_{i,1}$	$\alpha_{i,2}$	$\beta_{i,2}$	t_i

Table 4.1: SevEx severity definitions for masonry bridge elements.

Score	Severity Definitions
A	No visible defects to masonry. (Cracks are scored separately.)
B	Brickwork - depth of spalled and weakened/softened material < 10 mm. Stonework - depth of spalled and weakened/softened material < 20 mm. Or any evidence of the presence or effect of water (defined as percolation, run-off, etc).
C	Deterioration of pointing. (Record the maximum and typical depth lost.)
D	Brickwork - depth of spalled and weakened/softened material ≥ 10 mm but less than the depth of a header. Stonework - depth of spalled and weakened/-softened material ≥ 20 mm but less than the depth of a block.
E	Hollowness/Drumming. (Not associated with B or D.)
EX	Includes all incidences of: loose/wedged bricks/blocks - not displaced, loose/wedged bricks/blocks - displaced but not to the full depth of the structural element or missing brick/blocks - one or more, but not to the full depth of the structural element.
F	Choose most extensive from: bulging, distortion tilting (vertical alignment), displacement: loose and/or wedged displaced bricks/blocks to the full depth of the element or missing brick/block to the full depth of the element.

Table 4.2: SevEx extent definitions for masonry bridge elements.

Score	Extent Definitions
1	No visible defects to masonry (cracks are scored separately).
2	Localised defect due to local circumstances (such as mechanical damage).
3	Defect occupies less than 5% of surface of the structural element.
4	Defect occupies 5% to 10% of the surface of the structural element.
5	Defect occupies 10% to 50% of the surface of the structural element.
6	Defect occupies more than 50% of surface of the structural element.

where $i = 1, \ldots, n$ and $\alpha_{i,j}$ is the worst score at the j^{th} inspection, $\beta_{i,j}$ is the second worst score at the j^{th} inspection, $\alpha_{i,j}, \beta_{i,j} \in \mathcal{C}$ and $t_i \in \mathbb{R}, 0 < t < 18$. This process is repeated for all bridge elements that have had multiple inspections and the resulting tables are pooled into one data set.

The historic condition records are filtered to only include records which exhibit stationary behaviour or deterioration, i.e. $\{\alpha_{i,1}, \beta_{i,1}\} \leq \{\alpha_{i,2}, \beta_{i,2}\}$. Pairs of inspections that exhibit extreme cases of deterioration are also omitted as the deterioration is deemed to be the result of sudden deterioration rather than gradual deterioration. Extreme deterioration is identified using defined thresholds of reduction in the Bridge Condition Marking Index, as outlined by Network Rail.

4.1.2 Masonry Multiple Defect Condition States

To leverage the SevEx condition scale for any potential multiple defect model, some adaptations to the scale are required. The SevEx scale has the overall state of no defect defined as $A1$, whereas for multiple defect modelling a no defect state is required for each defect i.e. $A1 \rightarrow \{B1, C1, D1, E1, EX1, F1\}$. Thus, the SevEx conditions states for each defect type are as follows: $\mathcal{B} = \{B1, \ldots, B6\}$, $\mathcal{C} = \{C1, \ldots, C6\}$, $\mathcal{D} = \{D1, \ldots, D6\}$, $\mathcal{E} = \{E1, \ldots, E6\}$, $\mathcal{EX} = \{EX1, \ldots EX6\}$ and $\mathcal{F} = \{F1, \ldots, F6\}$. The inspection records for a multiple defect panel *should* be in the following format for all n records ($i = 1, \ldots, n$),

Record	**Inspection 1**						**Inspection 2**						**Interval**
	B	C	D	E	EX	F	B	C	D	E	EX	F	(Years)
r_i	$B_{i,1}$	$C_{i,1}$	$D_{i,1}$	$E_{i,1}$	$EX_{i,1}$	$F_{i,1}$	$B_{i,2}$	$C_{i,2}$	$D_{i,2}$	$E_{i,2}$	$EX_{i,2}$	$F_{i,2}$	t_i

where B_{ij} is the condition of Defect B in the j^{th} inspection of the i^{th} record with $B_{ij} \in \mathcal{B}$. C_{ij}, D_{ij}, E_{ij}, EX_{ij} and F_{ij} are described similarly. However, at each inspection only the two worst severity scores are recorded.

4.1.3 Score Ranking

The current format of inspection records contains the two worst scores; for any score inference, a definition of what ranking is used to determine worst scores is required. However, how the worst scores are defined is unclear, and consequently two candidate rules were considered:

- **Rule One**: The SevEx scores are ranked according to severity score, followed by the extent score, and thus the rule has the following order of precedence: $A1 < B2 < \cdots < B6 < C2 < \cdots < C6 < D2 < \cdots < D6 < E2 < \cdots < E6 < EX2 < \cdots < EX6 < F2 < \cdots < F6$.

- **Rule Two**: The SevEx scores have a numerical weight which is used in a Bridge Condition Marking Index (BCMI) calculation. Using the BCMI weight a 1D integer condition scale could be created to rank the different SevEx scores. The integer scale value for each SevEx score is shown in Table 4.3. Under this ranking, there are still possible cases were a tie-break rule would need to be developed.

Table 4.3: Network Rail assigned integer condition scale score for each SevEx score.

Severity \ Extent	**1**	**2**	**3**	**4**	**5**	**6**
B	1	2	2	3	4	5
C	1	4	4	5	6	7
D	1	7	7	8	11	12
E	1	7	9	11	13	14
EX	1	7	9	11	13	14
F	1	7	10	12	14	15

Documentation compiled by Network Rail describing the condition scores of bridges used at examinations states that the two most severe defects should be recorded at each inspection, and that the same severity rating can not be used

more than once (Network Rail, 2010). Moreover, the guidance for bridge inspectors states that with an ageing masonry bridge stock it would be rarely appropriate to categorise a bridge element as $A1$, and thus a minor defect, even if it is with little structural significance, should be reported. After consultation with Network Rail bridge engineers it was determined that the bridge inspectors adhere to rule one when determining the two worst scores to record for a bridge element at inspection. The use of the rule one avoids the arbitrary conversion weightings which rule two relies on. Moreover, the proposed methodology is applicable to any score ranking method.

Masonry Multiple Defect Score Inference

Score inference can be performed on the historic inspection records, to express the recorded score panel as a multiple defect inspection panel as fully as possible. Recall that for the i^{th} record, the worst score recorded at inspection j is given by $\alpha_{i,j}$, and the second worst score is denoted by $\beta_{i,j}$. Then, $Sev(\alpha_{i,j})$ denotes the severity score of the SevEx score of $\alpha_{i,j}$, similarly $Ex(\alpha_{i,j})$ denotes the extent score of the SevEx score of $\alpha_{i,j}$.

If the score panel at inspection is reported as, $\alpha_{i,j} = A1$ and $\beta_{i,j} = A1$ then the multiple defect panel will be $\{B1, C1, D1, E1, EX1, F1\}$. In the situation that a score panel of $\beta_{i,j} = A1$ and $\alpha_{i,j} \neq A1$ is reported at inspection, the multiple defect panel would have five defects that have an extent of one, the severity score of these five would be all γ that satisfy,

$$(\gamma \in \{B, C, D, E, Ex, F\}) \wedge (Sev(\alpha_{i,j}) \neq Sev(\gamma)). \tag{4.1.2}$$

For the one defect that has an extent score greater than one, which is $Sev(\alpha_{i,j})$, the extent score would be $Ex(\alpha_{i,j})$.

Finally, if an inspection is recorded such that $\alpha_{i,j} \neq A1$ and $\beta_{i,j} \neq A1$, it is still possible to make some assertions on the unobserved defects. The score inference relies on the assumption that, if an inspection score panel does not contain a high severity score, it must be due to the high severity defect being absent, otherwise the bridge examiner should have recorded the presence of that defect instead of the lower

severity defect. The ranking rule selected states that: $B < C < D < E < EX < F$. Consider the i^{th} record at the j^{th} inspection, where $\alpha_{i,j}$ and $\beta_{i,j}$ are known SevEx scores and they have two different severity scores, i.e. $Sev(\alpha_{i,j}) \neq Sev(\beta_{i,j})$. If a candidate score value is denoted as $\gamma_{i,j}$, then there are four possible severity scores that were not recorded at inspection but could possibly be inferred, i.e.

$$(Sev(\gamma_{i,j}) \notin \{Sev(\alpha_{i,j}), Sev(\beta_{i,j})\}) \wedge (Sev(\gamma_{i,j}) \in \{B, C, D, E, EX, F\}). \quad (4.1.3)$$

For each of the four severity values $\gamma_{i,j}$ can assume, an attempt of inferring the extent score can be sought by using the following inference rules:

$$\text{If } Sev(\gamma_{i,j}) > Sev(\alpha_{i,j}), \text{ then } Ex(\gamma_{i,j}) = 1. \quad (4.1.4)$$

$$\text{If } Sev(\gamma_{i,j}) < Sev(\alpha_{i,j}) \text{ and } Sev(\gamma_{i,j}) > Sev(\beta_{i,j}), \text{ then } Ex(\gamma_{i,j}) = 1. \quad (4.1.5)$$

Alternatively, if $Sev(\gamma_{i,j}) < Sev(\alpha_{i,j})$ and $Sev(\gamma_{i,j}) < Sev(\beta_{i,j})$ then $Ex(\gamma_{i,j})$ is unknown, otherwise $Ex(\gamma_{i,j}) = 1$. In other words, a more severe defect is not recorded if it is absent, while a less severe defect could be absent independent of its extent score.

Masonry Inference Examples

Consider the example panel data in Table 4.4, which can be explicitly defined as a multiple defect panel using the score inference rules, shown in Table 4.5. Both Records 1 and 2 can be explicitly defined as multiple defect panels, with Record 1 using the first score inference rule, (4.1.4) and Record 2 using both score inference rules, (4.1.4), (4.1.5). From Records 3 and 4 it can be observed that the multiple defect panel may not always be explicitly defined. For example, for inspection 1 of record 3, defects with severity scores D and EX were found. Consequently, any defect with severity score B or C would be excluded for being less severe, independently of extent. In the cases where a multiple defect panel is not explicitly defined, the inspection pair for a severity score can only be used in any data analysis if an extent score exists for the defect type at both inspections.

Table 4.4: Example bridge inspection panel data using NR's SevEx condition scale.

Record	Exam Inspection 1		Inspection 2		Time Interval
	$\alpha_{i,1}$	$\beta_{i,1}$	$\alpha_{i,2}$	$\beta_{i,2}$	(Years)
1	$C3$	$B2$	$C5$	$B3$	6.34
2	$E2$	$B3$	$E3$	$B6$	6.12
3	$EX2$	$D3$	$EX3$	$E4$	5.79
4	$F2$	$EX4$	$F2$	$EX5$	7.26

Table 4.5: Inferred multiple defect panel, using the score inference rules on the example bridge inspection panel data from Table 4.4. Dashes denote unknown scores.

Record	Inspection 1						Inspection 2						Time Interval (Years)
1	$B2$	$C3$	$D1$	$E1$	$EX1$	$F1$	$B3$	$C5$	$D1$	$E1$	$EX1$	$F1$	6.34
2	$B3$	$C1$	$D1$	$E2$	$EX1$	$F1$	$B6$	$C1$	$D1$	$E3$	$EX1$	$F1$	6.15
3	–	–	$D3$	$E1$	$EX2$	$F1$	–	–	–	$E4$	$EX3$	$F1$	5.79
4	–	–	–	–	$EX4$	$F2$	–	–	–	–	$EX5$	$F2$	7.26

Generally, the 'lower' severity scores will become unobserved when the bridge element exhibits 'higher' severity scores. Thus, any model will make the assumption that the rate of deterioration estimated for the lower severity scores which were observed continues to hold true when they become unobserved. As current industry practice is to base maintenance scheduling models off the worst score, this is seen as a reasonable assumption given the data available. However, in the future, Network Rail intend to record inspections by tracking particular defects by a unique identifier. This updated recording regime will make the whole multiple defect score panel observable all of the time and result in the score inference rules and deterioration behaviour assumption no longer being required.

Merging of Extent Scores

Whilst analysing the inspection records, it became clear that an extent score of 2, i.e. $\{B2, C2, D2, E2, EX2, F2\}$, was underutilised by bridge examiners. It was also apparent that the low number of observed records with extent score equal to 2 was common across all severity scores. The under reporting of this score could be due to the sojourn time of this condition state being considerably shorter than any inspection interval.

However, it was determined that a more likely explanation was the fact that an extent score of 2 and 3 are very similarly defined; extend score 2 is defined as, '*Localised defect due to local circumstances*' and extent score 3 defined as '*Defect occupies less than 5% of surface of the structural element*'. Thus, if a defect is not present it would be assigned $Ex(\alpha_{i,j}) = 1$, whereas if there is some defect but its' coverage is less than 5% of the surface, bridge inspectors are being cautious and assigning an extent score of 3.

To address the potential for any erroneous errors due to this, the extent scores of 2 and 3 were merged, with the extent scores used in this study defined in reference to the Network Rail extent scores, as shown in Table 4.6.

Table 4.6: The extent scores used in this study in reference to the NR extent scores.

	NR Extent Score					
	1	2	3	4	5	6
Study Extent Score	1	2	2	3	4	5

4.1.4 Masonry Deterioration Model

Due to the constraints of the data, discussed further in Section 4.1.5, it was determined that a continuous time Markov chain would be the most appropriate modelling technique. The proposed multiple defect deterioration model is shown in Figure 4.1. The predictive model reports the probability of an extent score for each of the six

severity scores, which for masonry bridges aligns with the extent of each of the six different defect types.

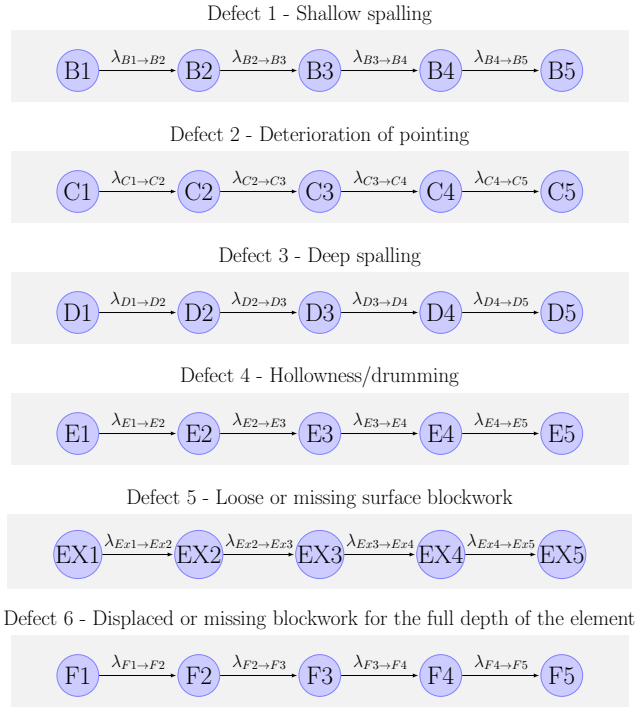

Figure 4.1: Multiple defect deterioration Markov model.

The transition rate matrix for severity B is described by,

$$Q_B = \begin{array}{c} \\ B_{1,j} \\ B_{2,j} \\ B_{3,j} \\ B_{4,j} \\ B_{5,j} \end{array} \begin{array}{c} \begin{array}{ccccc} B_{i,1} & B_{i,2} & B_{i,3} & B_{i,4} & B_{i,5} \end{array} \\ \begin{pmatrix} -\lambda_{B_1,B_2} & \lambda_{B_1,B_2} & 0 & 0 & 0 \\ 0 & -\lambda_{B_2,B_3} & \lambda_{B_2,B_3} & 0 & 0 \\ 0 & 0 & -\lambda_{B_3,B_4} & \lambda_{B_3,B_4} & 0 \\ 0 & 0 & 0 & -\lambda_{B_4,B_5} & \lambda_{B_4,B_5} \\ 0 & 0 & 0 & 0 & 0 \end{pmatrix} \end{array}. \tag{4.1.6}$$

The model described by (4.1.6) makes the assumption that a bridge element can only degrade instantaneously to an extent score of one more than the current extent score. The inability to make an instantaneous transition of more than one extent score is considered to be a more realistic representation of the physical process of bridge deterioration, as the defects will exhibit continuous growth. Moreover, the inability of the model to make 'state jumps' is deemed to be a helpful attribute to avoid the model being over-fitted to the data.

The transition rate matrices, Q_C, Q_D, Q_E, Q_{EX} and Q_F for severity scores C, D, E, EX and F respectively, are similarly described as Q_B. Thus, the entire model is described by the following transition rate matrix,

$$Q_{MD} = \begin{bmatrix} [Q_B] & & & & & \\ & [Q_C] & & & & \\ & & [Q_D] & & & \\ & & & [Q_E] & & \\ & & & & [Q_{EX}] & \\ & & & & & [Q_F] \end{bmatrix}. \tag{4.1.7}$$

The continuous time Markov chain approach as used in this study, assumes that there is no additional information of the bridge condition, or timing of condition transitions between the discrete observation times. However, the model does not implicitly assume that the bridge element will remain in its most recently observed condition state until an inspection reveals it to be otherwise. This model assumption is deemed to be reflective of the physical reality of continuous bridge deterioration. Notwithstanding, in a model that applied maintenance strategy, an inspection regime must be considered to reveal condition rather than assume a continuously reviewed state. However, the purpose of this model is to parameterise the deterioration mechanisms under a do-nothing maintenance strategy.

Methods such as partially-observable Markov processes can be used to incorporate the variability of inspections (Frangopol et al., 2004). However, the quantification of the inspection variability was deemed to be beyond the scope of this study. Additionally, there are several other organisations and agencies globally that use bridge condition scales akin to SevEx, however they may have different inspection regimes. The purpose of this model is to be as general as possible for maximum applicability as well as provide insight into the novel idea of modelling bridge degradation by defect group opposed to the traditional single condition index approach.

4.1.5 Parameter Estimation

Network Rail has a vast portfolio of bridges and the time and expense required to inspect is significant. The earliest record inspection record that Network Rail have

for a bridge asset is from 1999. Between 1999 and 2017, of the bridge elements that have had multiple inspections, 57.25% have had two inspections, 34.28% have had three and 8.47% have had four or more inspections.

Considering a structural element that has been inspected multiple times over a period of time; a record can be produced detailing the element's condition over time. An example of is shown in Figure 4.2a. The time-based approach considers the time it required to move from one condition to another, so the specific element records are used to determine the number of condition transitions for each observed time interval. An example of amalgamated records is shown in Figure 4.2b.

Many of the masonry bridges in the Network Rail portfolio were constructed during the Victorian era in the 19^{th} century (McKibbens et al., 2006), and thus have had an active service life of over 100 years in most cases. As there is an extensive gap between the construction of the masonry bridges in the Network Rail portfolio and the first recorded inspections as well as the maintenance interventions records, it was deemed that the use of bridge age to compute time-dependent transition rate matrices as shown in Kallen and Noortwijk (2006), would be inappropriate for the available data.

The approach used to produce Figure 4.2b is unsuitable for Network Rail records due to the size of the inspection intervals. When an second inspection shows deterioration from the first inspection, the inspection interval can not be assumed to be the exact time it took for that degradation to occur. As the inspection interval can be several years, it is impossible to ascertain how long the bridge element has been in the worse condition state before the inspection took place. An example of this is shown in Figure 4.3a.

Additionally, due to the large inspection intervals and lack of continuous monitoring, one can not deduce the route between the initial inspection and the second, if there is a score difference greater than one. For example, if the first inspection recorded a 1, and the second a 3, the route of deterioration is unrevealed. Moreover, as the deterioration route is unrevealed, one does not know whether the bridge condition degraded from condition 1 to condition 2 to condition 3 or from condition 1 directly to condition 3 (see Figure 4.3b).

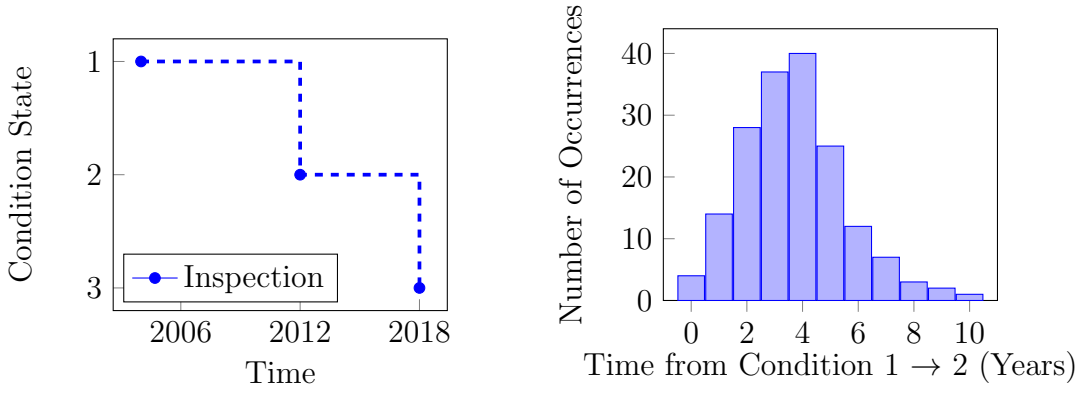

(a) An example of the history of an example bridge element, with inspections marked by dots.

(b) An example distribution of the different times for a bridge element to degrade from one condition to another.

Figure 4.2: An example between using historic inspection records to analyse a specific elements and a group of elements.

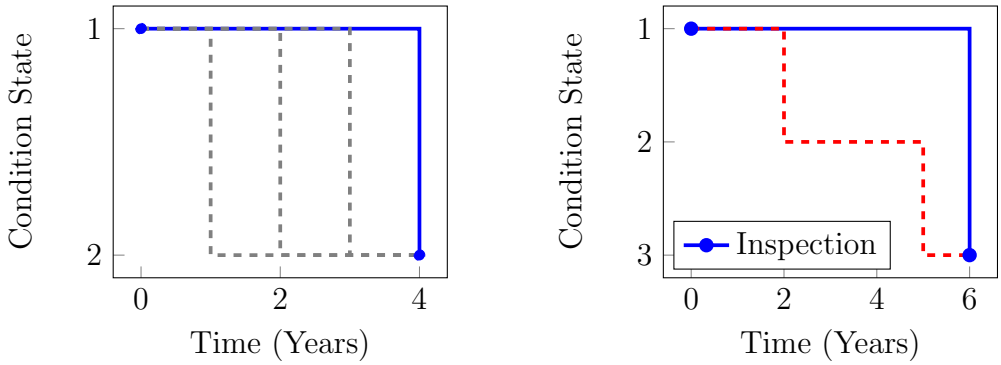

(a) An example of the various ways an element can degrade in discrete time.

(b) An example, showing the various ways an element can degrade between multiple condition scores.

Figure 4.3: Example plots showing the uncertainty in deterioration paths during the inspection interval and between the revealed condition states.

The censoring of time intervals and unknown deterioration paths are due to the data being a form of panel data or a longitudinal study. To address these issues a memoryless distribution is employed which does not require information on the previous histories of condition. A common implementation of this is to use discrete time Markov chains.

The estimation of parameters of a distribution describing bridge deterioration need to consider the defined frequency of inspections. In some organisations and jurisdictions the inspection intervals are a fixed size, which allows for the TPM to be computed. The number of records that show a transition from condition i to condition j is denoted as $n_{i,j}$. The probability $p_{i,j}$ of a transition from condition i to j can be computed by the following,

$$p_{i,j} = \frac{n_{i,j}}{n_i}, \tag{4.1.8}$$

where n_i is the sum of all inspections pairs which have an initial condition of i. When time is known to be both fixed and constant for all observations, $p_{i,j}$ has been shown to be a Maximum Likelihood Estimator (MLE) (Frankel, 1988). The changes in the probability distribution of a portfolio, $\mathbf{C}$, with N condition states, from time 0, to t, can be derived from the Chapman-Kolmogorov equation,

$$\begin{bmatrix} c_1^t & c_2^t & \dots & c_N^t \end{bmatrix} = \begin{bmatrix} c_1^0 & c_2^0 & \dots & c_N^0 \end{bmatrix} \begin{bmatrix} p_{1,1} & p_{1,2} & \cdots & p_{1,N} \\ 0 & \ddots & \ddots & p_{2,N} \\ \vdots & \ddots & \ddots & \vdots \\ 0 & 0 & 0 & 1 \end{bmatrix}^t, \tag{4.1.9}$$

where c_i^t is the probability of being in state i at year t.

For the Network Rail bridge portfolio the size of interval between detailed inspections is determined by the condition of the overall bridge at its previous inspection or if observations made at an annual visual inspection result in a detailed inspection being required. For example, stone bridges are categorised into lower, medium and high risk categories with medium and high risk bridges inspected every 6 years and low risk bridges every 12 years (Network Rail, 2014a). Additionally, curved or

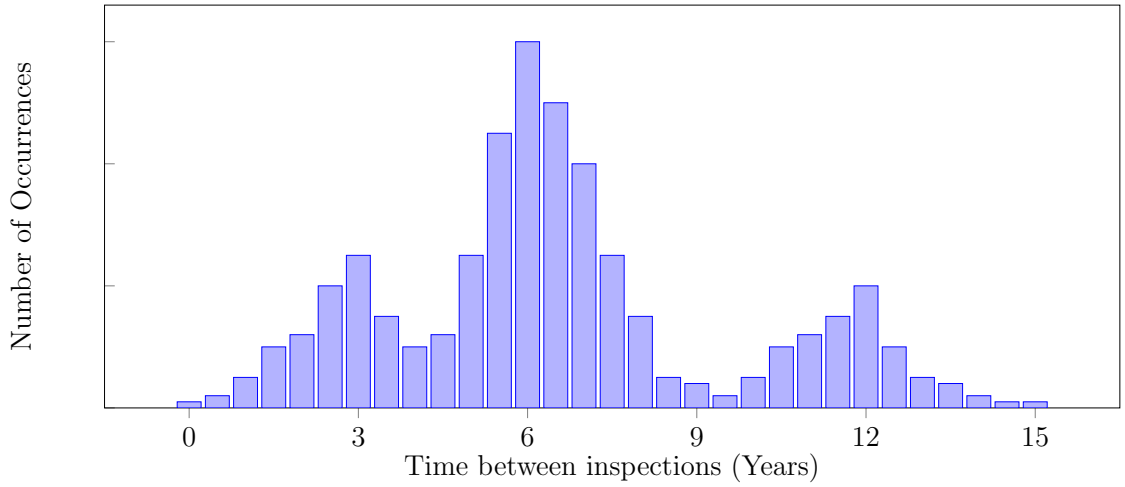

Figure 4.4: A typical distribution of time intervals between two inspections in the Network Rail inspection records. The distribution of inspection intervals has local maxima at 3 years, 6 years and 12 years.

straight masonry bridges of four or more spans with RA10[1] loading have maximum inspection intervals of 3 and 6 years respectively. An example distribution of inspection intervals is shown in Figure 4.4. Thus, any estimation technique will be required to analyse pairs of inspections with varying interval times.

4.1.6 Maximum Likelihood Estimation Approach

Due to the nature of the records available, a method of maximum likelihood applied to panel data is deemed the most appropriate for calculating the probabilities of condition transition events. The method is based on the seminal work by Kalbfleisch and Lawless (1985), which was later applied to a bridge portfolio in the Netherlands by Kallen and Noortwijk (2006) and to building facades by Silva et al. (2016) and Ferreira et al. (2018). In this approach, the parameters of the model, see (4.1.6) and (4.1.7) are computed by maximising the likelihood of the observed inspection results.

[1]RA10 refers to the route availability, which defines the axle weight that can be transported over a bridge.

Consider the observed discrete variable data, $\{x_1, x_2, \cdots, x_n\}$, the Likelihood function $L(\theta)$ is defined as the joint probability mass function of the observed data given θ. If $\{x_1, x_2, \cdots, x_n\}$ is a random sample from a distribution with probability function $f(x|\theta)$ then the Likelihood function is given by

$$L(\theta) = \prod_{i=1}^{n} f(x_i|\theta). \tag{4.1.10}$$

The MLE is the value of θ which maximises $L(\theta)$. The log-likelihood function, $F(\theta)$, is defined to be the natural logarithm of the likelihood function $L(\theta)$, as,

$$F(\theta) = \sum_{i=1}^{n} \ln\left(f(x_i|\theta)\right). \tag{4.1.11}$$

Note, that the natural logarithm is a monotonically increasing function, and thus maximising the likelihood function is equivalent to maximising the log-likelihood function.

Estimation of the Optimal Transition Rate Matrix

The likelihood is the predicted probability of the occurrence of the observed condition transitions:

$$L(Q_{MD}) = \prod_{r=1}^{N} p_r, \tag{4.1.12}$$

where N denotes the number of observed condition transition records for all severity scores and

$$p_r = p_{i,j,t}, \tag{4.1.13}$$

where i is the condition score at the first inspection of record r, j is the condition score at the second inspection of record r and t is the size of the inspection interval between the first and second inspection of record r. The $p_{i,j,t}$ value is found from the $(i,j)^{\text{th}}$ element from the appropriate transition probability matrix, $P(t)$, which is calculated as,

$$P(t) = e^{Q_{MD} \cdot t}, \tag{4.1.14}$$

where t is the time interval between inspections.

The MLE approach seeks to determine the set of parameters, θ, such that the transition rate matrix, Q_{MD}, maximises the following objective function,

$$F(\theta) = \log(L(Q_{MD})) = \sum_{i=1}^{N} \log(p_r). \tag{4.1.15}$$

Additionally, there is a constraint on all the parameters in the upper diagonal in the transition rate matrices, $Q_B, Q_C, Q_D, Q_E, Q_{EX}$ and Q_F in Q_{MD}, that they must be positive.

The MLE parameter values can be determined by taking derivatives of the log-likelihood function and using gradient-based optimisations techniques, this is the approach the `msm` package in `R` uses (Jackson, 2011). Derivative free optimisation algorithms are an alternative approach for maximising the objective functions and are suitable for a broad range of applications (Amaran et al., 2014; Conn et al., 2009; Rios and Sahinidis, 2013).

Examples of efficient derivative-free optimisation tools can be found in commercial software such as MATLAB (The Mathworks, 2020). MATLAB has several algorithms included in its environment including heuristic and direct search algorithms. Li et al. (2019) benchmarked the different algorithms across a range of criteria that included optimality, accuracy and reach-time amongst others, with the heuristic algorithms such as Particle Swarm Optimisation (PSO) and Genetic Algorithms (GA) returning favourable results.

PSO is a population based method and was first introduced by Kennedy and Eberhart (1995) and Shi and Eberhart (1998). GA is an algorithm inspired by the principles of natural selection of evolutionary biology (Goldberg, 1989). The MATLAB implementations of PSO and GA can be used by calling the `pswarm` and `ga` functions (The Mathworks, 2020). Note that each implementation seeks to minimise the provided objective function, and thus the objective function of maximising $F(\theta)$ was found by minimising $-F(\theta)$.

4.1.7 Validation of the Masonry Multiple Defect Model

To ensure that the score inference and multiple defect model are both accurate and robust, a series of validation checks were identified. The verification and validation

checks for the multiple defect model are:

1. Verify the multiple defect model using synthetic records. This requires the use of data, produced using known distributions, as well as the ordering rule to infer six scores from the observed two at each inspection.

2. Validate the multiple defect model using historic inspection records. The historic inspection records are split into training and test sets: to estimate transition rates and analyse the goodness of fit of the model, respectively.

The subsequent sections will explain the methods used to address the points above.

Verifying the Multiple Defect Model, using Synthetic Data

The multiple defect model is verified using synthetic records which was produced using known distributions. The process is as follows:

1. Assign values for the parameters that populate each of the severity score transition rate matrices.

2. Generate a number of samples of bridge element inspections by using Monte Carlo simulation of the defect model with the known transition rates. Moreover, the inspection time interval for each simulated synthetic record will be sampled from $\mathcal{N}(6, 1)$, and the initial condition for each severity score was sampled from a distribution reflecting observed initial conditions in the Network Rail data. Each of the six severity scores are recorded at both the first and second inspections.

3. Using the score ranking rules, determine the worst two scores and record in the same format as Network Rail historic inspection records.

4. Using the score inference rules, infer a multiple defect inspection record for each inspection.

5. Using the MLE parametric statistical inference method, estimate values for each transition rate from the inferred multiple defect inspection records.

6. Compare the estimated parameters from the synthetic data to the known parameters used to produce the synthetic data. As the number of synthetic records increases, the estimate parameter values should converge to the known values.

Example

The values of the parameters used to synthesise records are shown in Table 4.7. There were 25,000 records synthesised as described in Section 4.1.7, and then transition rates were estimated from the synthetic records using the MLE approach. The values of the estimated transition rates are shown in Table 4.7.

It can be observed that the estimated rates are a good approximation of the known transition rates, shown in Figure 4.5. The lower severity scores are more prone to estimation errors due to the lack of coverage of those scores in the inference rules when higher severity scores are present. This can be observed in the example estimation of severity C, however given the complexity of the problem being considered, this estimation was still deemed to be sufficiently accurate. Moreover, with the supply of more records, one would find further convergence to the known values. However, for the example 25,000 records were synthesised, as that number represents a typical sample size of records for a bridge element in the Network Rail data.

The number of synthesised records used is particularly relevant for the more severe defects as there are less of those records generated for the extensive stages of the severe defects. In particular, the initial condition before synthesising a sample inspection pair was based on a distribution that reflects the current bridge stock. For the more severe defects, there are less instances of them having an extent score greater than 1 in the bridge stock, so there are less records synthesised that would cover the more extensive stages of those mechanisms, hence the reduced levels of convergence to the known rates being particularly acute for the transitions $E3 \to E4$, $E4 \to E5$, $EX3 \to EX4$, $EX4 \to EX5$, $F3 \to F4$ and $F4 \to F5$. Moreover, these particular transitions have rather slow transition rates making them less likely to be captured in an inspection interval sampled from $\mathcal{N}(6, 1)$.

Table 4.7: Transition rates estimated from the synthetic data using MLE approach. All transitions rates are stated in (years^{-1}).

	B1 → B2	**B2 → B3**	**B3 → B4**	**B4 → B5**
Known	0.1500	0.0800	0.0850	0.0450
Estimated	0.1480	0.0790	0.0835	0.0443
% Error	1.4	1.2	1.7	1.5
	C1 → C2	**C2 → C3**	**C3 → C4**	**C4 → C5**
Observed	0.0810	0.0500	0.0600	0.0240
Estimated	0.0862	0.0490	0.0600	0.0240
% Error	6.4	2.0	0.05	0.1
	D1 → D2	**D2 → D3**	**D3 → D4**	**D4 → D5**
Known	0.0240	0.0600	0.0525	0.0140
Estimated	0.0248	0.0596	0.0512	0.0146
% Error	3.2	0.6	2.4	4.2
	E1 → E2	**E2 → E3**	**E3 → E4**	**E4 → E5**
Known	0.0090	0.0820	0.0400	0.0225
Estimated	0.0095	0.0828	0.0365	0.0209
% Error	5.4	0.9	8.8	7.1
	EX1 → EX2	**EX2 → EX3**	**EX3 → EX4**	**EX4 → EX5**
Known	0.0070	0.0435	0.0410	0.0555
Estimated	0.0070	0.0437	0.0381	0.0579
% Error	0.6	0.4	7.0	4.3
	F1 → F2	**F2 → F3**	**F3 → F4**	**F4 → F5**
Known	0.0055	0.1160	0.0860	0.0415
Estimated	0.0055	0.1138	0.0842	0.0439
% Error	0.3	1.9	2.1	5.8

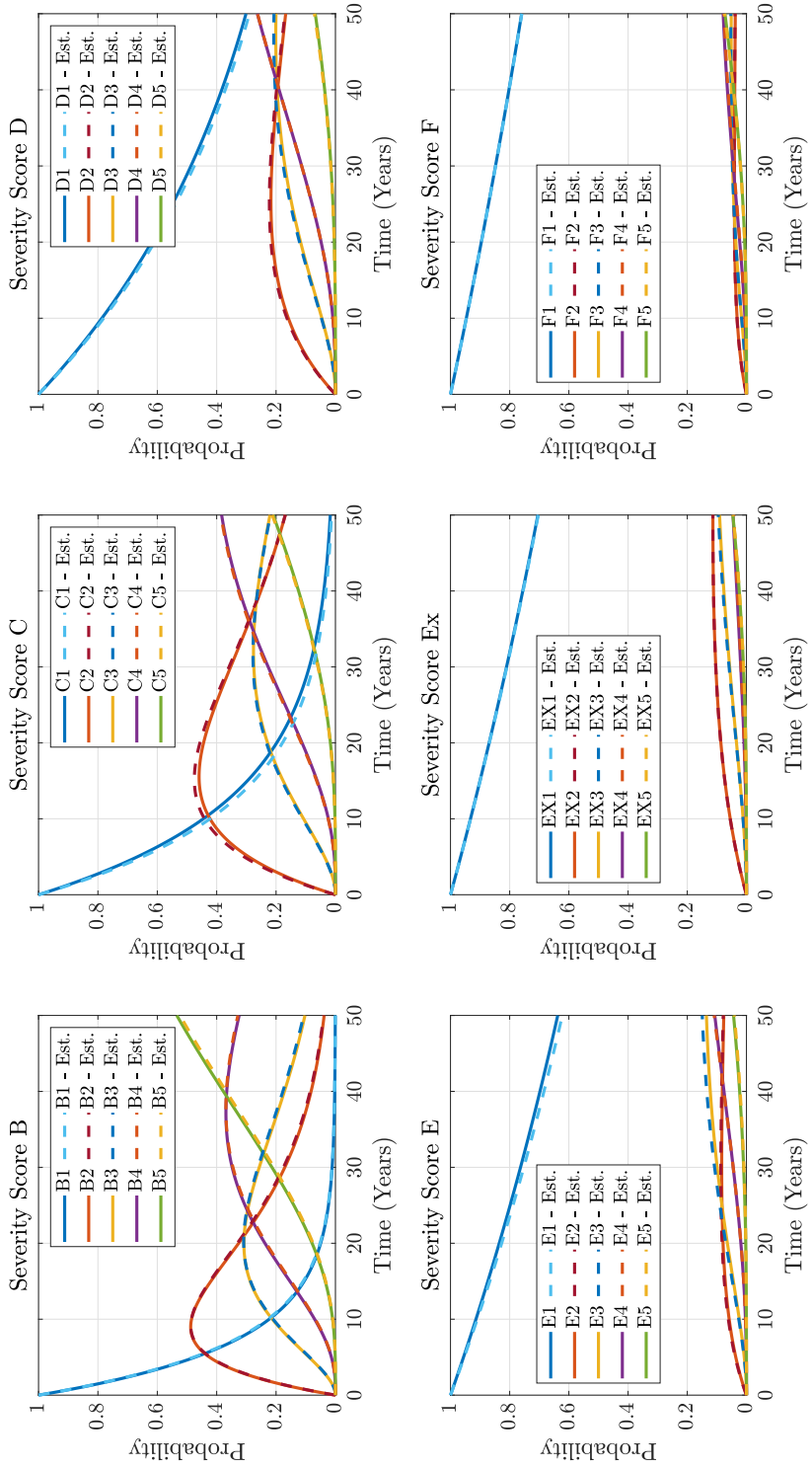

Figure 4.5: Deterioration profiles for defect types with the known distribution for the synthetic data and the estimated distributions.

Validating the Multiple Defect Model, using Historic Inspection Records

To validate the multiple defect model using historic inspection records, the data set is split into training and testing sets. The proposed random split between the two sets is a 3:1 ratio between training and test sets. The training set is used to estimate the values for transition rates from the observations and the test set is used to evaluate the goodness-of-fit of the model and the estimated transition rate values.

Masonry is commonly modelled as a homogeneous class of material; however, it can be easily sub-divided into two materials types: brick and stone. Analysis of the Network Rail data suggested that there were differences in the deterioration rate between brick and stone bridge elements. Moreover, there are subtle differences in the definition of the extent score for severity B and D, see Table 4.1. For the multiple defect model it was deemed that these two materials should have their records split into two cohorts for the purposes of parameter estimation. Additional factors have been shown to alter the deterioration profile of a bridge (Yianni et al., 2016), including local, structural and material characteristics. However, such cohort based studies reduce the amount of data available to calibrate each model. In this study, no further cohort analysis beyond material type was performed, to maximise the amount of data available for the severe defects, which are of rare occurrence.

Bridges are extremely heterogeneous and the structural hierarchy of bridges varies greatly. At inspection, Network Rail bridges have a score panel recorded for each structural element of the bridge e.g. abutment, spandrel wall, arch barrel etc. An example deterioration profile output of the multiple defect model for a brick, underbridge, spandrel wall is shown in Figure 4.6, with its transition rates shown in Table 4.8. A spandrel wall is a masonry wall that is positioned on the arch barrel and retains the back-fill (McKibbens et al., 2006). A railway underbridge is a bridge which carries the railway over a road, river etc.

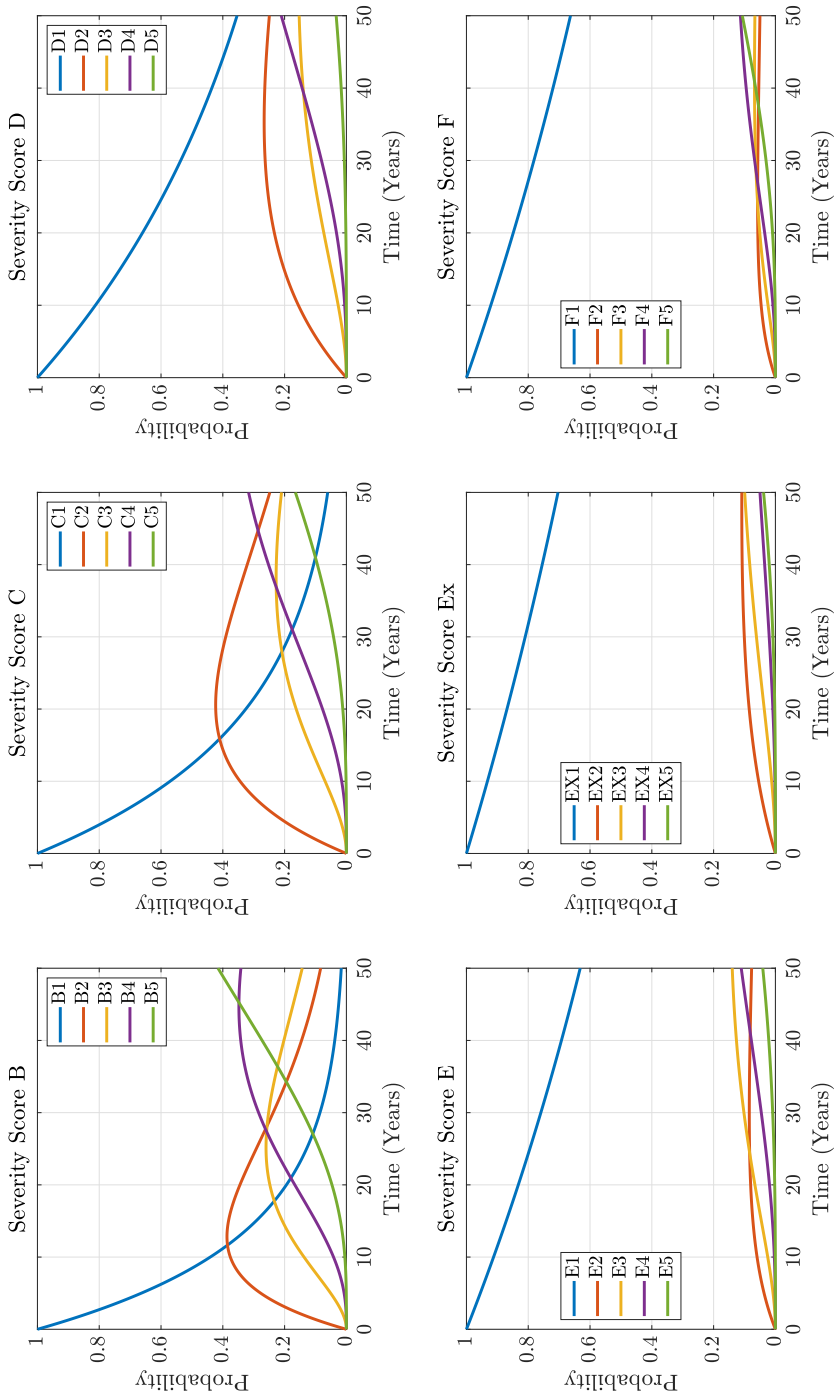

Figure 4.6: Deterioration profiles for all defect modes for a brick spandrel wall on a railway underbridge.

Table 4.8: Transition rates estimated from Network Rail inspection records for a brick spandrel wall on a railway underbridge. All transitions rates are stated in (years^{-1}).

	B1 → B2	**B2 → B3**	**B3 → B4**	**B4 → B5**
Estimated	0.0820	0.0741	0.0826	0.0413
	C1 → C2	**C2 → C3**	**C3 → C4**	**C4 → C5**
Estimated	0.0561	0.0418	0.0616	0.0248
	D1 → D2	**D2 → D3**	**D3 → D4**	**D4 → D5**
Estimated	0.0208	0.0375	0.0568	0.0092
	E1 → E2	**E2 → E3**	**E3 → E4**	**E4 → E5**
Estimated	0.0092	0.0826	0.0390	0.0206
	EX1 → EX2	**EX2 → EX3**	**EX3 → EX4**	**EX4 → EX5**
Estimated	0.0070	0.0461	0.0366	0.0434
	F1 → F2	**F2 → F3**	**F3 → F4**	**F4 → F5**
Estimated	0.0082	0.1166	0.0919	0.0413

Assessing Goodness of Fit

Pearson's chi-squared goodness of fit test is a type of hypothesis testing which is commonly used to assess the fit of models estimated using categorical panel data. To be able to use Pearson's chi-squared goodness of fit test, the events must be mutually exclusive and be from a random sample.

Consider n observations from sample data that are arranged in a frequency histogram having k class intervals. Let O_i be the observed frequency in the i^{th} interval and E_i, as the corresponding expected frequency as predicted by the fitted distribution from the observed data. The test statistic is expressed as,

$$\mathcal{X}^2 = \sum_{i=1}^{k} \frac{(O_i - E_i)^2}{E_i}. \tag{4.1.16}$$

It is common that the goodness of fit test is conducted at the 5% significance level,

although this should be taken as merely convention and not definitive (Sterne et al., 2001).

As shown in Kalbfleisch and Lawless (1985), the size of the time interval between inspections must be considered in the assignment of the intervals for the calculation of the test statistic. However, with the varying inspection intervals in the Network Rail data, there is an imbalance of interval values. This causes low frequencies to occur for some test statistic intervals. Pearson's chi-squared test is sensitive to the choice of the interval, however there is no optimal choice for interval width. Although for the test statistic to be a valid approximation of the chi-squared distribution, the expected number in an interval should exceed a minimum number, which is generally taken to be at least five (Yates, 1934).

The time between initial and final inspections will require discretisation to define interval limits for the test statistic. However, determining appropriate interval limits was challenging as the interval would require relatively large limits, e.g. a year in duration in many cases, before the expectation in each interval would exceed five. An interval width of a year is too wide to be a fair assessment of statistical significance of the goodness of fit of the model. In particular, for the faster acting defects such as spalling and pointing deterioration, a year represents a duration which could yield a large change in condition of multiple condition states. Consequently, it was deemed that the Pearson chi-squared test statistic was an inappropriate measure of fit for the data considered in this study.

Comparing the Observed and Predicted Final Inspection

To assess the goodness-of-fit, a comparison between the observed final condition and predicted final condition was performed. The records in the training set are used to calibrate the values of each of the transition rates and the records in the test set are used in the comparison. The process for the comparison requires:

- Compute the total number of observations of each condition state at the final inspection for all the observed records.
- Using the model, predict the final condition of each record, using the initial

inspection as an initial state and executing the model for the duration of the interval between inspections.

- Sum all the probabilities for each condition state for all predicted final conditions for all records.

For a brick underbridge, spandrel wall, the error rate for each condition state can be found in Table 4.9, with the mean percentage error and weighted mean percentage error for each severity score shown in Table 4.10. The weighted mean percentage error, W, for a particular severity score is calculated as follows:

$$W = \frac{\sum_{i=1}^{5} n_i \cdot e_i}{N}, \tag{4.1.17}$$

where n_i is the number of a observations in extent score i, e_i is the percentage error for extent score i from the model and N is the total number of observations for the severity score being considered.

Table 4.9: Errors between observed and predicted final conditions, for a brick spandrel wall on a railway underbridge.

	B1	**B2**	**B3**	**B4**	**B5**
Observed	488	615	360	240	127
Predicted	555.9	594.8	332.3	240.0	107.0
% Error	13.9	3.3	7.7	9.0×10^{-5}	15.7
	C1	**C2**	**C3**	**C4**	**C5**
Observed	1127	1073	350	209	59
Predicted	1039.4	1153.7	364.2	194.7	66.0
% Error	7.8	7.5	4.1	6.8	11.9
	D1	**D2**	**D3**	**D4**	**D5**
Observed	2304	848	209	88	19
Predicted	2262.0	853.9	231.5	107.2	13.5
% Error	1.8	0.7	10.7	21.8	29.2
	E1	**E2**	**E3**	**E4**	**E5**
Observed	3584	255	148	103	39
Predicted	3565.1	259.6	171.8	96.8	35.8
% Error	0.5	1.8	16.1	6.1	8.1
	EX1	**EX2**	**EX3**	**EX4**	**EX5**
Observed	4231	207	43	15	5
Predicted	4214.5	219.6	47.8	15.3	3.8
% Error	0.4	6.1	11.3	2.3	24.9
	F1	**F2**	**F3**	**F4**	**F5**
Observed	3651	175	168	180	147
Predicted	3653.2	188.1	140.4	183.8	155.6
% Error	0.1	7.5	16.4	2.1	5.8

Table 4.10: Mean percentage errors and weighted mean percentage errors for each severity score for a brick spandrel wall on a railway underbridge.

	B	**C**	**D**	**E**	**EX**	**F**
Mean % Error	8.12	7.61	12.86	6.51	8.99	6.37
Weighted Mean % Error	7.42	7.23	2.74	1.37	0.79	1.28

4.1.8 Results Discussion

Variability in recorded bridge inspection conditions is well documented in literature (Ben-Akiva et al., 1993; Berrade et al., 2013; Madanat, 1993; Moore et al., 2001; Neves and Frangopol, 2010; Phares et al., 2004), and thus it would be inappropriate to not recognise the impact of this in any model analysis. Consequently, the values for the errors and the mean errors are considered to be sufficiently low to be content that the model represents an appropriate goodness of fit.

For all the severe defects, i.e. D, E, EX and F, the absorbing state of extent score 5, is deemed to be a poor condition state, which would require immediate maintenance intervention. Moreover, for E, EX and F, this is true for some of the preceding states. Thus, maintenance activity would typically be scheduled in advance of defects progressing to such states and few observations would be made for these absorbing states. The low number of observations for these states can result in high prediction errors (e.g. $D5$, $EX5$), however these are rare events and represent less than 1% of the final observations for those particular defects. Whilst some of the states are low in frequency, the higher error rate for the more severe defects could also be due to the assumed independence of their development from the other less severe defects. The validity of modelling the multiple defect mechanisms independently is assessed in Chapter 5.

From Table 4.9, it can be seen that there is a low prediction error shown for $D1$, $E1$, $EX1$ and $F1$, and thus the model is accurate at predicting defect absence and presence. Furthermore, for these defects that pose the greatest risk to the structural integrity of the bridge, a Pearson's chi squared test of the predicted final observations

shows that the model is accurate to a statistical significance of 5%. Due to the data censoring, the errors for B and C are more significant. If the inspection regime at Network Rail were to be updated to monitor each distinct defect mechanism opposed to the current practice of recording only the worst two, the calibrated model would likely have much better prediction accuracy for the lower severity defects such as B and C. An example of a multiple defect mechanism model that was calibrated from fully observed mechanisms is shown for metallic components in Section 4.2.

The weighted mean is used to analyse the fit of the model without the metric being adversely impacted by low frequencies. From Table 4.10 it can be observed that the trend for the weighted mean percentage error is that the higher severity scores have smaller values. This would be expected as the score inference rule favours the higher severity scores over the lower scores, hence there are more revealed extent scores for the higher severity scores which results in an improved parameter estimation.

Figure 4.6 shows the deterioration profiles for a brick, underbridge, spandrel wall, with severity scores B, C and D exhibiting more rapid deterioration than severity scores E, EX and F. Severity scores B, C and D represent shallow spalling, deterioration pointing and deep spalling, respectively, which are faster acting defects than hollowness, loose block work and fully displaced block work, which are denoted by severity scores E, EX and F respectively. For faster acting defects, the accuracy of the rate of deterioration aids in the appropriate scheduling and budgeting of minor interventions. It is critical that the processes of hollowness, loose block work and displaced block work are also well understood, as whilst they are slower acting, they are the defects that are deemed to represent the most risk to the structural integrity of a bridge.

4.2 Metal Multiple Defect Deterioration Model

4.2.1 Condition Records

As aforementioned, Network Rail use an alpha-numeric condition scale known as Severity Extent (SevEx) to record the condition of the elements of bridges at inspection. For metallic bridge components an additional scale known as Coating-Metal (CM) is used to record the intactness of the paintwork or coating mechanism (Network Rail, 2017). The definition for metallic severity scores can be found in Table 4.11, metallic CM scores in Table 4.12 and the extent score which is common to SevEx and CM in Table 4.13.

From analysing the SevEx and CM scale definitions there are three distinct defect mechanisms that could be identified and monitored on metallic components in the Network Rail portfolio:

- Loss of coating or paintwork (Severity I to L);
- Corrosion (Severity B to F);
- Structural Component Failure (SCF) - Includes: buckling, permanent distortion/displacement and tearing/fracture (Severity G).

Table 4.11: SevEx severity definitions for metallic bridge elements (Network Rail, 2017).

Score	Severity Definitions
A	No visible defects to metal.
B	Corrosion less than 1mm deep.
C	Corrosion between 1mm and 5mm deep.
D	Corrosion between 5mm and 10mm deep.
E	Corrosion greater than 10mm but not through section.
F	Corrosion to full thickness of section.
G	Choose most extensive from: buckling, permanent distortion or displacement and tearing/fracture.

Table 4.12: CM severity definitions for metallic bridge elements (Network Rail, 2017).

Score	Severity Definitions
A	All coatings intact.
I	Presence of surface defects/abrasions. No corrosion of underlying element.
J	Flaking or blistering of top coat. No Corrosion of underlying metal.
K	Corrosion spots showing through coating.
L	Complete loss of coating to parent metal.

Table 4.13: SevEx/CM extent definitions for metallic bridge elements (Network Rail, 2017).

Score	Extent Definitions
1	No visible defects to metal/coating.
2	Localised defect due to local circumstances.
3	Defect occupies less than 5% of surface of the element.
4	Defect occupies between 5% to 10% of the surface of the element.
5	Defect occupies between 10% to 50% of the surface of the element.
6	Defect occupies more than 50% of the surface of the element.

At each inspection, for each metallic bridge element, the two worst SevEx scores and the two worst CM scores are recorded alongside the date of the inspection. Repeated observations form a longitudinal study and the records can be split to form exam pairs as shown in Table 4.14, where $i = 1, \ldots, n$ and $\alpha_{i,j}$ is the worst SevEx score at the j^{th} inspection, $\beta_{i,j}$ is the second worst SevEx score at the j^{th} inspection, $\gamma_{i,j}$ is the worst CM score at the j^{th} inspection, $\delta_{i,j}$ is the second worst CM score at the j^{th} inspection, $\alpha_{i,j}, \beta_{i,j}$ can assume a SevEx condition state and $\gamma_{i,j}, \delta_{i,j}$ can assume a CM condition state and $t_i \in \mathbb{R}, 0 < t < 18$.

Table 4.14: Example exam pair for a metallic bridge element.

Record	Inspection 1				Inspection 2				Time Interval
	SevEx 1	SevEx 2	CM 1	CM 2	SevEx 1	SevEx 2	CM 1	CM 2	(Years)
r_i	$\alpha_{i,1}$	$\beta_{i,1}$	$\gamma_{i,1}$	$\delta_{i,1}$	$\alpha_{i,2}$	$\beta_{i,2}$	$\gamma_{i,2}$	$\delta_{i,2}$	t_i

It can be assumed that the two worst SevEx scores recorded at inspection adhere to a similar score ranking for SevEx as masonry, i.e. the SevEx scores are ranked according to severity score, followed by the extent score: $A1 < B2 < \cdots < B6 < C2 < \cdots < C6 < D2 < \cdots < D6 < E2 < \cdots < E6 < F2 < \cdots < F6 < G2 < \cdots < G6$. Thus, if $Sev(\alpha_{i,j}) \neq G$ and $Sev(\beta_{i,j}) \neq G$ it can be assumed that SCF was not observed at that inspection, which can be denoted using the score of $G1$. Consequently, a condition state for each of the three metallic deterioration mechanisms is revealed at each inspection.

It is possible to devise a Markov model with discrete states that correspond to the discrete SevEx/CM states and the transitions between the states could be calibrated from the exam pairs that are formed from the condition records. However, to facilitate later work as detailed in Section 5.2, the discrete states for each defect mechanisms are amalgamated into a simpler model.

The SevEx and CM condition scales were transformed to a defect specific condition scale using Network Rail weightings for the SevEx/CM states (Network Rail, 2017), shown in Tables 4.15 and 4.16. For the paintwork node there are four states for this study, where $Pa1$ denotes no visible defects and $Pa4$ denotes extensive paintwork damage, with $Pa2$ and $Pa3$ as intermediate states of paintwork damage. Corrosion states, $C1$, $C2$, $C3$ and $C4$ are defined in a similar manner with $C4$ corresponding as the poor condition state that would trigger major maintenance interventions. For SCF, there are two states: $F1$ for when a SCF mode is absent and $F2$ denotes its presence. Two states were used for SCF as NR policy suggests maintenance intervention is required once a SCF mode is identified. Moreover, there is less prevalence of SCF being present in the records and two states were used to

reduce the likelihood of a model being over fitted to rare event data. The mapping between the study condition states and the Network Rail weightings are shown in Tables 4.17, 4.18 and 4.19.

Table 4.15: Network Rail assigned integer condition scale score for each SevEx score - Metal.

Severity \ Extent	**1**	**2**	**3**	**4**	**5**	**6**
A	1	-	-	-	-	-
B	-	2	3	4	5	6
C	-	3	6	7	8	9
D	-	5	7	8	10	12
E	-	7	8	11	12	13
F	-	8	11	13	14	15
G	1	8	12	13	14	15

Table 4.16: Network Rail assigned integer condition scale score for each CM score - Metal.

Severity \ Extent	**1**	**2**	**3**	**4**	**5**	**6**
A	1	-	-	-	-	-
I	-	2	3	4	5	6
J	-	4	6	7	8	9
K	-	6	7	8	9	10
L	-	7	8	9	11	12

Table 4.17: Paintwork Condition State - Integer Conversion Chart

Pa1	Pa2				Pa3			Pa4			
1	2	3	4	5	6	7	8	9	10	11	12

Table 4.18: Corrosion Condition State - Integer Conversion Chart.

C1	C2				C3				C4					
1	2	3	4	5	6	7	8	9	10	11	12	13	14	15

Table 4.19: SCF Condition State - Integer Conversion Chart.

F1	F2				
1	8	12	13	14	15

4.2.2 Metal Deterioration Model

A multiple defect deterioration model for metallic elements can be used to predict condition indicators for paintwork/coating, corrosion and SCF; the Markov model is shown in Figure 4.7.

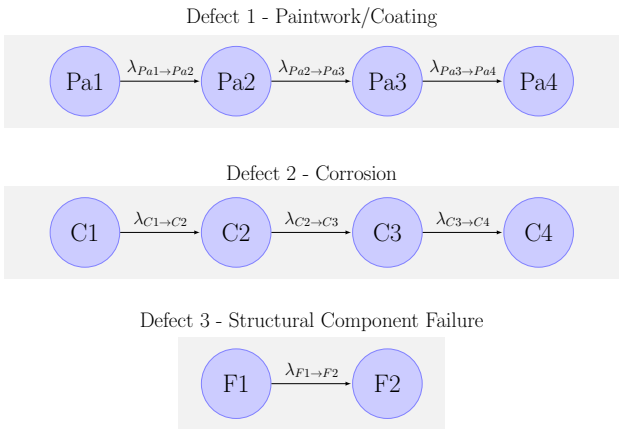

Figure 4.7: Multiple defect deterioration Markov model - Metal.

For a case study of the metallic multiple defect model, a model was calibrated using condition records for metallic exposed main girders from railway underbridges. The parameters calculated using the maximum likelihood method are shown in Table 4.20. The condition probability profiles for paintwork, corrosion and SCF are shown in Figure 4.8. Finally, a comparison of the observed final conditions for exam pairs and the predicted final condition for a test set of data using the model is given in Table 4.21.

Table 4.20: Parameters for independent multiple defect deterioration model.

Defect Type	**Transition**	**Transition Rate**
Paintwork	$P1 \rightarrow P2$	0.1751
Paintwork	$P2 \rightarrow P3$	0.1557
Paintwork	$P3 \rightarrow P4$	0.0342
Corrosion	$C1 \rightarrow C2$	0.1431
Corrosion	$C2 \rightarrow C3$	0.1148
Corrosion	$C3 \rightarrow C4$	0.0325
SCF	$F1 \rightarrow F2$	0.0095

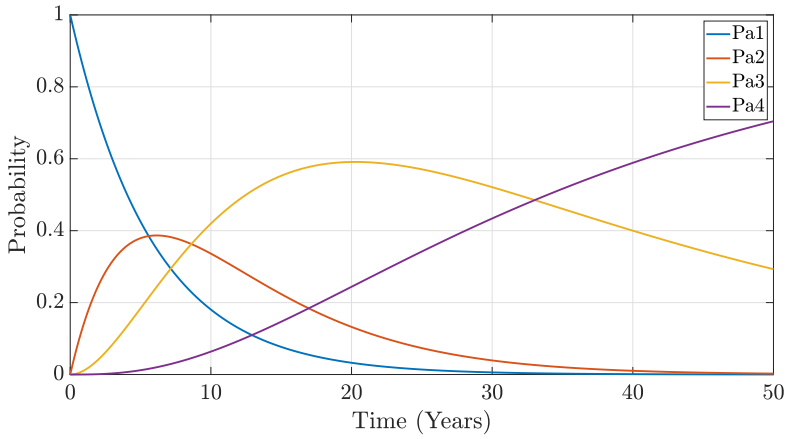

(a) Paintwork/Coating

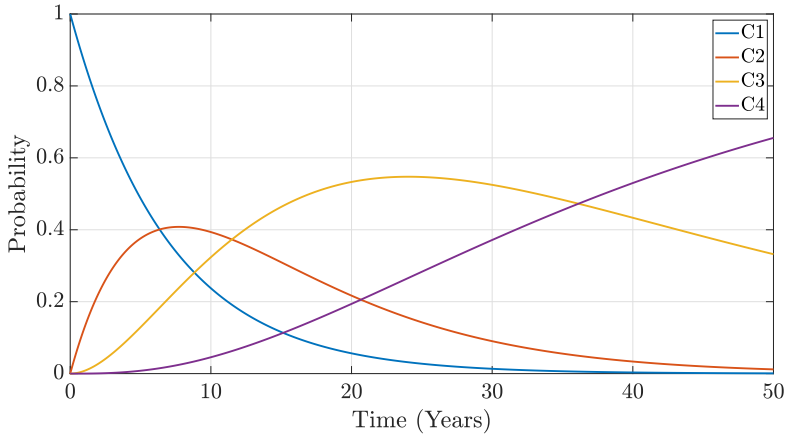

(b) Corrosion

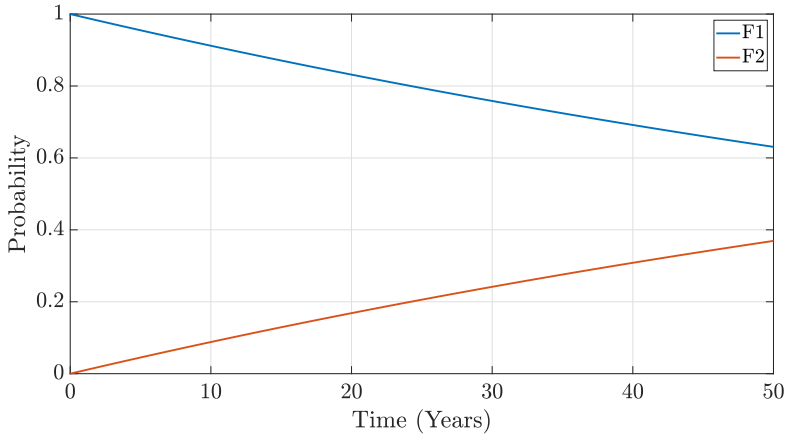

(c) SCF

Figure 4.8: Condition probability profiles for paintwork/coating, corrosion SCF for a metallic exposed main girder starting in $\{Pa1, C1, F1\}$.

Table 4.21: Errors between observed and predicted final conditions from the Markov model, for a metallic exposed main girder on a railway underbridge.

	Pa1	**Pa2**	**Pa3**	**Pa4**
Observed	154	376	2745	1725
Predicted	149.3	375.6	2714.9	1760.1
% Error	3.03	0.09	1.09	2.03
	C1	**C2**	**C3**	**C4**
Observed	105	520	2692	1683
Predicted	108.7	541.4	2687.4	1662.5
% Error	3.54	4.11	0.17	1.22
	F1	**F2**		
Observed	4392	608		
Predicted	4365.4	634.6		
% Error	0.60	4.37		

4.2.3 Results Discussion

The model for metallic bridge elements outputs condition indicators for three distinct deterioration mechanisms: deterioration of coating/paintwork, corrosion and SCF. From Figure 4.8 it can be observed that SCF occurs at a much slower rate than the other two defect mechanisms. This observation corresponds with what engineering experience would suggest as the deterioration of coating/paintwork and corrosion are faster acting defects which can be accelerated by the environment that a metallic element is exposed to. Moreover, the expected lifespan of element's coating will be considerably less than the expected lifespan of the element itself. SCF encompasses the structural failure of an element due to the occurrence of mechanisms such as buckling, permanent distortion or displacement and tearing/fracture, which are often the result of long term loading of a bridge element. Additionally, the occurrence of SCF typically has a serviceability consequence for a entire structure, and thus a larger mean time to occurrence is an expected outcome.

The goodness-of-fit of the multiple defect metallic deterioration model is evaluated by comparing the observed final conditions in exam record pairs and predicting the final condition for each initial condition of an exam record pair. From Table 4.21, for the test data, it can be noted that for each condition state there is sufficient prediction accuracy, with the maximum percentage error being 3.03%, 4.11% and 4.37%, for coating deterioration, corrosion and SCF respectively.

The calibration of the metallic deterioration model benefited from the fact that all three defect mechanisms had a condition state recorded at each inspection. In particular, the less severe defects for the metallic component, i.e. coating deterioration and corrosion, have similar prediction accuracy as the more severe defects of SCF. This is in contrast to the masonry model, which had less severe defects, i.e. shallow spalling and pointing deterioration, that suffered from unrevealed condition states at some inspections and there were more significant prediction errors when compared to the more severe defects, i.e. hollowness and blockwork displacement.

Finally, whilst the calibration of the metallic deterioration model is still susceptible to the impact of inspection variability, the consolidation of multiple of SevEx/CM conditions states into a smaller number of discrete condition states will minimise the effects of variability during model calibration.

4.3 Chapter Summary

This chapter presented a multiple defect approach for modelling bridge deterioration, which outputs multiple predictive condition profiles. Models were presented for both masonry and metallic bridge elements.

Bridge elements deteriorate through a variety of different defect modes, and thus the proposed multiple defect model offers more versatility than current predictive bridge deterioration models which only provide a single condition index.

An ideal inspection regime would record a complete multiple defect inspection panel, however in many organisations this is not the case and so a score inference technique using logic rules was also introduced to utilise existing Network Rail data. The score inference was shown to partially reveal all deterioration mechanisms for

masonry elements and fully reveal all the mechanisms for metallic components. A proven maximum likelihood parameter estimation technique can then be applied to estimate the transition rates between condition states.

In the contexts of the PPDAC cycle, a clear recommendation for future investigations is that if an asset manager seeks to evaluate a multiple defect mechanism deterioration model, it would be worthwhile recording all observed instances of defects present at inspection using unique identifiers and tracking their progression at subsequent inspections.

A limitation of the presented model is that it does not account for any interactions between the different defects modes. It is expected that the condition of a component in terms of one defect may alter the rate of development of other defect mechanisms. Such trends would impact on predictions of service life of the bridge element but additionally on the condition dynamics upon maintenance intervention. The next chapter considers methods for incorporating the interactions between multiple deterioration mechanisms.

Chapter 5

Modelling Interactions between Deterioration Mechanisms

The previous chapter proposed modelling deterioration by computing condition indicators for multiple defect mechanisms simultaneously. A major limitation of the presented approach was that the defect mechanisms were modelled independently from each other. However, engineering experience would suggest that for both masonry and metal their respective defect mechanisms would have interactions between other mechanisms.

This chapter will provide insight into the relationships between the different defect mechanisms for both masonry and metal bridge components. Additionally modelling methods and calibration techniques are presented that enable the incorporation of the interactions between defects under a data constrained scenario.

5.1 Masonry Multiple Defect Deterioration Model

5.1.1 Masonry Data Constraints

To investigate the interactions between masonry defect mechanisms, each defect type has two states defined, i.e. defect absent and defect present. The defect absent state corresponds to an extent score of 1 and the defect present state corresponds to any extent score between 2 and 6. The labelling for each defect's condition states

is shown in Table 5.1.

Table 5.1: Notation for each defect type being absent or present.

Defect Type	Defect Absent	Defect Present
Spalling	$\overline{S}$	S
Pointing	$\overline{P}$	P
Hollowness	$\overline{H}$	H
Displaced Blockwork	$\overline{B}$	B
Cracking	$\overline{C}$	C

Typically, predictive profiles of bridge deterioration express not only the absence or presence of a defect but how extensive the considered defect is on the bridge component. For the data available for masonry elements, a study beyond the absence or presence of defects was not possible when considering the interactions between defects due to the following data constraints:

- Record truncation - Network Rail record only the two worst scores at inspection rather than a full panel of defects present. Inference can be applied to determine the status of some of the unobserved defects, see Section 4.1.3, however the inference would not reveal sufficient information to analyse both the relationship between defects and their extensiveness.

- Variable inspection intervals - The inspection interval for bridges in the Network Rail portfolio depends on the condition at previous inspection and the technical specification of the bridge, and can range from 6 months to over 12 years, see Section 4.1.5. As such, to fit any model of defect extensiveness would be greatly limited by such a large variance in inspection interval.

- Partial lifetime history - Only a fraction of the life of the structure has been recorded using the defined inspection strategy.

If data were to become available which was not limited by these constraints, the methodology presented in this study could be adapted such that each defect with n

condition states would be modelled with a variable in the DBN which had n states, rather than the two in this study.

Recall from Section 4.1 that the SevEx condition scale for masonry encapsulates condition states that describe spalling, deterioration of pointing, hollowness and displaced blockwork. The different defect modes defined in the SevEx scale for masonry components are shown in Table 5.2.

Table 5.2: Defect types as defined by their SevEx score.

Defect Type	**Severity Score**
Spalling	B & D
Pointing	C
Hollowness	E
Displaced Blockwork	EX & F

Masonry spalling alludes to the breaking of the material into pieces and can be present on the surface of bricks or stone blocks. A common cause of spalling is the penetration of moisture into the material. The SevEx condition scale accounts for the spalled or weakened material and/or evidence that material is experiencing the effects of water, e.g. percolation. Ideally, this would be distinguished by separate states but as aforementioned, data constraints tied the study to only consider the absence or presence of defects. Thus, the spalling defect would be expected to have a small mean time to occurrence due to its definition. The pointing defect accounts for any degradation in the mortar between the block work. Hollowness or drumminess is the separation of masonry material from the face of the block work. The block work defect is the indicator that the block work has become displaced from its intended location, or is fully missing.

Additionally, as part of the bridge inspection regime of masonry bridges at Network Rail, a Cracked-Masonry (CM) score is recorded. The CM score is used by Network Rail to monitor the development and/or progression of cracking on a bridge component. The CM condition scale for masonry is also akin to SevEx and is an

alpha-numeric scale, with the letter grades denoting the defect present and the numeric scores denoting the extent of the defect.

The CM score has two classes: class one is used for abutments, piers, wing walls, spandrel walls, parapets and padstones, and class two for the arch barrels and face rings. Class one records the distinct defect mechanisms of vertical/diagonal cracking, and horizontal cracking. Class two records the distinct defect mechanisms of longitudinal cracking, transverse cracking and face ring separation. Upon analysing the CM records for the Network Rail bridge portfolio it was found that the majority of bridge components did not exhibit cracking at each inspection. Consequently, efforts to estimate the rate of deterioration between no cracking to each CM defect mechanism were inhibited. As such, in this study, any non-perfect CM score was considered as the same defect 'cracking'.

The condition records from visual examinations of bridges form a longitudinal study and typically these records cover only a fraction of the bridge's life span, in mature bridge stocks. Moreover, the year of construction and any major maintenance interventions may not be reliably known, which prohibits an accurate lifetime analysis. Consequently, any statistical analysis of these records must assume the memoryless property: the future condition state of a process is determined by the present condition state only, i.e. future condition is independent of past condition. Markov chains assume the memoryless property, as do DBNs.

Structural Health Monitoring (SHM) can be an effective means to reduce the uncertainty in the prediction models of structural performance and to improve the lifespan prediction accuracy of existing structures and enhance the design of new structures (Frangopol, 2011). Nonetheless, there are not many SHM data sources available at Network Rail for model calibration. There are examples of sensors being used, for example, on the Forth bridge in Scotland, however the objective of this study was to develop novel methods that could be calibrated and used for as many bridges as possible.

The deterioration of civil infrastructure is known to be a continuous degradation process, whilst DBN models are constrained to a temporal discretisation. The more severe modes of deterioration are slow-acting processes with many degrada-

tion mechanisms requiring years to first occur and then develop. Although surface defects such as spalling, and the deterioration of pointing are much faster acting than the more severe material defects of hollowness and displaced blockwork. After consultation with structural engineers, it was deemed that using a time step of one week to capture the continuous nature of degradation would satisfy any concerns that the time discretisation was not suitable for the faster acting defects. Moreover, the use of a DBN model enabled the inclusion of conditional probability distributions to account for the interactions between different deterioration mechanisms. Consequently, despite being tied to memoryless distributions, non-constant deterioration behaviour can still be incorporated as a model output.

5.1.2 Multiple Defect Masonry Bridge Deterioration DBN

In the SevEx scale there are four distinct defect modes: spalling, deterioration of pointing, the presence of hollowness, and the displacement of block work. A fifth defect type can be modelled when considering the CM condition records.

An adaption of the Markov model from Section 4.1, which considers the SevEx and CM defects independently will be considered. In this study, the defects will only be modelled to determine whether they are absent or present. The relationships between the different SevEx defects will then be modelled using a BBN, as shown in Figure 5.1. Finally, a third model is developed that encapsulates both the SevEx and CM defect types, and is shown in Figure 5.2. The structure of the SevEx DBN and SevEx-CM DBN were developed by analysing the structure of the condition scale, numerical experiment and expert judgment from Network Rail structural engineers.

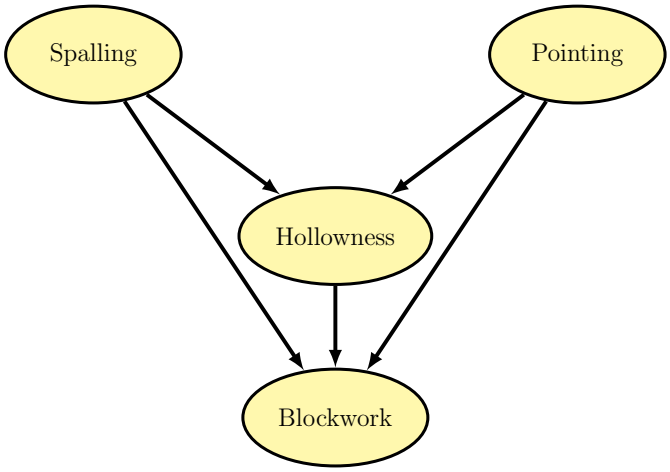

Figure 5.1: A BBN representing causal influences among masonry SevEx defect modes.

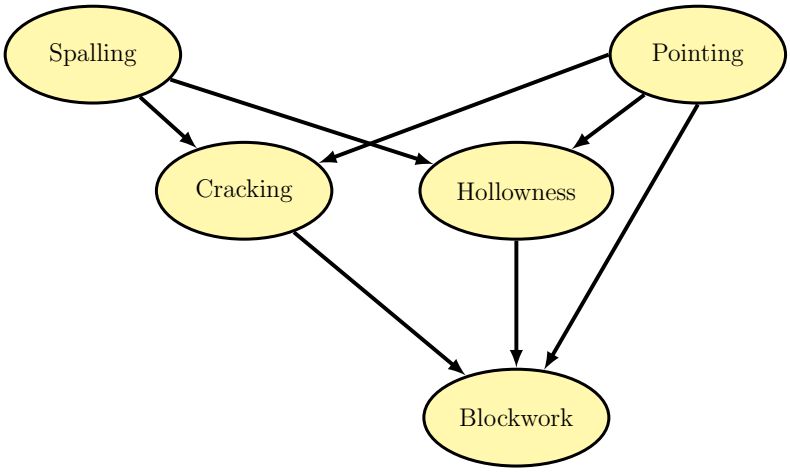

Figure 5.2: A BBN representing causal influences among masonry SevEx and CM defect modes.

To model the evolution of defects through time, a DBN is used. For each discrete time step, the corresponding time slide in the DBN has a BBN that is consistent with the one shown in Figure 5.1. However, it should be noted that the temporal link between time slices, for the multiple defect BBN, exists for each variable and its corresponding predecessor from the previous time slice, not only the root node of the time slice, as is commonly the case. The purpose of this model is to estimate deterioration profiles, which assume a do-nothing maintenance strategy, and thus once a defect becomes present, it should remain present. Consequently, temporal

links are required for each variable in the BBN, as each variable is not only influenced by the state of its parent variables but also the status of the considered variable at the previous time step. The multiple defect model is shown in Figure 5.3, with the red arrows denoting the temporal link between time slices.

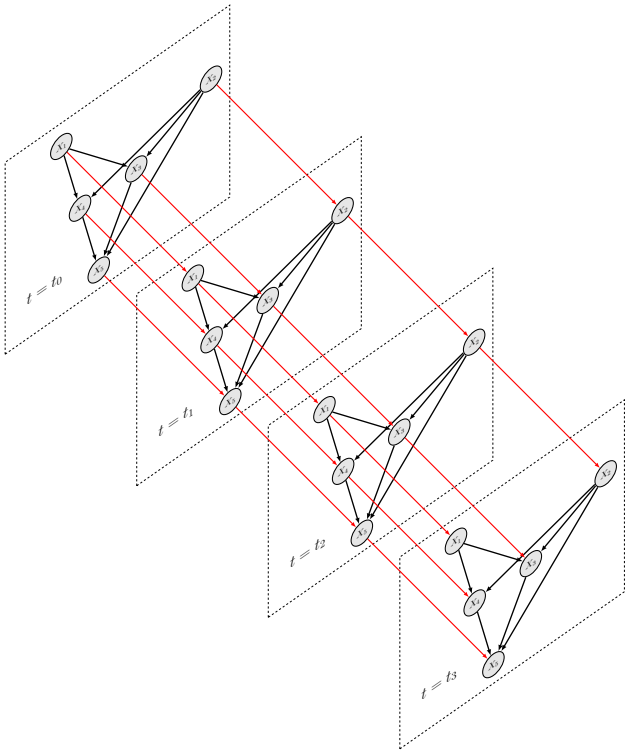

Figure 5.3: SevEx-CM multiple defect BBN expressed as a DBN.

The different time slices are connected through temporal links to form the complete model. If the time slices are identical and the temporal links stay the same, then the model is a DBN. Consequently, the DBN model can be assumed to be time homogeneous,

$$P(X_i^{j+1}|X_i^j \cap pa(X_i^{j+1})) = P(X_i^j|X_i^{j-1} \cap pa(X_i^j)), \tag{5.1.1}$$

where $i = 1, ...5$, $j = 1, ..., T$ and T is the final time slice to be calculated. The consequence of this property is that the CPT for each node on a time slice does not change over time.

5.1.3 Parameter Estimation

To populate a BBN or the time slices of a DBN, values are required to populate the CPTs of the network. For the model shown in Figure 5.2, there are 18 parameters required to populate all the required CPTs; 1 parameter each for spalling and deterioration of pointing, 4 parameters for hollowness, 4 parameters for cracking and 8 parameters for displaced block work. The structure of the spalling, deteriorated pointing and hollowness CPTs are shown in Tables 5.3, 5.4 and 5.5. It can be observed in these tables, that some scenarios have known probabilities, i.e. [0,1], in the CPT, this is due to the do-nothing maintenance strategy of the model, and thus if a defect becomes present, it will remain present. The CPTs for cracking and displaced block work are defined in a similar manner.

Table 5.3: Example CPT structure for spalling.

	Spalling	
	$\overline{S}_t$	S_t
$\overline{S}_{t-1}$	$1-p_1$	p_1
S_{t-1}	0	1

Table 5.4: Example CPT structure for deteriorated pointing.

	Pointing	
	$\overline{P}_t$	P_t
$\overline{P}_{t-1}$	$1-p_2$	p_2
P_{t-1}	0	1

Table 5.5: Example CPT structure for hollowness.

	Hollowness	
	$\overline{H}_t$	H_t
$\overline{H}_{t-1} \cap \overline{P}_{t-1} \cap \overline{S}_{t-1}$	$1 - p_3$	p_3
$\overline{H}_{t-1} \cap \overline{P}_{t-1} \cap S_{t-1}$	$1 - p_4$	p_4
$\overline{H}_{t-1} \cap P_{t-1} \cap \overline{S}_{t-1}$	$1 - p_5$	p_5
$\overline{H}_{t-1} \cap P_{t-1} \cap S_{t-1}$	$1 - p_6$	p_6
$H_{t-1} \cap \overline{P}_{t-1} \cap \overline{S}_{t-1}$	0	1
$H_{t-1} \cap \overline{P}_{t-1} \cap S_{t-1}$	0	1
$H_{t-1} \cap P_{t-1} \cap \overline{S}_{t-1}$	0	1
$H_{t-1} \cap P_{t-1} \cap \overline{S}_{t-1}$	0	1

In this study, the CPTs of a DBN were parameterised using the λ rate for the exponential distribution. This aided the optimisation process and provided numerical stability. Nonetheless, it should be noted that a direct parameterisation of the CPTs using probabilities for the discrete time transitions would be permissible and may be preferable depending on the calibration method used.

In this study, each defect has two states with one permitted transition: absent to present. Thus, the probability for the CPT could be computed analytically from the exponential cumulative distribution function,

$$p_i = 1 - e^{-\lambda_i \cdot t}, \tag{5.1.2}$$

where t is the size of interval between time slices in the DBN, p_i is a probability in the CPT for a particular state of causal influences and λ_i is its associated λ value for the exponential distribution.

Consider θ as the set of parameters that characterizes the CPT of every variable in a DBN. The likelihood of the observed condition transitions is:

$$L(\theta) = \prod_{r=1}^{N} p_r, \tag{5.1.3}$$

where N denotes the number of observed condition transition records,

$$p_r = p_{i,j,t}, \tag{5.1.4}$$

where i is the joint condition score at the first inspection in record r, and j is the joint condition score at the second inspection in record r, t is the size of the inspection interval between the first and second inspection of record r and N is the number of exam pair records that exist. For numerical stability, the log-likelihood function should be used,

$$F = \log(L(\theta)) = \sum_{r=1}^{N} log(p_r). \tag{5.1.5}$$

To compute the appropriate value for p_r using θ, the conditions of each variable at the first inspection were used as a belief state for each variable on the initial time slice. Then using exact inference on the DBN populated with θ, the joint probability of all the variables being in the state observed at time t were calculated. A MATLAB script was developed that made use of the `ga` function and determined the MLE for θ using the historic condition records to evaluate the objective function. Appendix A outlines how a GA operates.

5.1.4 Masonry Case Study

NR are responsible for maintaining the structural integrity of the entire portfolio of bridges on the railway in Great Britain. Part of the asset management strategy of this portfolio is an inspection regime, which ensures that every bridge component on each bridge is inspected at a frequency that adheres to the predefined inspection intervals at Network Rail. The worst and second worst SevEx score are recorded at each inspection, alongside, the worst and second worst CM score. Thus, the original records do not provide a complete panel of scores for all of the SevEx defects, all of the time. However, through the use of a score inference rule, as shown in Section 4.1.3, these can be more densely populated. These SevEx/CM scores can be converted into the condition states shown in Table 5.1.

Once the condition states are in a two-state scale, it is possible to further fill in any unrevealed defect states by using a *Known Failed Function* (KFF). Consider the case where a defect is observed to be present at the first inspection but is unrevealed at the second inspection. It would be unrevealed at the second inspection due to a more severe defect having developed during the inspection interval and now

being present (see Section 4.1.3). Thus, the bridge component exhibited an overall deterioration behaviour. Consequently, if the less severe defect was present at the first inspection, it is reasonable to assume it is still present at the second inspection. An example of the result of this assumption is shown as Record 1 in Table 5.6. The rule is not a complete 'fail safe', with some incomplete records not being fully populated by the rule, as shown for Record 2 in Table 5.6. However, Record 2 is not of any use in the estimation of the transition rates of absent to present for hollowness or displaced blockwork, as both of those defects are already present. After, the use of the KFF, approximately 85% of the desired records are a complete multiple defect score panel at both inspections in the two-state condition scale. The remaining 15%, whilst not known fully are of a similar format as Record 2. It is common practice to use the Expectation-Maximisation (EM) algorithm (Dempster et al., 1977), to estimate parameters for stochastic models with latent variables, however due to the nature of the latent variables and the temporal properties and censoring in this data, its use would not be applicable in this case study.

Table 5.6: Example bridge inspection data, shown as both the original and post Known Failed Function (KFF). The dashes indicate an unrevealed state.

Record	**Inspection 1**	**Inspection 2**
1 - Original	$\{S, P, \overline{H}, \overline{B}, \overline{C}\}$	$\{-, -, H, B, \overline{C}\}$
1- Post KFF	$\{S, P, \overline{H}, \overline{B}, \overline{C}\}$	$\{S, P, H, B, \overline{C}\}$
2 - Original	$\{-, -, H, B, \overline{C}\}$	$\{-, -, H, B, \overline{C}\}$
2- Post KFF	$\{-, -, H, B, \overline{C}\}$	$\{-, -, H, B, \overline{C}\}$

Example: Abutment

As a case study, the condition records for all the brick abutments on underbridges were used to estimate transition rates to compute the required probabilities for the model. An abutment can be found at the end of a bridge and are designed to support the lateral pressure of an arch (McKibbens et al., 2006). A railway underbridge is a bridge which carries the railway over a road, river etc.

Each model had its optimal θ determined as shown in (5.1.5). To compare the

fit between the different models, a test statistic such as a Pearson's chi-squared test could be used. However, due to the aforementioned variability in time intervals, there would be a considerable number of bins which have low frequencies and the test was deemed inappropriate. Instead, an analysis of observed final inspections compared to the predicted final inspections was performed, similar to what was outlined in Section 4.1.7.

The Mean Squared Error (MSE) is given by,

$$MSE = \frac{1}{n}\sum_{i=1}^{n}(Y_i - \hat{Y}_i)^2, \tag{5.1.6}$$

where n is the total number of predictions, generated from the n observations, across all variables. Y is a vector of the observations across all variables and $\hat{Y}$ is a vector of the predictions across all variables. The MSE can only take values that are non-negative and the closer the MSE value is to zero, the better the fit generated by the estimator.

The values for final observed and predicted inspections are shown in Table 5.7, and it can be observed that the predicted final conditions are consistent in magnitude as the observed final conditions. However, the SevEx and SevEx-CM models are typically closer to the observed value. In terms of the number of observed final conditions there are several states (e.g. states 2 and 4) that are considerably greater in observations than others (e.g. states 7 and 9). The discrepancy between the high and low observed states seems to cause some inaccuracies in the predicted number for the low observed states. This could be a consequence of the MLE parameter estimation technique used, which could introduce a bias for the most frequently observed states.

The variability of recorded condition states at inspection is a known issue with bridge condition records (Yianni et al., 2018). Consequently, the accuracy presented for these models is deemed to be be sufficiently accurate. Moreover, if there were consistently low errors between the observations and predictions, it would be likely that the model has been over fitted to the condition records.

Table 5.7: Number of observed and predicted final conditions, for the displacement of block work.

	Condition State	Observed	Predicted: Independent	Predicted: SevEx	Predicted: SevEx-CM
1	$\overline{\mathbf{B}} \cap \overline{\mathbf{H}} \cap \overline{\mathbf{P}} \cap \overline{\mathbf{S}}$	76	69.7	79.1	77.1
2	$\overline{\mathbf{B}} \cap \overline{\mathbf{H}} \cap \overline{\mathbf{P}} \cap \mathbf{S}$	1518	1338.5	1498.5	1495.4
3	$\overline{\mathbf{B}} \cap \overline{\mathbf{H}} \cap \mathbf{P} \cap \overline{\mathbf{S}}$	94	93.3	109.2	102.7
4	$\overline{\mathbf{B}} \cap \overline{\mathbf{H}} \cap \mathbf{P} \cap \mathbf{S}$	3433	3505.1	3446.6	3440.9
5	$\overline{\mathbf{B}} \cap \mathbf{H} \cap \overline{\mathbf{P}} \cap \overline{\mathbf{S}}$	19	14.5	10.5	10.6
6	$\overline{\mathbf{B}} \cap \mathbf{H} \cap \overline{\mathbf{P}} \cap \mathbf{S}$	112	232.6	156.1	155.2
7	$\overline{\mathbf{B}} \cap \mathbf{H} \cap \mathbf{P} \cap \overline{\mathbf{S}}$	0	13.1	5.4	4.9
8	$\overline{\mathbf{B}} \cap \mathbf{H} \cap \mathbf{P} \cap \mathbf{S}$	1580	1567.7	1544.8	1545.3
9	$\mathbf{B} \cap \overline{\mathbf{H}} \cap \overline{\mathbf{P}} \cap \overline{\mathbf{S}}$	2	4.6	0.9	1.8
10	$\mathbf{B} \cap \overline{\mathbf{H}} \cap \overline{\mathbf{P}} \cap \mathbf{S}$	62	126.7	60.9	61.7
11	$\mathbf{B} \cap \overline{\mathbf{H}} \cap \mathbf{P} \cap \overline{\mathbf{S}}$	0	6.5	0.5	5.9
12	$\mathbf{B} \cap \overline{\mathbf{H}} \cap \mathbf{P} \cap \mathbf{S}$	341	383.9	336.7	339.8
13	$\mathbf{B} \cap \mathbf{H} \cap \overline{\mathbf{P}} \cap \overline{\mathbf{S}}$	0	1.0	0.01	0.01
14	$\mathbf{B} \cap \mathbf{H} \cap \overline{\mathbf{P}} \cap \mathbf{S}$	0	19.5	1.1	1.0
15	$\mathbf{B} \cap \mathbf{H} \cap \mathbf{P} \cap \overline{\mathbf{S}}$	0	1.0	0.01	0.5
16	$\mathbf{B} \cap \mathbf{H} \cap \mathbf{P} \cap \mathbf{S}$	268	127.4	254.6	262.2

The MSE can be used to compare the goodness of fit between models and the value for each model can be found in Table 5.8. The original hypothesis was that the defects were not independent from each other but rather, the absence or presence of defects would influence the status of other defects. The independent model has the highest, and thus worse MSE value, which provides evidence to suggest that the hypothesis of there being interactions between mechanisms is true. The difference in the MSE value for the SevEx and SevEx-CM models suggests that the SevEx-CM model provides a better fit, however, the improvement is not as stark as the improvement by introducing conditionality. Nonetheless, the SevEx-CM does provide the best fit out of the three models, as well as outputting an additional defect type indicator, so was the DBN structure selected for further analysis.

Table 5.8: Mean Squared Error for each model based on the predictions shown in Table 5.7.

Model	MSE Value
Independent Model	10.4724
SevEx DBN	0.5727
SevEx-CM DBN	0.5172

SevEx-CM DBN Condition Profiles

The parameters for the SevEx-CM DBN model can be found in Table 5.9. All of the probability of occurrence profiles presented for this study are for a 100 year interval. There will be considerable uncertainty for such a large time period. However, the interval is used to best display the condition profile of the non-constant deterioration behaviour. Moreover, the plots of the probability of defects occurring have been initialised with a belief state of no defects being present, unless otherwise stated. The initial belief state of no defects present has been used so that a life cycle of a bridge element under a do-nothing strategy can be observed. The target node for each plot was the respective defect at time $t = 100$ years.

The condition profiles for the independent defects, i.e. spalling, and deteriorated pointing are shown in Figure 5.4. The rate of spalling developing, see Figure 5.4, is rather rapid and more pronounced than the rate of deteriorated pointing occurring. Whilst, this is plausible, it also could be explained by the definition of spalling in the SevEx condition scale, as it can be initiated with limited water damage on the surface as discussed in Section 5.1.1.

The use of the exponential distribution for modelling the transition times between state implies that for the independent model, each deterioration mode has a constant deterioration rate. The Markov assumption required for traditional Markov deterioration models has been thought to be a severe limitation, with Sobanjo (2011), empirically showing that bridge deterioration may be non-constant. Whilst, the

Table 5.9: List of required parameters for multiple defect DBN.

Defect Type	Transition	Transition Rate (years^{-1})	Parameter Number (Defect Index Number)
Spalling	$\overline{S} \rightarrow S$	0.2254	1 (S.1)
Pointing	$\overline{P} \rightarrow P$	0.0725	2 (P.1)
Hollowness	$\overline{H} \rightarrow H\|(\overline{P} \cap \overline{S})$	0.0020	3 (H.1)
	$\overline{H} \rightarrow H\|(\overline{P} \cap S)$	0.0042	4 (H.2)
	$\overline{H} \rightarrow H\|(P \cap \overline{S})$	2.2×10^{-08}	5 (H.3)
	$\overline{H} \rightarrow H\|(P \cap S)$	0.0205	6 (H.4)
Cracking	$\overline{C} \rightarrow C\|(\overline{P} \cap \overline{S})$	0.0097	7 (C.1)
	$\overline{C} \rightarrow C\|(\overline{P} \cap S)$	0.0184	8 (C.2)
	$\overline{C} \rightarrow C\|(P \cap \overline{S})$	0.0205	9 (C.3)
	$\overline{C} \rightarrow C\|(P \cap S)$	0.0228	10 (C.4)
Block work	$\overline{B} \rightarrow B\|(\overline{C} \cap \overline{H} \cap \overline{P})$	0.0020	11 (B.1)
	$\overline{B} \rightarrow B\|(\overline{C} \cap \overline{H} \cap P)$	0.0074	12 (B.2)
	$\overline{B} \rightarrow B\|(\overline{C} \cap H \cap \overline{P})$	2.1×10^{-08}	13 (B.3)
	$\overline{B} \rightarrow B\|(\overline{C} \cap H \cap P$	0.0179	14 (B.4)
	$\overline{B} \rightarrow B\|(C \cap \overline{H} \cap \overline{P})$	0.0042	15 (B.5)
	$\overline{B} \rightarrow B\|(C \cap \overline{H} \cap P)$	0.0158	16 (B.6)
	$\overline{B} \rightarrow B\|(C \cap H \cap \overline{P})$	7.1×10^{-07}	17 (B.7)
	$\overline{B} \rightarrow B\|(C \cap H \cap P)$	0.0339	18 (B.8)

DBN models in this study retain the Markov assumption, it can be seen in Figures 5.5, 5.6 and 5.7, for the marginal rate of occurrence of hollowness, cracking and displaced block work, respectively, the deterioration process is non-constant. Comparing the marginal probability to the independent probability it can be observed that the independent model would overestimate deterioration in the early years of a life cycle and underestimate the deterioration in the later stages of the life cycle.

Figure 5.5 shows various conditional profiles for hollowness occurring on a brick abutment on a railway bridge. The top dashed line represents the probability of hollowness being present, assuming the influencing defects are all present, all of the

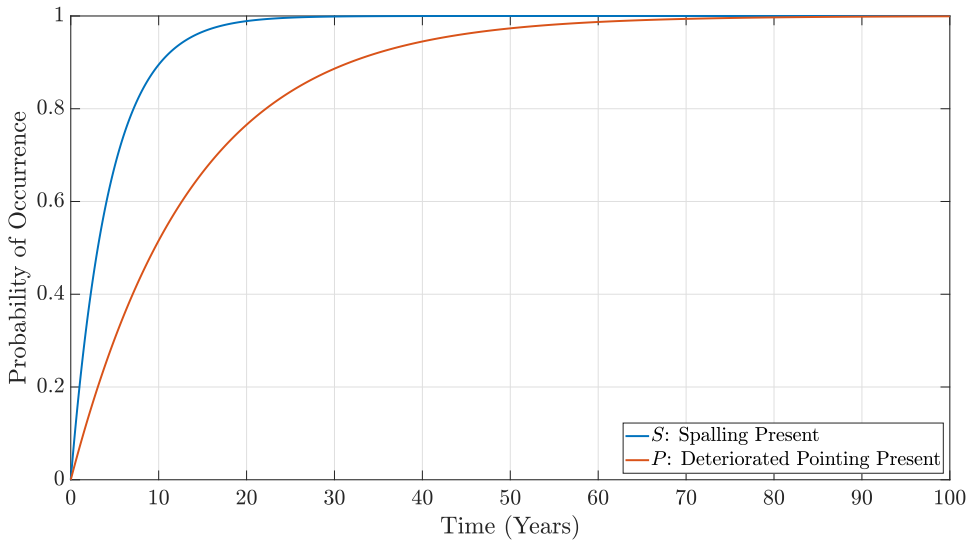

Figure 5.4: Probability profiles for the defects of spalling and deteriorated pointing occurring on a brick abutment, on a railway underbridge.

time, i.e. the 'worst' causal influence scenario. Conversely, the bottom dashed line represents the probability of hollowness being present, assuming the influencing defects are all absent, all of the time, i.e. the 'best' causal influence scenario. The identified 'worst and 'best' causal influence scenarios are consistent with the theoretical engineering expectation of bounding all other scenarios and is observed in the values obtained during model calibration for each considered defect. The orange line is the probability of hollowness occurring, if it were modelled as an independent defect. Finally, the yellow line presents the marginal probability of hollowness occurring, given the status of the influencing defects, where the influencing defects evolve through time as shown in Figure 5.4.

Figure 5.5 shows that for the independent defect model, the probability of hollowness occurring is greater than what is predicted by the conditional defect model for the first 40 years. After 40 years, the conditional defect model is predicting a greater prevalence of hollowness than the independent defect model. These observations can be explained by the fact that the rate of occurrence of hollowness when modelled independently from other defects is constant throughout time. In contrast, the rate of occurrence of hollowness is variable when hollowness is modelled with a conditional relationship with spalling and pointing deterioration. Moreover, when

spalling is absent, and pointing has not deteriorated, hollowness becomes present at a lower rate than when independently modelled. However, as time evolves and spalling becomes present and the pointing deteriorates, the occurrence of hollowness is predicted to occur at a higher rate than when modelled independently.

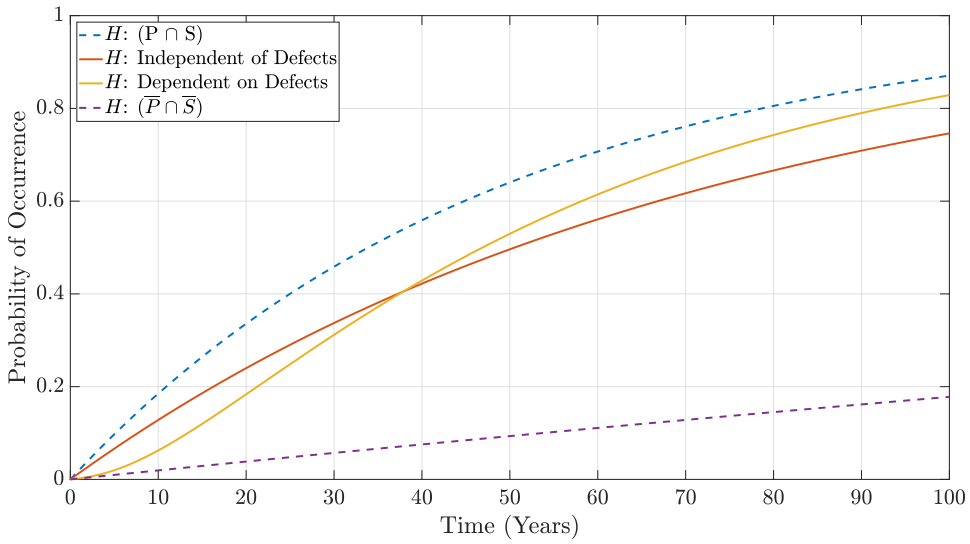

Figure 5.5: Probability profile for hollowness occurring on a brick abutment, on a railway underbridge.

Figures 5.6 and 5.7 show the conditional profiles for cracking and displaced block work, respectively, with similarly defined profiles as shown in Figure 5.5. For cracking, although the deterioration rate is non-constant, the variation in rate between different causal influences is small. The small variation in rate could be a result of the amalgamation of several different cracking processes into one modelled mechanism. Additionally, spalling and deteriorated pointing are being modelled as the influencing defects to cracking, but both are fast acting defects.

The smaller variation in rate between the 'worse case' causal influence and 'best case' causal influence for cracking compared to hollowness suggests that the development of cracking may be less sensitive to spalling and pointing condition than hollowness. However, such conclusions should be reserved until the extensiveness of spalling, deteriorated pointing and cracking can be evaluated in a model. The influences of spalling and pointing deterioration on cracking were ultimately retained in the model as the goodness of fit analysis suggests a better prediction accuracy with

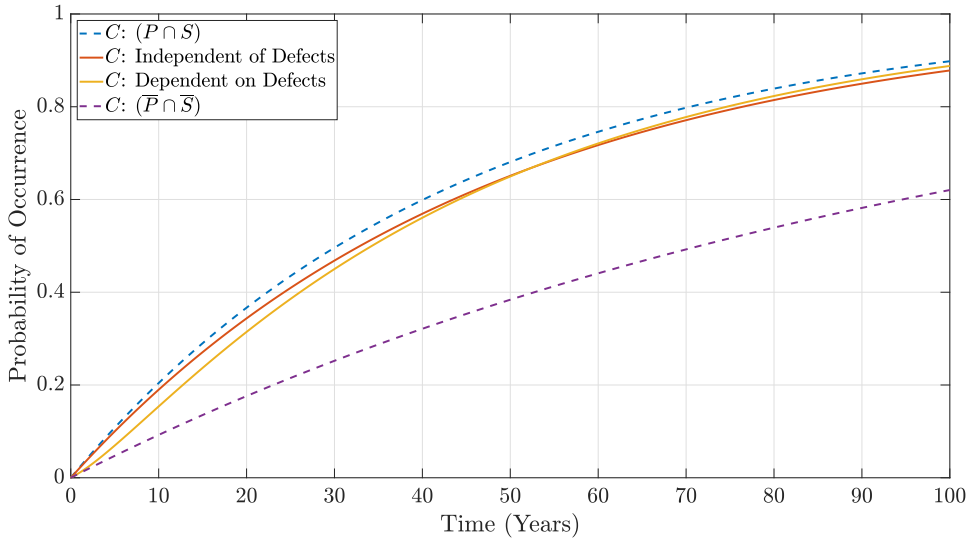

Figure 5.6: Probability profile for cracking occurring on a brick abutment, on a railway underbridge.

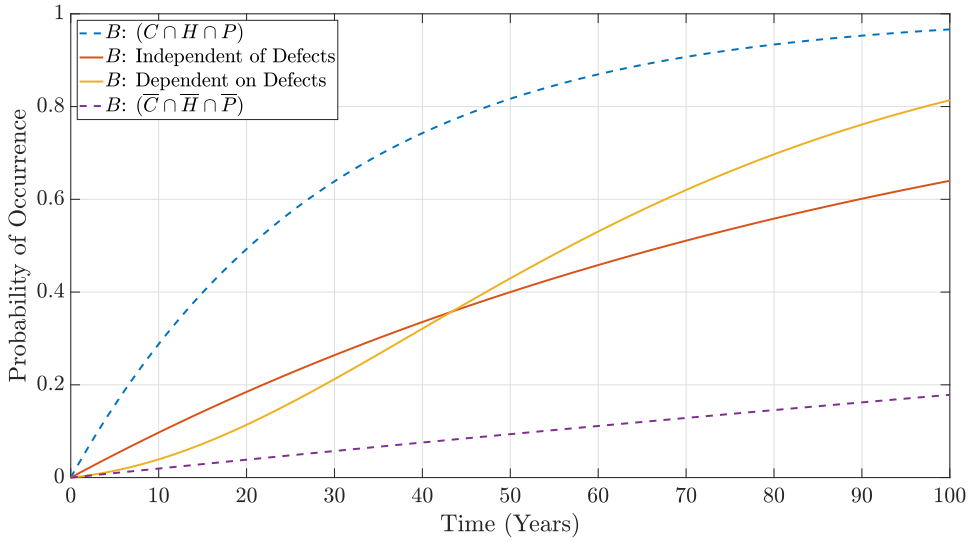

Figure 5.7: Probability profile of displaced block work occurring on a brick abutment, on a railway underbridge.

its inclusion. Additionally, the causal influences were consistent with the judgement of Network Rail engineers.

Displaced block work is the most severe defect type being considered and poses the greatest risk to the structural integrity of a masonry bridge asset. The model is deemed to provide an accurate insight into the rate of occurrence of this defect

whilst capturing the non-constant behaviour. It should be recalled that the profiles are modelling the existence of a defect on a bridge element and not how extensive the defect is, and thus very localised defects will be captured.

The model has the capability to determine a contextualised rate of occurrence given the presence of other influencing defects. Figure 5.8 shows an instance where a bridge element is initially at perfect condition i.e. no defects present. The blue line, denotes the probability of hollowness occurring given the initial belief state. However, after 6 years, an inspection is performed and the DBN can be updated with evidence. In the case where the inspection observes hollowness being present, the probability would trivially become one. However, in the cases where hollowness is observed as being absent, then there are four scenarios that could be used as belief states, i.e. the absence or presence of spalling and deteriorated pointing, its influencing defects. From Figure 5.8, the probability of hollowness occurring varies given the status of spalling and deteriorated pointing. The scenario where spalling and deteriorated pointing are both absent yields the lowest probability 6 years after inspection and both defects being present yields the highest probability of hollowness occurring, 6 years after inspection.

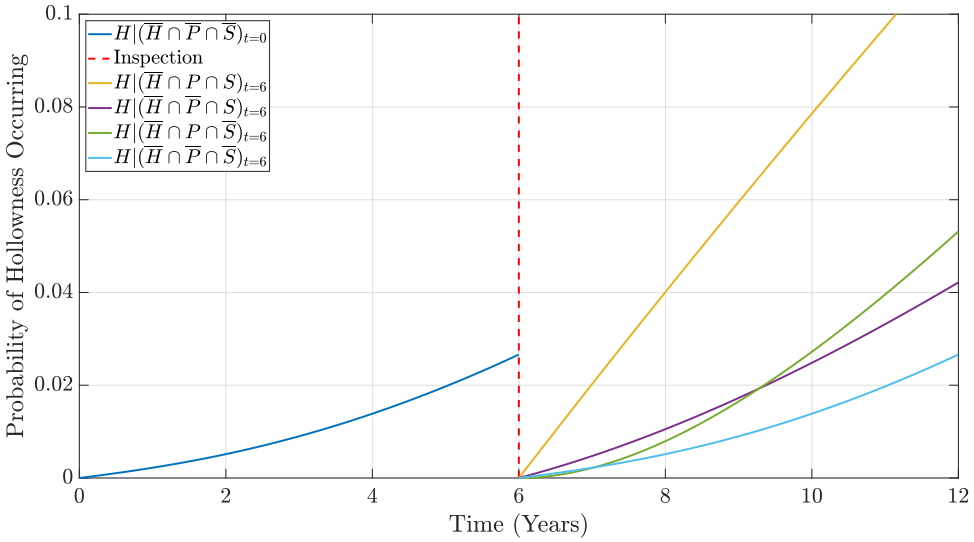

Figure 5.8: Contexualised rates for the occurrence of hollowness on a brick abutment, on a railway underbridge.

Propagation Analysis

Ideally any inspection regime would record all instances of each defect mechanism at inspection, so that all the defects being modelled can be updated with evidence. However, there is an increasing interest in deploying drones to inspect bridges to reduce the safety risk to examiners working on the railway and to reduce expense. In the situation where this is possible, the drone inspection could be used to reveal the absence/presence of the less severe surface defects of spalling, deteriorated pointing and cracking, before requiring a visual inspection of bridge at 'touching distance' by a bridge examiner.

Consider the example where a bridge component is in perfect condition at time $t = 0$. Moreover, a drone inspection occurs at time $t = 5$ years, which reveals the absence/presence state of spalling, deteriorated pointing and cracking. Upon, the condition of these defects becoming known, the model can be updated with the evidence and a propagation analysis performed to assess the updated probabilities of defect occurrence. An asset manager may be interested in the predicted presence of the severe defects after a further five years has elapsed, i.e. $t = 10$ years. The updated probabilities of hollowness and displaced blockwork being present at time $t = 10$ years are shown in Figure 5.9. From Figure 5.9, it can be observed that the revealed condition at $t = 5$ years can have a sizeable impact on the probability of hollowness and displaced block work occurring at $t = 10$ years. In particular, if pointing degradation is revealed to be present at $t = 5$ years, the probability of the 'severe' defect being present at $t = 10$ years, is more than doubled when compared to the calculated probability for the scenario when no inspection occurs at $t = 5$ years.

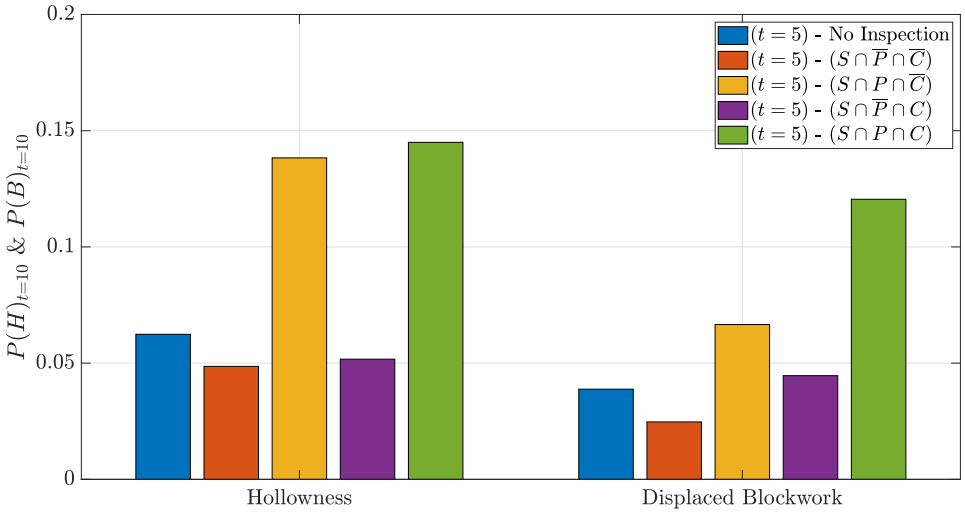

Figure 5.9: Probabilities of hollowness and displaced block work being present at $t = 10$ years with partial state reveal at $t = 5$ years.

Understanding the non-constant deterioration behaviour is fundamental when developing maintenance strategies. For example, if an infrastructure manager expends resources on an intervention for a less severe defect, such as spalling and deteriorated pointing, there needs to be a justification for this expense. If this strategy was assessed using the deterioration profiles shown above, this expense would not only alleviate the presence of spalling and/or pointing, but would additionally have the 'reward' of reducing the likelihood of the more severe defects, i.e hollowness, cracking and displaced block work. The modelling of this phenomena is not only important for more accurately replicating the physical process but by also introducing the means, to assess the effects of targeted maintenance interventions in a contextualised manner.

5.2 Metal Multiple Defect Deterioration Model

For metallic components the SevEx condition scale captures the development of corrosion and SCF mechanisms during an inspection and the CM scale indicates the intactness of the paintwork or coating mechanism. Whilst the defect mechanisms could be modelled using discrete condition states that align with the appropriate SevEx or CM score, Section 4.2.1 introduced consolidated four state condition scales for coating/paintwork and corrosion and a two state scale for SCF. The purpose of these consolidated scales was to facilitate an investigation of the interactions between mechanisms whilst each mechanism is developing i.e. the interactions between mechanisms at different levels of defect extensiveness. Masonry was constrained to evaluating the interactions between mechanisms on an absent/present basis due to the data constraints outlined in Section 5.1.1, however metallic condition records fully reveal the condition of each defect mechanism at every inspection enabling this additional analysis.

After consultation with Network Rail structural engineers, the deterioration model with interacting mechanisms was devised such that the condition of the coating influenced the rate of corrosion, which in turn influenced the rate at which SCF develops. The interactions between the deterioration mechanisms is shown in Figure 5.10 as a BBN, the temporal evaluation of the deterioration mechanisms is shown as a DBN in Figure 5.11.

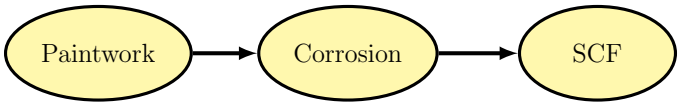

Figure 5.10: Bayesian Belief Network representing causal influences between metallic defect modes.

5.2.1 Metal Defect DBN Condition Profiles

As a case study of the metallic multiple defect DBN deterioration model, the records for all the metallic exposed main girders on railway underbridges in the database were used to calibrate the model.

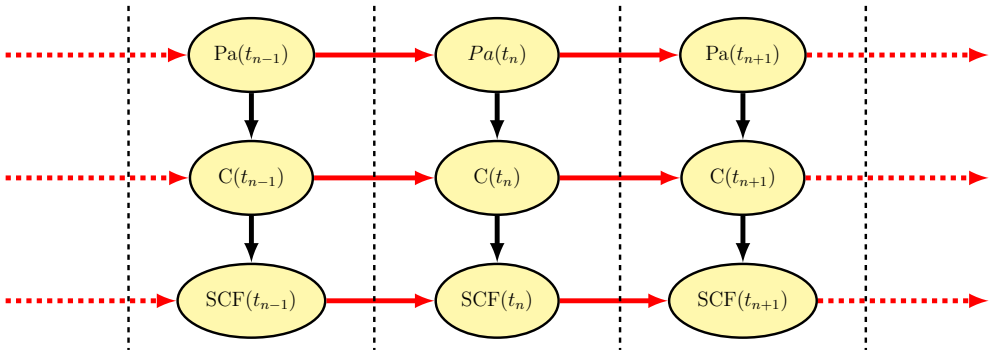

Figure 5.11: DBN deterioration model, where the red lines denote temporal links.

The probability values for the CPTs of the DBN model shown in Figure 5.11 are parametrised using a λ rate for an exponential distribution, similar to what was shown in Section 5.1.3 for the masonry DBN model. The DBN model for metallic defect mechanisms only permits transitions to successive condition states, with no state jumping permitted i.e. a direct transition from C1 to C3 is not possible, the model requires a transition from C1 to C2 and then to C3. Consequently, the probability of transition occurring during one time step can be computed analytically from the exponential cumulative distribution function,

$$p_{ij|c} = 1 - e^{-\lambda_{ij|c} \cdot t}, \tag{5.2.7}$$

where $p_{ij|c}$ is the probability of transition from condition state i to j given the causal influence c, $\lambda_{ij|c}$ is its associated exponential distribution parametrisation and t is the size of the interval between the time slices in the DBN. Thus, the probability of staying in the current condition state is $p_{ii|c} = 1 - p_{ij|c}$.

The DBN model also had some parameter manipulations to exert expert judgement. The $C2 \rightarrow C3$ and $C3 \rightarrow C4$ transitions, each only had 2 distinct parameters to capture the causal relationships, opposed to the 4 distinct parameters that $C1 \rightarrow C2$ and $F1 \rightarrow F2$ each had. The reason was that there were fewer records for each of these transitions to be calibrated with. Moreover, the model required a monotonic increase in rate for the causal relationship between $Pa1$, $Pa2$, $Pa3$ and $Pa4$. However, in this study constraints were not used to enforce that criteria to enable the statistical significance testing between models that is described in Chapter 7.

Theoretically one may anticipate that if the paintwork is in $Pa1$, i.e. perfect condition then corrosion should not occur and that the $C1 \rightarrow C2|Pa1$ value should be zero. However, in reality there is no such thing as absolutely perfect paintwork repair and consequently some corrosion may still occur, hence the λ value for $C1 \rightarrow C2|Pa1$ should be set to a non-zero value using expert judgement prior to model calibration.

Each model had its optimal θ determined using the function shown in (5.1.5) in a GA optimisation, as outlined in Section 5.1.3 and Appendix A. The parameter values for the DBN deterioration model are shown in Table 5.10.

The condition profiles for coating, corrosion and SCF calculated using the DBN model are shown in Figure 5.12. Additionally, the condition profiles from the independent multiple defect model, as detailed in Section 4.2.2, are also shown in Figure 5.12. Note that the bridge element has an initial belief condition state of $P1$, $C1$ and $F1$, representing a new bridge element.

It can be observed from the condition probability profiles for both models that corrosion and coating damage are much more rapid in progression than SCF. This model outcome aligns with the engineering expectation that SCF would develop over a much longer time period. The condition probability profiles for paintwork are shown to be consistent between the independent Markov and DBN models, which corresponds with paintwork being the root variable in the DBN model. However, for corrosion and SCF it can be observed that the DBN model returns condition profiles that have quite a large discrepancy in the returned probabilities for being in a particular condition at any given time.

The discrepancy in the condition profiles for corrosion and SCF between the independent and DBN models is due to the DBN model having variable probabilities of corrosion and SCF state transitions based on their respective influencing defects.

For the example shown in Figure 5.12, the DBN model indicates that the corrosion and SCF occur at a slower rate. However, this is only true as the model was initialised with the conditions of $Pa1, C1$, and $F1$ and the slower rate is not necessarily always the case. For transitions between conditions states for corrosion and SCF, the probability of transitions is dictated by the condition of the influencing

Table 5.10: List of parameters for multiple defect DBN deterioration model.

Defect Type	**Transition**	**Transition Rate** (years^{-1})
Paintwork	$Pa1 \rightarrow Pa2$	0.1761
Paintwork	$Pa2 \rightarrow Pa3$	0.1553
Paintwork	$Pa3 \rightarrow Pa4$	0.0335
Corrosion	$C1 \rightarrow C2 \vert Pa1$	0.0050
Corrosion	$C1 \rightarrow C2 \vert Pa2$	0.1818
Corrosion	$C1 \rightarrow C2 \vert Pa3$	0.4304
Corrosion	$C1 \rightarrow C2 \vert Pa4$	0.6918
Corrosion	$C2 \rightarrow C3 \vert Pa1$	0.0471
Corrosion	$C2 \rightarrow C3 \vert Pa2$	0.0471
Corrosion	$C2 \rightarrow C3 \vert Pa3$	0.1545
Corrosion	$C2 \rightarrow C3 \vert Pa4$	0.1545
Corrosion	$C3 \rightarrow C4 \vert Pa1$	0.0331
Corrosion	$C3 \rightarrow C4 \vert Pa2$	0.0331
Corrosion	$C3 \rightarrow C4 \vert Pa3$	0.0340
Corrosion	$C3 \rightarrow C4 \vert Pa4$	0.0340
SCF	$F1 \rightarrow F2 \vert C1$	0.0015
SCF	$F1 \rightarrow F2 \vert C2$	0.0036
SCF	$F1 \rightarrow F2 \vert C3$	0.0087
SCF	$F1 \rightarrow F2 \vert C4$	0.0156

defect. Moreover, the transitions which have their rates determined by an influencing defect exhibit a monotonic increase in rate of transition as the condition of the influencing defect worsens.

For example, the $C1 \rightarrow C2$ has $\lambda = 0.0050$ when paintwork is in $Pa1$, which increases to $\lambda = 0.1818$ for $Pa2$, $\lambda = 0.4304$ for $Pa3$ and finally $\lambda = 0.6918$ for $Pa4$. Similar trends can be observed for $C2 \rightarrow C3$, $C3 \rightarrow C4$ and $F1 \rightarrow F2$.

Thus, depending on the condition of the influencing defects, the rate of corrosion and SCF can occur at a slower or faster rate than the independent model would suggest. However, in general for a metallic element starting in perfect condition, the independent model would overestimate the rate of deterioration at the earlier stages of a component life span and underestimate the rate of deterioration in the later stages.

The values for the $C1 \rightarrow C2$ transition are notably higher than the other transitions for corrosion, which suggests that $C1 \rightarrow C2$ occurs quite rapidly. $C1$ is defined in accordance with the SevEx state $A1$, which is defined such that a bridge component has no visible defects to the metal, see Table 4.11. However, for a component to be scored as $C2$, corrosion does not need to be particularly well developed but just present, i.e. the corrosion could be less than 1mm deep. Consequently, the transition from $C1 \rightarrow C2$ is likely to be quite rapid and faster than $C2 \rightarrow C3$ or $C3 \rightarrow C4$ as these transitions reflect more substantial development of corrosion. Given that the $C1 \rightarrow C2$ transition is reasonably rapid in general, it follows that the transition for $C1 \rightarrow C2$ when paintwork is in its worst condition $Pa4$ is notably large in value.

For similar reasons as outlined in Section 5.1.4 to evaluate the prediction accuracy of the metallic DBN model, an analysis of observed condition at second inspection compared to the predicted condition at second inspection was performed. The breakdown for all condition state permutations is shown in Table 5.11.

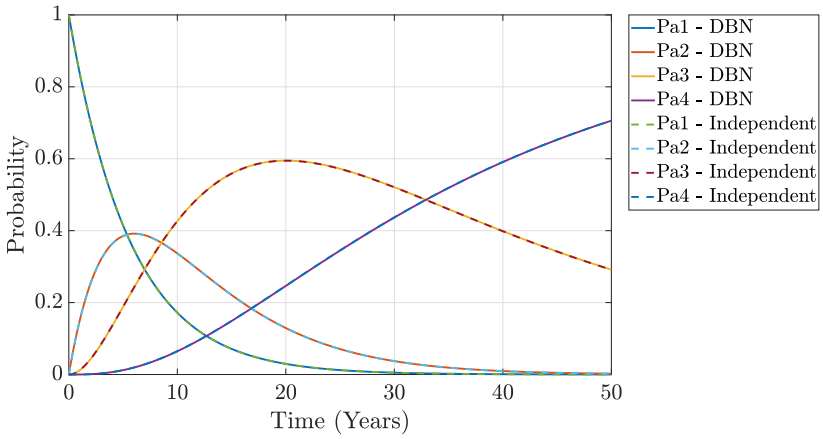

(a) Paintwork

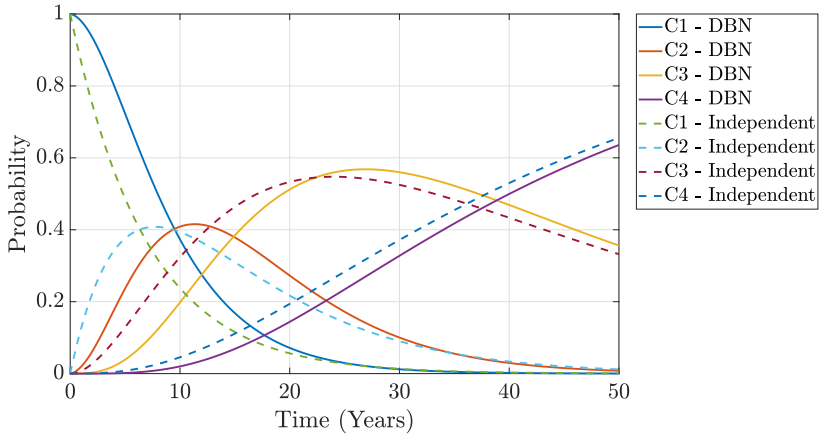

(b) Corrosion

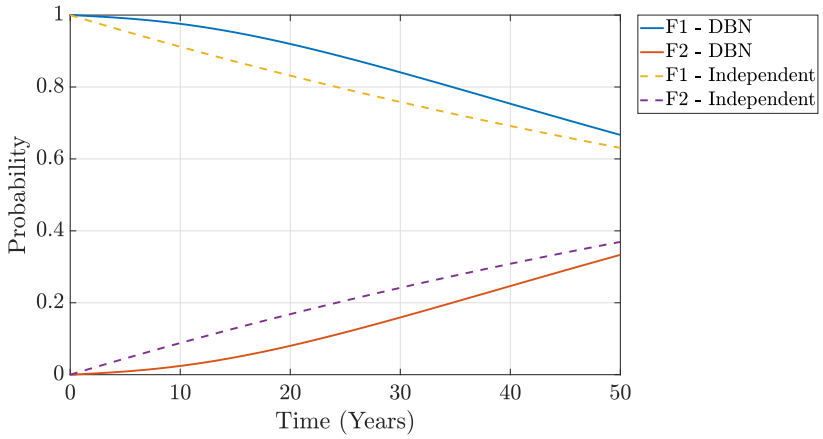

(c) SCF

Figure 5.12: Comparison of the condition probability profiles for paintwork, corrosion and SCF for a metallic girder starting in $\{P1, C1, F1\}$, between the DBN and independent CTMC models.

Table 5.11: Number of observed and predicted final conditions for metallic defect mechanisms.

	Condition State	Observed	Predicted: Independent	Predicted: Metal DBN
1	$F1 \cap C1 \cap Pa1$	223	101.76	214.78
2	$F1 \cap C1 \cap Pa2$	167	140.42	178.23
3	$F1 \cap C1 \cap Pa3$	36	141.52	71.73
4	$F1 \cap C1 \cap Pa4$	0	19.43	3.65
5	$F1 \cap C2 \cap Pa1$	74	117.44	59.42
6	$F1 \cap C2 \cap Pa2$	642	377.95	528.48
7	$F1 \cap C2 \cap Pa3$	1101	1146.79	1119.68
8	$F1 \cap C2 \cap Pa4$	181	328.55	286.18
9	$F1 \cap C3 \cap Pa1$	143	182.95	132.62
10	$F1 \cap C1 \cap Pa2$	337	583.26	441.17
11	$F1 \cap C3 \cap Pa3$	5604	5240.81	5406.83
12	$F1 \cap C3 \cap Pa4$	3356	3275.61	3347.54
13	$F1 \cap C4 \cap Pa1$	117	128.99	119.24
14	$F1 \cap C4 \cap Pa2$	173	253.50	232.97
15	$F1 \cap C4 \cap Pa3$	2640	2811.53	2755.67
16	$F1 \cap C4 \cap Pa4$	2525	2474.30	2414.49
17	$F2 \cap C1 \cap Pa1$	4	5.60	3.68
18	$F2 \cap C1 \cap Pa2$	1	8.65	3.26
19	$F2 \cap C1 \cap Pa3$	3	13.42	2.19
20	$F2 \cap C1 \cap Pa4$	3	4.47	0.45
21	$F2 \cap C2 \cap Pa1$	11	11.02	6.36
22	$F2 \cap C2 \cap Pa2$	26	31.46	25.46
23	$F2 \cap C2 \cap Pa3$	80	122.10	76.04
24	$F2 \cap C2 \cap Pa4$	16	41.81	25.84
25	$F2 \cap C3 \cap Pa1$	7	17.64	12.32
26	$F2 \cap C1 \cap Pa2$	35	63.79	47.24
27	$F2 \cap C3 \cap Pa3$	681	726.50	705.97
28	$F2 \cap C3 \cap Pa4$	464	497.01	487.90
29	$F2 \cap C4 \cap Pa1$	21	19.32	21.64
30	$F2 \cap C4 \cap Pa2$	47	40.73	45.62
31	$F2 \cap C4 \cap Pa3$	696	592.22	670.48
32	$F2 \cap C4 \cap Pa4$	587	480.45	553.86

The MSE values for the independent defect model and the DBN model are shown in Table 5.12, with the DBN model providing a better overall prediction accuracy than the independent model.

From Table 4.21 in Section 4.2.3 the independent Markov model was found to be provide reasonable prediction accuracy for independent defects. However, this is only true when considering observed final condition states across an entire portfolio. For specific instances of a bridge component with a particular condition score permutation of paintwork, corrosion and SCF, the DBN model has a higher accuracy of predicting the condition states of the combined defect mechanisms than the independent model. The improved accuracy for specific instances of components will be beneficial when modelling asset management strategies for specific instances of bridge elements.

Table 5.12: Mean Squared Error for each model based on the predictions of final condition.

Deterioration Model	**Mean Squared Error**
Independent	19.5254
DBN	5.4180

Additionally, a log-likelihood ratio test statistic can be used to show that the improved fit of the model is statistically significant given the increase in parameters for the DBN model. The log-likelihood ratio test is given by

$$LR = -2(F_{Ind} - F_{DBN}), \tag{5.2.8}$$

where F_{Ind} is the log-likelihood of the independent model with its optimal parameter θ values and F_{DBN} is similarly defined for the DBN model. The null hypothesis for the likelihood ratio test is true when LR is small and rejected if the LR values have a significant difference. The LR statistic approximately follows a chi-squared distribution, with the degrees of freedom equal to the difference between the number of parameters used in each model. For the independent and DBN models the LR statis-

tic is 423.3. Using a significance level of 5%, the null hypothesis can be rejected, and thus conclude that the DBN model improvement is statistically significant despite the increased number of parameters in the model.

5.2.2 Comparison to Single Indicator Model

The comparison of predictive accuracy between the multiple defect DBN deterioration model and a typical single indicator bridge deterioration model can be a challenging task depending on the condition scales used for each model type.

Network Rail model future condition of metallic bridge components using a Markov chain approach, where condition is denoted using an integer condition scale. The SevEx condition states for metallic components are converted to the integer condition scale using the assigned values shown in Table 4.15. Currently at Network Rail, only SevEx scores are considered for model calibration, i.e. the CM scores are omitted.

To compare the multiple indicators from the multiple defect model and the single condition scale a common metric or indicator is required. Ideally, one would calculate the multiple indicators in the multiple defect model and select the worst score to compare against the single condition scale. However, this is not possible for the metallic model as the study conditions of $C1, C2, C3$ and $C4$ for corrosion and $F1$ and $F2$ for SCF are a consolidation of multiple condition states from the integer scale.

The integer condition scale has 15 distinct condition states which correspond to different SevEx states. If the integer value for SevEx state of G2 is assigned a new value of 12 for this analysis, it is then possible to perform a comparison between models using the states outlined in Table 5.13.

Table 5.13: States used to compare multiple defect models to single indicator model.

Condition State	Integer Scale	Multiple Defect Scale
Defects Absent - Perfect Condition	1	C1 and F1
Defects Present - Fair Condition	2-9	(C2 and F1) or (C3 and F1)
Defects Present - Poor Condition	10-15	(C4 and F1) or F2

A CTMC model was calibrated using the same condition records as the multiple defect model, however the scores were stated in the revised integer condition scale. The calibrated CTMC model was developed to match internal Network Rail models and allowed the instantaneous transition of a condition state of up to five states worse than the current state.

The calibrated CTMC and DBN models were then used to predict the second recorded inspection score of an exam pair when given the initial inspection and inspection interval using their own respective condition scales. The DBN model has a state space of 32 states and the CTMC model has a state space of 15, both of which were transformed to the condition scale denoted in Table 5.13. Note that the DBN model retained the CM score for model calibration and was used to influence the appropriate causal relationships when modelling records, however the Pa score is not used in the state mapping which is used in the comparison study. The values for observed and predicted scores using the DBN and CTMC models are shown in Table 5.14.

From Table 5.14 it can be observed that the DBN model has the highest prediction accuracy for the Fair and Poor condition states. However, the DBN returns the lowest prediction accuracy for the Perfect condition state, which can be partially attributed to the exertion of expert judgement on the corrosion transition of $C1 \rightarrow C2$ when paintwork is in $Pa1$. Nonetheless, the perfect condition states represent approximately 2% of the records considered, and thus on a weighted basis the DBN model is clearly more accurate. Additionally, for maintenance scheduling and determining residual value of an asset portfolio, the total of components predicted to be in poor condition is a more critical value to an asset manager.

Table 5.14: Number of observed and predicted final conditions for metallic defect mechanisms using DBN and CTMC models.

	Perfect (% Error)	Fair (% Error)	Poor (% Error)
Observed	426	11438	8222
DBN - Conditional	468.39	11321.94	8295.67
	(9.95)	(-1.01)	(0.90)
CTMC - Multiple Defect	403.13	11253.36	8429.50
	(-5.37)	(-1.61)	(2.52)
CTMC - Single Indicator	417.718	12808.74	6859.54
	(-1.94)	(11.98)	(-16.57)

One critical trend that is observable for the single indicator model in Table 5.14 is that the single indicator model grossly underestimated the number of exam pairs that had a final score in poor condition. The underestimation of the poor condition state would correspond with similar findings in literature that that Markov models of bridge deterioration overstate the expected service life of assets.

5.2.3 Bridge Condition Under Different Maintenance Strategies

The comparisons of different asset management strategies is a significant task for transportation infrastructure asset managers, with industry stakeholders requiring prudent strategic decisions. Such comparisons require an evaluation of the outcomes on bridge condition and capability, safety risk, service risk etc., for each strategy and the associated impact on WLCC.

To evaluate the life cycle consequence of using contextualised deterioration rates and the effects of targeted maintenance interventions, a simple maintenance case study was performed by applying maintenance interventions to uplift the paintwork score to perfect condition. The three maintenance strategies considered are:

- Strategy 1 - Instant repair of paintwork upon entering state $Pa2$;
- Strategy 2 - Instant repair of paintwork upon entering state $Pa3$;
- Strategy 3 - Instant repair of paintwork upon entering state $Pa4$.

The instant repair strategy assumes a continuously revealed condition state, no budgetary limitations and allocates no delay for scheduling and performing the intervention. These assumptions do not relate to the real-world scenario of managing a bridge portfolio, however the example serves to show the impact of considering defect interactions and modelling using contextualised rates. The average condition of each defect predicted over 50 years with each maintenance strategy and a do-nothing approach are shown in Figure 5.13.

It can be observed from Figure 5.13a that if a maintenance strategy is applied to service the paintwork, the average paintwork condition will ultimately reach an equilibrium value which is greater than the do-nothing approach, which continually degrades. Moreover, the earlier the paintwork intervention is scheduled for, the lower the equilibrium value obtained for average condition score. Recall that a lower average condition score denotes a better condition.

The multiple defect DBN deterioration model incorporates the influence of paintwork condition on the rate of corrosion. Whilst the maintenance strategies considered in this study only intervene on paintwork, that targeted intervention still results in an uplift of the average condition of corrosion for all three scenarios. Nonetheless, it can be observed from Figure 5.13b that the earlier paintwork is intervened on, the greater the reduction in corrosion prevalence. For Strategy 3, the paintwork intervention seems to be so delayed that the difference in the average condition of corrosion for Strategy 3 and the do-nothing approach is minimal. The model accounts for an influence of corrosion on the occurrence of SCF. The reduced prevalence of corrosion due to the paintwork interventions, elicits a reduction in the occurrence of SCF.

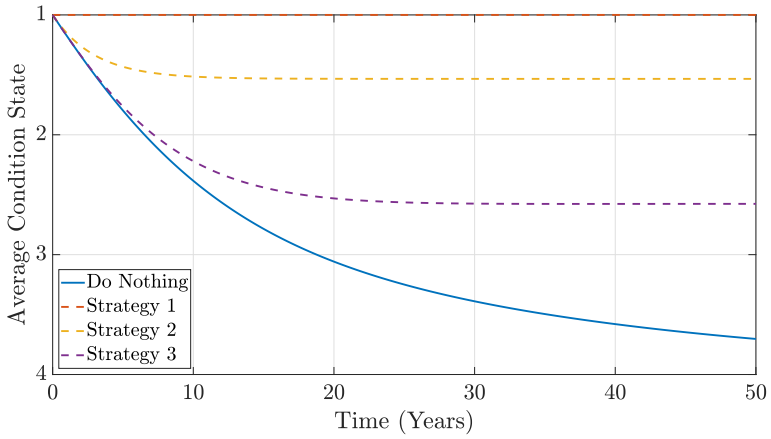

(a) Paintwork

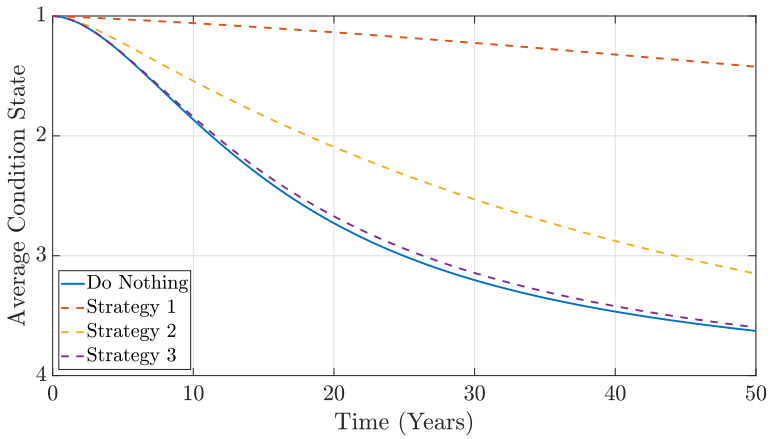

(b) Corrosion

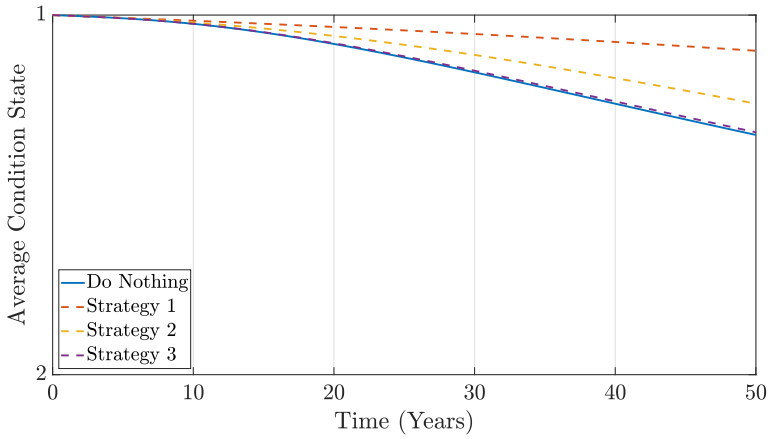

(c) SCF

Figure 5.13: Average condition of paintwork, corrosion and SCF under different paintwork maintenance strategies.

The reduced evolution of defects is a critical trend that represents a desired modelling capability for asset managers, as states C2 and F2 represent the bridge element being in poor condition and posing a risk to the structural integrity of the element and the overall bridge. Having a model that can isolate these physical phenomena and enables the study of the effects of maintenance strategy is a hugely desirable tool for asset managers to develop and present strategies to stakeholders and more efficiently allocate resources.

5.3 Chapter Summary

An accurate life cycle analysis is required to be able to distinguish the cost effects of competing asset management strategies. This is a requisite component to the decision making process for many infrastructure asset managers. Commonly in literature and in industry, bridge deterioration is reported using a single condition index, however deterioration is a heterogeneous process composed of several distinct processes acting simultaneously.

In Chapter 4 CTMCs were found to be an effective means of modelling multiple defects simultaneously, however the method omitted the interactions between the defects. The DBN models presented in this chapter incorporated the interactions between mechanisms, and the DBN models were found to have better prediction accuracy when compared to the CTMC models. Thus, the DBN models are the preferred approach for modelling multiple defect mechanisms under a do-nothing assumption.

The earlier parts of the chapter presented a model for bridge components that are constructed from masonry. The defects of spalling and deteriorated pointing were considered as independent processes, whereas hollowness, cracking and displaced block work, were influenced by the status of other defect modes. The consequence of modelling influences between defect modes is the ability to calculate non-constant deterioration profiles for defect mechanisms even when the underlying probability distributions used are from a memoryless distribution. The incorporation of non-constant deterioration behaviour represents a desired modelling capability for bridge

asset managers.

Although the proposed framework facilitates the modelling of different condition states, in terms of severity and extent, the current implementation for masonry only models the absence or presence of defects, due to data constraints for model calibration. In the advent of a more complete dataset for masonry components, the method can be implemented to include multiple condition states at each of the defect nodes and model the absence or extensiveness of a defect. However, for metallic components a more appropriate dataset was available.

The metallic DBN deterioration modelled the deterioration of paintwork/coating as an independent defect and that the paintwork condition influenced the rate of corrosion. Moreover, the model incorporated the relationship between corrosion and structural component failure. The metallic DBN model was parameterised to include the effects of these interactions not only on a defect absent/present basis but also on the extensiveness of a defect.

A limitation of the presented models is that the defects must ultimately have an acyclic relationship between each other, due to that being an inherent property of BBNs and DBNs. As the condition scales used in this research have a well defined hierarchy it is not thought to be a major concern, however for future studies the feasibility of cyclic relationships between defects should be considered.

Modelling multiple defects simultaneously enables an improvement in predictive accuracy of deterioration as well as outputting additional bridge condition indicators for informing decision modelling. The additional indicators specific for each defect can be employed to develop specific maintenance strategies as opposed to the traditional qualitative maintenance actions. In Section 5.2.3 a simple example exhibited the benefits of applying specific maintenance interventions on paintwork and the resultant reduction in the progression of corrosion and structural component failure. Chapter 6 provides further consideration of the incorporation of multiple defect condition indicators in a life cycle analysis and management strategy development.

Chapter 6

Incorporating Defect Specific Condition Indicators in a Bridge Life Cycle Analysis

The consequences of structural failure of a bridge can be devastating including serious human injury, fatalities and huge reductions in the economic and social well-being of local geographic regions (Smale, 2018; Xie and Levinson, 2011). As part of the efforts to avert such failures infrastructure owners devise asset management strategies. For large bridge portfolios it is a requisite of strategy development to perform a life cycle analysis to ascertain the cost implications of particular strategies as well as to forecast future resource requirements and to present strategies to stakeholders.

In this chapter, the deterioration of bridge condition is modelled using defect specific condition scales and indicators at element level as shown in Chapter 5. The evaluation of different asset management strategies in a life cycle analysis will be executed using a Petri net model. To model the Dynamic Bayesian Network within the Petri net framework a novel Dynamic Conditional Transition is defined. The additional condition indicators can be used to model targeted defect specific maintenance strategies. The quantification of the benefits of early maintenance interventions or servicing programs is a desired modelling capability for many asset managers and is explored in the later parts of the chapter.

6.1 Petri Net Bridge Life Cycle Modelling

Whilst there are many effective approaches for modelling deterioration, Section 3.5.2 outlined the advantages of using the Petri net methodology for modelling deterioration due to the flexibility of the method for incorporating an extensive range of stochastic process. Moreover, for life cycle analysis modelling, PNs are very effective in capturing the unique properties of different management strategies due to the ability of defining detailed state specific actions and developing bespoke solutions under a standardised framework.

The PN bridge deterioration model proposed by Yianni et al. (2017) models bridge condition on a two-dimensional scale, which considers both the type of defect and its associated magnitude. This approach produces deterioration profiles that correspond to the physical process of deterioration, however it is limited by only monitoring the score for the worst defect present, disregarding others.

Le and Andrews (2016) presented a bridge asset management model which encapsulated a series of sub-models for each bridge element, with each sub-model also defined for the element material type. The sub-models incorporated multiple degradation mechanisms dependent on the material. For metallic components the mechanisms considered included protective paint flaking, minor metal corrosion and major corrosion. Multiple mechanisms were also considered for concrete and masonry components.

To model the dependencies between the different degradation mechanisms, Place Conditional Transitions (PCT) were included in the Le and Andrews (2016) PN model. A PCT is a transition which has its firing delay sampled from a probability distribution but the distribution that samples are taken from is dependent on the marking of a predefined list of places upon the transition becoming enabled (Andrews, 2013). Graphically the list of associated places for a PCT is denoted using black dashed arcs.

A limitation of PCTs is that if the marking of the places changes after the enabling of the transition but before the PCT fires, the firing delay is not re-sampled to reflect the updated marking. Consider a slow-acting process that is being modelled with PCTs and the process is conditional on places denoting a fast-acting process.

If the PCT samples a large time for the slow-acting process, the fast-acting process could deteriorate rapidly which could have warranted a different and shorter firing delay for the slow-acting process, but this cannot be reflected for any enabled transitions. Moreover, if the fast-acting process is something that could be regularly intervened on or serviced, the PCT for the slow-acting process could end up having a firing delay sampled from a distribution based on an out-of-date marking and have a firing delay that is too short when considered against the updated marking. The latter scenario is problematic when trying to model and evaluate different maintenance strategies and assess the benefits of early interventions.

There are several additional formalisms for incorporating Bayesian methods or conditionality into PNs. Andrews and Fecarotti (2017) introduced a formalism known as BP-Net which was based on PNs and BBNs, where PN models were used to generate the probabilities for model CPTs. An alternative tool known as Bayesian Stochastic Petri Nets (BSPN) was introduced by Taleb-Berrouane et al. (2020). BSPNs are also a combination of BBNs and Stochastic PNs, although BSPNs enabled the evaluation of continuous input data, negating the need for time discretisation. However, the BSPN method was only applied to a relatively simple case study and there is limited discussion on how to extend the method to large scale and/or complex systems (Moradi and Groth, 2020).

An accurate prediction of future condition requires the ability to dynamically update the stochastic process given changing influencing conditions. To address the limitations of PCTs and extend the methods in literature the next section proposes a new transition; *Dynamic Conditional Transitions*.

6.1.1 Dynamic Conditional Transitions

Consider two distinct processes, α and β, both of which can be described by two discrete states. However, at any given instance the state of α influences the state that β assumes, i.e. β is dependent on α. If α and β are failure mechanisms, and the state of each process is known at initial time t_0, one could predict the evolution of α and β provided a conditional probability distribution is defined for each causal state permutation. A probability distribution for $\alpha(t_n)$ can be determined from the

probability distribution for $\alpha(t_{n-1})$ and the conditional probability distribution for α. The probability distribution of $\beta(t_n)$, the dependent process, can be evaluated if the probability distributions for $\alpha(t_n)$ and $\beta(t_{n-1})$ and the conditional probability distribution for β are known. A common methodology to model this phenomena is using DBNs as discussed in Chapter 5. A DBN implementation of the described scenario is shown in Figure 6.1.

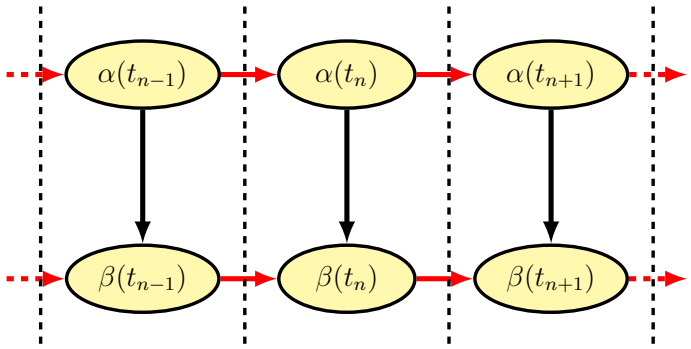

Figure 6.1: A DBN representing the causal influence of defect α on defect β over time. The red arrows denote temporal links between different time steps.

Modelling dynamically conditional processes is not possible using existing defined transition types for PN. Whilst PCTs do sample a firing delay conditionally on the marking of a predefined set of places, if the net marking were to change before the transition fires, the transition firing delay is not resampled. To overcome this limitation, a bespoke transition known as the Dynamic Conditional Transition (DCT) is defined.

Consider the example shown in Figure 6.2. Place P01 denotes the working state of α, P02 its failed state. Similarly, P03 is the working state of β and P04 is the failed state. T01 is a standard stochastic transition which samples its firing delay from a probability distribution and it represents α changing from the working state to the failed state. The firing operations of stochastic transitions are well defined in the literature (Marsan et al., 1984). T02 is a DCT and models the time for β to change from the working state to the failed state. The reachability graph for the PN is shown in Figure 6.3.

A DCT has input arcs, output arcs and '*causal arcs*', where the causal arcs are denoted with dashed blue lines in Figure 6.2. T02 would be enabled if a token is

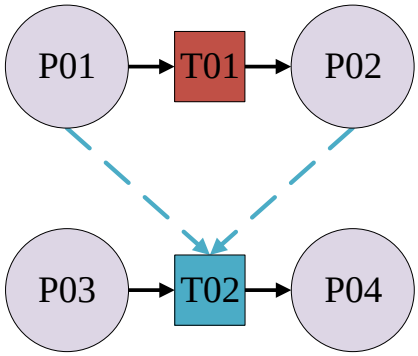

Figure 6.2: PN modelling the DBN shown in Figure 6.1 using a DCT.

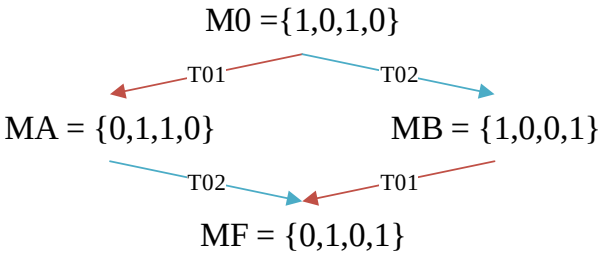

Figure 6.3: Reachability graph for the PN shown in Figure 6.2, where $\{\dots\}$ represents the marking of P01, P02, P03 and P04 respectively.

present in P03 (marking M0 or MA). Upon a DCT becoming enabled, it will attempt to fire after δt, where δt corresponds to the size of interval between a DBN time slice. After δt has elapsed during the simulation, the DCT will analyse its *causal arc place marking* (CAPM). For example, if the PN has a marking of M0 then the CAPM for T02 would be $\{1, 0\}$ ({P1, P2}). When a DCT attempts to fire, a random number, r, is sampled from $\mathcal{U}(0, 1)$. Then r is compared against the DCT firing probability, f, with the value of f dependent on the CAPM. In the example shown in Figure 6.2, the CAPM will be dictated by whether $T01$ has already fired or not. All possible values of f are stored in a conditional probability table.

If the value of $r \leq f$, the DCT will fire. Otherwise, the DCT will not fire but will remain enabled. Whilst the DCT remains enabled, the DCT will not attempt to fire again until a further period of δt has elapsed, at which point it will determine its current CAPM, reselect f and resample r. An algorithm charting out the full

firing mechanism for DCTs is shown in Algorithm 1.

A DCT provides the capability of conditional firing delay times to adapt to new markings at its conditional places as the global simulation time evolves and not just be conditional at the initialisation of the simulation, or at the time of a transition becoming first enabled.

Note that the mechanisms or processes described by stochastic transitions and that do not possess causal arcs, e.g. α, can be described by any probability distribution for firing delay, when using DCTs and not just an exponential distribution. Additionally, DCTs can not be implemented for all structures of DBN but rather the DBNs that have temporal arcs for each variable that features on a time slice, analogous to the structure shown in Figure 6.1. The state of stochastic process at the future time step must be conditional on the state of the stochastic process at the current time step, for all stochastic process.

DBN-DCT Condition Profile Comparison

The metallic multiple defect deterioration model was simulated to determine condition probability profiles for 35 years. The DBN model was simulated using the parameters shown in Table 5.10. The model was additionally simulated using an analogous PN implementation of the model using DCTs. The probability values of being in particular condition state after 35 years is reported for each modelling method in Table 6.1. There is a difference in probability values between the PN and DBN models which can be attributed to issues regarding numerical precision and convergence of the PN using Monte Carlo simulations.

The probabilities shown in Table 6.1 are probabilities of being in a condition state after 35 years using both DBNs and PNs. The results for the PN model are the mean probabilities for each state after 100,000 simulations. 100,000 simulations were used as that is a sufficient number of simulations to achieve convergence on the performance metrics of the wider life cycle analysis, as shown later in the chapter. In general, the convergence of the PN-DCT model after 100,000 simulations is such that the returned probabilities are the same as the DBN values to three decimals places. For the PN-DCT model to have convergence such that the returned probabilities are

Algorithm 1: DCT firing sequence for transition t_j

```
1  G, global simulation time,
2  I(t_j), t_j marking input function (Boolean),
3  ζ, enabled status of t_j (Boolean),
4  T_e, time t_j became enabled
5  if I(t_j) = 1 ∧ ζ = 0 then
6      ζ = 1    %Transition is enabled;
7      T_e = G    %Time transition became enabled
8  while ζ = 1 do
9      if G = T_e + δt then
10         if I(t_j) = 1 then
11             ζ = 1
12             Obtain CAPM
13             Select f value based on CAPM
14             Sample r value from U(0, 1)
15             if r ≤ f then
16                 t_j fires ;
17                 ζ = 0
18             else
19                 ζ = 1 ;
20                 T_e = T_e + δt
21         else
22             ζ = 0 ;
```

accurate to five decimals places would require a significant increase in the number simulations. Moreover, it was deemed that such convergence in the deterioration model to such a tolerance would be unnecessary as the convergence of the wider life cycle analysis performance indicators would already be satisfactory.

Note that the percentage difference between the PN-DCT probabilities and the DBN probabilities have values that are less than 0.5%, with most values significantly less than this. The reason why the values of percentage differences vary is that the lack of convergence to the fourth and fifth decimal places has more significance for condition states that have a smaller probability value. Consequently, the DCT implementation in a PN model of the DBN model provides a sufficiently accurate condition output to facilitate the modelling of deterioration and application of intervention activities in a life cycle model.

Table 6.1: Probabilities of being in a condition state after 35 years using both DBN and PN-DCTs.

Defect Type	**Condition State**	**DBN Probability**	**PN-DCT Probability**	**% Difference**
Paintwork	$Pa1$	0.01225	0.01223	0.15219
Paintwork	$Pa2$	0.07071	0.07060	0.16266
Paintwork	$Pa3$	0.57186	0.57085	0.17532
Paintwork	$Pa4$	0.34516	0.34630	-0.32921
Corrosion	$C1$	0.02958	0.02963	-0.16363
Corrosion	$C2$	0.17192	0.17265	-0.42557
Corrosion	$C3$	0.56430	0.56307	0.21694
Corrosion	$C4$	0.23418	0.23463	-0.18964
SCF	$F1$	0.88213	0.88214	0.00001
SCF	$F2$	0.11787	0.11786	0.00291

6.2 Multiple Defect, Bridge Asset Management PN Model

A PN model was developed to model the deterioration of paintwork, prevalence of corrosion and the development of SCF, alongside the inspection, scheduling and maintenance processes for a bridge component. The PN model is shown in Figure 6.4 with a key of the various PN nodes shown in Figure 6.5.

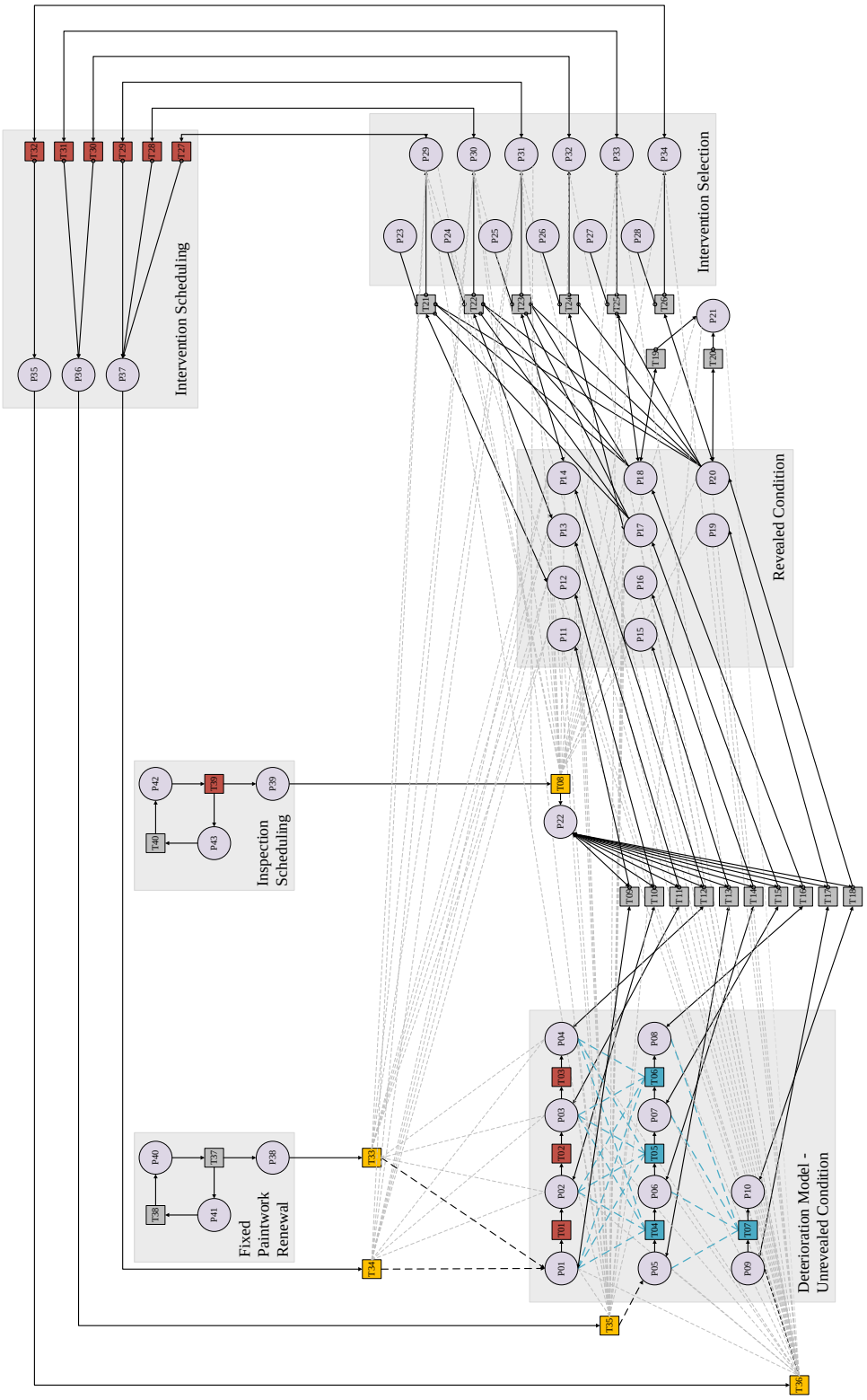

Figure 6.4: Petri net for modeling the asset management of a metallic bridge component.

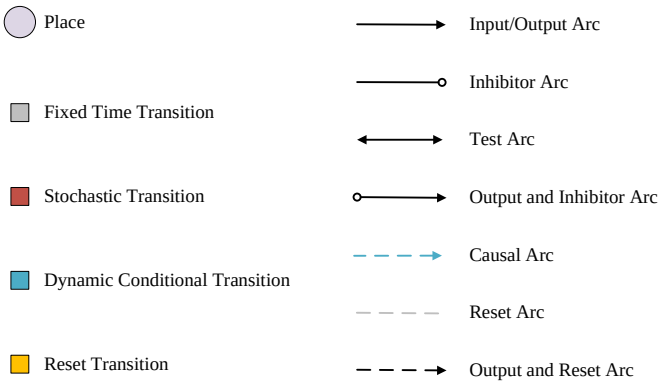

Figure 6.5: Key of Petri net nodes and arcs used in Figure 6.4.

The unrevealed condition states of paintwork, corrosion and SCF are denoted by P01-P10. The transitioning between condition states is controlled by the firing rules of T01-T07, where T04-T07 are DCTs. The configurations of these places, transitions and arcs is such that the PN is providing an analogous condition output as the DBN model, see Table 6.1.

The unrevealed condition states correspond to the condition of the component in real time. However, the condition of the component will only become known upon being inspected, and thus a second group of places (P11-P20) are defined to represent the revealed condition state of the component. After inspection, a maintenance strategy may require a certain intervention to be scheduled upon a revealed condition state, P29-P34 are designated to represent this. By default, the PN will schedule and execute all appropriate intervention types upon particular conditions being revealed. However, particular maintenance strategies only require some of the possible intervention types. To be able to use the same PN structure to evaluate different maintenance strategies P23-P28 are used to inhibit particular interventions when testing different maintenance strategies.

Upon designating the requirement for a particular intervention to occur, there will be a delay between scheduling the intervention and it being executed, in the model T27-T32 are used to assign a time delay for this action. In this study, the delay between an intervention being scheduled and occurring was sampled from $\mathcal{N}(3, 0.5)$. This distribution was set based on the analysis of asset policy documents and engineering judgement. P35-P37 are used to signal that the particular mainte-

nance intervention is ongoing. After the intervention is complete the PN is reset to reflect the updated condition scores.

Reset transitions are used to update the marking of a number of places in a net upon a particular action occurring. For example, as part of the inspection process, reset transitions are used to set the marking of places P11-P20 to zero prior to transitions T09-T18 firing to update the new revealed condition. Additionally, after an intervention is complete, T33-T36 are used to reset the PN to reflect the updated condition scores. A reset of the net can be performed using traditional PN features but the traditional approach typically requires additional transitions and increases the model complexity (Andrews, 2013).

This PN models the life cycle of a single metallic bridge element, as the purpose of this study was to investigate the functionality of DCTs and to showcase the feasibility of quantifying the benefits of maintenance strategies that favour early intervention. However, to implement the entire asset management procedure there were some specific places and transitions required in lieu of a whole structure model. For example, the interval between inspections can vary and is normally determined by the amalgamated score of multiple elements at the previous inspection. As the presented PN is for a single component, there is a local inspection loop of (P42, P43, T39, T40), which deposits tokens in P39 to initiate an inspection. However, if a whole structure model was to be deployed, all that is required is that a token is deposited into P39 to prompt an inspection of the component. The inspection interval for this case study was sampled from $\mathcal{N}(6, 1)$, which was determined by analysing Network Rail data, assessing asset policy documents and expert judgement.

A perfect inspection is an inspection where the revealed condition is an accurate representation of the unrevealed condition at the time of inspection. Transitions T09-T18 in the model are standard transitions, which were used to update the places that indicate the revealed condition, assuming a perfect inspection. However, the inspection process is not always perfect, see Section 3.4.3.

Imperfect inspections could be modelled in the PN model by using probabilistic transitions as part of the modelled inspection process (Yianni et al., 2018). To incorporate imperfect inspections into the PN model, transitions T09-T18 could be

restated as probabilistic transitions, with the output arcs to the places indicating revealed condition having a probability distribution relating to the variability in inspection. However, calibrating a probability distribution to reflect the variability of examiners during the inspection process is a challenging endeavour and was beyond the scope of this study.

To enable an analysis of strategies requiring fixed-interval paintwork renewal, the following places and transitions were included in the PN model: P40, P41, T37, T38. In the case of a whole structure model these nodes could be substituted for, provided there was an output arc to deposit tokens in P38. Finally, T27-T32 could have additional input arcs to alter the scheduling behaviour of maintenance interventions based on the condition of the overall structure and/or to facilitate studies under constrained budget scenarios. The defined physical representation for each place can be found in Table 6.3.

The parameter values for the defect mechanisms were calibrated using a method of maximum likelihood applied to the condition data for Network Rail metallic girders, as shown in Section 5.1.3. The degradation of paintwork is determined by T01-T03, which are stochastic transitions using exponential distributions with the following parameter values: $\lambda_{T01} = 0.1761$, $\lambda_{T02} = 0.1553$ and $\lambda_{T03} = 0.0335$. For the development of corrosion and SCF, T03-T06 and T07 were used respectively, all of which are DCTs. The f values used for the DCTs are shown in Table 6.2, which illustrates that the probability of each DCT firing monotonically increases as the marking of its influencing defect exhibits degradation.

It should be noted that the PN model shown in Figure 6.4 could be restated using the CPN formalism described in Section 2.2.6 to reduce the net size of the model. However, the model is shown as a PN to assist with reproducibility.

Table 6.2: Conditional probability table for model DCTs. Note that $\delta t = \frac{1}{52}$ years.

	CAPM	f
T04 Fires,	{1,0,0,0}	9.9995×10^{-5}
CAPM = {P1, P2, P3, P4}	{0,1,0,0}	0.0036
	{0,0,1,0}	0.0086
	{0,0,0,1}	0.0137
T05 Fires,	{1,0,0,0}	9.4188×10^{-4}
CAPM = {P1, P2, P3, P4}	{0,1,0,0}	9.4188×10^{-4}
	{0,0,1,0}	0.0031
	{0,0,0,1}	0.0031
T06 Fires,	{1,0,0,0}	6.6124×10^{-4}
CAPM = {P1, P2, P3, P4}	{0,1,0,0}	6.6124×10^{-4}
	{0,0,1,0}	6.8001×10^{-4}
	{0,0,0,1}	6.8001×10^{-4}
T07 Fires,	{1,0,0,0}	3.0185×10^{-5}
CAPM = {P1, P2, P3, P4}	{0,1,0,0}	7.2268×10^{-5}
	{0,0,1,0}	1.7336×10^{-4}
	{0,0,0,1}	3.1122×10^{-4}

Table 6.3: Descriptions of the physical representation of each place in Figure 6.4.

Place	Representation
P01-P04	Unrevealed – Paintwork 1-4
P05-P08	Unrevealed – Corrosion 1-4
P09-P10	Unrevealed – SCF 1-2
P11-P14	Revealed – Paintwork 1-4
P15-P18	Revealed – Corrosion 1-4
P19-P20	Revealed – SCF 1 - 2
P21	Revealed – Poor Condition
P22	Perform Inspection
P23-P25	Inhibit Pa Repair on Pa2-Pa4
P26-P27	Inhibit C Repair on C3 -C4
P28	Inhibit SCF Repair on B2
P29-P31	Schedule P Repair on Pa2 -Pa4
P32-P32	Schedule C Repair on C3-C4
P34	Schedule SCF Repair on B2
P35	Repair Paintwork
P36	Repair Corrosion
P37	Repair Buckling
P38	Fixed Renewal of Paintwork
P39	Enable Inspection of Element
P40	Pre-Fixed Renewal of Paintwork
P41	Fixed Paintwork Renewal
P42	Global Inspection Scheduled
P43	Performing Inspection

6.2.1 Case Study

The primary purpose of the PN model is to enable the evaluation of the impacts of a range of different maintenance strategies. The PN model has a versatile design such that all the different strategies can be simulated using the same net, with the only required amendment being different initial markings for a specific set of places, P23-P28 and P40, which are used to inhibit the scheduling of particular interventions. To showcase the functionality of the PN several strategies are considered:

- **Do Nothing**
- **Strategy 1** - Fixed renewal of paintwork every five years.
- **Strategy 2** - Fixed renewal of paintwork every ten years.
- **Strategy 3** - Paintwork intervention when revealed {Pa4} reached.
- **Strategy 4** - No paintwork-only interventions.

For strategies 1-4, there were two additional repair actions that were always enabled:

- Corrosion repair when condition C4 is revealed. This intervention restores corrosion to C1 and paintwork to Pa1. Example repair types include adding metal to strengthen components/plating repair. Additionally, the paintwork restoration is included as Network Rail expertise suggests that when an intervention occurs, the engineers would ensure that the paintwork is fully restored to maximise the impact of taking possession of the bridge.
- Component replacement when condition F2 is revealed. This will restore the component model to the states of Pa1, C1 and F1. If C4 and F2 are revealed at the same time, component replacement is prioritised over corrosion repair.

6.2.2 Simulation Results

The model was analysed using Monte-Carlo simulations with 100,000 simulations per strategy. The central limit theorem can be used to evaluate the confidence interval for a Monte-Carlo sample after n simulations to a particular confidence level,

$$[a, b] = \left[\frac{\overline{z} - \lambda s(z)}{\sqrt{n}}, \frac{\overline{z} + \lambda s(z)}{\sqrt{n}} \right], \tag{6.2.1}$$

where a is the lower confidence interval limit, b is the upper confidence interval limit, $\overline{z}$ is the sample mean, $s(z)$ sample standard deviation and λ is a coefficient which relate to the desired nominal confidence limit. For a confidence limit of 95%, $\lambda = 2$ (Dunn and Shultis, 2011). The confidence limits over the course of 100,000 simulations for Strategy 1 are shown in Figure 6.6. After 100,000 simulations the sample mean for Strategy 1 was 233.1 and with a 95% confidence interval of the true mean being within [232.07, 234.19]. Similar convergence was found for Strategies 2-4.

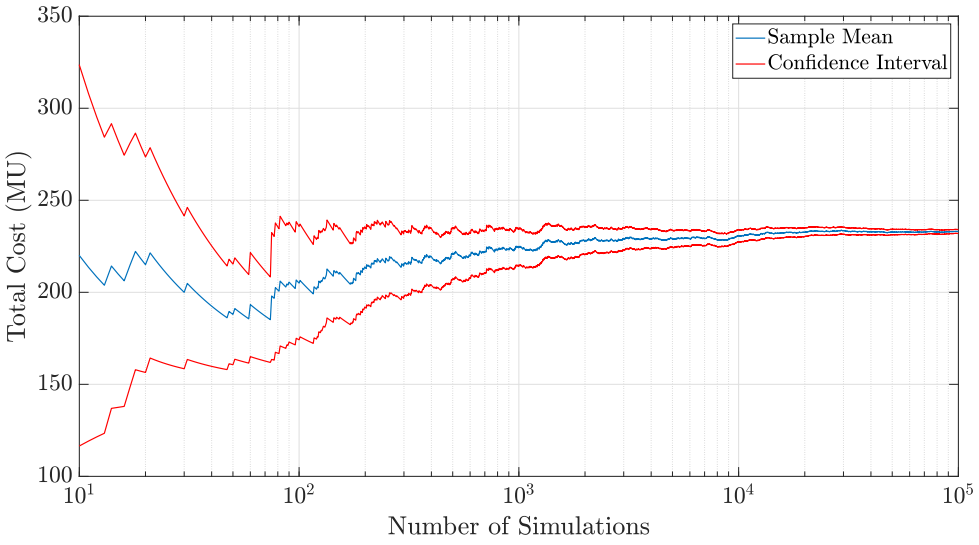

Figure 6.6: Convergence confidence interval of 95% for PN simulation of Strategy 1.

For n conditions states, an integer score can be assigned to each, $C_1, \ldots, C_n$, then the average condition of a defect at time t is determined from

$$\sum_{i=1}^{n} (C_i \cdot p_i), \tag{6.2.2}$$

where p_i is the probability of being in C_i at time t. The average conditions of paintwork, corrosion and SCF over time, for each strategy are shown in Figures 6.7, 6.8 and 6.9 respectively. From Figure 6.7, it can be observed for the strategies that instigated earlier repainting of the component, lower values were obtained for average paintwork condition.

The policy for corrosion repair was consistent for each of the four strategies, i.e. to schedule corrosion repair upon an inspection revealing C4 being reached. Nonetheless, from Figure 6.8, it can be observed that there is a variation between the values obtained for average corrosion condition. This observed result is a consequence of the variation in the paintwork strategy, as paintwork condition is modelled as a causal influence on corrosion progression. Thus the variation in paintwork strategy alone, alters progression of paintwork degradation which corresponds to varying rates of corrosion development. Hence, the strategies that favour early paintwork intervention, i.e. Strategies 1 and 2, result in reduced levels of corrosion, when compared to Strategies 3 and 4.

For the SCF defect modes a similar observation can be made, due to corrosion acting as a causal influence to SCF development. Thus, the maintenance strategies that schedule paintwork renewal earlier, result in an improved average condition for paintwork which mitigate the levels of corrosion and instances of SCF developing.

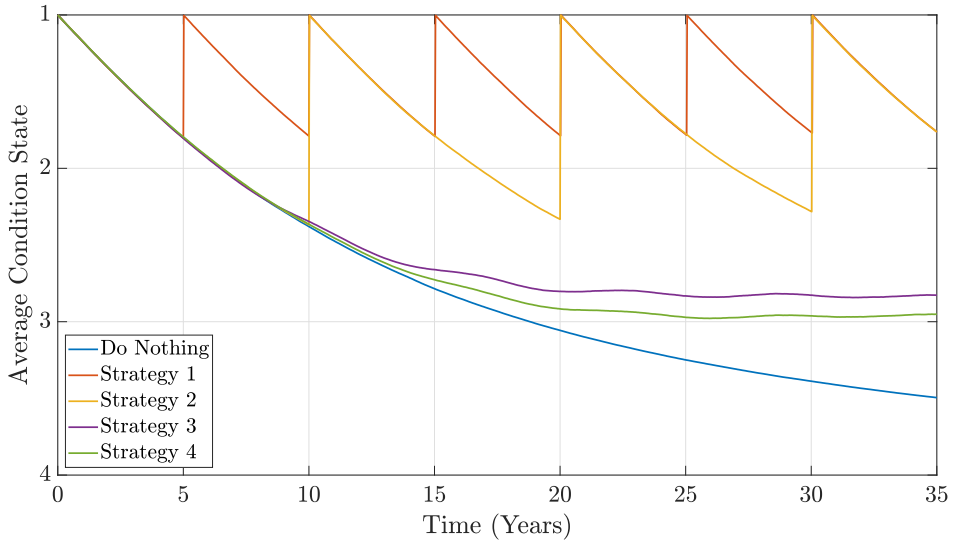

Figure 6.7: Average condition of paintwork under different maintenance strategies.

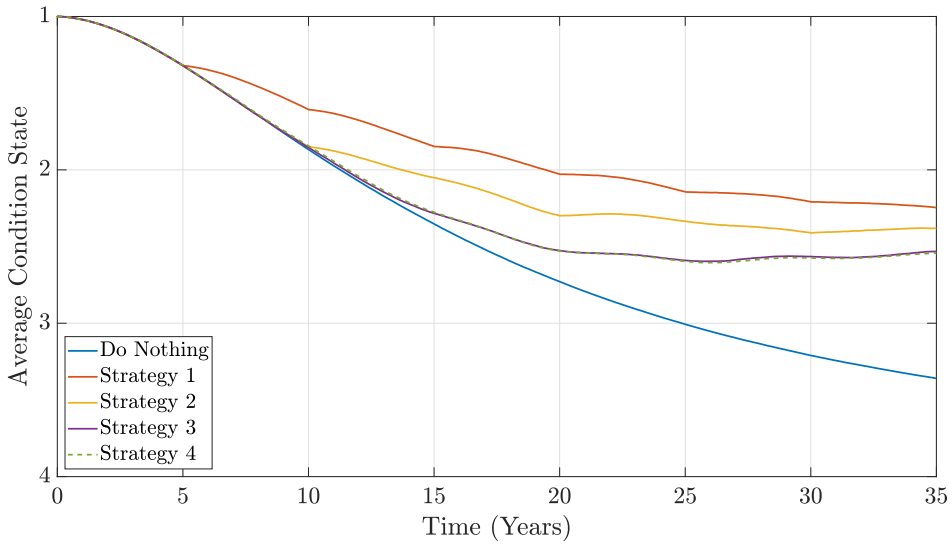

Figure 6.8: Average condition of corrosion under different maintenance strategies.

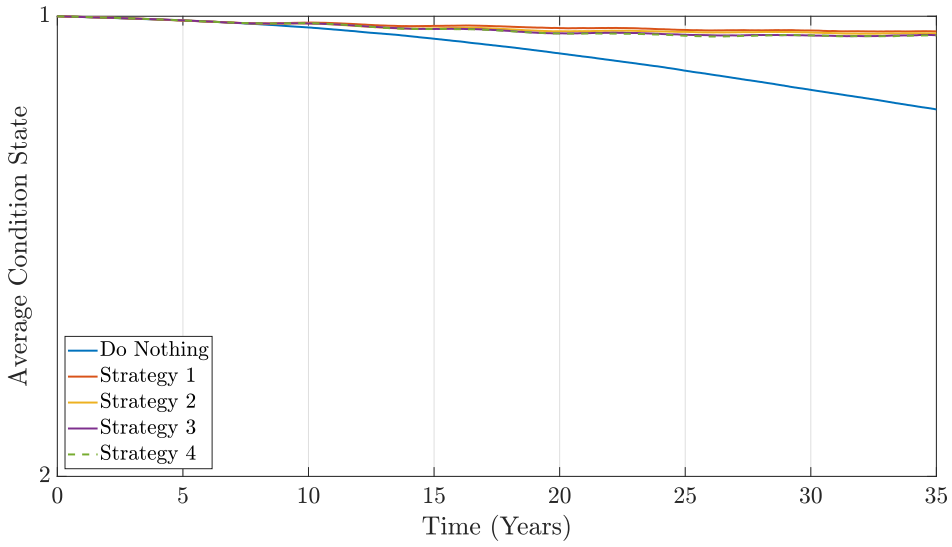

Figure 6.9: Average condition of SCF under different maintenance strategies.

An asset manger's task of maintenance strategy selection is a multi-criteria problem. Asset condition is one of many factors that must be considered when selecting strategy and presenting decisions to stakeholders. Other factors such as service disruption and strategy cost must also be considered, see Section 3.2. Ultimately infrastructure is managed to maintain safe, reliable and operation for network usage, and the minimisation of service disruption is a key priority. In this study, the

minimisation of service disruption was monitored by determining the average time the bridge component spent in poor condition.

For Network Rail condition scales, poor condition is a well defined state that triggers the scheduling of maintenance interventions and is reportable to regulators. The condition states of $C4$ and $F2$ as defined in this study correspond to the defined Network Rail poor condition states for metallic elements. The time spent in poor condition can be determined by analysing how long a poor condition state was marked during the course of simulation. An average is found by analysing each of the simulations performed during the Monte Carlo analysis.

As a baseline, the average time spent in poor condition for the do-nothing strategy was 5.34 years. The average total time in poor condition for each of the maintenance strategies is shown in Figure 6.10. It can be noted that the strategies favouring early paintwork intervention return the lowest average values for total time in poor condition. Moreover, the strategies that have increased values in average total time in poor condition are caused by increases in both time spent in $C4$ and $F2$. This trend conforms to the previous finding that strategies that mandate early paintwork interventions not only result in a reduction in the prevalence of corrosion but also in there being less instances of SCF developing.

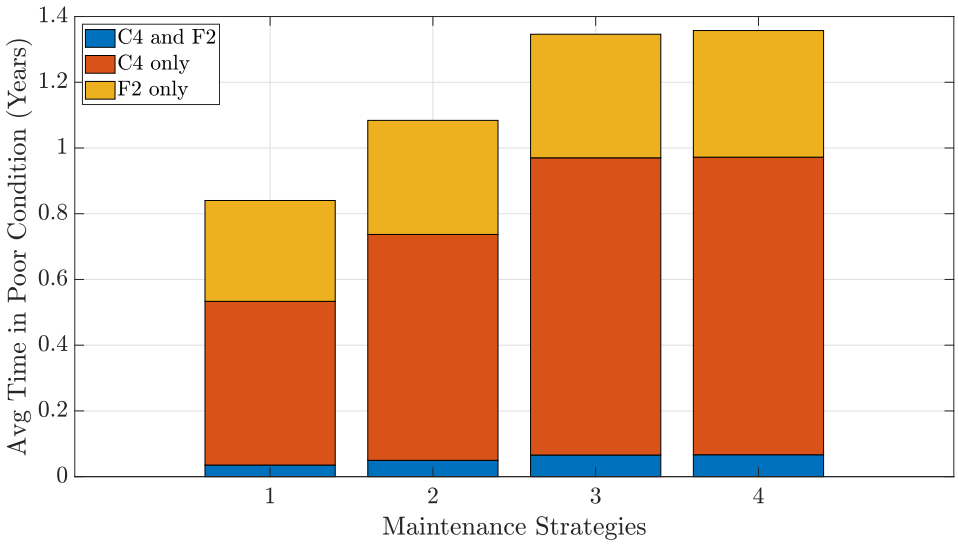

Figure 6.10: Average total time in poor condition over 35 years, under different maintenance strategies.

Finally, another critical concern for asset managers is the cost implication of each strategy. The average cost for each strategy can be calculated by analysing the number of executed maintenance interventions during the simulated period. The number of interventions can be determined by summing the number of times that transitions T33-T36 fire throughout the duration of the simulation. The predicted average cost of each strategy can be calculated using the number of interventions and a defined cost distribution for each type of intervention. For this study, arbitrary fixed costs for each different maintenance intervention were assigned, the costs are denoted in arbitrary monetary units (MU):

- Fixed paintwork renewal - 25 MU
- Paintwork repair upon condition reveal - 50 MU
- Corrosion repair - 200 MU
- Component replacement - 500 MU

Across all model outputs there are minimal differences between Strategy 3 and Strategy 4. The similarities between strategies would indicate that there is limited benefit to waiting until the paintwork is in poor condition to repaint the component as the negative impact on corrosion would have already occurred.

Figure 6.11 shows the predicted average cost of each strategy over time alongside the probability of being in poor condition. Strategy 1 results in the lowest probability of being in poor condition over the course of the entire 35 year simulation period. Nonetheless, Strategy 1 can also be identified as being the most expensive strategy, as there are regular fixed costs for paintwork renewal. The remaining three strategies all result in lower overall costs than Strategy 1, however the probability of being in poor condition is increased. Strategies 3 and 4 obtain a lower cost than Strategy 1 and 2, however the costs are composed of increased replacement costs which would be indicative that there was an assessment of greater risk of structure failure.

Note that the cost analysis has only considered maintenance and replacement costs. Inspection costs are the same across the four strategies, with an average of 5.33 inspections taking place over the simulated 35 years.

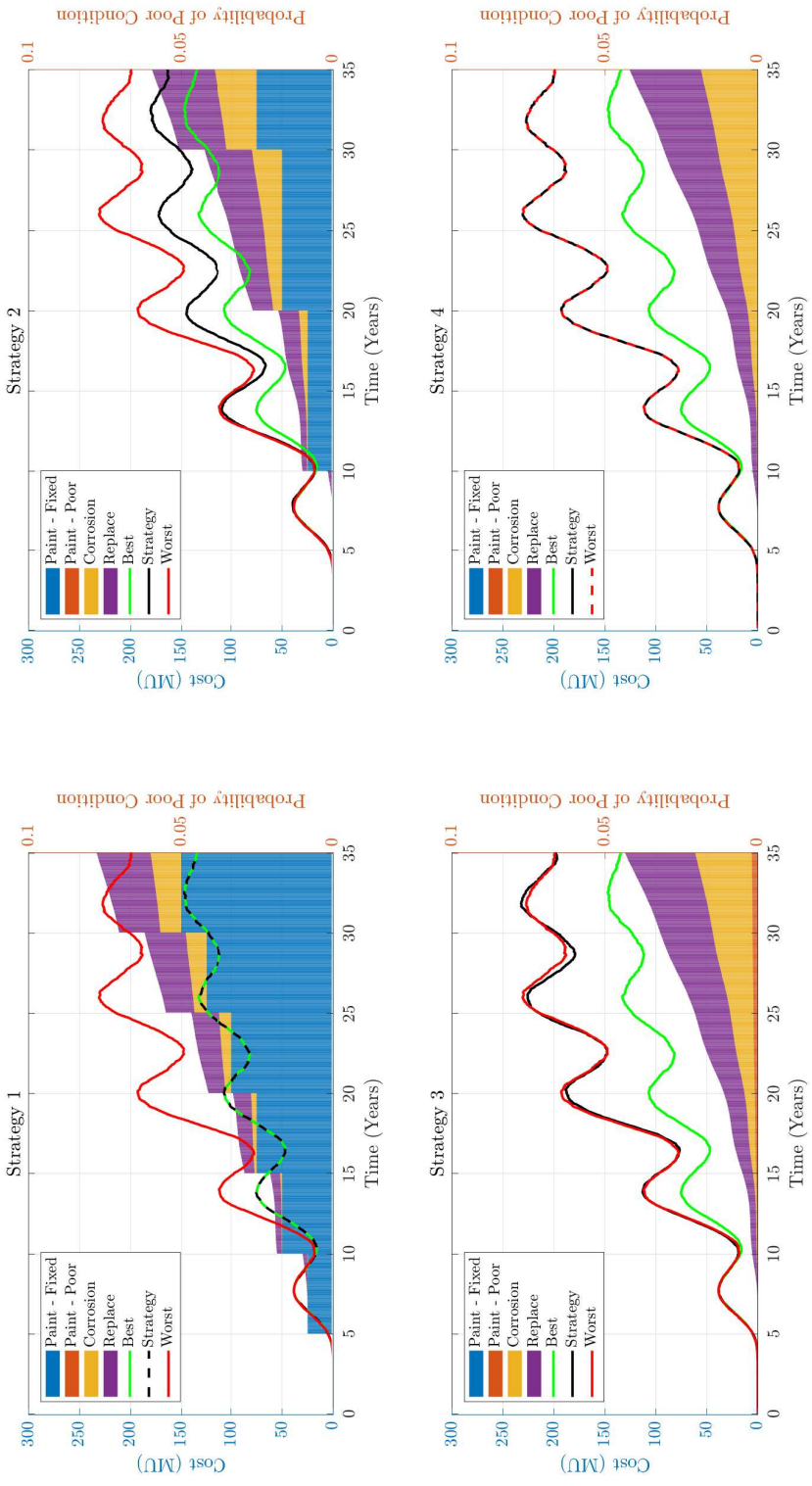

Figure 6.11: Predicted maintenance costs and probability of revealed poor condition over time for Strategies 1-4.

The values for average time in poor condition, average costs and probability of being in poor condition after 35 years can be found in Table 6.4. Strategy 1 returns the lowest values for average total time in poor condition and the probability of being in poor condition after 35 years. However, Strategy 1 is the most expensive strategy and is 30.4% more expensive than Strategy 2. From analysing the cost values, Strategy 2 would be the favoured strategy in a cost constrained scenario. Strategy 2 has a 42.0% increase in overall costs when compared to the strategy with the lowest costs, Strategy 4, and yields a 20.6 % reduction in the average total time in poor condition when compared to Strategy 4. Note that any reduction in average total time in poor condition would translate to increased adherence to capability and serviceability requirements.

Table 6.4: Model outputs for each strategy after 100,000 simulations of 35 years.

Strategy	Average Total Time in Poor Condition (Years)	Average Maintenance Cost (MU)	Average Replacement Cost (MU)	Average Total Cost (MU)	Probability of Poor Condition at $t = 35$ years
1	0.84	180.2	52.9	233.1	0.0448
2	1.08	117.1	61.7	178.8	0.0545
3	1.35	61.3	68.8	130.1	0.0657
4	1.36	55.8	70.1	125.9	0.0661

6.3 Chapter Summary

Infrastructure asset managers are tasked with ensuring that their civil infrastructure is maintained to conform to strict safety standards and deliver safe, reliable and functional operation. This task must be delivered whilst making optimal use of the available resources. A common approach to present management strategies to stakeholders is utilising the outputs of life cycle modelling.

In this chapter, a novel approach to bridge deterioration was presented, whereby multiple condition indicators were developed that were specific to distinct defect mechanisms. The additional indicators encapsulated the interactions between de-

fects and the reality that the absence or presence may alter the rate of development of other defects. The considered defects were the degradation of paintwork, corrosion and the occurrence of SCF defect modes. These relationships were quantified from industrial condition data for metallic girders from railway bridges in the United Kingdom and modelled using a DBN.

To perform a life cycle analysis which modelled the condition of bridge components and the application of inspection and maintenance policy, a PN model was presented. However, to incorporate the deterioration model, a novel transition type, DCT, was defined to enable the modelling of multiple interacting deterioration mechanisms within the PN methodology. A case study of four different maintenance strategies with specific and targeted maintenance interventions was analysed. The multiple defect approach to modelling, provides additional indicators which are critical to the detailed evaluation of competing maintenance strategies, which can be defined as targeted defect specific actions. In this study, the considered model outputs for each strategy were average component condition, average total time spent in poor condition and average predicted maintenance cost.

DBN models are an effective method for modelling multiple defects simultaneously whilst also incorporating the interactions between the defects. Moreover, the DBN model does not require Monte Carlo simulations as it can be solved analytically. Whilst the deterioration part of the PN model provides analogous results to the DBN model, the computational expense for the PN model is far greater than the DBN. Thus, for calibrating the CPT parameters, the DBN method is a more effective approach. However, the capability of PN models to encapsulate bespoke asset policies means that they are more appropriate technique for a life cycle analysis.

It should be noted that the model presented in this chapter could have been developed as generalised Monte Carlo simulations. However, the proposed model was presented as a PN model to improve the reproducibility of the model for future research. Simulations are not necessarily irreproducible but the PN methodology enhances the reproducibility and provides a convenient framework for visualising the model.

The optimisation process in the life cycle management of deteriorating structures

is an important part of developing asset management strategies for many infrastructure owners, see Section 3.3.3. However, depending on how the model is being used, an optimisation may or may not be important. For example, at Network Rail life cycle models are used for two distinct purposes: a life cycle model may be used to predict costs, work volumes and asset condition over the medium term under different prescribed strategies and scenarios, or a model may be used to determine optimal asset policy. The PN model presented in this chapter was used to predict costs, work volumes and asset condition over the medium term using different specified strategies. In particular, the model provides a novel contribution in terms of being able to quantitatively evaluate the outcomes of preventative maintenance programs such as repainting. Moreover, the analysis of different well specified strategies was deemed to be an appropriate way to showcase the consequences of the novel approach to including conditional deterioration processes in a PN model.

The PN model could be used in a wider optimisation of asset management strategy by including the parameters for different asset processes to be altered by the optimisation, e.g. inspection interval, intervention scheduling delay etc. However, such work was deemed to be beyond the scope of the study. In particular, a limitation of the presented PN model was that it was defined and analysed for a single bridge component. However, the model has been designed to have input/output functionality to facilitate inclusion into a hierarchical whole structure model in the future, which should enable the reporting of additional factors such as required asset possession time for interventions. Before modelling at the level of the whole structure, further analysis should be performed to identify the correlation between defect mechanisms across multiple bridge components. Additionally, the methodology could be extended to additional material types such as masonry, which have their own respective mechanisms and interactions.

Chapter 7

Incorporating the Effects of Local, Material and Structural Properties on Metallic Bridge Deterioration

Deterioration models are critical when analysing the life cycle of bridges. Any maintenance modelling requires an accurate prediction of bridge condition to enable the most appropriate intervention type to be modelled and condition uplift applied. An additional indicator that bridge asset managers are interested in is the predicted service life of a bridge under a do-nothing strategy. The service life prediction under such strategies is required when calculating the residual value of a bridge asset and for determining asset value across an entire portfolio.

Chapter 5 shown that it is possible to model bridge deterioration by analysing multiple degradation mechanisms and the interactions between mechanisms. Moreover, the additional indicators from monitoring multiple mechanisms facilitated an enhanced evaluation of intervention strategy in Chapter 6. This is critical as distinct mechanisms such as corrosion can be identified as a common cause for damage and structural failure in metallic bridges (Imam and Chryssanthopoulos, 2012; Wardhana and Hadipriono, 2003). Thus, being able to model the development of corrosion and its influence on other structural failure modes is a desired capability for bridge asset managers.

The rate of corrosion is contingent on multiple factors, such as environmental

exposure conditions, the specific coating or protection system applied to the metallic component as well as the condition uplift that is resultant of particular maintenance intervention types. The advanced development of corrosion can result in reduced structural performance and capability and ultimately instigate structural failure. Nonetheless, its is common that corrosion can be assessed to be unacceptable in terms of a condition score rating before any structural failure occurs (Kallias et al., 2017). Yianni et al. (2016) showed that the incorporation of local environmental factors in a deterioration model can have a large consequence on predictions of cumulative cost for bridges located in different environments, with the lowest and highest cumulative costs for the least and most aggressive environment being calculated as 1,800 and 27,500 cost units respectively.

For corrosion, existing literature suggests that particular element types will experience different rates of deterioration for corrosion (Hutchins and McKenzie, 1973; Tamakoshi et al., 2006). In Section 7.1, the rate of corrosion, loss of coating and structural component failure for different element types will be analysed using condition records for metallic main girders from UK railway bridges. Moreover, the analysis will compare the deterioration rates between inner and exposed main girders, as well as comparing constituent girders from underbridges and overbridge girders.

Upon determining baseline deterioration rates for the unique element types, Section 7.2 analyses the effect that several local, material and structural properties have on the deterioration rate of particular defect mechanisms and element types. Moreover, a scaling factor method is introduced to incorporate the multiple co-variates into a deterioration model simultaneously. Section 7.4 proceeds to analyse the life cycle implications of incorporating these additional co-variates in the deterioration model.

7.1 Element Specific Deterioration Rates

Bridges represent a diverse asset class, with each bridge having its own distinct composition of structural elements. To facilitate intervention co-ordination and strategy development, bridges are commonly described by a hierarchical decomposition of ele-

ments. For example, at Network Rail the hierarchy for structural assets is defined by asset groups (e.g. underbridge), asset sub-groups (e.g. construction material, design principles), major elements (e.g. deck) and minor elements (e.g. inner main girder). When aggregating minor elements to determine an overall score for an asset, particular minor elements have a designation of being a principal loading bearing element, which are used to attribute a greater weighting for elements that are structurally integral to the loading capability of a bridge.

The inspection regime at Network Rail records the condition of each distinct bridge element at each inspection. These records are then used to calibrate specific deterioration rates for particular minor element types. The overall deterioration of a bridge is described by the simultaneous modelling of its constituent bridge elements. However, the existing Network Rail model, like many models, report an overall condition indicator as opposed to multiple defect specific indicators.

As an initial study, parameters were calibrated for cohorts at different hierarchical levels for the multiple defect deterioration DBN model for metallic bridge components, see Section 5.2. For metallic main girders, there are four model/hierarchical levels considered,

- Model 1 - 14 Parameters - Generalised metallic main girders.
- Model 2 - 28 Parameters - Metallic main girders, with specific parameters depending on whether a girder belonged to an underbridge (BU) or an overbridge (BO).
- Model 3 - 28 Parameters - Metallic main girders, with specific parameters depending on whether a girder belonged was an inner (MGI) or exposed girder (MGE).
- Model 4 - 56 Parameters - Metallic main girders, with specific parameters depending on whether a girder belonged to an underbridge or an overbridge, and whether it was an inner or exposed girder.

A railway underbridge has the railway line going over the deck of the bridge. Conversely, a railway overbridge has the railway line going under the deck of the

bridge. It is generally expected that an underbridge will deteriorate at a faster rate than the overbridge given that the underbridge has the loading of the railway on its deck. The MGE and MGI classifications are used to denote the exposed and inner main girders, respectively. The term of main girder is used to describe a longitudinal main girder or beam that spans between the abutments, piers or columns. The outer two beams on any deck are classified as MGE with the remaining main girders classified as MGI, see Figure 7.1.

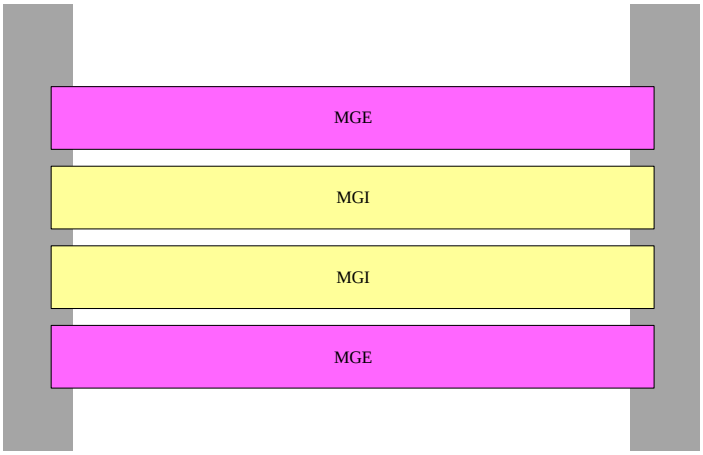

Figure 7.1: Bridge girder schematic of MGI and MGE elements.

The transition rates between different condition states are shown in Table 7.1. Note that the MGE-BU parameters in this study and the parameters in Table 5.10 will have a slight difference. The difference in values is due to the requirement of each record being used to calibrate the model in this study having known material, coastal proximity and track category, which was not the case in the original study.

The parameter values of Model 1 somewhat served as an 'average' parameterisation, with the calibrated model being reflective of the composition of the structural properties across the asset portfolio. However, the composition of inner and exposed girders belonging to underbridges and overbridges is not uniformly distributed and each permutation of characteristics does not necessarily deteriorate at similar rates to other permutations. For models that are calibrated to parameterise the additional characteristics, i.e. Model 4, there are quite distinct fluctuations in the transition values from Model 1 and across the different characteristic permutations of Model

4, as shown in Table 7.1. Whilst Model 4 offers a positive development in incorporating the different deterioration behaviour across the asset inventory it exposes the vulnerability of a model not including characteristics that influence deterioration. Section 7.2 will consider the inclusion of additional properties that may influence the deterioration process.

Table 7.1: List of parameters for multiple defect DBN deterioration model for different cohorts. Rates are stated in $years^{-1}$.

Transition	**General**	**BU**	**BO**	**MGI**	**MGE**	**MGI-BU**	**MGE-BU**	**MGI-BO**	**MGE-BO**
	Model 1	Model 2	Model 2	Model 3	Model 3	Model 4	Model 4	Model 4	Model 4
$(Pa1 \rightarrow Pa2)$	0.1670	0.1844	0.1269	0.1641	0.1701	0.1952	0.1769	0.1193	0.1441
$(Pa2 \rightarrow Pa3)$	0.1631	0.1571	0.1874	0.1651	0.1602	0.1606	0.1529	0.1777	0.2132
$(Pa3 \rightarrow Pa4)$	0.0351	0.0309	0.0463	0.0327	0.0378	0.0284	0.0332	0.0415	0.0563
$(C1 \rightarrow C2)\|Pa1$	0.0050	0.0050	0.0050	0.0050	0.0050	0.0050	0.0050	0.0050	0.0050
$(C1 \rightarrow C2)\|Pa2$	0.1702	0.1864	0.1232	0.1634	0.1786	0.1969	0.1753	0.1075	0.2014
$(C1 \rightarrow C2)\|Pa3$	0.3965	0.3820	0.4539	0.4027	0.3885	0.3523	0.4274	0.5439	0.2185
$(C1 \rightarrow C2)\|Pa4$	0.9050	0.8082	0.9923	0.9976	0.9981	0.9526	0.7014	0.8976	1.0132
$(C2 \rightarrow C3)\|Pa1$	0.0650	0.0688	0.0508	0.082019	0.04605	0.0957	0.0453	0.0505	0.0503
$(C2 \rightarrow C3)\|Pa2$	0.0650	0.0688	0.0508	0.082019	0.04605	0.0957	0.0453	0.0505	0.0503
$(C2 \rightarrow C3)\|Pa3$	0.1417	0.1342	0.1699	0.1279	0.1641	0.1172	0.1545	0.1515	0.2435
$(C2 \rightarrow C3)\|Pa4$	0.1417	0.1342	0.1699	0.1279	0.1641	0.1172	0.1545	0.1515	0.2435
$(C3 \rightarrow C4)\|Pa1$	0.0236	0.0287	0.0107	0.0160	0.0339	0.0219	0.0341	0.0047	0.0237
$(C3 \rightarrow C4)\|Pa2$	0.0236	0.0287	0.0107	0.0160	0.0339	0.0219	0.0341	0.0047	0.0237
$(C3 \rightarrow C4)\|Pa3$	0.0269	0.0291	0.0232	0.0211	0.0352	0.0247	0.0367	0.0165	0.0389
$(C3 \rightarrow C4)\|Pa4$	0.0269	0.0291	0.0232	0.0211	0.0352	0.0247	0.0367	0.0165	0.0389
$(F1 \rightarrow F2)\|C1$	0.0018	0.0022	0.0010	0.0017	0.0016	0.0038	0.0013	0.0010	0.0035
$(F1 \rightarrow F2)\|C2$	0.0040	0.0046	0.0025	0.0049	0.0036	0.0054	0.0035	0.0021	0.0052
$(F1 \rightarrow F2)\|C3$	0.0064	0.0073	0.0047	0.0051	0.0083	0.0060	0.0094	0.0041	0.0070
$(F1 \rightarrow F2)\|C4$	0.0138	0.0136	0.0144	0.0095	0.0166	0.0103	0.0157	0.0077	0.0184

7.1.1 Condition Probability Profiles

The condition probability profiles for the underbridge and overbridge related model parameters from Table 7.1 are shown in Figure 7.2 and Figure 7.3, respectively. The probability profile of being a defect absorbing state, i.e. Pa4, C4 or F2, is shown in Figure 7.4 for all four models. In general, it can be stated that inner main girders degrade at a slower rate than exposed main girders for loss of paintwork, corrosion and SCF. However, the variance in the condition probability profiles for the overbridge parameters is considerably higher than the underbridge parameters. This observation could be at least be partially explained by the fact that overbridges commonly have road traffic going over the deck, which will have road gritting procedures in places during the autumn and winter seasons. The gritting procedures will increase the quantity of chlorides in the vicinity of a bridge, however the exposed girders will be particular vulnerable to the 'overspill' of such materials, whereas inner girders are typically better shielded from such contamination. Consequently, if there are more chlorides from non-atmospheric sources, it follows that particular elements may suffer from accelerated rates of paintwork degradation and corrosion, particularly for components that feature on an overbridge.

The curves show that the different cohorts within a model and the different models return different rates of deterioration. In general, there are trends that are maintained with no crossing over, that signifies that one type of cohort is deteriorating at a faster rate or slower rate than another cohort. For example, there is an expectation that inner girders' paintwork would deteriorate at a slower rate than that of an exposed main girder, and that this dynamic would be the same for corrosion. For such trends, one may assume that

$$\lambda_i^{MGI} \leq \lambda_i^{MGE}, \quad i = \{1, 2, \dots 15\}, \tag{7.1.1}$$

however, this is not necessarily the case when calibrated from the data.

There are various reasons why a strict adherence to (7.1.1) is not obtained when calibrating from the condition records. For example, imperfect inspections could add to the uncertainty of the model when calibrating from condition records. However, the primary reason for a lack of adherence is that cohorts in Models 2-4 assume

that each cohort in a model is composed of similar girders that have similar factors that may influence deterioration. There are more factors that influence the rate of deterioration in a girder than were considered in Models 2-4, and the factors are not uniformly distributed between the cohorts that were considered. Consequently, the calibrated values for transitions rates do not strictly adhere to (7.1.1), which in turn causes some of the condition probability profiles to cross over each other.

The model calibration could have constraints put in place to enforce inequalities for transition rates using expert judgement. However, such enforcement of inequality constraints in the calibration limits or invalids the choice of goodness of fit tests. Alternatively, the additional factors that may influence deterioration could be included in the hope that (7.1.1) is adhered to, however this approach would require further splits in the data and is likely to over parameterise sparse cohorts.

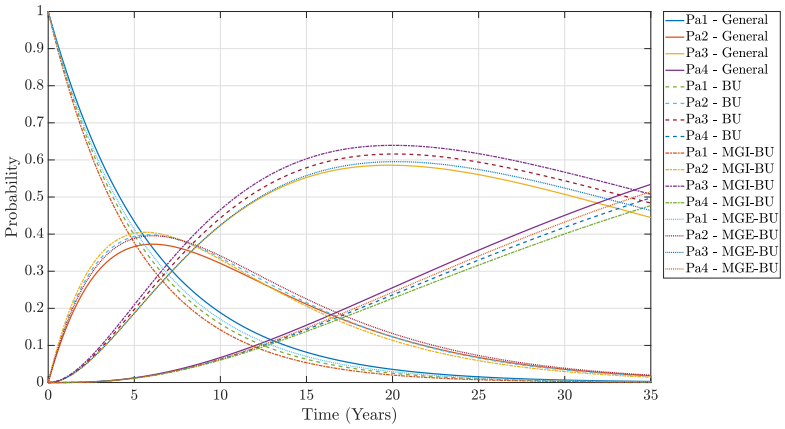

(a) Paintwork

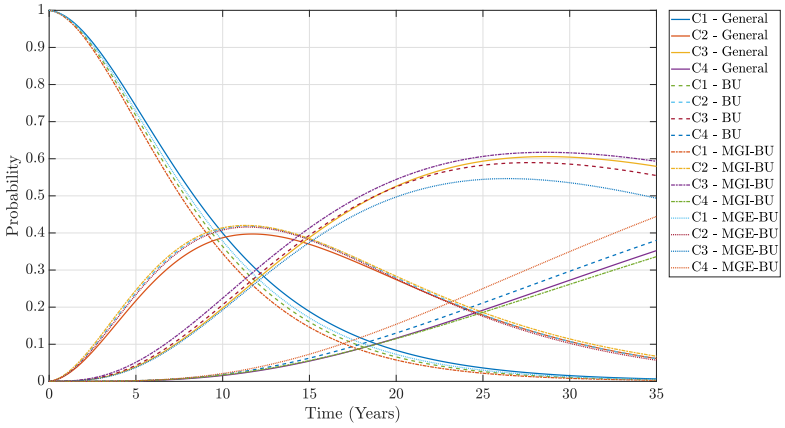

(b) Corrosion

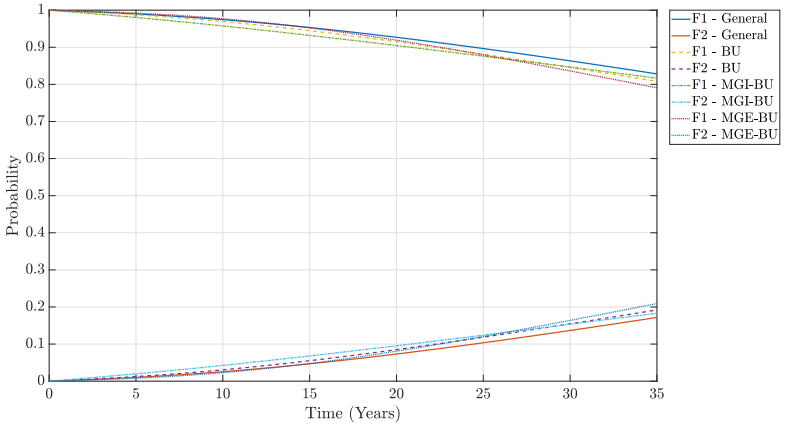

(c) SCF

Figure 7.2: Condition profiles for 35 years for different parametrisations of main girders from railway underbridges.

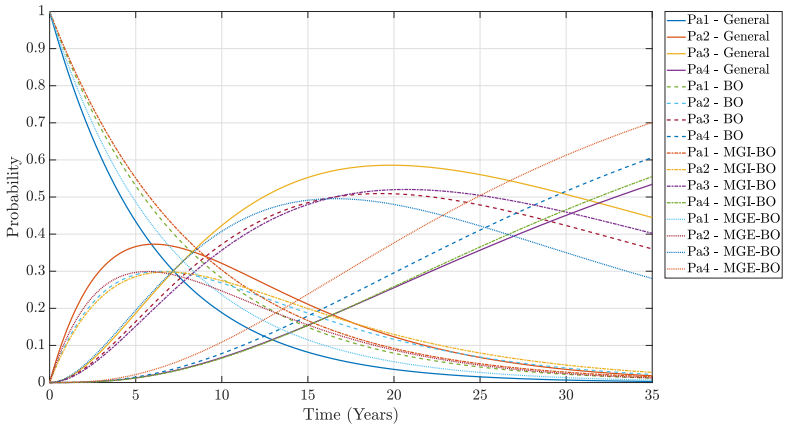

(a) Paintwork

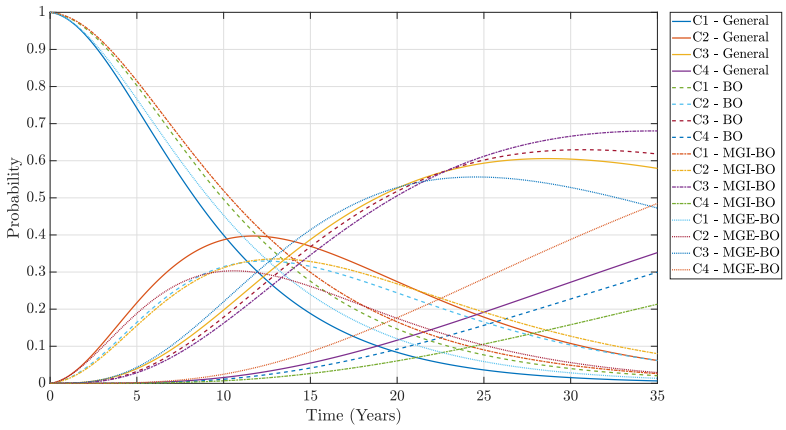

(b) Corrosion

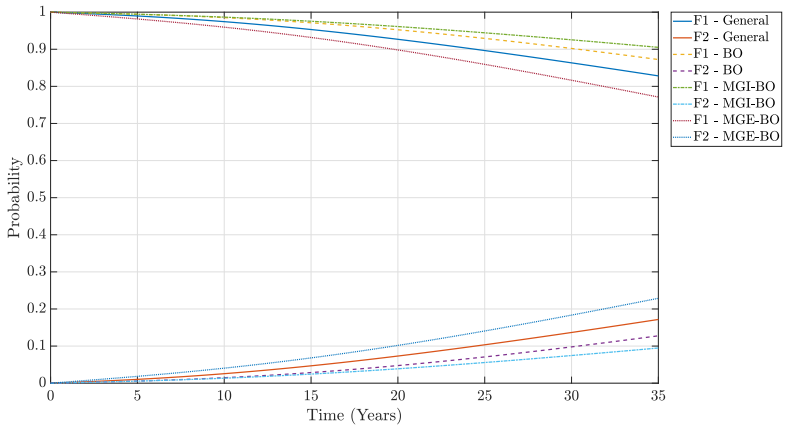

(c) SCF

Figure 7.3: Condition profiles for 35 years for different parametrisations of main girders from railway overbridges.

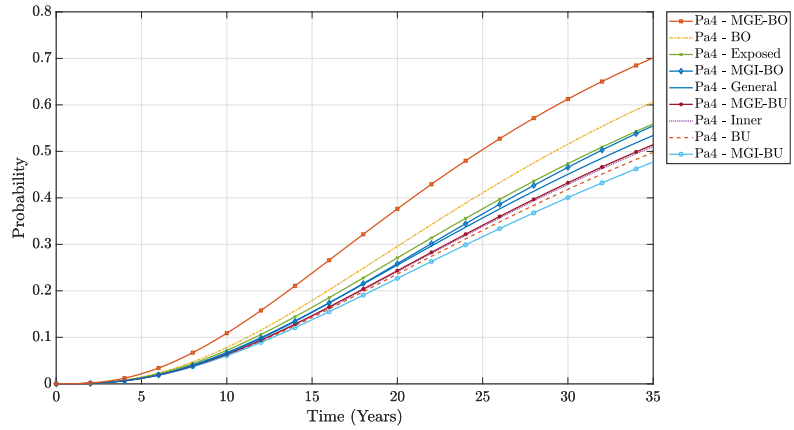

(a) Paintwork

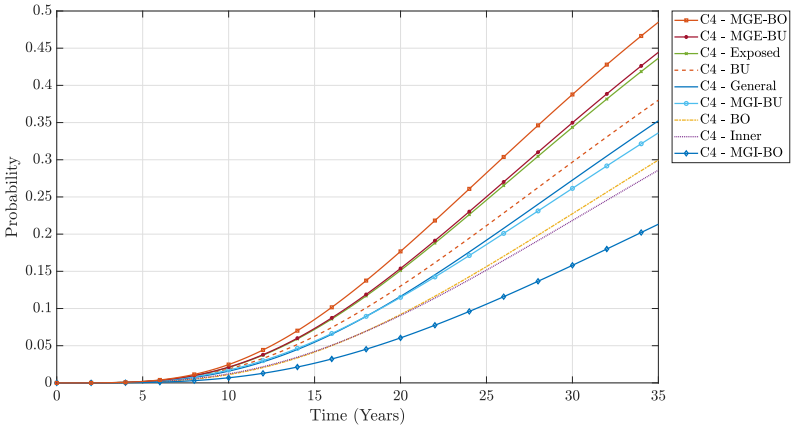

(b) Corrosion

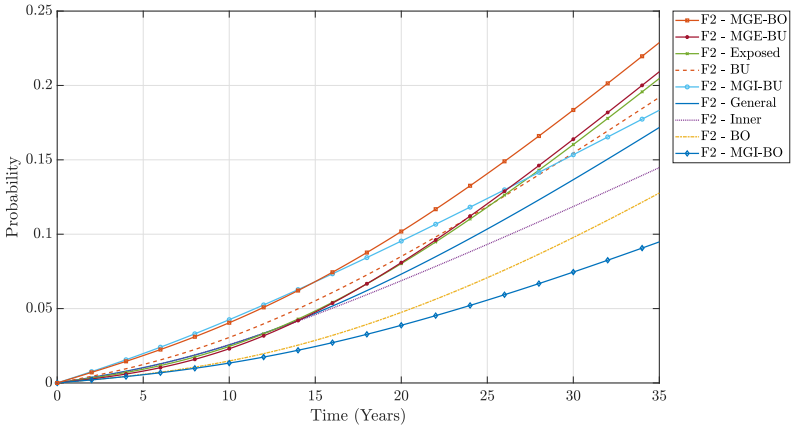

(c) SCF

Figure 7.4: Probability of being in defect absorbing state for different parameterisations of main girders.

7.1.2 Service Life Predictions

A common way to evaluate the service life of a bridge or bridge component is by calculating the expected time to reach an absorption state, i.e. $Pa4$, $C4$ and $F2$ from a starting condition. The expected time to reach an absorbing state or the Mean Time To Poor condition (MTTP) is given by,

$$\tau = \sum_{i=1}^{\infty} t_i \cdot f_i, \tag{7.1.2}$$

where τ is the MTTP and

$$f_i = p_i - p_{i-1}. \tag{7.1.3}$$

The calculation can be terminated at time T, when T satisfies the following,

$$\sum_{i=1}^{T} f_i \approx 1. \tag{7.1.4}$$

The calculated values for MTTP for each set of parameters are shown in Figure 7.5. From Figure 7.5 it can be observed that for both underbridges and overbridges, an exposed main girder degrades faster than an inner main girder and consequently has a shorter MTTP. The discrepancy in MTTP for inner and exposed main girders is particularly large for SCF, which is of great interest to infrastructure managers as the presence of SCF would have direct implications of the serviceability of their infrastructure. Moreover, it can be seen for Corrosion and SCF that Model 1, i.e. generalised main girder, would underestimate the MTTP for general main girders from overbridges and overestimate the MTTP for general main girders from underbridges (Model 2).

7.1.3 Model Selection

To assess the goodness of fit between two candidate models, the likelihood-ratio test can be employed. The models must be nested which requires that one model has been calibrated across the complete parameter space and the second model is calibrated using a constrained parameter space of the first model. The likelihood-ratio test statistic is given by,

$$\lambda_{LR} = -2 \ln \left(\frac{L(\theta_0)}{L(\theta)} \right), \tag{7.1.5}$$

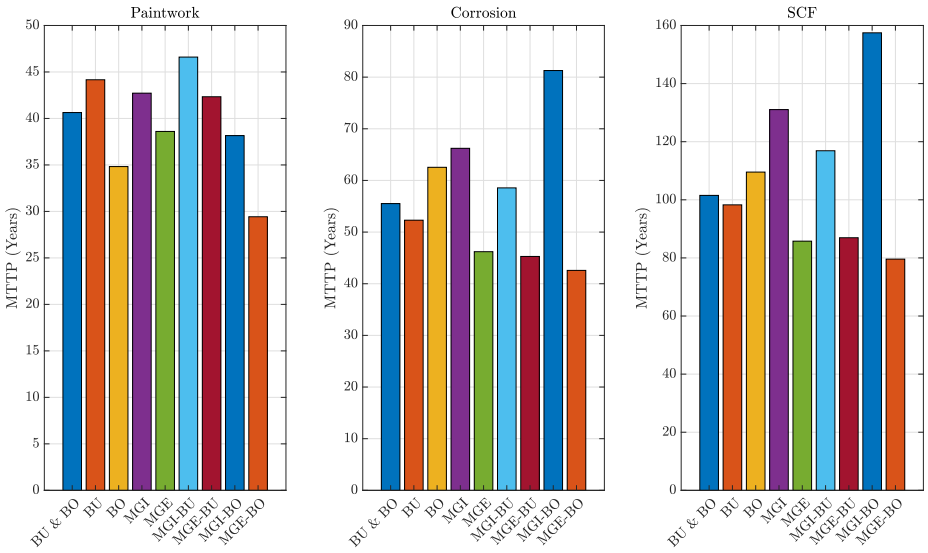

Figure 7.5: The Mean Time to Poor Condition for the deterioration of paintwork, corrosion and SCF using a starting condition of {Pa1, C1, F1} using Models 1, 2 , 3 and 4.

where $L(\theta_0)$ is the maximum likelihood for the constrained model and $L(\theta)$ is the maximum likelihood for the model calibrated using the complete parameter space. The log-likelihood ratio test statistic can be expressed as the difference between the log-likelihoods,

$$\lambda_{LR} = -2(l(\theta_0) - l(\hat{\theta})). \tag{7.1.6}$$

For hypothesis testing, the model parameterised using θ_0 is the null hypothesis, H_0 and the model parameterised using θ is the alternative hypothesis H_1. The model with parameters θ will at least have as good a fit as the model using θ_0 but typically the fit as measured by the log-likelihood will be greater due to the extra parameters.

To determine if an improvement in goodness of fit is significant, given the increased number of parameters, one assigns a $p-$value for the improved fit of the model with increased parameters being due to chance alone, assuming the model with θ_0 is true. The hypothesis test works as the likelihood-ratio test statistic will be asymptotically chi-squared distributed with the degrees of freedom equal to the difference in the number of parameters between θ and θ_0 (Wilks, 1938). The comparison between the test statistic and the chi-squared value can be then used to determine if the models are different with statistical significance.

Whilst out-of-sample testing is the best method for ascertaining the predictive performance a model, due to the complexity of some of the models considered and the limited data availability this study calibrated each model using all of the available data. The Akaike Information Criterion (AIC) is an estimator of the out-of-sample prediction error and is used in model selection to assess goodness of fit and candidate model's parameter dimensionality (Akaike, 1973, 1974). AIC is computed as,

$$AIC = 2k - 2\ln(\hat{L}), \tag{7.1.7}$$

where k is the number of estimated parameters in the model and $\hat{L}$ is the maximum value for the likelihood function for a candidate model. The model with the lowest AIC value is deemed to be the preferred candidate model. The AIC assess the goodness of fit against the number of parameters and the $2k$ serves as a penalty function against increasing numbers of parameters, as an increase in the number of parameters typically results in an improvement in the goodness of fit.

Bayesian Information Criterion (BIC) is similar to the AIC (Schwarz, 1978), but BIC has greater penalisation for model complexity and also accounts for the number of data points used in model calibration. BIC is expressed as,

$$BIC = k\ln(n) - 2\ln(\hat{L}), \tag{7.1.8}$$

where k is the number of parameters, n is the number of data points in the observed data and $\hat{L}$ is the maximum value of the likelihood function.

The Log-likelihood, AIC and BIC for each model are shown in Table 7.2. The λ_{LR} between model 1 and 2 is 465.0, between model 1 and 3 is 548.8 and between model 1 and 4 is 1145.4. Additionally, the λ_{LR} between models 3 and 4 is 596.7. After obtaining the p-value for each test statistic, all of which are negligible to zero, it can be stated that there is a statistically significant difference ($\alpha = 0.01$) between model 1 and model 2, models 1 and 3, models 1 and 4, models 2 and 4, and between model 3 and 4. Model 4 returns the lowest value for both the AIC and BIC and is the preferred candidate model despite it having the largest number of parameters.

Table 7.2: Main girder model test statistics.

Model	No. Parameters	Log-likelihood	AIC	BIC
1	14	-54968.8	109965.7	110090.1
2	28	-54736.3	109528.7	109777.3
3	28	-54694.4	109444.9	109693.6
4	56	-54396.1	108904.2	109401.5

7.2 Local, Structural and Material Properties

Studies have observed material loss due to corrosion can be described by an exponential function,

$$C = A \cdot t^B, \tag{7.2.9}$$

where C is the average corrosion penetration, t is the elapsed time, and A and B are coefficients from a regression analysis of the experimental data (Komp, 1987). The rate of corrosion can be influenced by the metal type, surface coating, structural factors, environmental factors and stress (Albrecht and Naeemi, 1984; Kayser and Nowak, 1989b). Additionally, the prevalence of corrosion can have a negative consequence on the loading capability of a bridge with the increasing likelihood of structural defects occurring (Kayser and Nowak, 1989a).

Although the defect models in this study are calibrated using inspection records rather than experimental data, it is still critical that the aforementioned properties that alter deterioration behaviour are considered in the model calibration. Previous studies have analysed additional properties that can influence deterioration such as traffic volumes, asset age, coastal proximity, structure type amongst others (Huang et al., 2010; Jiang and Sinha, 1989; Morcous et al., 2002a; Yianni et al., 2016) and shown that their consideration is statistically significant to calibrated deterioration models. However, the early studies were often limited to analysing properties independently from each other, which is problematic for scenarios when more than one property has been identified as influencing deterioration and an asset manager wants to incorporate all of the properties simultaneously.

For those studies that were able to incorporate multiple properties simultaneously, they were still limited to using a single indicator to denote asset condition. Incorporating multiple properties whilst simultaneously outputting multiple condition indicators is a challenging task in a data constrained scenario, as one wants to avoid developing an over-fitted model.

The previous section confirmed that accounting for the structural configuration of the element is appropriate when calibrating a multiple defect deterioration model. However, it is critical that additional properties that influence deterioration are also incorporated in the model calibration. In this study, coastal proximity, material type and track category, which incorporates annual loading and track line speed, are simultaneously incorporated into a multiple defect deterioration model.

7.2.1 Atmospheric Environment

The rate of corrosion of a metallic component can be determined by the atmospheric environment. Moreover, atmospheric corrosion is driven by properties such as environmental moisture, surface chlorides and the absorption of sulphur dioxide (Dean, 2001). Environmental moisture depends on the local climate. Chlorides will be abundant in marine environments and where gritting polices are in place for highway roads. A primary source for sulphur dioxide is the combustion of fossil fuels.

Ideally for analysing the effects of atmospheric environment, environmental corrosivity would be described by a single variable. This corrosivity variable could be obtained by performing a principal component analysis of multiple climatic conditions. Alternatively, it could be obtained from empirical measurements of metallic corrosion rates across a geographical area. In the UK, the Galvanizers Association have recorded the average corrosion rate for zinc ($\mu m/yr$) for 10 km^2 grid squares across British Isles (Galvanizers Association, 2020). Observed corrosion rates range are recorded in 0.5 $\mu m/yr$ intervals from $0 - 2.5$ $\mu m/yr$. Unfortunately, 88% of metallic structures in the Network Rail portfolio are located in areas with a rate of 1 or 1.5 $\mu m/yr$, which according to ISO 9223 (BSI, 2012) is the same corrosivity category, so there is limited scope for using this metric to split the bridges into

cohorts.

The model shown in Section 7.1 makes the distinction between under and over bridges, alongside girders being inner or exposed, which will already incorporate any difference in chloride abundance due to road gritting. The proximity of a structure to the coast could be a means of assessing the effects of a marine environment.

Coastal Proximity

Bridges situated in close proximity to the coast are exposed to high atmospheric salinity and prevailing winds, which can accelerate the deterioration of structural components. To determine the proximity of a bridge to the coast, the co-ordinates of the bridge were evaluated against 51,043 reference co-ordinates of the coastline from the Global Self-consistent, Hierarchical, High-resolution Geography Database (GSHHG) (National Oceanic and Atmospheric Administration (NOAA), 2015). Note that the Network Rail bridge portfolio has bridges on the Isle of Anglesey (including Holy Island), the Isle of Wight and Portsea Island as well as the island of Great Britain, see Figure 7.6.

The great-circle distance is the minimal distance between two surface points of a sphere. The great-circle distance d between two points can be computed as,

$$d = r \cdot \Theta, \tag{7.2.10}$$

where r is the radius of the sphere and Θ is the central angle between the two points on sphere surface. Let (ϕ_i, λ_i) denoted the longitude and latitude for point i, measured in radians. Then using the haversine formula (Van Brummelen, 2013), the distance d can be computed as,

$$d = 2r \arcsin\left(\sqrt{\sin^2\left(\frac{\phi_2 - \phi_1}{2}\right) + \cos(\phi_1)\cos(\phi_2)\sin^2\left(\frac{\lambda_2 - \lambda_1}{2}\right)}\right). \tag{7.2.11}$$

Note that (7.2.11) has been stated explicitly and not in terms of the haversine function.

Upon, determining the proximity to the coast for all bridges, the bridges were split into two cohorts,

- CP1 - Less than or equal to 10 km from the coast

- CP2 - More than 10 km from the coast

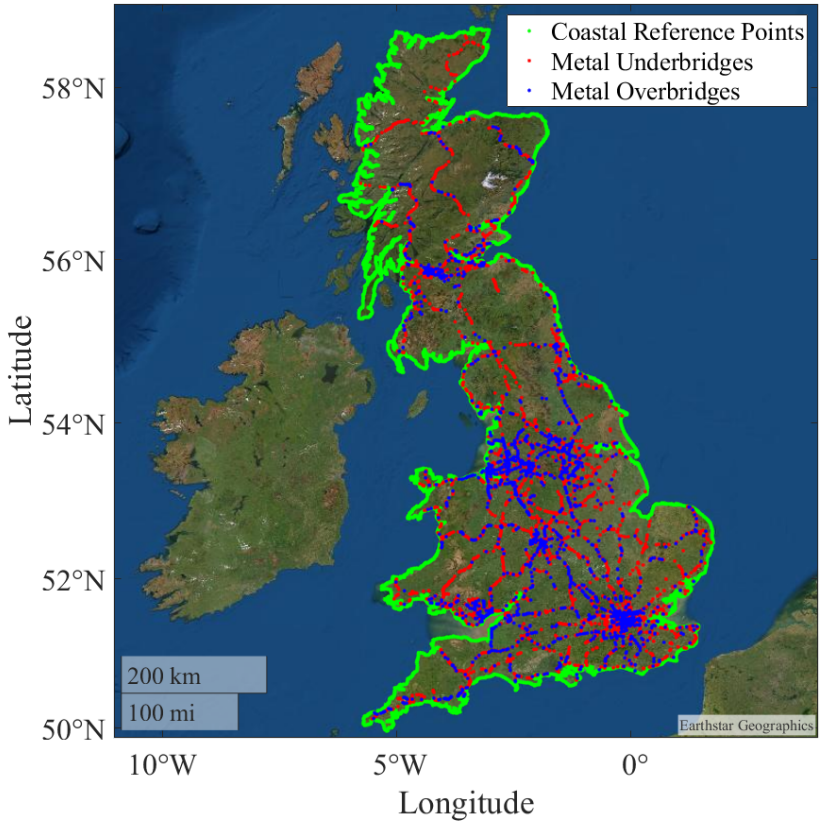

Figure 7.6: Coastline reference points for Great Britain, the Isle of Anglesey (including Holy Island), the Isle of Wight and Portsea Island and the co-ordinates of the Network Rail metal bridge portfolio (Network Rail, 2019b).

7.2.2 Material

Corrosion is "*an irreversible interfacial reaction of a material (metal, ceramic, polymer) with its environment which results in consumption of the material or in dissolution into the material of a component of the environment*" (Heusler et al., 1989).

Across a network of bridges and even a bridge, metallic bridge elements can be constructed out of different metal materials. These different metals will corrode at different rates. For example, Agrawal et al. (2010) analysed highway bridges in New York state, where from around 1968 metal bridges were constructed using weathering steel, which was a different steel composition than was typically used

before 1968, called 'steel'. In the Weibull-based analysis, weathering steel was found to deteriorate at a slower rate than the steel after 20 years.

The Network Rail portfolio contains metal bridges constructed out of cast iron, wrought iron, early steel, weathering steel and steel. 'Early Steel' is steel that was manufactured prior to 1956 (Network Rail, 2006) and 'Steel' denotes steel manufactured from 1956 onwards. For the purposes of this study, three cohorts were formed based on material type,

- M1 - Wrought Iron;
- M2 - Early Steel;
- M3 - Steel.

Cast iron was omitted from the study due to discrepancies in the recording of condition for this material at Network Rail.

7.2.3 Track Category

For road bridges, it is common to consider the traffic volume and road system when determining cohorts for model calibration (Scherer and Glagola, 1994). Road traffic volume is commonly measured using Annual Average Daily Traffic (AADT), which is the total volume of traffic for a year, divided by 365 days. The road system indicates the type of road system a bridge is situated on e.g. interstate/motorway, primary or secondary. Moreover, Zhang and Cai (2012) shown that increased vehicle speed has a negative effect on fatigue reliability of bridge components.

Track categorisation considers annual tonnage for a section of track and the designated line speed for trains on that section of track. The categories are used to specify requirements relating to design, maintenance, renewal and inspection of track. For railway underbridges, track category can be used as an indicator of traffic loading and route type. Tonnage is measured using Equivalent Million Gross Tonnes Per Annum (EMGTPA), which accounts for the variations caused by different rolling stock. The calculation that Network Rail uses for EMGTPA is similar to the calculation for "*theoretical traffic load*" specified by the International

Union of Railways (UIC, 2009). Line speed is measured in miles per hour and track sections with a greater permitted line speed are typically located on strategically important routes e.g. mainline services.

At Network Rail there are seven track categories, Cat 1, 1A, 2, 3, 4, 5 and 6. For this study, there are two track category cohorts considered

- TC1 - Cat 1, 1A and 2;
- TC2 - Cat 3, 4, 5 and 6.

The boundary between the track category definitions is a line speed of 91 mph between 0 and 7.2 EMGTPA. For annual tonnage greater than 7.2 EMGTPA, the line speed is defined as $-55 \cdot log(w) + 200$, where w is the annual tonnage in EMGTPA of the track section, as shown in Figure 7.7. The boundaries for categories are based on historical and experimental data (Network Rail, 2011).

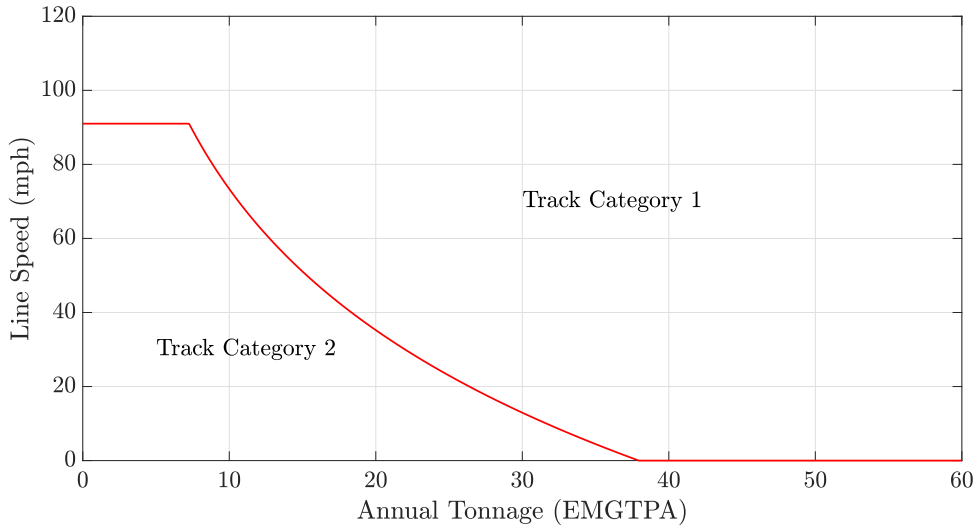

Figure 7.7: Defined boundary for track categories TC1 and TC2.

7.2.4 Data Breakdown

For this study, the condition records of 36,075 main girders are considered. When additional properties are incorporated into the deterioration model, the records used in model calibration are split into smaller cohorts. For example, of the 36,075 main girders considered, 24,847 are a constituent of an underbridge and 11,228 are a

constituent of an overbridges. The inclusion of coastal proximity, material type, track category and being an inner or exposed girder in a more detailed model will increasingly limit the size of the available data for specific instances of model calibration, see Table 7.3. The next section will consider a method to include influences of all these properties simultaneously, whilst ensuring that the minimal number of additional parameters are used.

Table 7.3: Number of main girders considered in the study, broken down by local, material and structural properties.

				M1	M2	M3
Underbridge	Inner	CP1	TC1	143	62	205
			TC2	736	466	1477
		CP2	TC1	824	411	1990
			TC2	1684	1226	2860
	Exposed	CP1	TC1	132	60	300
			TC2	1000	611	1587
		CP2	TC1	586	340	1794
			TC2	1759	1284	3310
Overbridge	Inner	CP1		662	208	733
		CP2		1341	1068	3299
	Exposed	CP1		302	206	466
		CP2		972	516	1455

7.3 Incorporating Multiple Factors into One Model

For the defect condition state transitions shown in Table 7.1, it can be observed that the rate monotonically increases as the causal influence defect progressively worsens.

This trend was obtained during an unconstrained model calibration, however, is a key trend that reflects the physical phenomena of deterioration but also has huge importance for any outputs from a life cycle analysis.

To incorporate deterioration altering properties, one could calibrate the multiple defect model and calculate a complete parameter set for a particular property cohort. However, scaling factors were introduced to the model to incorporate the effects of different deterioration altering properties whilst minimising the increase in parameter count to avoid over-fitting and to ensure that this monotonic increase in rate was retained.

If distinct rates or a scaling factor permutation were calibrated that did not maintain the monotonic increase, the model could output the perverse scenario that the more degraded an influencing defect is, the slower the corresponding defect degradation rate is. For example, if the rate for $C1 \rightarrow C2|Pa3$ is 0.675 and the rate for $C1 \rightarrow C2|Pa4$ is 0.55, the model would be returning a lowering rate of corrosion as the paintwork condition degrades. This scenario would ultimately disincentivise paintwork maintenance interventions when performing a life cycle analysis, which goes against engineering judgement.

To include multiple properties simultaneously, they could be strategically input into the model on a per defect basis. The multiple defect model shown in Section 7.1 incorporates the underbridge/overbridge and exposed/inner status of the component for all of the defects in the deterioration model. However, each of the additional properties that influence deterioration is then input to the existing model for a particular defect type:

- The paintwork scaling factors are specific to the proximity of the bridge component to the coast.
- The corrosion scaling factors are specific to the material type that the bridge component is constructed out of.
- The SCF scaling factors are specific to the component's bridge track category.

The relationship between the local, structural and material properties is shown in Figure 7.8. This particular model configuration ensures that there are minimal ad-

ditional parameters being added to the model to avoid the over parameterisation of the condition data. However, if a girder being close to the coast results in increased paintwork degradation, corrosion will occur at a great rate due to the worse paintwork condition. Similarly if a particular material type corrodes at a faster rate, the instances of SCF occurring will increase due to the causal influence between those defects.

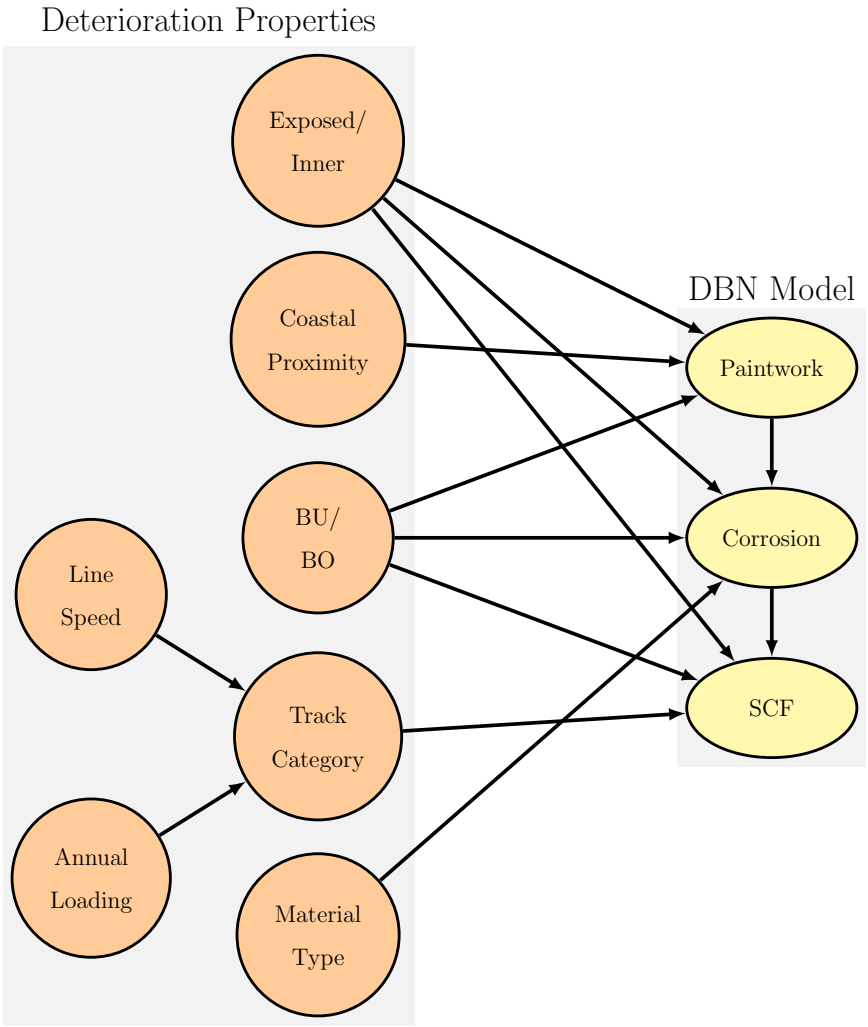

Figure 7.8: Influencing properties for defect deterioration model.

As aforementioned, scaling factors for the calibrated transition rates were introduced to avoid having to calibrate a complete set of parameters for each unique cohort. The transition rates that incorporate additional properties are calculated as,

$$\lambda_i = \alpha_i \cdot \beta_i^{EIID}, \tag{7.3.12}$$

where β_i is the baseline transition rate that corresponds to the element type of the component and α_i is the scaling factor that corresponds to the associated property. The scaling factors are listed in Table 7.4, with the associated Paintwork ID (PaID), Corrosion ID (CoID) and SCF ID (StrID) defined in Table 7.5. Table 7.5 provides a mapping between different properties of a bridge component and the index (ID) for the appropriate scaling factor for each defect. Using Tables 7.4 and 7.5 to determine the appropriate parameters for a particular type of bridge component enables the evaluation of (7.3.12).

Table 7.4: Defect transition rates and scaling factors for Paintwork, Corrosion and SCF.

Transition	**Transition Rate**	**Baseline Rate**	**Scaling Factor**
$(Pa1 \rightarrow Pa2)$	λ_1	β_1^{ElID}	$\alpha_1 = \gamma_A^{PaID}$
$(Pa2 \rightarrow Pa3)$	λ_2	β_2^{ElID}	$\alpha_2 = \gamma_A^{PaID}$
$(Pa3 \rightarrow Pa4)$	λ_3	β_3^{ElID}	$\alpha_3 = \gamma_A^{PaID}$
$(C1 \rightarrow C2)\|Pa1$	λ_4	β_4^{ElID}	$\alpha_4 = 1$
$(C1 \rightarrow C2)\|Pa2$	λ_5	β_5^{ElID}	$\alpha_5 = \gamma_B^{CoID}$
$(C1 \rightarrow C2)\|Pa3$	λ_6	β_6^{ElID}	$\alpha_6 = \gamma_B^{CoID}$
$(C1 \rightarrow C2)\|Pa4$	λ_7	β_7^{ElID}	$\alpha_7 = \gamma_B^{CoID}$
$(C2 \rightarrow C3)\|Pa1$	λ_8	β_8^{ElID}	$\alpha_8 = \gamma_B^{CoID}$
$(C2 \rightarrow C3)\|Pa2$	λ_9	β_9^{ElID}	$\alpha_9 = \gamma_B^{CoID}$
$(C2 \rightarrow C3)\|Pa3$	λ_{10}	β_{10}^{ElID}	$\alpha_{10} = \gamma_B^{CoID}$
$(C2 \rightarrow C3)\|Pa4$	λ_{11}	β_{11}^{ElID}	$\alpha_{11} = \gamma_B^{CoID}$
$(C3 \rightarrow C4)\|Pa1$	λ_{12}	β_{12}^{ElID}	$\alpha_{12} = \gamma_B^{CoID}$
$(C3 \rightarrow C4)\|Pa2$	λ_{13}	β_{13}^{ElID}	$\alpha_{13} = \gamma_B^{CoID}$
$(C3 \rightarrow C4)\|Pa3$	λ_{14}	β_{14}^{ElID}	$\alpha_{14} = \gamma_B^{CoID}$
$(C3 \rightarrow C4)\|Pa4$	λ_{15}	β_{15}^{ElID}	$\alpha_{15} = \gamma_B^{CoID}$
$(F1 \rightarrow F2)\|C1$	λ_{16}	β_{16}^{ElID}	$\alpha_{16} = \gamma_C^{StrID}$
$(F1 \rightarrow F2)\|C2$	λ_{17}	β_{17}^{ElID}	$\alpha_{17} = \gamma_C^{StrID}$
$(F1 \rightarrow F2)\|C3$	λ_{18}	β_{18}^{ElID}	$\alpha_{18} = \gamma_C^{StrID}$
$(F1 \rightarrow F2)\|C4$	λ_{19}	β_{19}^{ElID}	$\alpha_{19} = \gamma_C^{StrID}$

Table 7.5: Defect Parameter IDs for Paintwork, Corrosion and SCF*.

Structure Type	Element Type	M	CP	TC	ElID	PaID	CoID	StrID
B/U	MGI	1	1	1	1	1	1	1
B/U	MGI	1	1	2	1	1	1	2
B/U	MGI	1	2	1	1	2	1	1
B/U	MGI	1	2	2	1	2	1	2
B/U	MGI	2	1	1	1	1	2	1
B/U	MGI	2	1	2	1	1	2	2
B/U	MGI	2	2	1	1	2	2	1
B/U	MGI	2	2	2	1	2	2	2
B/U	MGI	3	1	1	1	1	3	1
B/U	MGI	3	1	2	1	1	3	2
B/U	MGI	3	2	1	1	2	3	1
B/U	MGI	3	2	2	1	2	3	2
B/U	MGE	1	1	1	2	3	4	3
B/U	MGE	1	1	2	2	3	4	4
B/U	MGE	1	2	1	2	4	4	3
B/U	MGE	1	2	2	2	4	4	4
B/U	MGE	2	1	1	2	3	5	3
B/U	MGE	2	1	2	2	3	5	4
B/U	MGE	2	2	1	2	4	5	3
B/U	MGE	2	2	2	2	4	5	4
B/U	MGE	3	1	1	2	3	6	3
B/U	MGE	3	1	2	2	3	6	4
B/U	MGE	3	2	1	2	4	6	3
B/U	MGE	3	2	2	2	4	6	4

* M - Material, CP - Coastal Proximity, TC - Track Category, ElID - Element ID, PaID - Paintwork ID, CoID - Corrosion ID, StrID - SCF ID

7.3.1 Underbridge Case Study

As a case study, the enhanced multiple defect deterioration model from the previous section was calibrated using the Network Rail condition records for railway underbridges. Note that the baseline deterioration rates for MGI-BU and MGE-BU from Table 7.1 remain the same in the calibration of the deterioration model with scaling factors. The scaling factors that maximised the log-likelihood function for the condition records used in calibration are shown in Tables 7.6, 7.7 and 7.8 for paintwork, corrosion and SCF respectively.

Table 7.6: Scaling factors for paintwork.

		CP1 (γ^{CP1})	CP2 (γ^{CP2})
MGI	γ_A	1.3580	0.9096
MGE	γ_A	1.2223	0.9210

Table 7.7: Scaling factors for corrosion.

		M1 (γ^{M1})	M2 (γ^{M2})	M3 (γ^{M3})
MGI	γ_B	1.4048	1.2562	0.8108
MGE	γ_B	1.4031	1.2966	0.7621

Table 7.8: Scaling factors for SCF.

		TC1 (γ^{TC1})	TC2 (γ^{TC2})
MGI	γ_C	1.6822	0.7235
MGE	γ_C	1.1430	0.9354

It can be observed that for each of the scaling factors, components with the more aggressive properties, i.e. CP1, M1, M2 and TC1, have a value greater than one and the components with the less aggressive properties, i.e. CP2, M3 and TC2, have a factor value less than one. This enables the components with aggressive properties

to deteriorate at a faster rate than the baseline rate and conversely, the components with less aggressive properties can deteriorate at a slower rate than the baseline rates. Consequently, each component would have a contextualised deterioration rates for its composition of local, structural and material properties. The variation of predicted condition for MGI-BU and MGE-BU with each property composition are shown in Figures 7.9 and 7.10.

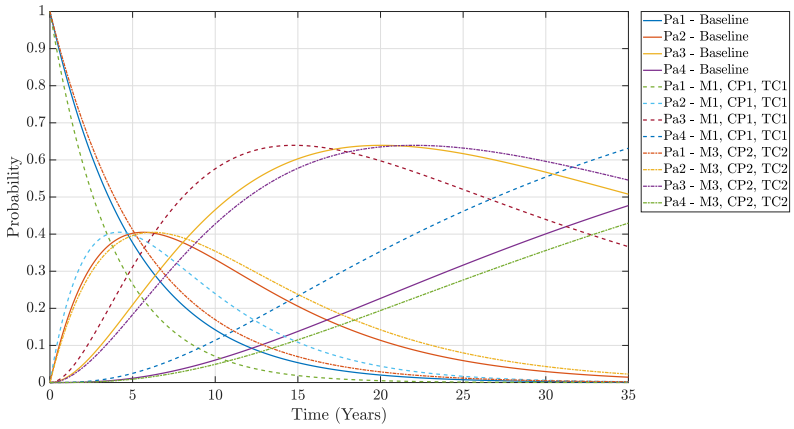

(a) Paintwork

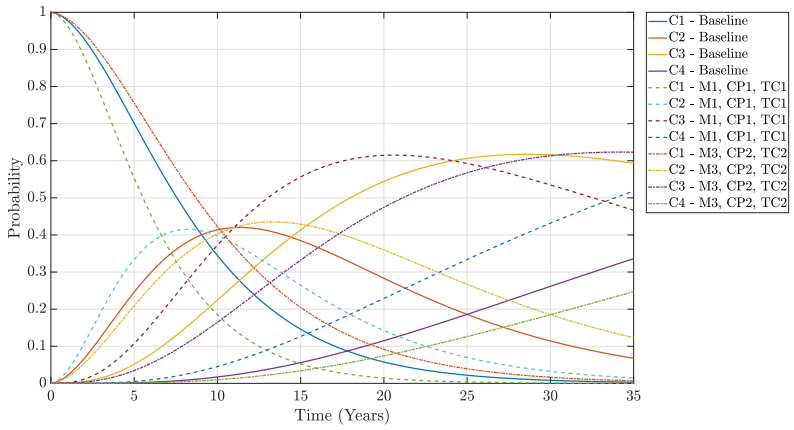

(b) Corrosion

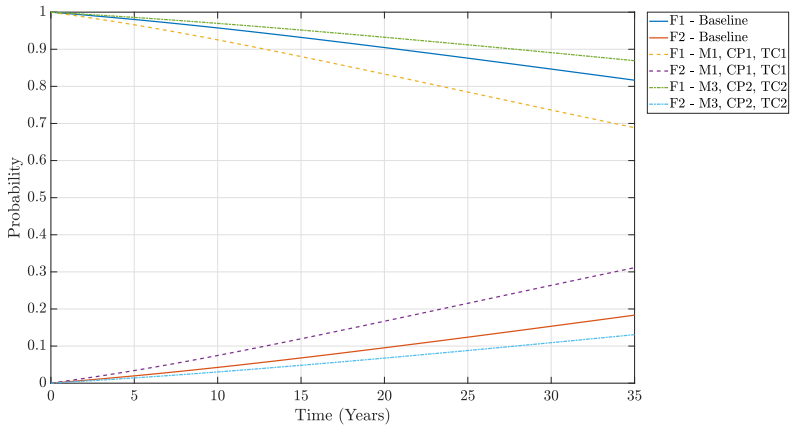

(c) SCF

Figure 7.9: Condition profiles for 35 years for different parametrisations of MGI-BU girders incorporating additional deterioration properties.

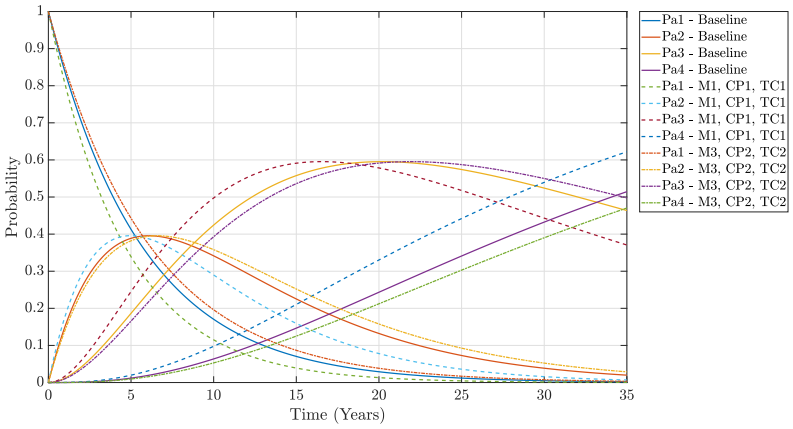

(a) Paintwork

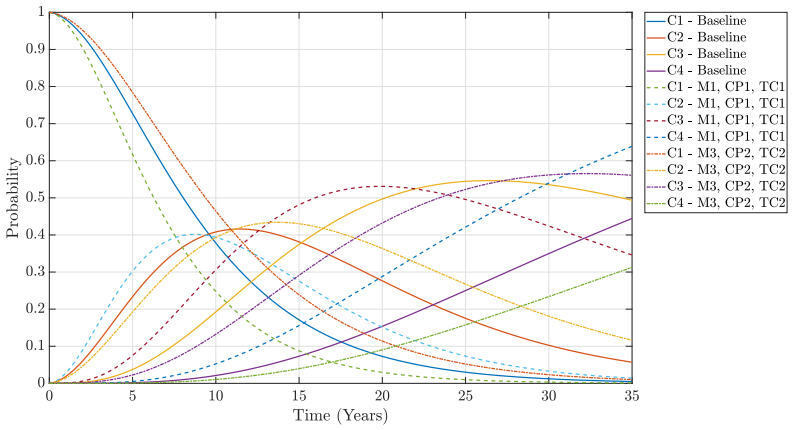

(b) Corrosion

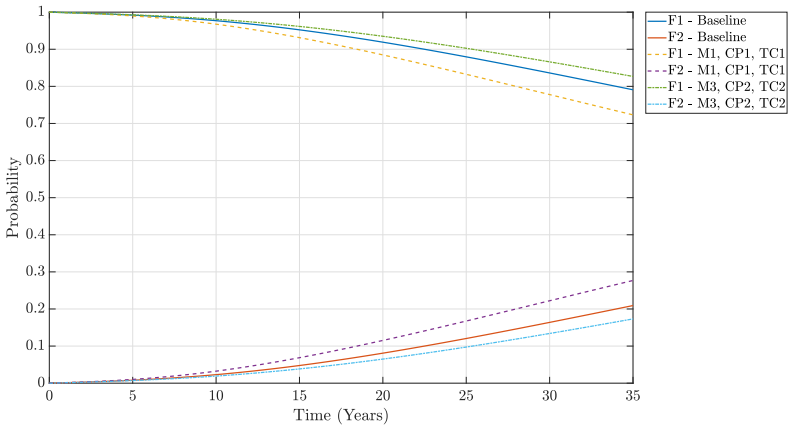

(c) SCF

Figure 7.10: Condition profiles for 35 years for different parametrisations of MGE-BU girders incorporating additional deterioration properties.

Engineering expertise would suggest that the closer a bridge is to the coast, the greater the rate of deterioration, similarly, wrought iron and early steel would deteriorate faster than steel and finally that the greater the bridge loading or line speed is, the greater the rate of deterioration. This is observed in the deterioration factor values and the values obtained in the initial case study adhere to the following inequalities,

$$\gamma_A^{CP1} \geq \gamma_A^{CP2}, \tag{7.3.13}$$

$$\begin{aligned} \gamma_B^{M1} &\geq \gamma_B^{M3}, \\ \gamma_B^{M2} &\geq \gamma_B^{M3}, \end{aligned} \tag{7.3.14}$$

$$\gamma_C^{TC1} \geq \gamma_C^{TC2}. \tag{7.3.15}$$

The consequence of the different rates of deterioration is a difference in the predicted service life of the bridge component. Figure 7.11 shows the MTTP for paintwork, corrosion and SCF respectively. It can be observed that the local, structural and material properties cause quite large differences between the different configurations. For example, considering MGI-BU,

- CP3 has a 49.3% greater MTTP for coating degradation than CP1.
- M2, CP3 has a 70.3% greater MTTP for corrosion than M1, CP1.
- TC2, M2, CP3 has a 106.6% greater MTTP for SCF than TC1, M1, CP1.

Such discrepancies in the predicted service life of a component would have great consequence when performing a life cycle analysis and ascertaining the most appropriate intervention strategy.

The significant peaks in Figure 7.11c are for MGI-BU elements identified as TC2, i.e. lower annualised loading and/or lower line speed. The reduced loading and reduced line speed should result in a reduced rate of SCF occurring, which is why λ_C^{TC2} is 0.7235, i.e. less than 1. A reduced level of SCF is expected, however there seems to be a sizeable difference for the MTTP values for TC2 inner girders and TC2 exposed girders.

Recall that SCF is structural component failure which encompasses a range of defect modes including buckling, tearing, displacement, fracture etc. The discrepancy in SCF MTTP values for inner and exposed girders could be due to the inner

girder's SCF modes being more dependent on loading, whereas SCF in exposed girders whilst still influenced by loading are also more environmentally driven. The paintwork degrades faster on an exposed girder than an inner girder and the exposed girder corrodes faster too, suggesting that an exposed girder is more vulnerable to environmental factors. Moreover, the large discrepancy between inner and exposed girders in TC2 bridges could suggest that there is a greater level of unused redundancy for inner girders in the bridge design, i.e. the bridges are 'over-engineered'. However, a more tactical investigation of specific bridges would be required to confirm this hypothesis.

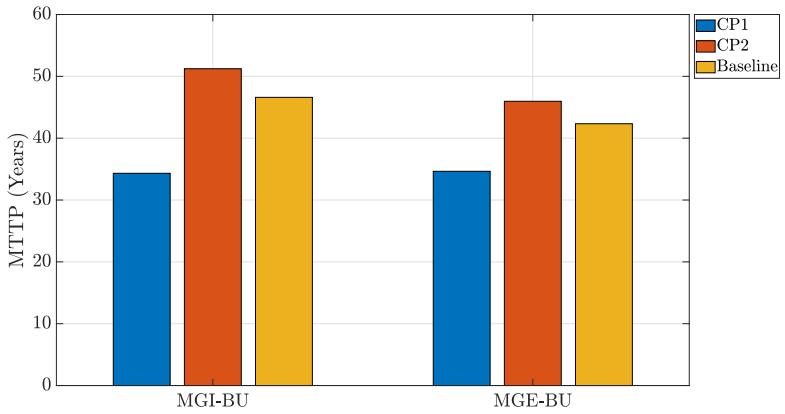

(a) Paintwork

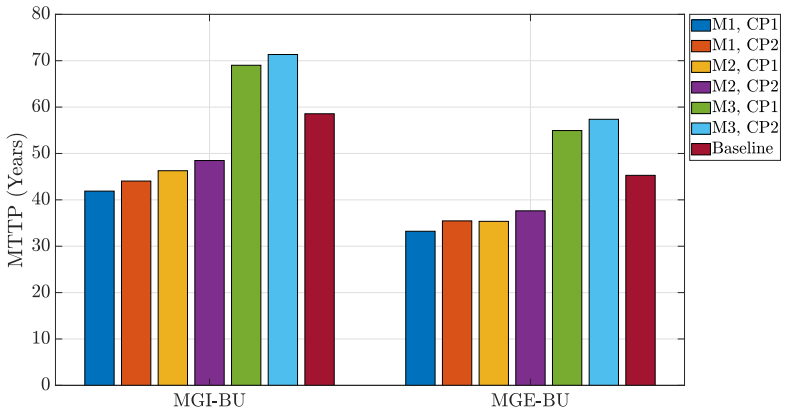

(b) Corrosion

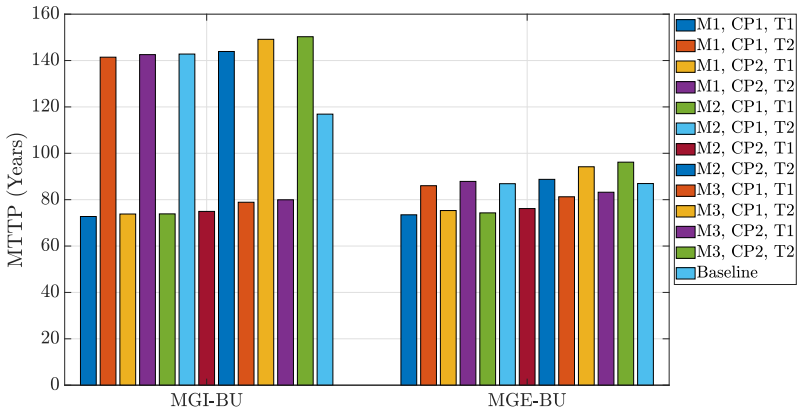

(c) SCF

Figure 7.11: The Mean Time to Poor Condition for loss of paintwork, corrosion and SCF using a starting condition of {Pa1, C1, F1} for Model B for BU main girders.

7.3.2 Model Selection

For the initial case study for underbridges there are two models,

- Model A - 28 Parameters (Baseline transition rates used for MGI/MGE BU girders)
- Model B - 42 Parameters (28 Baseline Parameters, 7 Deterioration Factors for MGI and 7 Deterioration Factors for MGE)

The test statistics for Model A and B are shown in Table 7.9. The likelihood ratio test statistic is 875.5, which gives a p-value that is infinitesimal ($< 10^{-5}$) and suggests that the difference between Model A and B is statistically significant. This is again supported by Model B having the lowest value for AIC and BIC, making it the preferred candidate model despite its increased parameters.

Table 7.9: Initial deterioration properties model (BU) test statistics.

Model	No. Parameters	Log-likelihood	AIC	BIC
A	28	-39017.8	78091.6	78163.2
B	42	-38580.1	77244.1	77351.4

7.3.3 Further Model Development

Model B as presented in the previous section incorporated multiple additional factors that could influence the development and progression of multiple defect mechanisms, however it only considered one property per defect mechanism. This model was proposed with this particular structure to enable the model to generalise well across different bridge elements, particular for those elements which may not have the same amount of condition records available for model calibration.

However, the model could be extended further to include multiple factors for a particular defect. For example, corrosion may be influenced by the construction material as well as coastal proximity, in addition to the coating condition. The additional model structures considered are presented in Figure 7.12. The increased

inclusion of the properties that can influence the progression of a defect mechanism results in the conditions used for model calibration being subdivided into smaller cohorts. Small cohorts for model calibration are problematic as the model may over-fit a condition profile that is non-representative of the physical phenomena or return a skewed output due to an unknown bias in the maintenance strategy that may exist for particularly aggressive cohorts.

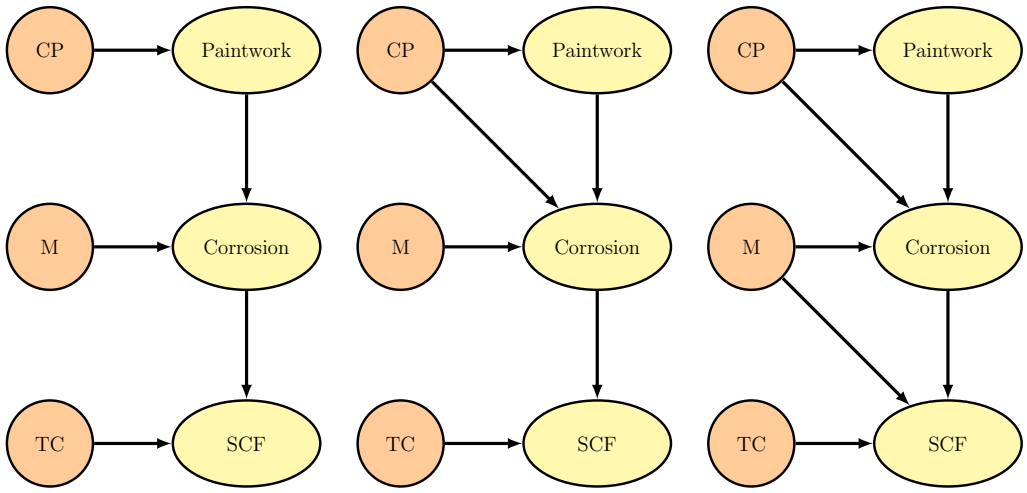

(a) Model B (b) Model C (c) Model D

Figure 7.12: Influencing properties for various enhanced defect deterioration models for main girders from a railway underbridge. Note that each model also used the appropriate MGI/MGE and BU baseline parameters.

A model user can incorporate expert judgement to prevent any returned condition profiles being in conflict of the conjectured behaviour between property types. For example, if coastal proximity and material are being calibrated to influence the rate of corrosion, one would anticipate that for the same material, the girders closer to the coast would corrode at a faster rate than girders further inland.

However, in preliminary attempts, whilst the calibrated γ_B for CP1 was larger than for CP2, for early steel and steel in Model C, this was not the case for wrought iron. This output could be due to a sparse dataset for that particular cohort or that Network Rail engineers already enact enhanced maintenance interventions for that cohort, or it could just be the reality for some unknown reason. To avoid the deterioration model and associated life cycle analysis being adversely impacted by

this parameter, expert judgement can be used to alter the model for these scenarios, potential approaches are:

i Place inequality constraints on the parameters to ensure that the CP1 returns a faster rate of corrosion than CP2. Note that inequality constraints would make the use of AIC and BIC inappropriate in model selection (Anraku, 1999; Kuiper et al., 2011).

ii Revert to using a simpler model structure for the particular cohort configurations that are in conflict with engineering judgement. For example, instead of using material and coastal proximity, use material only.

iii Revert to using the baseline rate for the particular cohort configurations that are in conflict with engineering judgement.

iv Set appropriate values using engineering expertise and evaluation of similar element types.

In this study, the second approach was considered for the particular cohorts that conflicted with the expected behaviour for coastal proximity and track category, as shown in (7.3.13) and (7.3.15). The models that incorporate these assumptions are denoted as C_e and D_e.

The test statistics for the different models are shown in Table 7.10. It can be observed that Model D should be selected as the most appropriate model given its log-likelihood, AIC and BIC scores. However, between Models A, B, C_e and D_e, i.e. the models adhering to the expected engineering outcomes, Model D_e should be selected. The scaling factors for corrosion and SCF for Model D_e are shown in Tables 7.11 and 7.12, with any simplified cohorts indicated, the associated defect MTTP values are shown in Figure 7.13.

Table 7.10: Enhanced deterioration properties model (BU) test statistics.

Model	No. Parameters	Log-likelihood	AIC	BIC
A	28	-39017.8	78091.6	78163.2
B	42	-38580.1	77244.1	77351.4
C	48	-38537.9	77171.8	77294.5
D	56	-38505.5	77123.0	77266.0
C_e	46	-38547.4	77186.9	77304.4
D_e	52	-38521.8	77147.6	77280.4

Table 7.11: Scaling factors for corrosion for Model D_e.

	M1		M2		M3	
	CP1 (γ_i^1)	CP2 (γ_i^2)	CP1 (γ_i^3)	CP2 (γ_i^4)	CP1 (γ_i^5)	CP2 (γ_i^6)
MGI	1.4048*	1.4048*	1.7754	1.0876	0.8774	0.8003
MGE	1.4031*	1.4031*	1.7662	1.1335	0.8236	0.7431

* indicates a parameter that was sampled from a simpler model configuration.

Table 7.12: Scaling factors for SCF for Model D_e.

	M1		M2		M3	
	TC1 (γ_i^1)	TC2 (γ_i^2)	TC1 (γ_i^3)	TC2 (γ_i^4)	TC1 (γ_i^5)	TC2 (γ_i^6)
MGI*	1.6822*	0.7235*	1.3850	0.5300	1.5377	0.7192
MGE	2.1122	1.1427	1.3739	0.7765	1.1430*	0.9354*

* indicates a parameter that was sampled from a simpler model configuration.

7.3.4 Overbridge Case Study

For overbridges, similar models as underbridges were considered for incorporating properties that influence deterioration, see Figure 7.14. Note that track category was omitted from the calibrated models as the railway line goes under the deck in

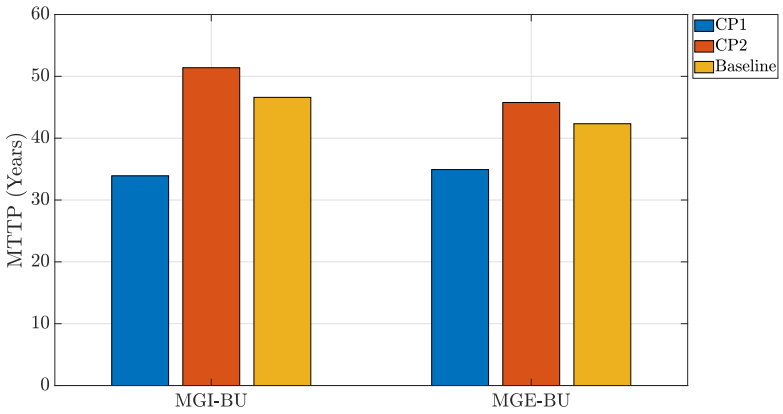

(a) Paintwork

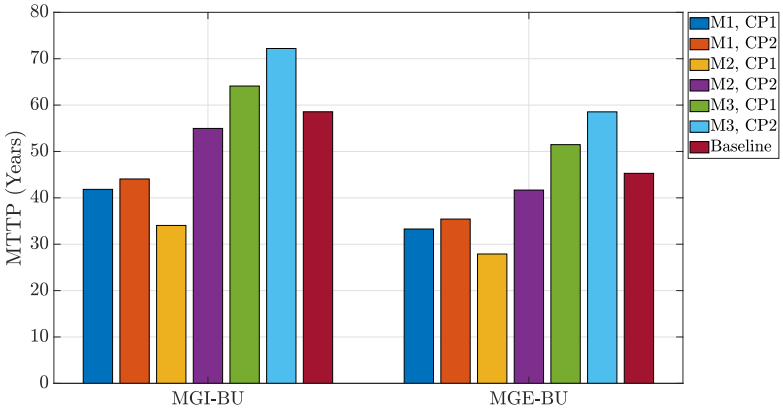

(b) Corrosion

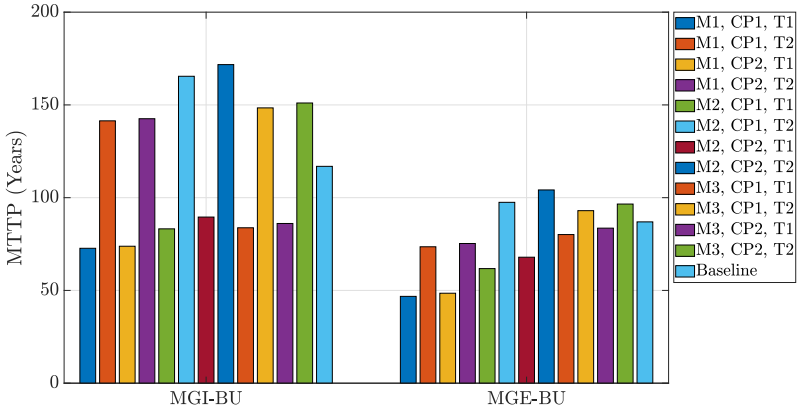

(c) SCF

Figure 7.13: The Mean Time to Poor Condition for the deterioration of paintwork using a starting condition of {Pa1, C1, F1} for Model D_e for BU main girders.

a overbridge, and thus would not be an appropriate characterisation of the bridge loading.

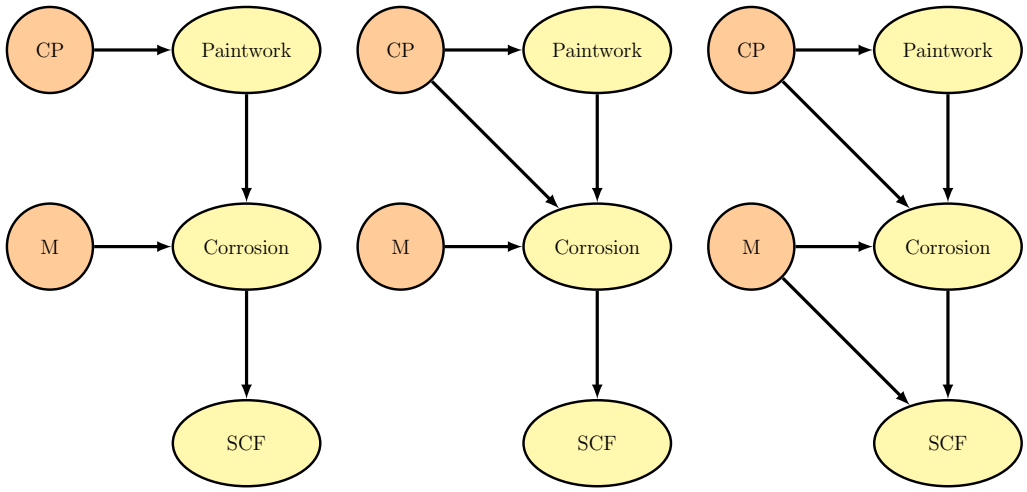

(a) Model B (b) Model C (c) Model D

Figure 7.14: Influencing properties for various defect deterioration models for main girders from a railway overbridge. Note that each model also used the appropriate MGI/MGE and BO baseline parameters.

The test statistics for each model for overbridges is shown in Table 7.13. Again it can be observed that Model D is the most appropriate given the three test statistics. The scaling factors for overbridges, for Model D are listed in Tables 7.14, 7.15 and 7.16. The MTTP values for Model D are shown in Figure 7.15. Note that Model D did not require any manipulation or model simplification to exert engineering judgement.

Table 7.13: Deterioration properties model (BO) test statistics.

Model	No. Parameters	Log-likelihood	AIC	BIC
A	28	-15378.3	30812.6	30875.7
B	38	-15253.9	30583.8	30669.4
C	44	-15237.1	30562.1	30661.2
D	50	-15218.2	30536.3	30648.9

Table 7.14: Scaling factors for paintwork (BO).

		CP1 (γ_i^1)	CP2 (γ_i^2)
MGI	γ_A	1.2611	0.9439
MGE	γ_A	1.1384	0.9638

Table 7.15: Scaling factors for corrosion (BO).

		M1		M2		M3	
		CP1 (γ_i^1)	CP2 (γ_i^2)	CP1 (γ_i^3)	CP2 (γ_i^4)	CP1 (γ_i^5)	CP2 (γ_i^6)
MGI	γ_B	1.2153	1.0636	1.8308	1.8006	1.1787	0.7557
MGE	γ_B	1.2521	1.2363	1.6241	1.2490	0.8940	0.7711

Table 7.16: Scaling factors for SCF (BO).

		M1 (γ_i^1)	M2 (γ_i^2)	M3 (γ_i^3)
MGI	γ_C	1.1979	1.3750	0.6976
MGE	γ_C	1.1423	1.1585	0.7305

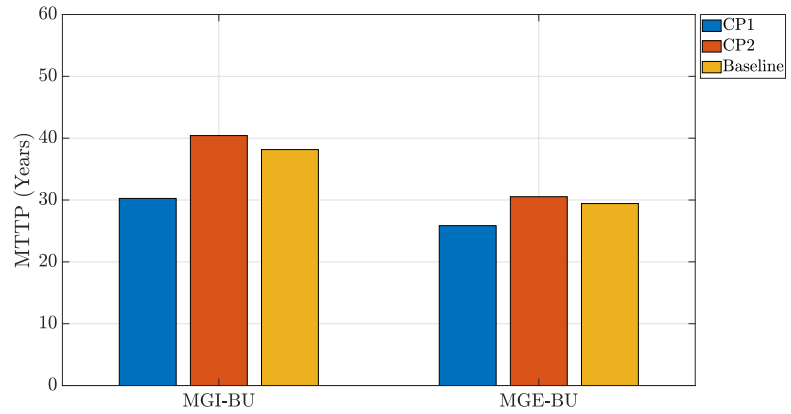

(a) Paintwork

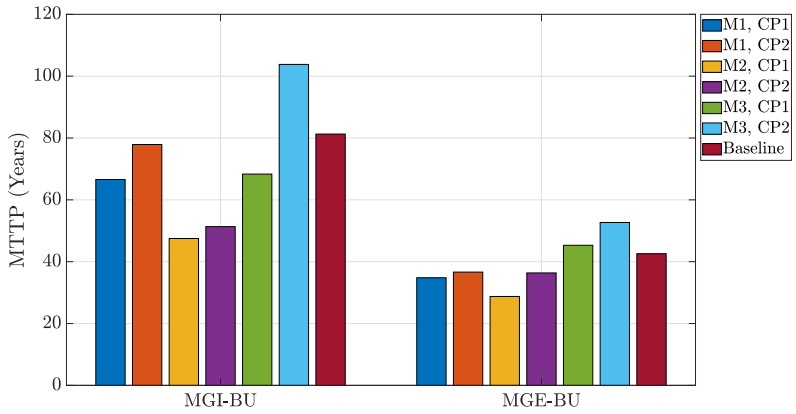

(b) Corrosion

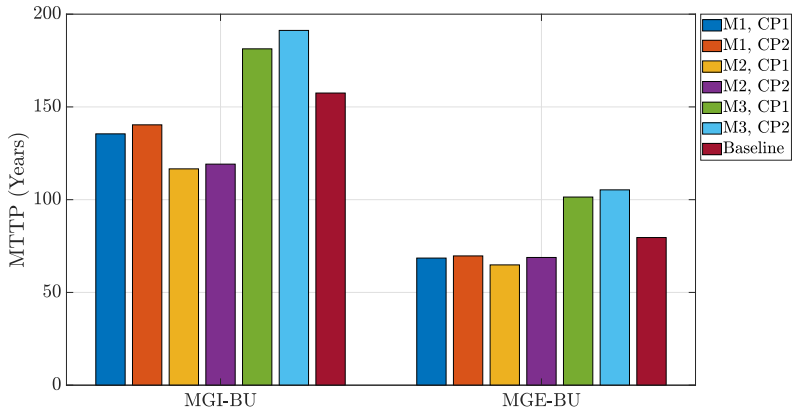

(c) SCF

Figure 7.15: The Mean Time to Poor Condition for the deterioration of paintwork, corrosion and SCF using a starting condition of {Pa1, C1, F1} for Model D for BO main girders.

7.4 Life Cycle Analysis of Different Deterioration Properties

The previous section incorporated multiple properties that influence the rate of paintwork/coating degradation, corrosion and occurrence of SCF and it was found these have a large effect on the predicted condition profiles and MTTP values. However, the MTTP analysis assumed a do-nothing maintenance strategy. In this section a life cycle analysis will performed to evaluate the effects of the different deterioration properties under different maintenance strategies. Deterioration rates for several cohorts from the baseline model and model D_e for main girders for railway underbridges will be considered,

- Cohort 1 - MGI-BU Baseline
- Cohort 2 - MGI-BU, M1, CP1, TC1
- Cohort 3 - MGI-BU, M3, CP2, TC2
- Cohort 4 - MGE-BU Baseline
- Cohort 5 - MGE-BU, M1, CP1, TC1
- Cohort 6 - MGE-BU, M3, CP2, TC2

The different cohorts will be assessed using three different maintenance strategies,

- Strategy A - Fixed renewal of paintwork every five years.
- Strategy B - Fixed renewal of paintwork every ten years.
- Strategy C - No paintwork-only interventions.

For all three strategies, there were two additional repair actions that were always enabled:

- Corrosion repair when condition $C4$ is revealed. This intervention restores corrosion to $C1$ and paintwork to $Pa1$. The paintwork restoration is included

as Network Rail expertise suggests that when an intervention occurs, the engineers would ensure that the paintwork is fully restored to maximise the impact of taking possession of the bridge.

- Component replacement when condition $F2$ is revealed. This will restore the component model to the states of $Pa1$, $C1$ and $F1$. If $C4$ and $F2$ are revealed at the same time, component replacement is prioritised over corrosion repair.

A life cycle analysis was performed using a Petri model which simulated the deterioration of a component, inspection regime and application of each maintenance strategy. The model is described in Section 6.2.

7.4.1 Performance Indicators

The probability profiles of being in poor condition are shown in Figures 7.16, 7.17 and 7.18 for Strategies A, B and C respectively, alongside the predicted average total cost over time, broken down by intervention type.

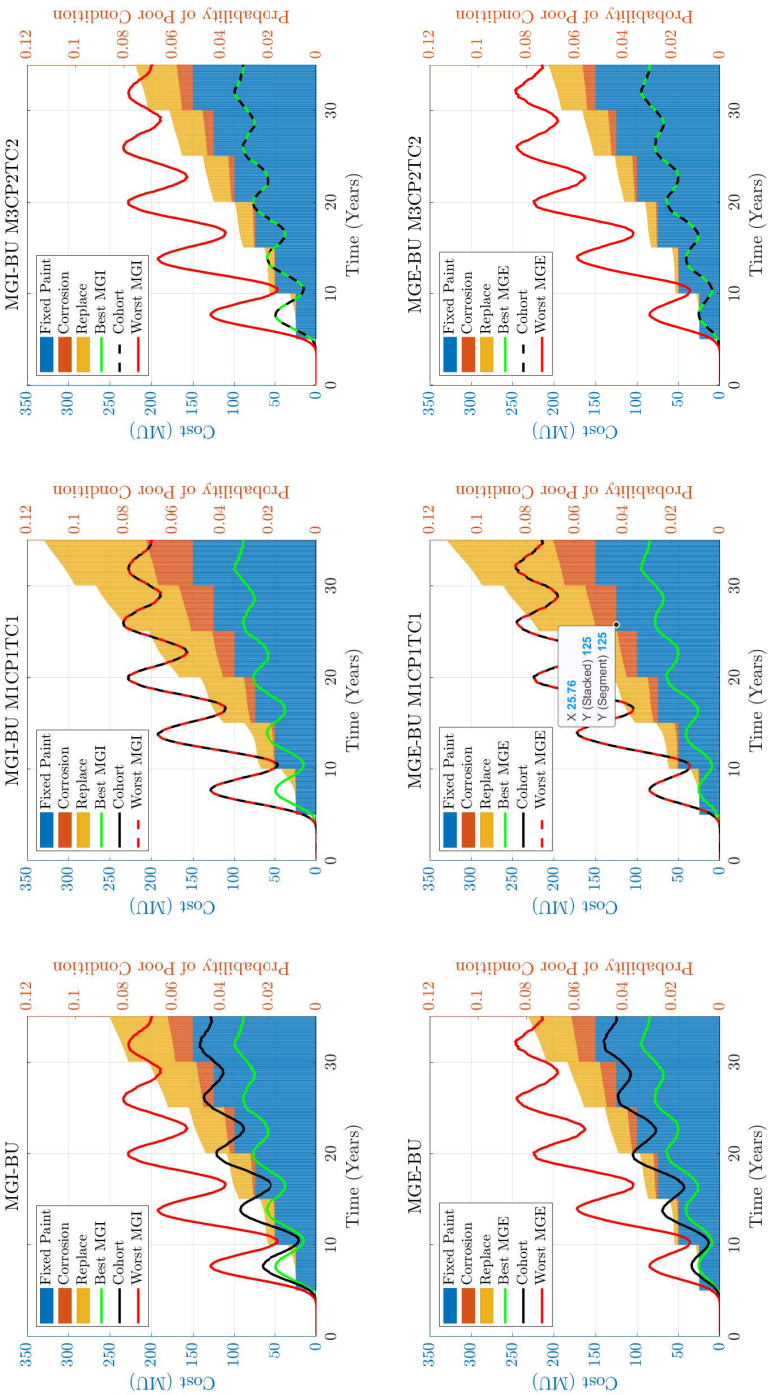

Figure 7.16: Probability of being in poor condition and predicted costs over time for Strategy A, with a starting condition of {Pa1, C1, F1}.

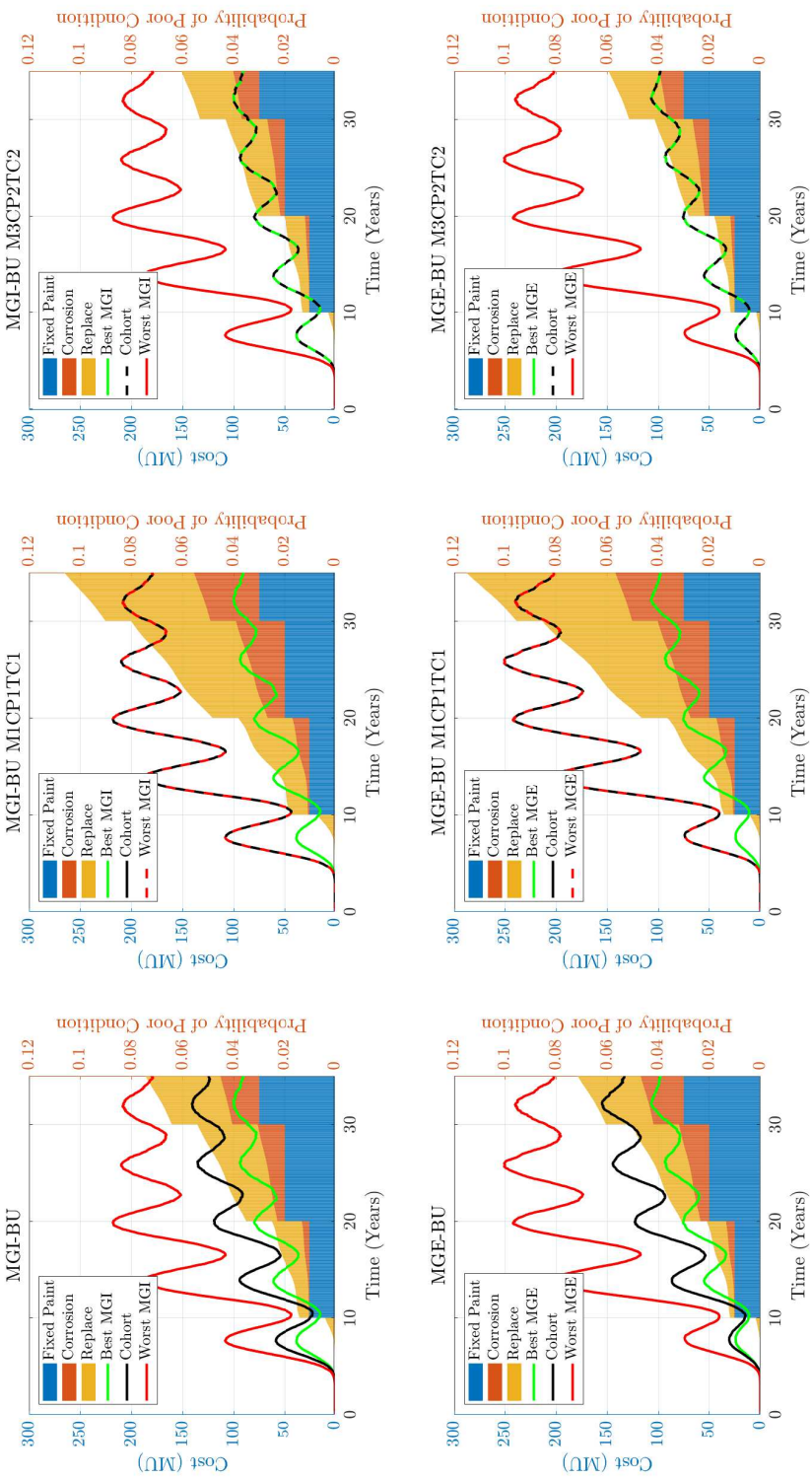

Figure 7.17: Probability of being in poor condition and predicted costs over time for Strategy B, with a starting condition of {Pa1, C1, F1}.

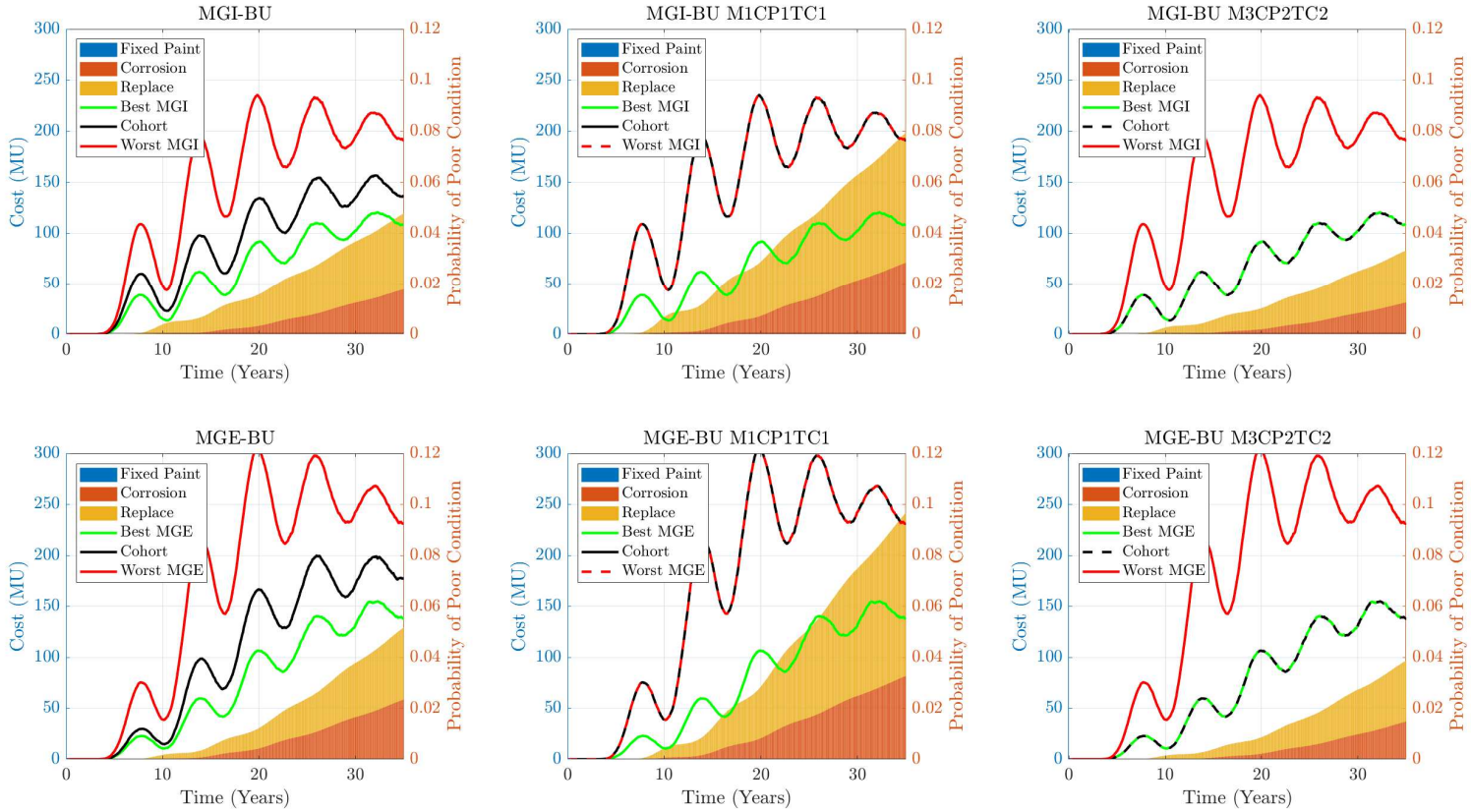

Figure 7.18: Probability of being in poor condition and predicted costs over time for Strategy C, with a starting condition of {Pa1, C1, F1}.

To compare between the different cohorts and strategies, there are two Key Performance Indicators (KPI) considered for the 35 year simulation period,

- Average total Time in Poor Condition (ATPC),
- Average Total Costs,

which are shown in Figures 7.19 and 7.20 respectively.

For each cohort there is a general trend that the ATPC increases from Strategy A to B to C. However, the reduced ATPC comes at a cost, with a trend that Strategy A is the most expensive and Strategy C is the least expensive. These observed trends corresponds with what engineering expertise would predict as Strategy A dictates a more regular preventative maintenance schedule. Additionally, for any given strategy it can be observed that the following inequalities are satisfied,

$$\begin{aligned} \text{ATPC}_2 > \text{ATPC}_1 > \text{ATPC}_3, \\ \text{ATPC}_5 > \text{ATPC}_4 > \text{ATPC}_6, \end{aligned} \tag{7.4.16}$$

$$\begin{aligned} \text{Cost}_2 > \text{Cost}_1 > \text{Cost}_3, \\ \text{Cost}_5 > \text{Cost}_4 > \text{Cost}_6, \end{aligned} \tag{7.4.17}$$

where ATPC_i indicates the ATPC for cohort i and Cost_i indicates the total cost for cohort i.

The expressions in (7.4.16) and (7.4.17) state that the cohorts (Cohorts 2 and 5) with the most aggressive properties, i.e. CP1, M1 and TC1, return the upper limit for total cost and ATPC. Conversely, the cohorts (Cohorts 3 and 6) with the least aggressive properties, i.e. CP2, M3 and TC2, returns the lower limit for total cost and ATPC. It was expected that the least aggressive and most aggressive cohorts would act as bounds for cost and ATPC indicators. Moreover, the baseline cohorts (Cohorts 1 and 4) return values for total cost and ATPC between the two limits, which conforms with the expectation that the baseline cohorts serve as an average based on the asset composition of the calibration data.

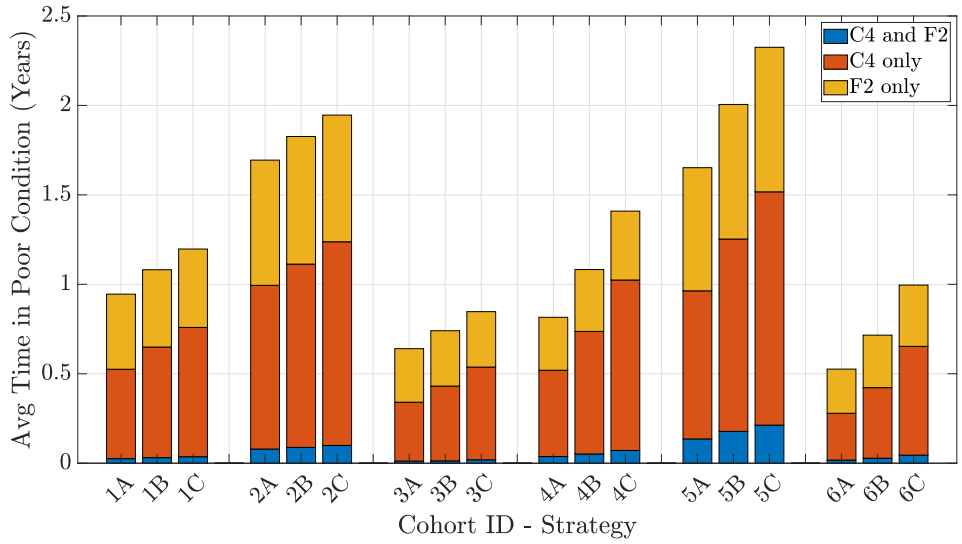

Figure 7.19: Average Total Poor Time in Poor Condition for 35 year simulation using a starting condition of {Pa1, C1, F1}.

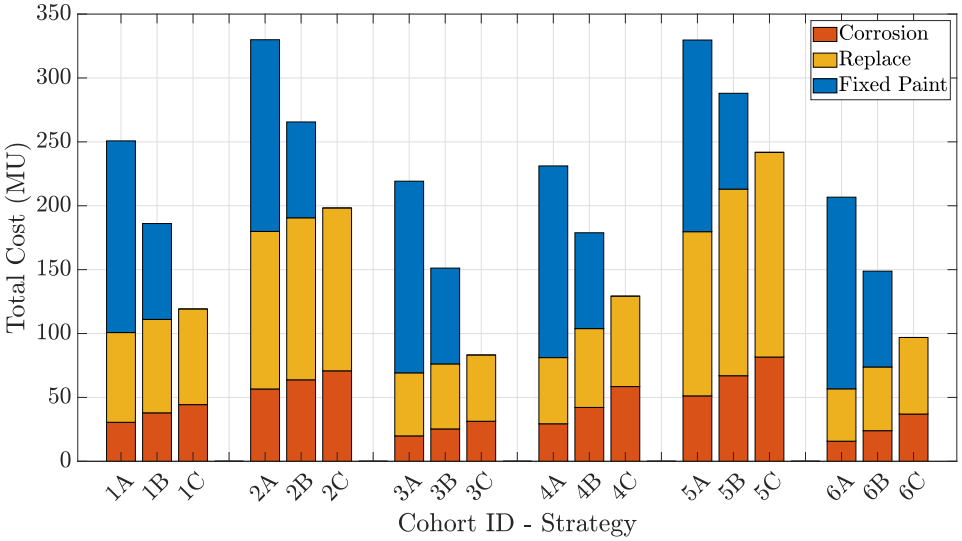

Figure 7.20: Average total costs over the course 35 years using a starting condition of {Pa1, C1, F1}.

The study KPIs are presented in Figure 7.21 as a scatter plot, where it can be observed that there are three clusters formed from different cohorts and maintenance strategies. The red ellipse includes the KPIs for Cohorts 2 and 5 under strategies A, B and C; these cohorts represented the most aggressive scaling factors, with wrought iron, a coastal proximity of within 10km of the coast and belonging to a

track category with the greatest loading/highest line speeds. Conversely, the green ellipse includes the cohorts from the least aggressive scaling factors. The yellow ellipse includes the KPI results for the baseline parameters for inner and exposed main girders.

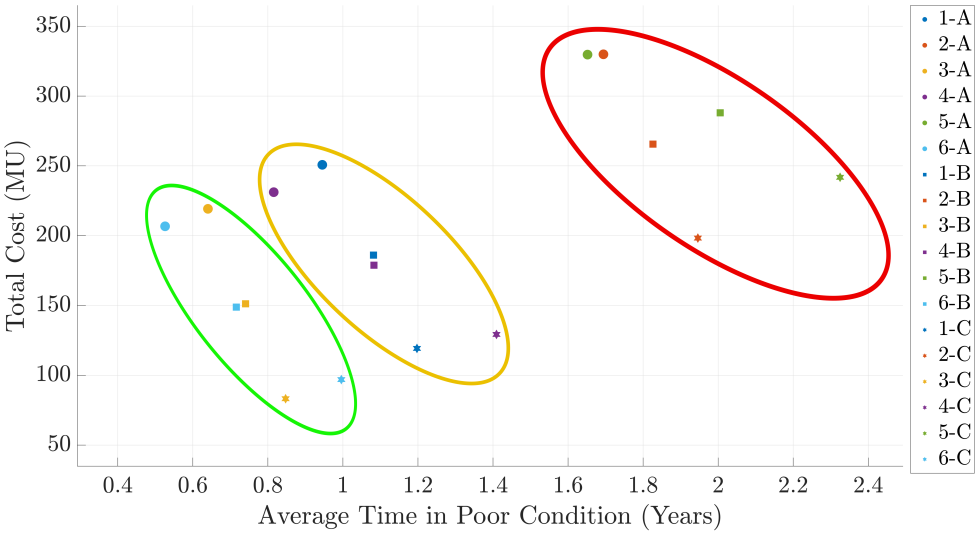

Figure 7.21: Scatter plot of cost and condition KPIs, where $i-j$ denotes the Cohort ID and Strategy ID respectively.

From Figure 7.21, it is observable that both the scaling factors and the maintenance strategy have a great impact on the resultant KPIs. The traditional breakdown of inner and exposed main girders returns a smaller difference in KPIs when compared to the differences between KPIs between the same element type and different deterioration properties. Moreover, for any of the simulated results, for any given strategy, the following expressions hold true,

$$\begin{aligned} \text{Cost}_1 - \text{Cost}_3 &< \text{Cost}_2 - \text{Cost}_1, \\ \text{Cost}_4 - \text{Cost}_6 &< \text{Cost}_5 - \text{Cost}_4, \end{aligned} \tag{7.4.18}$$

$$\begin{aligned} \text{ATPC}_1 - \text{ATPC}_3 &< \text{ATPC}_2 - \text{ATPC}_1, \\ \text{ATPC}_4 - \text{ATPC}_6 &< \text{ATPC}_5 - \text{ATPC}_4, \end{aligned} \tag{7.4.19}$$

where the numeric subscript denotes the cohort identifier.

From (7.4.18), it can be stated that the savings in total cost for the least aggressive cohort compared to the baseline is less than the added expense of the most

aggressive cohort compared to the baseline. Similarly from (7.4.19), the reduction in ATPC for the least aggressive cohort to the baseline is less than the increase in ATPC for the most aggressive cohort compared to the baseline. Such observations have huge importance when allocating resources in a constrained budget scenario.

The difference in cost and ATPC between the least aggressive and baseline cohorts, and the difference between the most aggressive and baseline cohorts were expected not to be equal. Moreover, there are more components that feature in the less aggressive cohort than the most aggressive cohort. Consequently, it would make sense that the values obtained by the least aggressive cohort are closer to the baseline values, as the baseline cohort is ultimately an average result based on the composition of all cohorts, so will be skewed to larger cohorts.

For network level modelling and decision making, having decision support models that incorporate the differences between maintenance strategies is critical, however the incorporation of properties that influence deterioration is no less important. The improved accuracy in the predictive deterioration model would translate to the life cycle analysis model, however the improved accuracy is only one advantage in adopting the deterioration factors, they also enable more informed decision making and strategy development.

An asset manager trying to ascertain the best strategy under a constrained budget scenario will have to consider other factors such as service obligations, criticality of the bridge location on the network and other strategic priorities. For example, if an asset manager was developing a strategy for exposed main girders, a sample of the KPIs that could be considered are shown in Table 7.17. One could compare the percentage improvement in ATPC to the increase in total costs on both an absolute and percentage basis. However, if an asset manager is aware of the service obligations and requires all predicted ATPCs to be below a threshold of 2, then they may select to conserve funds from Cohort 6 by selecting Strategy C for them to be used for Strategy A on Cohort 5 under a constrained budget scenario. This example assumes that the bridges being considered represent the same criticality and strategic importance on the network but the example shows the enhanced versatility in decision support by incorporating deterioration factors.

Table 7.17: KPIs for Cohorts 5 and 6 under Strategies A and C across different administrative regions.

Cohort	Strategy	Total Cost (MU)	ATPC (Years)
5	A	329.7	1.65
5	C	241.8	2.33
6	A	206.7	0.53
6	C	96.9	0.97

7.4.2 Network Level Decision Support

Asset management activities may be coordinated strategically at a network level, however it is common that such activities are operationally managed in smaller administrative regions. For example, Network Rail manage their portfolio as five regions and fourteen routes, see Figure 7.22. The composition of bridges in each region and route will vary, with some regions having a disproportionate amount of assets with aggressive deterioration properties and vice versa. The inclusion of the aforementioned deterioration properties enables a more equitable allocation of resources between regions and routes to better accommodate the local asset management concerns.

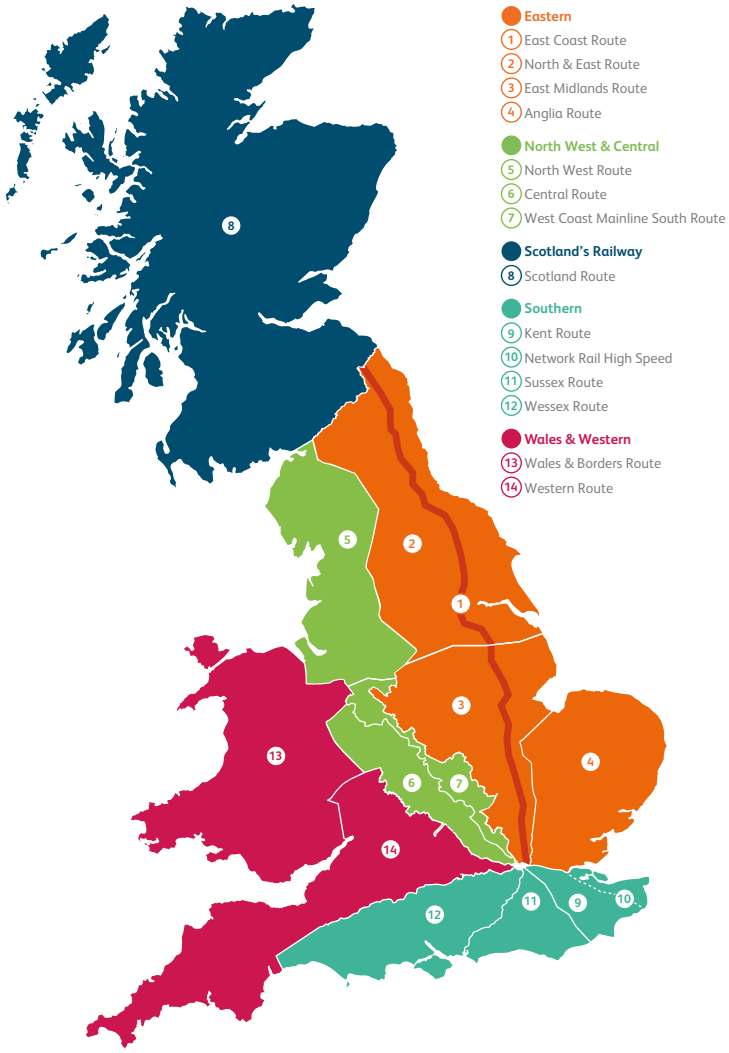

Figure 7.22: Network Rail's routes and regions (Network Rail, 2019a).

As an example, the total costs for maintaining main girders on railway underbridges under strategies A, B and C were calculated for five regions using the costs from model D_e and the costs for the baseline model (Model β_a). The cumulative costs for each region, strategy and model are shown in Figure 7.23.

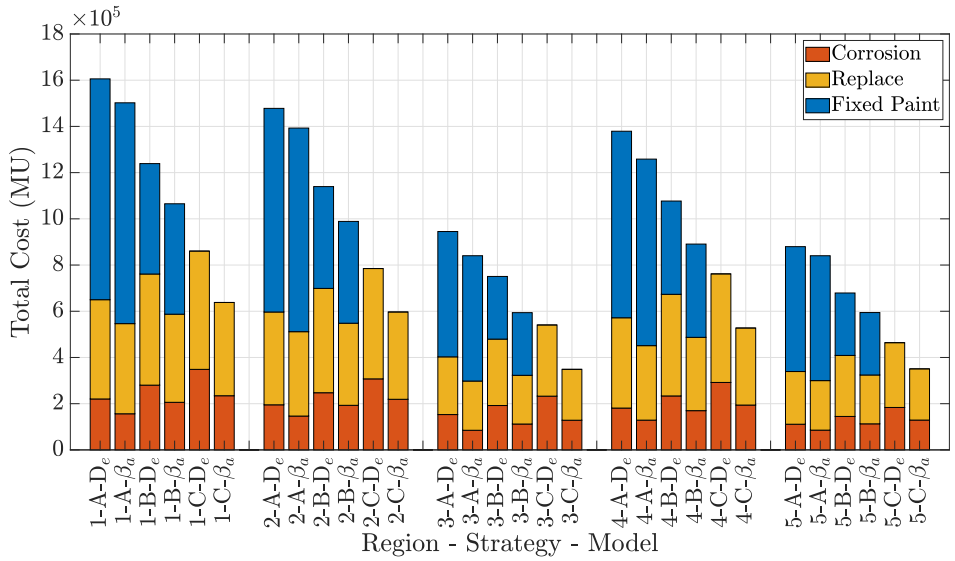

Figure 7.23: Regional costs for main girders on railway underbridges.

It can be observed from Figure 7.23 that the baseline model would underestimate the total cost for all five regions and for all three intervention strategies. However, the percentage of underestimation in total cost varies between the different strategies. For example, model D_e returns a total cost that is on average 7.94% greater than the baseline model for Strategy A but for Strategy C the total cost is on average 39.62% greater, a full breakdown is shown in Table 7.18. This increase can be partly explained by the fact that the majority of Strategy A's total cost is coming from the fixed paintwork renewal. Nonetheless, the inclusion of the local, material and structural properties into the life cycle analysis model can have a large consequence on the predicted total costs and is more reflective of the local needs of particular regions based on their asset composition. The local fluctuation in resource requirements is exhibited in Table 7.18 with the variation in percentage increases in total costs for particular regions under the same strategy.

It is feasible that a region with a large quantity of assets with less aggressive deterioration properties could yield a total cost that is less than what the baseline model would suggest. However, as the cost saving for girders with less aggressive deterioration properties is less than the added expense of assets with more aggressive properties, as shown in Figure 7.21 and (7.4.18), this overestimation in total costs has not been observed for the regional asset breakdowns considered in this study.

Table 7.18: Percentage increase in total costs between models D_e and β_a.

Region	Strategy A	Strategy B	Strategy C
1	6.89	16.32	34.86
2	6.12	15.24	31.50
3	12.47	26.38	55.05
4	9.59	20.91	44.41
5	4.68	14.24	32.29
Average	7.95	18.62	39.62

7.5 Chapter Summary

The study in this chapter analysed deterioration rates for main girders from metallic bridges. An initial set of deterioration rates were calibrated for the traditional cohort breakdown of underbridges/overbridges and inner/exposed main girders using conditions records from the bridge inspection regime on the British railway.

Statistical analysis confirmed that the inclusion of these structural properties increase the accuracy of the multiple defect deterioration model without over-fitting the model due to the additional parameters. Moreover, there was quite a large discrepancy in the mean time to poor condition for an element with 'favourable' properties compared to the elements with 'unfavourable' properties, which is critical when using life cycle analysis to determine intervention strategies.

Existing literature has shown that there are additional properties aside from the aforementioned structural properties that alter the deterioration rates of bridge components. In this study the deterioration factors of coastal proximity, component material type, bridge loading and railway line speed were considered. Commonly, properties that alter deterioration rates are identified by calibrating models by data cohort splitting, however this typically results in the inability of including multiple factors due to data sparsity. This chapter presented a novel approach to incorporate multiple deterioration factors by including the factors on a per defect basis with the

defects also having causal influences. The incorporation of the deterioration factors was shown to provide a statistically significant improvement in model accuracy.

Finally, the enhanced deterioration model with the multiple deterioration factors integrated into a wider asset management PN model to perform a life cycle analysis. The life cycle analysis revealed that the different deterioration factors returned quite diverse values for the considered KPIs of average total time in poor condition and average total cost. Moreover, the incorporation of the deterioration factors in the life cycle analysis enables increased decision support capabilities for asset managers by facilitating targeted intervention strategy development particularly for constrained budget scenarios, and developing equitable resource allocation for different administrative regions.

In future work and in the advent of additional data, additional deterioration properties may be identified and included in the metallic bridge component deterioration model. Moreover, properties may be identified for additional material types.

Chapter 8

Conclusions

8.1 Summary of Work

The successful operation of transportation networks is contingent on the safe performance of bridges. Infrastructure asset managers are tasked with ensuring that bridges assets adhere to the rigorous safety standards with the finite resources available for maintenance, repair and rehabilitation activities across a portfolio of bridges. To maximise the impact of any invested resources decision support tools are commonly employed to facilitate a life cycle analysis.

The purpose of Chapter 2 was to provide an overview of stochastic methodologies that are commonly employed to model bridge deterioration for portfolio decision support and to outline the methods which were used in the remainder of the thesis. The chapter introduced the mathematical formalisms for Markov models, Petri Nets (PN), Bayesian Belief Networks (BBN) and Dynamic Bayesian Networks (DBN). Each methodology has its own set of advantages and limitations, however to determine which methodology is the most appropriate to use, requires a well posed problem and a clear understanding of the limitations of any available data for model calibration.

Chapter 3 presented a literature review of bridge asset management with a particular focus on managing bridges at network level. From the literature it is evident that performance evaluation of bridges is a complex task with Frangopol et al. (2017) stating that bridge managers seek to determine the optimal balance between

structural reliability, risk, utility, sustainability and life-cycle cost. Decision support tools known as Bridge Management Systems (BMS) have found widespread use at transportation agencies across the world, with many governments and stakeholders mandating their expected functionality in statutory codes and regulations. Moreover, the outputs from such decision support tools commonly have a required level of accountability to support any selected decision.

The life cycle modelling capabilities of a BMS are typically derived from two components: a deterioration model and decision model. The deterioration model is used to predict future condition over time under a do-nothing maintenance strategy and a decision model is used to evaluate the effects of different intervention strategies. The capabilities and modelling methodology of a deterioration model is typically dictated by the most appropriate data that is available for model calibration. Appropriate data includes condition records from visual inspections, maintenance records from interventions and experimental measurements from techniques such as non-destructive testing and structural health monitoring. Despite concerns that condition records are vulnerable to subjectivity, they have been found to be the most widely utilised for calibrating deterioration models. The use of condition records for model calibration is acceptable as bridges/components that are found to be in poor condition or unacceptable at inspection are typically prioritised for maintenance intervention. Additionally, for many jurisdictions the recording of condition of at visual inspections is mandated, and thus is an abundant data source for assets across an entire network.

A range of stochastic models that are calibrated using condition records was considered including Markovian models, BBNs, PNs and Artificial Intelligence (AI) models. Each method had its own composition of advantages and disadvantages and offered different predictive capabilities but ultimately the use of each method is commonly driven by the data available for calibration. Chapter 3 concluded that further development of life cycle modelling capabilities for bridges/bridge components requires a holistic problem-based approach. The development of life cycle modelling capabilities is not only driven by the available data, but the development of new capabilities provides justification to reform data collecting procedures in a

continual adaptive process.

An aim of the research was to develop enhanced methodologies for modelling deterioration to support life cycle analysis. Chapter 4 introduced the idea of leveraging a particular format of condition records known as Severity Extent to calibrate a deterioration model that could provide simultaneous predictions for multiple distinct defect mechanisms. The modelling of multiple defect mechanisms for masonry components was found to be reasonably accurate despite instances of mechanisms not being fully revealed at every inspection. For metallic components, the records fully revealed the condition of each considered mechanism at each inspection. The models in this chapter provided insight into the feasibility of modelling bridge condition as a composition of multiple simultaneous processes but also exhibited the importance of revaluating the procedures for recording condition at inspection.

A limitation of the models presented in Chapter 4 was that the models assumed that the distinct defect mechanisms acted independently from each other. However, engineering experience would suggest that mechanisms may interact with other mechanisms such that accelerated deterioration behaviour is observed. Chapter 5 presented models for modelling multiple defect mechanisms simultaneously whilst incorporating the interactions between mechanisms. The interactions between mechanisms were incorporated into the model through causal relationships in a DBN. Chapter 5 again exhibited the importance of revaluating data collection procedures when addressing a research problem. Due to the unrevealed nature of some of the masonry defects at inspection, the model was limited to an analysis of the interactions on a defect absent/present basis. However, the model for metallic components exhibited that with appropriate data the interactions between defect mechanisms could be modelled in a fashion that also encapsulated the extensiveness of defects. Moreover, the inclusion of interactions enabled the assessment of non-constant behaviour which has enormous consequences when evaluating management strategies.

Chapter 6 introduced an approach for life cycle analysis modelling that incorporated the developments of the previous chapters for deterioration modelling. The life cycle analysis model was implemented using the PN framework. Modelling si-

multaneous processes and providing multiple condition indicators is possible using standard PN modelling. However, to include the interactions between mechanisms over the temporal domain, a novel dynamic condition transition was developed. The life cycle model was then applied to a case study which considered a metallic exterior main girder from a railway underbridge and applied different management strategies. Due to the interactions between defect mechanisms being included, the life cycle analysis model has the capability of evaluating the benefits and costs of strategies that favour early interventions.

There are many properties that can alter the expected service life of bridge components and their expected service life can vary by a large amount dependent on these properties. For example, main girders are traditionally broken into cohorts based on whether they are an inner or exposed girder and whether they are a constituent of an underbridge or overbridge. The early parts of Chapter 7 confirm that this traditional cohort breakdown remains statistically significant when modelling deterioration on a multiple defect basis. The later parts of Chapter 7 considered the effects that additional local, material and structural properties may have on deterioration and expected service life. A novel approach for including additional properties into a model simultaneously was presented in this thesis.

There are three modelling methodologies employed in this thesis: Continuous Time Markov Chains (CTMC), DBNs and PNs . The preliminary research in this thesis was performed using CTMCs due to their popularity in literature and their applicability given the limitations of condition data from longitudinal studies. The multiple defect CTMC models presented in Chapter 4 offered insight into the additional data processing and analysis required for modelling deterioration as multiple defects, however, the approach assumed an independence between the defects. The CTMC deterioration model was superseded by the DBN model that is shown in Chapter 5, as the DBN model can incorporate the interactions between the considered defect mechanisms and yields an improved prediction accuracy. A strength of the DBN model is that condition probability profiles can be obtained using an analytical expression, which does not require a great deal of computational expense. The final methodology employed in this thesis was the PN method for simulating a

life cycle model. PNs were selected to perform the life cycle analysis in this thesis, as they offer the capability to model bespoke processes and scenarios, whilst also enabling reproducibility of the model for future analysis.

A contribution of this thesis has been the development of multiple defect models and testing to verify and validate their applicability to support asset investment planning models. However, a reader of this thesis may be left questioning which method should they implement for their own multiple defect modelling. The most appropriate method is dependent on whether an individual is only interested in deterioration modelling or extending the deterioration model to include intervention scenario planning as part of a life cycle analysis. If an individual is only interested in deterioration modelling, under a do-nothing assumption, then the DBN models presented in Chapter 5 are the most appropriate as they have an analytical expression to compute a solution. However, if an individual is interested in the multiple defect approach to condition deterioration modelling as part of a wider life cycle analysis, then PNs should be used. It should be noted that the calibration of the parameters for the CPTs can be yielded from both the DBN and PN models, however, the DBN model is a much more computationally efficient means of calculating the joint probability distributions required for the maximum likelihood calculation.

The stated aim of this research project was to develop enhanced methodologies for modelling the deterioration of bridges, to facilitate enhanced life cycle modelling at network level, which maximises the impact of investments and minimises the safety risk to infrastructure users. The remainder of this chapter will outline the contributions of the research, how the aims and objectives have been satisfied, the limitations of the presented work and what future work is required.

8.2 Research Conclusions

The research featured in this thesis has provided the following contributions to the scientific knowledge:

- **A novel approach of modelling deterioration by accounting for multiple defect mechanisms** - A multiple defect approach for modelling de-

terioration was shown to be accurate for both masonry and metallic bridge components particularly as both material types have their structural integrity reduced by multiple mechanisms. The modelling of multiple defects simultaneously provides additional indicators for decision modelling. A score inference technique was developed to reveal missing condition records from a score panel; however, it is recommended that scores for each mechanism are recorded at every future inspection. The calibration of the model was tied to a memoryless distribution due to the condition records forming a longitudinal study. Although an appropriate method to calibrate deterioration rates using longitudinal data from literature was applied.

- **Identification and parametrisation of the interactions between multiple defect mechanisms** - Whilst modelling deterioration as distinct deterioration mechanisms is useful for forecasting defect prevalence across a portfolio of bridges, for specific bridges the independent modelling of mechanisms is an assumption that is not reflective of the physical phenomena of deterioration. The extensiveness of one defect type could influence the rate of development of another. Models were developed using DBNs to incorporate the interactions between mechanisms. The incorporation of these interactions provides additional predictive accuracy, especially when considering specific instances of components and the status of the defects on a component. Additionally, the incorporation of the interactions of defects enables the non-constant deterioration behaviour to be encapsulated in the model due to deterioration rates of one mechanism being variable to the status of other mechanisms.

- **A novel approach to bridge life cycle modelling that evaluates the effects of strategies that favour early interventions** - This thesis developed a life cycle model that included modelling deterioration with multiple defect mechanisms and the interactions between mechanisms. The life cycle model facilitated the evaluation of management strategies with targeted maintenance interventions on a per-defect basis. The enhanced evaluation of strategies enables a more accurate determination of cost. Additionally, the

evaluation of targeted maintenance interventions enables an asset manager to ascertain the benefits and consequences of intervening earlier (or later) on an element to address particular defects.

- **The inclusion of local, material and structural properties** – Traditionally condition records are broken into cohorts to reflect the different structural properties of a cohort. For main girders this includes whether they are an inner or exposed girder and whether they are a constituent of an underbridge or overbridge. Such cohort analysis was confirmed to still be statistically significant for the multiple defect models. Additional properties that can impact component life cycle were included in the deterioration model by leveraging the multiple defect structure of the model. Properties such as coastal proximity, material type, line speed and annual loading were incorporated into the model and their life cycle effects evaluated. A life cycle analysis revealed that it is critical that such properties are included as their returned values for KPIs such as average time in poor condition and total cost can greatly fluctuate. Moreover, the inclusion of the additional properties facilitates increased decision support capabilities for asset managers by enabling targeted intervention strategy development, particularly for constrained budget scenarios, and developing equitable resource allocations for different administrative regions.

8.3 Limitations and Future Work

Upon consideration of the contributions of this thesis, there have been several areas of limitation and future work identified:

- **Condition recording at inspection** – Whilst models were presented in this thesis for both masonry and metallic bridge components, the modelling capabilities for masonry components were more limited due to the constraints of the available data. When using a condition scale such as Severity Extent, future recording of condition at visual inspections should record all observed instances of defects, ideally using unique identifiers so that the progression of each instance can be tracked.

- **Whole structure modelling** - The deterioration and life cycle models presented in this thesis only considered a bridge component on a railway bridge. However, an asset manager will need such modelling and analysis to be performed for entire structures across a network. The modelling of entire structures could be completed by executing the presented models and aggregating results to match the structural configuration of a bridge, assuming no correlation of deterioration between components. However, there is a clear necessity to consider correlation of deterioration between components on a per-defect basis before proceeding to perform whole structure modelling.

- **Determining an optimal management strategy** - The multiple defect approach provides additional indicators for monitoring bridge component condition. Additionally, the thesis has shown the capabilities of the PN model to ascertain the effects of strategies with different scheduling of interventions. There is scope for further analysis to determine optimal schedules for interventions using optimisation techniques such as GA. However, such work would have most impact when the aforementioned whole structure modelling concerns have been addressed.

- **Precursor event identification** - A typical inspection regime is mandated by a network regulator or other statutory body of the network's jurisdiction. The interval between inspections is usually explicitly stated as a fixed amount of time or is based on the observed condition of the bridge at its most recent inspection. Detailed visual inspections can be quite expensive, sometimes requiring specialist equipment or specially trained inspectors that can abseil. The multiple defect deterioration model could facilitate a risk-based approach to reduce inspection costs by employing preliminary inspections that are less expensive to execute. Section 5.1.4 provided an example into a propagation analysis of condition based off of a drone inspection. However, further analysis is required to identify possible precursor condition events, which could influence the inspection regime, condition recording policies and strategy development without jeopardising the high safety standards instituted by stake-

holders. Additionally, the models presented in this thesis only considered the development of progressive deterioration, however with further analysis the models could incorporate the condition risks of sudden deterioration.

- **Calibrating models from multiple data sources** – The models used to support network level decision making and predict future condition are typically calibrated using one data type, e.g. condition records. The models in this thesis were calibrated using condition records from visual inspections. However, the multiple condition indicators output from the deterioration model are less arbitrary than the traditional single indicator that returns a condition on a scale from 'as-new' to 'very poor' or something similar. Analysis should be performed to compare expected times to poor condition and service life for particular defects using the models calibrated from condition records and from experimental data. Such comparative studies between data sources may also facilitate quantification of the variability of visual inspections which could address the concerns regarding the subjectivity of condition records.

References

AASHTO (1997). Aashto guide for commonly-recognized (core) structural elements. techreport, American Association of State Highway and Transportation Officials, Washington D.C.

AASHTO (2010). Aashto bridge element inspection manual. Technical report, American Association of State Highway and Transportation Officials, Washington D.C.

AASHTOWare (2013). *5.1.3 Official Release - May 2013. https://goo.gl/Jze9Wc.* Last Checked: 27/03/2018.

Abdel-Hameed, M. (1975). A Gamma Wear Process. *IEEE Transactions on Reliability R-24*(2), 152–153.

Agrawal, A., A. Kawaguchi, and Z. Chen (2009). Bridge element deterioration rates. Technical report, New York State DoT, Albany, NY, USA.

Agrawal, A. K., A. Kawaguchi, and Z. Chen (2010). Deterioration Rates of Typical Bridge Elements in New York. *Journal of Bridge Engineering 15*(4), 419–429.

Ajmone Marsan, M. and G. Chiola (1987). On petri nets with deterministic and exponentially distributed firing times. In *Lecture Notes in Computer Science*, Volume 266, pp. 132–145. Springer Verlag.

Akaike, H. (1973). Acute and prophylactic treatment of migraine. In B. N. Petrov and F. Caski (Eds.), *Proceeding of the Second International Symposium on Information Theory*, Budapest, pp. 267–281. Akadémiai Kiadó.

Akaike, H. (1974). A New Look at the Statistical Model Identification. *IEEE Transactions on Automatic Control 19*(6), 716–723.

Al-Mohy, A. H. and N. J. Higham (2009). A New Scaling and Squaring Algorithm for the Matrix Exponential. *SIAM Journal on Matrix Analysis and Applications 31*(3), 970–989.

Albrecht, P. and A. H. Naeemi (1984). *Performance of Weathering Steel in Bridges*.

Amaran, S., N. V. Sahinidis, B. Sharda, and S. J. Bury (2014). Simulation optimization: a review of algorithms and applications. *4OR - A Quarterly Journal of Operations Research 12*(4), 351–380.

Andrews, J. (2013). A modelling approach to railway track asset management. *Proceedings of the Institution of Mechanical Engineers, Part F: Journal of Rail and Rapid Transit 227*(1), 56–73.

Andrews, J. and C. Fecarotti (2017). System design and maintenance modelling for safety in extended life operation. *Reliability Engineering and System Safety 163*, 95–108.

Andrews, J. and T. R. Moss (2002). *Reliability and Risk Assessment*. London and Bury St Edmunds, UK: Professional Engineering Publishing Limited.

Andrews, J., D. Prescott, and F. De Rozières (2014). A stochastic model for railway track asset management. *Reliability Engineering and System Safety 130*, 76–84.

Ang, A. H. and D. De Leon (1997). Determination of optimal target reliabilities for design and upgrading of structures. *Structural Safety 19*(1), 91–103.

Ang, A. H.-S. and W. H. Tang. (2007). *Probability concepts in engineering : emphasis on applications in civil & environmental engineering* (2nd ed.). Hoboken, N.J.: Wiley.

Ang, A.-S. and W. Tang (1984). *Probability concepts in engineering planning and design*. New York: Wiley.

Anraku, K. (1999). An information criterion for parameters under a simple order restriction. *Biometrika 86*(1), 141–152.

ASCE (2017). *ASCE Grand Challenge. www.asce.org/grand-challenge/.* Last Checked: 01/10/2020.

Attoh-Okine, N. O. and S. Bowers (2006). A Bayesian belief network model of bridge deterioration. *Proceedings of the Institution of Civil Engineers (ICE): Bridge Engineering 159*(2), 69–72.

Bayes, T. (1763). An essay towards solving a problem in the doctrine of chances. *Philosophical Transactions of the Royal Society of London 53*, 370–418.

Bellman, R. (1978). *An introduction to artificial intelligence: can computers think?* Boyd & Fraser Publishing Company.

Ben-Akiva, M., F. Humplick, S. Madanat, and R. Ramaswamy (1993). Infrastructure Management under Uncertainty: Latent Performance Approach. *Journal of Transportation Engineering 119*(1), 43–58.

Bentley-Systems (2015). Pontis Release 5.2.1 User's Manual. Technical report, AASHTO Inc., Washington DC.

Berrade, M. D., P. A. Scarf, C. A. Cavalcante, and R. A. Dwight (2013). Imperfect inspection and replacement of a system with a defective state: A cost and reliability analysis. *Reliability Engineering and System Safety 120*, 80–87.

Biondini, F. and D. M. Frangopol (2016). Life-cycle performance of deteriorating structural systems under uncertainty: Review. *Journal of Structural Engineering (United States) 142*(9), 1–17.

Bonet, P. and C. Lladó (2007). PIPE v2. 5: A Petri net tool for performance modelling. *Proc. of 23rd Latin American Conference on Informatics (CLEI 2007)*, 12.

Box, G. (1979). *Robustness in the Strategy of Scientific Model Building.* Academic Press, Inc.

Box, G. E. P. (1976). Science and statistics. *Journal of the American Statistical Association 71*(356), 791–799.

British Standards Institution (2014). BS ISO 55000 Asset Management Standards. Technical report, BSI.

British Standards Institution (2017). ISO 15686-5:2017: Buildings and constructed assets - Service life planning - Part 5: Life-cycle costing.

Brownlow, S. A. and S. R. Watson (1987). Structuring Multi-Attribute Value Hierarchies. *The Journal of the Operational Research Society 38*(4), 309–317.

Brundtland, G. H. (1987). *Our Common Future*. Oxford University Press.

BSI (2012). BS EN ISO 9223 : 2012 BSI Standards Publication Corrosion of metals and alloys — Corrosivity of atmospheres — Classification , determination and estimation. Technical report, British Standards Institution, London, UK.

Bu, G., J. Lee, H. Guan, M. Blumenstein, and Y.-c. Loo (2014). Development of an Integrated Method for Probabilistic. *Journal of Performance of Constructed Facilities 28*(April), 330–340.

Bu, G. P., J. B. Son, J. H. Lee, H. Guan, M. Blumenstein, and Y. C. Loo (2013). Typical deterministic and stochastic bridge deterioration modelling incorporating backward prediction model. *Journal of Civil Structural Health Monitoring 3*(2), 141–152.

Bush, S. J. W., T. F. P. Henning, A. Raith, and J. M. Ingham (2017). Development of a Bridge Deterioration Model in a Data-Constrained Environment. *Journal of Performance of Constructed Facilities 31*(5), 1–8.

Cabinet Office (2019). Public Summary of Sector Security and Resilience Plans. Technical report, The Cabinet Office, London, UK.

Callow, D., J. Lee, M. Blumenstein, H. Guan, and Y. C. Loo (2013). Development of hybrid optimisation method for Artificial Intelligence based bridge deterioration model - Feasibility study. *Automation in Construction 31*, 83–91.

Cattan, J. and J. Mohammadi (1997). Analysis of bridge condition rating data using neural networks. *Microcomputers in Civil Engineering 12*(6), 419–429.

CEN (2010). En 1990:2002+a1:2005 - eurocode - basis of structural design. Technical report.

Ceravolo, R., M. Pescatore, and A. De Stefano (2009). Symptom-based reliability and generalized repairing cost in monitored bridges. *Reliability Engineering and System Safety 94*(8), 1331–1339.

Cesare, M. A., C. Santamarina, C. Turkstra, and E. H. Vanmarcke (1992). Modeling bridge deterioration with Markov chains. *Journal of Transportation Engineering 118*(6), 820–833.

Cha, Y. J., W. Choi, and O. Büyüköztürk (2017). Deep Learning-Based Crack Damage Detection Using Convolutional Neural Networks. *Computer-Aided Civil and Infrastructure Engineering 32*(5), 361–378.

Chen, L., T. F. Henning, A. Raith, and A. Y. Shamseldin (2015). Multiobjective optimization for maintenance decision making in infrastructure asset management. *Journal of Management in Engineering 31*(6), 1–9.

Chew, S. P., S. J. Dunnett, and J. D. Andrews (2008). Phased mission modelling of systems with maintenance-free operating periods using simulated Petri nets. *Reliability Engineering and System Safety 93*(7), 980–994.

Ching, W.-K., X. Huang, M. K. Ng, and T.-K. Siu (2013). *Markov Chains: Models, Algorithms and Applications* (2nd ed.). Springer.

Chojaczyk, A. A., A. P. Teixeira, L. C. Neves, J. B. Cardoso, and C. Guedes Soares (2015). Review and application of Artificial Neural Networks models in reliability analysis of steel structures. *Structural Safety 52*(Part A), 78–89.

Conn, A. R., K. Scheinberg, and L. N. Vicente (2009). *Introduction to Derivative-Free Optimization* (1st ed.). Philadelphia, PA: Society for Industrial and Applied Mathematics.

Cooke, R. M. (1991). *Experts in Uncertainty: Opinion and Subjective Probability in Science*. Environmental Ethics and Science Policy. Oxford University Press.

Dagum, P. and A. Galper (1995). Time series prediction using belief network models.

Dagum, P., A. Galper, and E. Horvitz (1992). Dynamic Network Models for Forecasting. In *Proceedings of the Eighth Conference on Uncertainty in Artificial Intelligence*, Stanford, CA, pp. 41–48.

Darwin, C. (1859). *On the Origin of Species by Means of Natural Selection, or the Preservation of Favoured Races in the Struggle for Life*. London, UK.

Dean, S. W. (2001). Natural Atmospheres: Corrosion. In *Encyclopedia of Materials: Science and Technology* (2nd ed.)., pp. 5930–5938. Elsevier.

Dean, T. and K. Kanazawa (1989). A model for reasoning about persistence and causation. *Computational Intelligence 5*(2), 142–150.

Decò, A., P. Bocchini, and D. M. Frangopol (2013). A probabilistic approach for the prediction of seismic resilience of bridges. *Earthquake Engineering and Structural Dynamics 42*, 1469–1487.

Decò, A. and D. M. Frangopol (2011). Risk assessment of highway bridges under multiple hazards. *Journal of Risk Research 14*(9), 1057–1089.

Dempster, A. P., N. M. Laird, and D. B. Rubin (1977). Maximum Likelihood from Incomplete Data Via the EM Algorithm. *Journal of the Royal Statistical Society: Series B (Methodological) 39*(1), 1–22.

Department of Homeland Security (2013). NIPP 2013: Partnering for Critical Infrastructure Security and Resilience. Technical report, Department of Homeland Security.

DeStefano, P. D. and D. A. Grivas (1998). Method for estimating transition probability in bridge deterioration models. *Journal of Infrastructure Systems 4*(2), 56–62.

Dingle, N. J. and W. J. Knottenbelt (2009). PIPE2 : A Tool for the Performance Evaluation of Generalised Stochastic Petri Nets. *ACM SIGMETRICS Performance Evaluation review 36*(4), 34–39.

Dobbs, R., H. Pohl, D.-Y. Lin, J. Mischke, N. Garemo, J. Hexter, S. Matzinger, R. Palter, and R. Nanavatty (2013). Infrastructure productivity: how to save $1 trillion a year. *McKinsey Global Institute*.

Dong, Y. and D. M. Frangopol (2016). Performance-based seismic assessment of conventional and base- isolated steel buildings including environmental impact and resilience. *Earthquake Engineering and Structural Dynamics 45*, 739–756.

Dong, Y., D. M. Frangopol, and S. Sabatino (2015). Optimizing bridge network retrofit planning based on cost-benefit evaluation and multi-attribute utility associated with sustainability. *Earthquake Spectra 31*(4), 2255–2280.

Dong, Y., D. M. Frangopol, and D. Saydam (2014). Sustainability of highway bridge networks under seismic hazard. *Journal of Earthquake Engineering 18*(1), 41–66.

Duffy, L. (2004). Development of Eirspan: Ireland's Bridge Management System. *Proceedings of the ICE - Bridge Engineering 157*(3), 139–146.

Dugan, J. B., K. S. Trivedi, R. M. Geist, and V. F. Nicola (1985). Extended stochastic petri nets: Applications and analysis. In *Performance '84 Proceedings of the Tenth International Symposium on Computer Performance Modelling, Measurement and Evaluation*, pp. 507–519. North-Holland.

Dunn, W. L. and J. K. Shultis (2011). *Exploring Monte Carlo Methods*. Elsevier Science.

Ellingwood, B. R. (2001). Acceptable risk bases for design of structures. *Progress in Structural Engineering and Materials 3*(2), 170–179.

Ellingwood, B. R. (2005). Risk-informed condition assessment of civil infrastructure: state of practice and research issues. *Structure and Infrastructure Engineering 1*(1), 7–18.

Ellingwood, B. R. and D. M. Frangopol (2016). Introduction to the state of the art collection: Risk-based lifecycle performance of structural systems. *Journal of Structural Engineering 142*(9).

Elmasry, M., A. Hawari, and T. Zayed (2017). Defect based deterioration model for sewer pipelines using Bayesian belief networks. *Canadian Journal of Civil Engineering 44*(9), 675–690.

Enright, M. P. and D. M. Frangopol (1999). Condition Prediction of Deteriorating Concrete Bridges using Bayesian Updating. *J. Struct. Eng. 125*(10), 1118–1125.

Estes, A. C. and D. M. Frangopol (1999). Repair Optimization of Highway Bridges Using System Reliability Approach. *Journal of Structural Engineering 125*(7), 766–775.

Everett, T. D., P. Weykamp, H. A. Capers, W. R. Cox, T. S. Drda, L. Hummel, P. Jensen, D. A. Juntunen, T. Kimball, and G. A. Washer (2008). Bridge Evaluation Quality Assurance in Europe. Technical report, Federal Highway Administration, U.S. Department of Transportation, Washington D.C.

Fenton, N. and M. Neil (2013). *Risk Assessment and Decision Analysis with Bayesian Networks*. CRC Press.

Ferreira, C., L. Neves, A. Silva, and J. de Brito (2018). Stochastic Petri net-based modelling of the durability of renderings. *Automation in Construction 87*, 96–105.

FHWA (1987). Bridge management systems. techreport Demonstration Project No. 71, Federal Highway Administration, Washington D.C.

FHWA (1995). Recording and Coding Guide for the Structure Inventory and Appraisal of the Nation's Bridges.

Fiorillo, G. and H. Nassif (2019). Application of Machine Learning Techniques for the Analysis of National Bridge Inventory and Bridge Element Data. *Transportation Research Record 2673*(7), 99–110.

Fiorillo, G. and H. Nassif (2020a). Development of a Risk Assessment Module for Bridge Management Systems in New Jersey. *Transportation Research Record*.

Fiorillo, G. and H. Nassif (2020b). Improving the conversion accuracy between bridge element conditions and NBI ratings using deep convolution neural networks. *Structure and Infrastructure Engineering 16*(12).

Flaig, K. and R. Lark (2000). The development of UK bridge management systems. *Proceedings of the ICE -Transport 141*(2), 99–106.

Foulliaron, J., L. Bouillaut, A. Barros, and P. Aknin (2015). Dynamic Bayesian Networks for reliability analysis: From a Markovian point of view to semi-Markovian approaches. *IFAC-PapersOnLine 28*(21), 694–700.

Frangopol, D. M. (2011). Life-Cycle performance, management, and optimisation of structural systems under uncertainty: Accomplishments and challenges. *Structure and Infrastructure Engineering 7*(6), 389–413.

Frangopol, D. M. and P. Bocchini (2012). Bridge network performance, maintenance and optimisation under uncertainty: Accomplishments and challenges. *Structure and Infrastructure Engineering 8*(4), 341–356.

Frangopol, D. M., Y. Dong, and S. Sabatino (2017). Bridge life-cycle performance and cost: analysis, prediction, optimisation and decision-making. *Structure and Infrastructure Engineering 13*(10), 1239–1257.

Frangopol, D. M., M.-J. Kallen, and J. M. van Noortwijk (2004). Probabilistic models for life-cycle performance of deteriorating structures: review and future directions. *Progress in Structural Engineering and Materials 6*(4), 197–212.

Frangopol, D. M., K.-Y. Lin, and A. C. Estes (1997). Life-Cycle Cost Design of Deteriorating Structures. *Journal of Structural Engineering 123*(10), 1390–1401.

Frangopol, D. M. and M. Liu (2007). Maintenance and management of civil infrastructure based on condition, safety, optimization, and life-cycle cost. *Structure and Infrastructure Engineering 3*(1), 29–41.

Frangopol, D. M. and T. B. Messervey (2007). Integrated life-cycle health monitoring, maintenance, management and cost of civil infrastructure. (May 16-18, 2007).

Frangopol, D. M., A. Strauss, and S. Kim (2008). Use of monitoring extreme data for the performance prediction of structures: General approach. *Engineering Structures 30*(12), 3644–3653.

Frankel, E. (1988). *Systems Reliability and Risk Analysis* (2nd ed.). Kluwer Academic Publishers.

Freytag, T. and M. Sänger (2014). WoPeD - An educational tool for workflow nets. *CEUR Workshop Proceedings 1295*, 31–35.

Fu, G. and D. Devaraj (2008). Methodology of homogeneous and non-homogeneous markov chains for modelling bridge element deterioration: Final report to michigan dot. Technical report, Wayne State University.

Galvanizers Association (2020). Corrosion Map.

Ghosn, M., L. Dueñas-Osorio, D. M. Frangopol, T. P. McAllister, P. Bocchini, L. Manuel, B. R. Ellingwood, S. Arangio, F. Bontempi, M. Shah, M. Akiyama, F. Biondini, S. Hernandez, and G. Tsiatas (2016). Performance indicators for structural systems and infrastructure networks. *Journal of Structural Engineering 142*(9), 1–18.

Ghosn, M., D. M. Frangopol, T. P. McAllister, M. Shah, S. M. Diniz, B. R. Ellingwood, L. Manuel, F. Biondini, N. Catbas, A. Strauss, and X. L. Zhao (2016). Reliability-based performance indicators for structural members. *Journal of Structural Engineering 142*(9), 1–13.

Ghosn, M. and F. Moses (1986). Reliability calibration of bridge design code. *Journal of Structural Engineering 112*(4), 745–763.

Glaser, S. D., M. Li, M. L. Wang, J. Ou, and J. Lynch (2007). Sensor technology innovation for the advancement of structural health monitoring: A strategic

program of US-China research for the next decade. *Smart Structures and Systems 3*(2), 221–244.

Golabi, K., R. B. Kulkarni, and G. B. Way (1982). A Statewide Pavement Management System. *Interfaces 12*(6), 5–21.

Golabi, K. and R. Shepard (1997). Pontis: A system for maintenance optimization and improvement of US bridge networks. *Interfaces 27*(1), 71–88.

Goldberg, D. E. (1989). *Genetic algorithms in search, optimization and machine learning*. Addison-Wesley Publishing.

Goodfellow-Smith, M. E., C. D. F. Rogers, and M. R. Tight (2020a). Infrastructure Value Maximisation: Finance and Insurance Appraisal. *Infrastructure Asset Management 7*(2), 103–110.

Goodfellow-Smith, M. E., C. D. F. Rogers, and M. R. Tight (2020b). Infrastructure Value Maximisation: Overcoming the Valley of Death for Sustainable Infrastructure. *Infrastructure Asset Management 7*(2), 95–102.

Grinstead, C. M. and J. L. Snell (1997). *Introduction to probability*. American Mathematical Society.

Guo, H.-Y., Y. Dong, and X.-L. Gu (2020). Two-step translation method for time-dependent reliability of structures subject to both continuous deterioration and sudden events. *Engineering Structures 225*, 111291.

Harmon, K. M. (2003). Conflicts between owner and contractors: Proposed intervention process. *Journal of Management in Engineering 19*(3), 121–125.

Hauck, M., C. Giezen, S. C. Calvert, E. E. Keijzer, S. E. de Vos-Effting, D. van Vliet, and J. Voskuilen (2017). Economic, environmental and social cost-benefit analysis of road construction works. In *Life-Cycle of Engineering Systems: Emphasis on Sustainable Civil Infrastructure - 5th International Symposium on Life-Cycle Engineering, IALCCE 2016*, pp. 901–906.

Hawk, H. (1999). BRIDGIT: User-friendly approach to bridge management. *TRB Transportation Research Circular 498*, 1–15.

Hawk, H. and E. P. Small (1998). The BRIDGIT Bridge Management System. *Structural Engineering International 8*(4), 309–314.

Health and Safety Executive (2001). *Reducing risks, protecting people*. HSE Books.

Hearn, G., J. Puckett, I. Friedland, T. Everett, K. Hurst, G. Romack, G. Christian, R. Shepard, T. Thompson, and R. Young (2005). Bridge preservation and maintenance in Europe and South Africa. Technical report, Federal Highway Adminstration, U.S. Department of Transport, Washington D.C.

Heath, B., R. Hill, and F. Ciarallo (2009). A survey of agent-based modeling practices (January 1998 to July 2008). *Journal of Artificial Societies and Social Simulation 12*(4).

Heusler, K. E., D. Landolt, and S. Trasatti (1989). Electrochemical corrosion nomenclature. *Pure and Applied Chemistry 61*(1), 19–22.

Higham, N. J. (2005). The Scaling and Squaring Method for the Matrix Exponential Revisited. *SIAM Journal on Matrix Analysis and Applications 26*(4), 1179–1193.

Highways Agency (2007a). *Inspection Manual for Highway Structures*, Volume 1: Reference Manual. The Stationary Office.

Highways Agency (2007b). *Inspection Manual for Highway Structures*, Volume 2: Inspector's Handbook. The Stationary Office.

Holland, J. H. (1975). *Adaptation in natural and artificial systems.* Ann Arbor, MI: University of Michigan Press.

Hopcroft, J. E. and J. D. Ullman (1969). *Formal Languages and their relation to automata*. Addison-Wesley Series in Computer Science and Information Processing. Addison-Wesley Publishing.

Hossain, N. U. I., F. Nur, S. Hosseini, R. Jaradat, M. Marufuzzaman, and S. M. Puryear (2019). A Bayesian network based approach for modeling and assessing

resilience: A case study of a full service deep water port. *Reliability Engineering and System Safety 189*(April), 378–396.

Howard, R. A. (1971). *Dynamic Probabilistic Systems, Volume II: SemiMarkov and Decision Processes*. New York: John Wiley & Sons.

Huang, R. Y., I. S. Mao, and H. K. Lee (2010). Exploring the deterioration factors of RC bridge decks: A rough set approach. *Computer-Aided Civil and Infrastructure Engineering 25*(7), 517–529.

Huang, Y. H. (2010). Artificial neural network model of bridge deterioration. *Journal of Performance of Constructed Facilities 24*(6), 597–602.

Hutchins, J. S. and M. McKenzie (1973). Characterisation of bridge locations by corrosion and environmental measurements - first year results. Technical report, Transport and Road Research Laboratory, Crowthorne, Berkshire.

Imam, B. M. and M. K. Chryssanthopoulos (2012). Causes and consequences of metallic bridge failures. *Structural Engineering International 22*(1), 93–98.

Institute of Civil Engineers (2018). State of the Nation 2018: Infrastructure Investment. Technical report.

International Organization for Standardization (2015). Iso 2394:2015 - general principles on reliability for structures. Technical report.

ISO/IEC (2010). BS ISO/IEC 15909-1:2004+A1:2010 Systems and software engineering - High-level Petri nets, Part 1: Concepts, definitions and graphical notation. Technical report, British Standards.

ISO/IEC (2011). BS ISO/IEC 15909-2:2011 Systems and software engineering - High-level Petri nets, Part 2: Transfer format. Technical report, British Standards.

Jacinto, L., L. C. Neves, and L. O. Santos (2016). Bayesian assessment of an existing bridge: a case study. *Structure and Infrastructure Engineering 12*(1), 61–77.

Jackson, C. H. (2011). Multistate models for panel data: The msm Package for R. *Journal Of Statistical Software 38*(8).

JCSS (2001). Probabilistic model code. Technical report.

Jensen, F. V. (2001). *Bayesian networks and decision graphs*. New York: Springer.

Jensen, K. (1997). *Coloured Petri Nets* (2nd ed.). Springer Verlag.

Jensen, K. and L. M. Krietensen (2009). *Coloured Petri Nets: Modelling and Validation of Concurrent Systems*. Springer.

Jensen, K., L. M. Kristensen, and L. Wells (2007). Coloured Petri Nets and CPN Tools for modelling and validation of concurrent systems. *International Journal on Software Tools for Technology Transfer 9*(3-4), 213–254.

Jiang, Y., M. Saito, and K. C. Sinha (1988). Bridge Performance Prediction Model Using the Markov chain. *Transportation Research Record 1180*(1), 25–32.

Jiang, Y. and K. C. Sinha (1989). Bridge Service Life Prediction Model Using the Markov Chain. *Transportation Research Record 1223*, 24–30.

Jiménez, A., S. Ríos-Insua, and A. Mateos (2003). A decision support system for multiattribute utility evaluation based on imprecise assignments. *Decision Support Systems 36*(1), 65–79.

Kabir, S. and Y. Papadopoulos (2019). Applications of Bayesian networks and Petri nets in safety, reliability, and risk assessments: A review. *Safety Science 115*(February), 154–175.

Kalbfleisch, J. D. and J. F. Lawless (1985). The Analysis of Panel Data Under a Markov Assumption. *Journal of the American Statistical Association 80*(392), 863–871.

Kallen, M. J. (2007). *Markov processes for maintenance optimization of civil infrastructure in the Netherlands*. Ph. D. thesis, Delft University of Technology.

Kallen, M. J. and J. M. V. Noortwijk (2006). Statistical inference for Markov deterioration models of bridge conditions in the Netherlands. In *Third International Conference on Bridge Maintenance, Safety and Management (IABMAS)*, pp. 535–536.

Kallias, A. N., B. Imam, and M. K. Chryssanthopoulos (2017). Performance profiles of metallic bridges subject to coating degradation and atmospheric corrosion. *Structure and Infrastructure Engineering 13*(4), 440–453.

Kalman, R. E. (1960). A new approach to linear filtering and prediction problems. *Journal of Basic Engineering 82*(1), 35–45.

Kalyviotis, N., C. D. F. Rogers, M. R. Tight, G. J. Hewings, and H. Doloi (2020). Defining the Social Value of Transport Infrastructure. *Infrastructure Asset Management 7*(2), 111–119.

Kammouh, O., P. Gardoni, and G. P. Cimellaro (2020). Probabilistic framework to evaluate the resilience of engineering systems using Bayesian and dynamic Bayesian networks. *Reliability Engineering and System Safety 198*, 106813.

Kayser, J. R. and A. S. Nowak (1989a). Capacity loss due to corrosion in steel-girder bridges. *Journal of Structural Engineering (United States) 115*(6), 1525–1537.

Kayser, J. R. and A. S. Nowak (1989b). Reliability of corroded steel girder bridges. *Structural Safety 6*(1), 53–63.

Kendall, A., G. A. Keoleian, and G. E. Helfand (2008). Integrated Life-Cycle Assessment and Life-Cycle Cost Analysis Model for Concrete Bridge Deck Applications. *Journal of Infrastructure Systems 14*(3), 214–222.

Kennedy, J. and R. Eberhart (1995). Particle Swarm Optimization. In *Proceedings of the IEEE International Conference on Neural Networks*, pp. 1942–1948.

Kilsby, P., R. Remenyte-Prescott, and J. Andrews (2017). A modelling approach for railway overhead line equipment asset management. *Reliability Engineering and System Safety 168*(February), 326–337.

Kilsby, P., R. Remenyte-Prescott, and J. Andrews (2018). A Petri Net-based life cycle cost analysis approach. *Proceedings of the Institution of Mechanical Engineers, Part F: Journal of Rail and Rapid Transit 0*(0), 1–13.

Kleiner, Y. (2001). Scheduling Inspection and Renewal of Large Infrastructure Assets. *Journal of Infrastructure Systems 7*(4), 136–143.

Komp, M. E. (1987). Atmospheric corrosion ratings of weathering steels - Calculations and significance. *Materials Performance 26*(7), 42–44.

Kosgodagan-Dalla Torre, A., T. G. Yeung, O. Morales-Nápoles, B. Castanier, J. Maljaars, and W. Courage (2017). A Two-Dimension Dynamic Bayesian Network for Large-Scale Degradation Modeling with an Application to a Bridges Network. *Computer-Aided Civil and Infrastructure Engineering 32*(8), 641–656.

Kroese, D., T. Taimre, and Z. Botev (2011). *Handbook of Monte Carlo Methods*. Wiley.

Kroese, D. P., T. Brereton, T. Taimre, and Z. I. Botev (2014). Why the Monte Carlo method is so important today. *Wiley Interdisciplinary Reviews: Computational Statistics 6*(6), 386–392.

Kuhn, K. D. and S. M. Madanat (2005). Model uncertainty and the management of a system of infrastructure facilities. *Transportation Research Part C: Emerging Technologies 13*(5-6), 391–404.

Kuiper, R. M., H. Hoijtink, and M. J. Silvapulle (2011). An Akaike-type information criterion for model selection under inequality constraints. *Biometrika 98*(2), 495–501.

Langseth, H. and L. Portinale (2007). Bayesian networks in reliability. *Reliability Engineering and System Safety 92*(1), 92–108.

Lauridsen, J. and B. Lassen (1999). The Danish bridge management system DANBRO. In P. C. Das (Ed.), *Management of highway structures*, pp. 61–70. London: Thomas Telford.

Le, B. and J. Andrews (2013). Modelling railway bridge asset management. *Proceedings of the Institution of Mechanical Engineers, Part F: Journal of Rail and Rapid Transit 227*(6), 644–656.

Le, B. and J. Andrews (2015). Modelling railway bridge degradation based on historical maintenance data. *The Journal of the Safety and Reliability Society 35*(2), 32–55.

Le, B. and J. Andrews (2016). Petri net modelling of bridge asset management using maintenance-related state conditions. *Structure and Infrastructure Engineering 12*(6), 730–751.

Le, B., J. Andrews, and C. Fecarotti (2017). A Petri net model for railway bridge maintenance. *Proceedings of the Institution of Mechanical Engineers Part O: Journal of Risk and Reliability 231*(3), 306–323.

Le, B. L. H. (2014). *Modelling Railway Bridge Asset Management*. Ph. D. thesis, University of Nottingham.

LeBeau, K. and S. Wadia-Fascetti (2010). Predictive and diagnostic load rating model of a prestressed concrete bridge. *Journal of Bridge Engineering 15*(4), 399–407.

LeBeau, K. H. and S. J. Wadia-Fascetti (2000). A fault tree model of bridge deterioration. In *8th ASCE Speciality Conference on Probabilistic mechanics and structural reliability*, University of Notre Dame.

LeCun, Y., Y. Bengio, and G. Hinton (2015). Deep learning. *Nature 521*(7553), 436–444.

Lee, J., K. Sanmugarasa, M. Blumenstein, and Y. C. Loo (2008). Improving the reliability of a Bridge Management System (BMS) using an ANN-based Backward Prediction Model (BPM). *Automation in Construction 17*(6), 758–772.

Leemis, L. M. (1995). *Reliability, probabilistic models and statistical methods*. Prentice-Hall.

Li, L., A. A. F. Saldivar, Y. Bai, Y. Chen, Q. Liu, and Y. Li (2019). Benchmarks for Evaluating Optimization Algorithms and Benchmarking MATLAB Derivative-Free Optimizers for Practitioners' Rapid Access. *IEEE Access 7*, 79657–79670.

Li, Z. (2019). *Transportation Asset Management*. Boca Raton, Florida: CRC Press.

Limnios, N. and G. Oprisan (2001). *Semi-Markov processes and reliability*. Statistics for industry and technology. Boston: Birkhauser.

Litherland, J., G. Calvert, J. Andrews, and A. Kirwan (2019). Development of an Extended RAMS Framework for Railway Networks. In M. B. Beer and E. Zio (Eds.), *Proceedings of the 29th European Safety and Reliability Conference*, pp. 3489–3496. Research Publishing, Singapore.

Liu, H. and Y. Zhang (2020). Bridge condition rating data modeling using deep learning algorithm. *Structure and Infrastructure Engineering 16*(10), 1447–1460.

Liu, M. and D. M. Frangopol (2006). Probability-Based Bridge Network Performance Evaluation. *Journal of Bridge Engineering 11*(5), 633–641.

Liu, M., D. M. Frangopol, and S. Kim (2009a). Bridge safety evaluation based on monitored live load effects. *Journal of Bridge Engineering 14*(4), 257–269.

Liu, M., D. M. Frangopol, and S. Kim (2009b). Bridge system performance assessment from structural health monitoring: A case study. *Journal of Structural Engineering 135*(6), 733–742.

Lounis, Z. and T. P. McAllister (2016). Risk-based decision making for sustainable and resilient infrastructure systems. *Journal of Structural Engineering 142*(9), 1–14.

Lundie, S., G. M. Peters, and P. C. Beavis (2004). Life cycle assessment for sustainable metropolitan water systems planning. *Environmental Science and Technology 38*(13), 3465–3473.

Luque, J. and D. Straub (2016). Reliability analysis and updating of deteriorating systems with dynamic Bayesian networks. *Structural Safety 62*, 34–46.

Luque, J. and D. Straub (2019). Risk-based optimal inspection strategies for structural systems using dynamic Bayesian networks. *Structural Safety 76*(August 2018), 68–80.

MacKay, R. J. and R. W. Oldford (2000). Scientific method, statistical method and the speed of light. *Statistical Science 15*(3), 254–278.

Madanat, S. (1993). Optimal infrastructure management decisions under uncertainty. *Transportation Research Part C: Emerging Technologies 1*(1), 77–88.

Marquez, D., M. Neil, and N. Fenton (2010). Improved reliability modeling using Bayesian networks and dynamic discretization. *Reliability Engineering and System Safety 95*(4), 412–425.

Marsan, M. A., G. Conte, and G. Balbo (1984). A class of generalized stochastic Petri nets for the performance evaluation of multiprocessor systems. *ACM Transactions on Computer Systems 2*(2), 93–122.

Martinez, P., E. Mohamed, O. Mohsen, and Y. Mohamed (2020). Comparative Study of Data Mining Models for Prediction of Bridge Future Conditions. *Journal of Performance of Constructed Facilities 34*(1), 1–9.

Mašović, S. and R. Hajdin (2014). Modelling of bridge elements deterioration for Serbian bridge inventory. *Structure and Infrastructure Engineering 10*(8), 976–987.

Matos, J. C., P. J. Cruz, I. B. Valente, L. C. Neves, and V. N. Moreira (2016). An innovative framework for probabilistic-based structural assessment with an application to existing reinforced concrete structures. *Engineering Structures 111*, 552–564.

McKibbens, L. D., C. M. N. Sawar, and C. S. Gaillard (2006). Masonry arch bridges: condition, appraisal and remedial treatment. Technical report, CIRIA, London, UK.

Melchers, R. E. and A. T. Beck (2018). *Structural Reliability Analysis and Prediction* (3rd ed.). Hoboken, N.J.: Wiley.

Middleton, C. (2004). Bridge Management and Assessment in the UK. In *5th Austroads Bridge Conference*.

Mirzaei, Z., B. T. Adey, L. Klatter, and J. S. Kong (2012). The IABMAS Bridge Managment Committee - Overview of Existing Bridge Management Systems 2012. Technical report, IABMAS.

Mirzaei, Z., B. T. Adey, L. Klatter, and P. D. Thompson (2014). The IABMAS Bridge Managment Committee - Overview of Existing Bridge Management Systems 2014. Technical report, IABMAS.

Mishalani, R. G. and S. M. Madanat (2002). Computation of Infrastructure Transition Probabilities Using Stochastic Duration Models. *Journal of Infrastructure Systems 8*(4), 139–148.

Moler, C. (1986). Matrix Computation on Distributed Memory Multiprocessors. In M. T. Heath (Ed.), *Hypercube Multiprocessors*. Philadelphia, PA: Society for Industrial and Applied Mathematics.

Moler, C. and C. Van Loan (2003). Nineteen Dubious Ways to Compute the Exponential of a Matrix, Twenty-Five Years Later. *SIAM Review 45*(1), 3–49.

Molloy, M. (1982). Performance Analysis Using Stochastic Petri Nets. *IEEE Transactions on Computers C-31*(9), 913–917.

Moore, M., B. Phares, B. Graybeal, D. Rolander, and G. Washer (2001). Reliability of visual inspection for highway bridges, volume i: Final report. Technical Report FHW A-RD-01-020, Federal Highway Administration.

Moradi, R. and K. M. Groth (2020). Modernizing risk assessment: A systematic integration of PRA and PHM techniques. *Reliability Engineering and System Safety 204*, 107194.

Moran, P. (1954). A probability theory of dams and storage systems. *Australian Journal of Applied Science 5*(2), 119–124.

Morcous, G. (2006). Performance Prediction of Bridge Deck Systems Using Markov Chains. *Journal of Performance of Constructed Facilities 20*(2), 146–155.

Morcous, G. and Z. Lounis (2006). Integration of stochastic deterioration models with multicriteria decision theory for optimizing maintenance of bridge decks. *Canadian Journal of Civil Engineering 33*(6), 756–765.

Morcous, G., H. Rivard, and A. M. Hanna (2002a). Case-based reasoning system for modeling infrastructure deterioration. *Journal of Computing in Civil Engineering 16*(2), 104–114.

Morcous, G., H. Rivard, and A. M. Hanna (2002b). Modeling Bridge Deterioration Using Case-based Reasoning. *Journal of Infrastructure Systems 8*(3), 86–95.

Murata, T. (1989). Petri Nets: Properties, Analysis and Applications. *Proceedings of the IEEE 77*(4), 541–580.

Murphy, K. P. (2002). *Dynamic Bayesian Networks: Representation, Inference and Learning*. Ph. D. thesis, University of California, Berkeley.

Nathwani, J., N. Lind, and M. Pandey (1997). *Affordable Safety By Choice: Affordable Safety By Choice*.

National Oceanic and Atmospheric Administration (NOAA) (2015). Global Self-consistent, Hierarchical, High-resolution Geography Database (GSHHG).

Naybour, S., J. Andrews, and M. Chiachio-Ruano (2019). Efficient Risk Based Optimization of Large System Models using a Reduced Petri Net Methodology. *Proceedings of the 29th European Safety and Reliability Conference*.

Network Rail (2006). The structural assessment of underbridges. Technical Report NR/GN/CIV/025, Network Rail, London, UK.

Network Rail (2010). Handbook for the examination of structures part 2c: Condition marking of bridges. Technical Report NR/L3/CIV/006/1C, Network Rail.

Network Rail (2011). Categorisation of track. Technical Report NR/L1/TRK/002, Network Rail.

Network Rail (2014a). Handbook for the examination of structures - part 1c: Determining the examination regime. Technical Report NR/L3/CIV/006/1C, Network Rail.

Network Rail (2014b). Structures Asset Policy (BCAM-TP-0165). Technical Report Issue 1.1, Network Rail.

Network Rail (2017). Handbook for the examination of structures. Technical Report NR/L3/CIV/006, Network Rail.

Network Rail (2018). Asset management policy. Technical report, Network Rail.

Network Rail (2019a). Annual report and accounts 2019. Technical report, Network Rail.

Network Rail (2019b). BCMI, CARRS and UGMS datasets.

Neumann, T., B. Dutschk, and R. Schenkendorf (2019). Analyzing uncertainties in model response using the point estimate method: Applications from railway asset management. *Proceedings of the Institution of Mechanical Engineers, Part O: Journal of Risk and Reliability 233*(5), 761–774.

Neves, L. and D. Frangopol (2010). Optimization of bridge maintenance actions considering combination of sources of information: Inspections and expert judgment. *Bridge Maintenance, Safety, Management and Life-Cycle Optimization - Proceedings of the 5th International Conference on Bridge Maintenance, Safety and Management*, 1913–1919.

Neves, L. A. C., D. M. Frangopol, and P. J. S. Cruz (2006a). Probabilistic Lifetime-Oriented Multiobjective Optimization of Bridge Maintenance : Single Maintenance Type. *Journal of Structural Engineering 132*(6), 991–1005.

Neves, L. A. C., D. M. Frangopol, and P. J. S. Cruz (2006b). Probabilistic Lifetime-Oriented Multiobjective Optimization of Bridge Maintenance: Combination of Maintenance Types. *Journal of Structural Engineering 132*(11), 1821–1834.

Neves, L. C. and D. M. Frangopol (2005). Condition, safety and cost profiles for deteriorating structures with emphasis on bridges. *Reliability Engineering and System Safety 89*(2), 185–198.

Ng, S.-K. and F. Moses (1996). Prediction of bridge service life using time-dependent reliability analysis. In J. Harding, G. Parke, and M. Ryall (Eds.), *Bridge Management 3*, ISBN: 1001168063. E & FN Spon.

Ng, S.-K. and F. Moses (1998). Bridge deterioration modeling using semi-Markov theory. *Structural Safety and Reliability*, 113–120.

Ni, Y. Q., Y. W. Wang, and C. Zhang (2020). A Bayesian approach for condition assessment and damage alarm of bridge expansion joints using long-term structural health monitoring data. *Engineering Structures 212*(November 2019).

Nicolai, R. P., R. Dekker, and J. M. van Noortwijk (2007). A comparison of models for measurable deterioration: An application to coatings on steel structures. *Reliability Engineering and System Safety 92*(12), 1635–1650.

Norris, J. R. (1997). *Markov Chains* (1st ed.). Cambridge University Press.

Okasha, N. M. and D. M. Frangopol (2009). Lifetime-oriented multi-objective optimization of structural maintenance considering system reliability, redundancy and life-cycle cost using GA. *Structural Safety 31*(6), 460–474.

Okasha, N. M., D. M. Frangopol, and A. D. Orcesi (2012). Automated finite element updating using strain data for the lifetime reliability assessment of bridges. *Reliability Engineering and System Safety 99*, 139–150.

Orcesi, A. D. and C. F. Cremona (2010). A bridge network maintenance framework for Pareto optimization of stakeholders/users costs. *Reliability Engineering and System Safety 95*(11), 1230–1243.

Orcesi, A. D. and D. M. Frangopol (2011). Optimization of bridge maintenance strategies based on structural health monitoring information. *Structural Safety 33*(1), 26–41.

Padgett, J. E., J. Ghosh, and K. Dennemann (2009). Sustainable infrastructure subjected to multiple threats. In *TCLEE 2009: Lifeline Earthquake Engineering in a Multihazard Environment*, Oakland, California, pp. 703–713. ASCE.

Pandey, M. D. and J. S. Nathwani (2004). Life quality index for the estimation of societal willingness-to-pay for safety. *Structural Safety 26*(2), 181–199.

Pandey, M. D., J. S. Nathwani, and N. C. Lind (2006). The derivation and calibration of the life-quality index (LQI) from economic principles. *Structural Safety 28*(4), 341–360.

Pandey, M. D. and J. M. van Noortwijk (2004). Gamma process model for time-dependent structural reliability analysis. In *Proceedings of the 2nd International Conference on Bridge Maintenance, Safety, and Management (IABMAS '04)*.

Pandey, M. D., X. X. Yuan, and J. M. van Noortwijk (2005). Gamma process model for reliability analysis and replacement of aging structural components. In *Nineth International Conference on Structural Safety and Reliability*, Rome, Italy, pp. 2439–2444.

Pearl, J. (1988). *Probabilistic reasoning in intelligent systems: Networks of plausible inference*. Morgan Kaufmann Series in Representation and Reasoning. Morgan Kaufmann.

Petcherdchoo, A., L. A. C. Neves, and D. M. Frangopol (2004). Combination of probabilistic maintenance actions for minimum life-cycle cost of deteriorating bridges. In E. Watanabe, D. M. Frangopol, and T. Utsunomiya (Eds.), *Proceedings of the 2nd International Conference on Bridge Maintenance, Safety, and Management (IABMAS '04)*, Kyoto, Japan. CRC Press.

Peterson, J. L. (1977). Petri Nets. *Computing Surveys 9*(3), 223–252.

Peterson, J. L. (1981). *Petri Net Theory and the Modeling of Systems*. Englewood Cliffs, NJ, USA: Prentice-Hall.

Petri, C. and W. Reisig (2008). Petri net. *Scholarpedia 3*(4), 6477.

Petri, C. A. (1962). *Communicating with automata*. Ph. D. thesis, Technical University Darmstadt, Germany.

Phares, B. M., G. a. Washer, D. D. Rolander, B. a. Graybeal, and M. Moore (2004). Routine Highway Bridge Inspection Condition Documentation Accuracy and Reliability. *Journal of Bridge Engineering 9*(4), 403–413.

Poole, D. L., A. K. Mackworth, and R. G. Goebel (1998). *Computational Intelligence: A Logical Approach*. New York: Oxford University Press.

Pregnolato, M. (2019). Bridge safety is not for granted – A novel approach to bridge management. *Engineering Structures 196*(June), 109193.

Privault, N. (2013). *Understanding Markov Chains* (1st ed.). Springer.

PwC (2014). Capital project and infrastructure spending: Outlook to 2025. Technical report, PricewaterhouseCoopers LLP.

Rabiner, L. (1989). A tutorial on hidden Markov models and selected applications in speech recognition.

Rackwitz, R. (2002). Optimization and risk acceptability based on the life quality index. *Structural Safety 24*, 297–331.

Rafiq, M. I., M. K. Chryssanthopoulos, and S. Sathananthan (2015). Bridge condition modelling and prediction using dynamic Bayesian belief networks. *Structure and Infrastructure Engineering 11*(1), 38–50.

Ramamoorthy, C. V. and G. S. Ho (1980). Performance Evaluation of Asynchronous Concurrent Systems Using Petri Nets. *Software Engineering, IEEE Transactions on SE-6*(5), 440–449.

Reeves, J., R. Remenyte-Prescott, J. Andrews, and P. Thorley (2018). A sensor selection method using a performance metric for phased missions of aircraft fuel systems. *Reliability Engineering and System Safety 180*, 416–424.

Reisig, W. (2013). *Understanding Petri Nets* (1st ed.). Springer-Verlag Berlin Heidelberg.

ReliaSoft (2020). *The Weibull Distribution. www.reliawiki.com* Last Checked: 01/10/2020.

Rios, L. M. and N. V. Sahinidis (2013). Derivative-free optimization: A review of algorithms and comparison of software implementations. *Journal of Global Optimization 56*(3), 1247–1293.

Robelin, C.-A. and S. M. Madanat (2007). History-Dependent Bridge Deck Maintenance and Replacement Optimization with Markov Decision Processes. *Journal of Infrastructure Systems 13*(3), 195–201.

Roelfstra, G., R. Hajdin, B. Adey, and E. Brühwiler (2004). Condition evolution in Bridge Management Systems and Corrosion-Induced Deterioration. *Journal of Bridge Engineering 9*(3), 268–277.

Ross, S. M. (2006). *Introduction to Probability Models*. San Diego: Elsevier Science & Technology.

Rubino, G. and B. Sericola (2014). *Markov chains and dependability theory* (1st ed.). Cambridge University Press.

Ryall, M. J. (2010). *Bridge Management* (2nd ed.). Elsevier Ltd.

Sabatino, S., D. M. Frangopol, and Y. Dong (2015). Sustainability-informed maintenance optimization of highway bridges considering multi-attribute utility and risk attitude. *Engineering Structures 102*, 310–321.

Sánchez-Silva, M., D. M. Frangopol, J. Padgett, and M. Soliman (2016). Maintenance and operation of infrastructure systems: Review. *Journal of Structural Engineering 142*(9), 1–16.

Saydam, D., D. M. Frangopol, and Y. Dong (2013). Assessment of Risk Using Bridge Element Condition Ratings. *Journal of Infrastructure Systems 19*(3), 252–265.

Scherer, W. T. and D. M. Glagola (1994). Markovian Models for Bridge Maintenance Management. *Journal of Transport Engineering 120*(1), 37–51.

Schneeweiss, W. G. (1999). *Petri Nets for Reliabiltiy Modeling*. LiLoLe-Verlag Publishing.

Scholten, L., A. Scheidegger, P. Reichert, and M. Maurer (2013). Combining expert knowledge and local data for improved service life modeling of water supply networks. *Environmental Modelling and Software 42*, 1–16.

Schwarz, G. (1978). Estimating the dimension of a model. *Annals of Statistics 6*(2), 461–464.

SETRA (1996). Classification des Ouvrages. Technical report, Service d'Etudes Techniques des Roultes et Autoroutes.

Shekhar, S. and J. Ghosh (2020). A metamodeling based seismic life-cycle cost assessment framework for highway bridge structures. *Reliability Engineering and System Safety 195*, 106724.

Shekhar, S., J. Ghosh, and J. E. Padgett (2018). Seismic life-cycle cost analysis of ageing highway bridges under chloride exposure conditions: modelling and recommendations. *Structure and Infrastructure Engineering 14*(7), 941–966.

Shi, Y. and R. Eberhart (1998). A Modified Particle Swarm Optimizer. In *Proceedings of IEEE International Conference on Evolutionary Computation.*, pp. 69–73.

Sianipar, P. R. and T. M. Adams (1997). Fault-tree model of bridge element deterioration due to interaction. *Journal of Infrastructure Systems 3*(3), 103–110.

Silva, A., L. C. Neves, P. L. Gaspar, and J. De Brito (2016). Probabilistic transition of condition: Render facades. *Building Research and Information 44*(3), 301–318.

Smale, K. (2018). Polcevera Viaduct Collapse: Engineers reveal structure's vulnerabilities. *New Civil Engineer* (September), 08–09.

Sobanjo, J. O. (1997). A Neural Network Approach to Modeling Bridge Deterioration. In *Computing in Civil Engineering*, pp. 623–626. ASCE.

Sobanjo, J. O. (2011). State transition probabilities in bridge deterioration based on Weibull sojourn times. *Structure and Infrastructure Engineering 7*(10), 747–764.

Sobanjo, J. O. and P. D. Thompson (2011). Enhancement of the FDOT's Projects Level and Network Level Bridge Management Analysis Tools. Technical report, Florida Department of Transportation.

Spiegelhalter, D. (2019). *The Art of Statistics: Learning from Data* (1st ed.). Pelican Books.

Srikanth, I. and M. Arockiasamy (2020). Deterioration models for prediction of remaining useful life of timber and concrete bridges: A review. *Journal of Traffic and Transportation Engineering 7*(2), 152–173.

Srinivasan, R. and A. K. Parlikad (2017). An approach to value-based infrastructure asset management. *Infrastructure Asset Management 4*(3), 87–95.

Stein, S. M., G. K. Young, R. E. Trent, and D. R. Pearson (1999). Prioritizing Scour Vulnerable Bridges Using Risk. *Journal of Infrastructure Systems 5*(3), 95–101.

Sterne, J. A., G. D. Smith, and D. R. Cox (2001). Sifting the evidence—what's wrong with significance tests? *British Medical Journal 322*(7280), 226–231.

Stewart, M. G. (2001). Reliability-based assessment of ageing bridges using risk ranking and life cycle cost decision analyses. *Reliability Engineering and System Safety 74*(3), 263–273.

Straub, D. (2009). Stochastic Modeling of Deterioration Processes through Dynamic Bayesian Networks. *Journal of Engineering Mechanics 135*(10), 1089–1099.

Straub, D. and A. Der Kiureghian (2010a). Bayesian Network Enhanced with Structural Reliability Methods: Application. *Journal of Engineering Mechanics 136*(10), 1259–1270.

Straub, D. and A. Der Kiureghian (2010b). Bayesian Network Enhanced with Structural Reliability Methods: Methodology. *Journal of Engineering Mechanics 1326*(10), 1248–1258.

Strauss, A., D. M. Frangopol, and S. Kim (2008). Use of monitoring extreme data for the performance prediction of structures: Bayesian updating. *Engineering Structures 30*(12), 3654–3666.

Taleb-Berrouane, M., F. Khan, and P. Amyotte (2020). Bayesian Stochastic Petri Nets (BSPN) - A new modelling tool for dynamic safety and reliability analysis. *Reliability Engineering & System Safety 193*, 106587.

Tamakoshi, T., Y. Yoshida, S. Yoshinaga, and S. Fukunaga (2006). Analysis of damage occurring in steel place girder bridges on national roads in Japan. In *22nd US–Japan Bridge Engineering Workshop*, Seattle, WA.

Tan, C. J. K. (2002). The PLFG parallel pseudo-random number generator. *Future Generation Computer Systems 18*(5), 693–698.

The Mathworks (2020). *MATLAB and Optimization Toolbox Release 2020a*. Natick, MA: The Mathworks, Inc.

Thoft-Christensen, P. and M. J. Baker (1982). *Structural reliability theory and its applications*. Berlin: Springer-Verlag.

Thomas, O. and J. Sobanjo (2016). Semi-Markov models for the deterioration of bridge elements. *Journal of Infrastructure Systems 22*(3), 1–12.

Thomopoulos, N. T. (2013). *Essentials of Monte Carlo SImulation; Statistical Methods for Building Simulation Models* (1st ed.). New York: Springer.

Thompson, P. D. and R. W. Shephard (1994). Pontis. *Transportation Research Record 324*, 35–42.

Thompson, P. D., E. P. Small, M. Johnson, and A. R. Marshall (1998). The Pontis Bridge Management System. *Structural Engineering International 8*(4), 303–308.

Tokdemir, O. B., C. Ayvalik, and J. Mohammadi (2000). Prediction of Highway Bridge Performance by Artificial Neural Networks and Genetic Algorithms. *Proceedings of the 17th IAARC/CIB/IEEE/IFAC/IFR International Symposium on Automation and Robotics in Construction*.

Trivedi, K. S. and A. Bobbio (2017). *Reliability and Availability Engineering: Modeling, Analysis, and Applications*. Cambridge University Press.

UIC (2009). Classification of lines for the purpose of track maintenance. Technical Report Leaflet 714, Union Internationale des Chemins de Fer.

US Department of Transportation, Federal Highway Administration (2018). *Glossary*. Last Checked: 27/03/2018: *https://www.fhwa.dot.gov/planning/glossary/glossary_listing.cfm*.

Vagnoli, M. (2019). *Railway Bridge Condition Monitoring and Fault Diagnostics*. Ph. D. thesis, University of Nottingham.

Vagnoli, M., R. Remenyte-Prescott, and J. Andrews (2018). Railway bridge structural health monitoring and fault detection: State-of-the-art methods and future challenges. *Structural Health Monitoring 17*(4), 971–1007.

Van Brummelen, G. (2013). *Navigating by the Stars: The Forgotten Art of Spherical Trigonometry*. Princeton University Press.

van Noortwijk, J. M. (2009). A survey of the application of gamma processes in maintenance. *Reliability Engineering and System Safety 94*(1), 2–21.

van Noortwijk, J. M., J. A. van der Weide, M. J. Kallen, and M. D. Pandey (2007). Gamma processes and peaks-over-threshold distributions for time-dependent reliability. *Reliability Engineering and System Safety 92*(12), 1651–1658.

Vickerman, R. (2007). Cost - benefit analysis and large-scale infrastructure projects: State of the art and challenges. *Environment and Planning B: Planning and Design 34*(4), 598–610.

Wang, R., L. Ma, C. Yan, and J. Mathew (2012). Condition deterioration prediction of bridge elements using Dynamic Bayesian Networks (DBNs). In *Proceedings of 2012 International Conference on Quality, Reliability, Risk, Maintenance, and Safety Engineering, ICQR2MSE 2012*, pp. 566–571. IEEE.

Wardhana, K. and F. C. Hadipriono (2003). Analysis of recent bridge failures in the United States. *Journal of Performance of Constructed Facilities 17*(3), 144–150.

Weber, P. and L. Jouffe (2003). Reliability modelling with dynamic Bayesian networks. *IFAC Proceedings Volumes 36*(5), 57–62.

Weber, P., G. Medina-Oliva, C. Simon, and B. Iung (2012). Overview on Bayesian networks applications for dependability, risk analysis and maintenance areas. *Engineering Applications of Artificial Intelligence 25*(4), 671–682.

Wild, C. J. and M. Pfannkuch (1999). Statistical thinking in empirical enquiry. *International Statistical Review 67*(3), 223–248.

Wilks, S. S. (1938). The Large-Sample Distribution of the Likelihood Ratio for Testing Composite Hypotheses. *The Annals of Mathematical Statistics 9*(1), 60–62.

Xie, F. and D. Levinson (2011). Evaluating the effects of the I-35W bridge collapse on road-users in the twin cities metropolitan region. *Transportation Planning and Technology 34*(7), 691–703.

Yang, D. Y. and D. M. Frangopol (2018). Probabilistic optimization framework for inspection/repair planning of fatigue-critical details using dynamic Bayesian networks. *Computers and Structures 198*, 40–50.

Yang, D. Y. and D. M. Frangopol (2019). Life-cycle management of deteriorating civil infrastructure considering resilience to lifetime hazards: A general approach based on renewal-reward processes. *Reliability Engineering and System Safety 183*, 197–212.

Yang, S. I., D. M. Frangopol, Y. Kawakami, and L. C. Neves (2006). The use of lifetime functions in the optimization of interventions on existing bridges considering maintenance and failure costs. *Reliability Engineering and System Safety 91*(6), 698–705.

Yang, S. I., D. M. Frangopol, and L. C. Neves (2004). Service life prediction of structural systems using lifetime functions with emphasis on bridges. *Reliability Engineering and System Safety 86*(1), 39–51.

Yates, F. (1934). Contingency Tables Involving Small Numbers and the $\chi 2$ Test. *Supplement to the Journal of the Royal Statistical Society 1*(2), 217–235.

Yianni, P. C., L. C. Neves, D. Rama, and J. D. Andrews (2018). Accelerating Petri-Net simulations using NVIDIA Graphics Processing Units. *European Journal of Operational Research 265*(1), 361–371.

Yianni, P. C., L. C. Neves, D. Rama, J. D. Andrews, and R. Dean (2016). Incorporating local environmental factors into railway bridge asset management. *Engineering Structures 128*, 362–373.

Yianni, P. C., L. C. Neves, D. Rama, J. D. Andrews, N. Tedstone, and R. Dean (2018). Quantifying the impact of variability in railway bridge asset management. In *Life-Cycle Analysis and Assessment in Civil Engineering: Towards an Integrated Vision - Proceedings of the 6th International Symposium on Life-Cycle Civil Engineering, IALCCE 2018*, pp. 1395–1402.

Yianni, P. C., D. Rama, L. C. Neves, J. D. Andrews, and D. Castlo (2017). A Petri-Net-based modelling approach to railway bridge asset management. *Structure and Infrastructure Engineering 13*(2), 287–297.

Zhang, H. and D. W. R. Marsh (2018). Generic Bayesian network models for making maintenance decisions from available data and expert knowledge. *Proceedings of the Institution of Mechanical Engineers, Part O: Journal of Risk and Reliability 232*(5), 505–523.

Zhang, H. and D. W. R. Marsh (2020). Multi-state deterioration prediction for infrastructure asset: Learning from uncertain data, knowledge and similar groups. *Information Sciences 529*, 197–213.

Zhang, H. and D. W. R. Marsh (2021). Managing infrastructure asset: Bayesian

networks for inspection and maintenance decisions reasoning and planning. *Reliability Engineering & System Safety 207*, 107328.

Zhang, H., D. William, and R. Marsh (2017). Bayesian network models for making maintenance decisions from data and expert judgment. In *ESREL 2016: Risk, Reliability and Safety: Innovating Theory and Practice*, pp. 1056–1063.

Zhang, W. and C. S. Cai (2012). Fatigue reliability assessment for existing bridges considering vehicle speed and road surface conditions. *Journal of Bridge Engineering 17*(3), 443–453.

Zhang, X., D. Rajan, and B. Story (2019). Concrete crack detection using context-aware deep semantic segmentation network. *Computer-Aided Civil and Infrastructure Engineering 34*(11), 951–971.

Zimmermann, A. (2017). Modelling and Performance Evaluation With TimeNET 4 . 4. In *14th International Conference on Quantitative Evaluation of SysTems ()QEST*.

Zuberek, W. M. (1980). Timed Petri nets and preliminary performance evaluation. In *Proceedings of the 7th annual symposium on Computer Architecture - ISCA '80*, pp. 88–96.

Appendix A

Genetic Algorithms

Genetic Algorithms (GA) are an optimisation technique popularised by Holland (1975) and are based on the principles of natural selection from evolutionary biology (Darwin, 1859). To determine a solution for an optimisation problem using a GA, an initial population is required. A population refers to several potential solutions that can be evaluated against the fitness function. An individual solution is a set of variables that can be used to evaluate the fitness function. Each variable or parameter in a solution can be referred to as a gene, with a complete set of genes forming a chromosome. The fitness function is the indicator that is used to compare different solutions and ascertain which chromosomes have the more favourable genes. During an iteration, the population of solutions is evaluated using the fitness function: chromosomes that can yield the 'fittest' solutions are then selected to pass their genes onto the next generation.

The selection process takes place to ensure that the solutions deemed to be the 'fittest' are allocated a greater opportunity to act as parents and reproduce to pass their genes onto the next generation. Pairs of individual chromosomes are selected based on their fitness scores and act as a pair of parents that are mated to yield a new chromosome. The mating of two parents is a phase of GA known as crossover, whereby a crossover point is selected at random in the chromosome of both parents and offspring are created through the exchange of genes between parents. The offspring chromosomes then form the population of the next generation.

An additional phase of GA is the mutation phases which is the probabilistic

manipulation of genes when forming offspring. The probability of mutation is typically low, e.g. $< 1\%$ and is unlikely to drastically change the composition of a large number of the solutions (Goldberg, 1989). The purpose of the mutation phase is to ensure adequate diversity in the chromosomes of a population, enable potential solutions that did not exist in the previous generation and to avoid the optimisation converging before the global optimum has been reached. However, one should be adverse to a high level of mutation as the optimisation process would increasingly become akin to a random selection and convergence may never be achieved.

The convergence of the optimisation is specified by criteria determining whether there has been significant changes in the offspring of two successive generations. An example convergence criteria is comparing the computed mean value between generations. However, the optimisation can be terminated due to other factors beyond convergence such as maximum number of generations, maximum execution time/-cost and generational stalling (no improvement in the objective function between multiple generations, or less than a defined amount). A pseudocode of a typical GA is shown in Algorithm 2.

Algorithm 2: Genetic algorithm pseudocode

```
1 Generate initial population;
2 Evaluate fitness of initial population;
3 while Termination criteria is false do
4     Selection;
5     Crossover;
6     Mutation;
7     Fitness Evaluation;
```

The advantages of a GA include:

- Works with optimisation problems with both discrete and continuous variables.
- Can be implemented to leverage parallel computing which reduces computational execution time.

- Technique can be easily adapted to resolve a wide variety of problems and problems with a large set of variables.
- Does not require derivative information of the objective function.

The disadvantages of GA include:

- GA optimisations are vulnerable to premature convergence, particularly if the initial population was initialised with sub-optimal parameters e.g. a small population size.
- There a wide range of optimisation parameters required to initialise an optimisation e.g. selection rate, initial population size, crossover characteristics.